Catalytic dehydrogenations of ethylbenzene to styrene

Christian Nederlof

Catalytic dehydrogenations of ethylbenzene to styrene

Proefschrift

ter verkrijging van de graad van doctor
aan de Technische Universiteit Delft,
op gezag van de Rector Magnificus prof.ir. K.C.A.M. Luyben,
voorzitter van het College voor Promoties,
in het openbaar te verdedigen
op maandag 26 november 2012 om 12.30 uur

door

Christian NEDERLOF

scheikundig ingenieur
geboren te Bernisse, Nederland

Dit proefschrift is goedgekeurd door de promotoren:
Professor dr. F. Kapteijn
Professor dr.ir. M. Makkee

Samenstelling promotiecommissie:

Rector Magnificus,	voorzitter
Professor dr. F. Kapteijn	TU Delft, promotor
Professor dr.ir. M. Makkee	UNITO Turin / TU Delft, promotor
Professor dr. R. Schlögl	Fritz Haber Institut, Duitsland
Professor dr.ir. L. Lefferts	Universiteit Twente
Professor dr. J.A. Moulijn	TU Delft
Dr. B. Kimmich	CB&I Lummus Technology, USA
Dr. I.V. Melián-Cabrera	Rijksuniversiteit Groningen
Professor dr.ir. M.T. Kreutzer	TU Delft, reservelid

The research reported in this thesis was conducted in the Catalysis Engineering section of the Chemical Engineering department of the Faculty of Applied Sciences (TNW) of the Delft University of Technology.
This research is supported by the Dutch Technology Foundation STW, which is part of the Netherlands Organisation for Scientific Research (NWO) and which is partly funded by the Ministry of Economic Affairs, Agriculture and Innovation.
The author wants to thank Lummus Technology, a CB&I company, for their financial contribution.

Thesis, Delft University of Technology
Met samenvatting in het Nederlands / with summary in Dutch
ISBN 978-90-8891-521-5

Cover design: Stephan Timmers, Total Shot Productions, www.totalshot.nl
Printed by: Proefschriftmaken.nl || Uitgeverij BOXPress
Published by: Uitgeverij BOXPress, ‘s-Hertogenbosch

Table of contents

Voor Ingrid
en Robin

1

Introduction into styrene production

Abstract

Styrene monomer is a very important monomer, its number of applications and demand are still growing. Currently, styrene is produced by catalytic dehydrogenation, or by a peroxidation process together with propene oxide. These processes have several disadvantages such as high energy demands, low equilibrium conversions, lack in product flexibility and high capital costs. Improvements in the current processes are not expected, but other dehydrogenation processes show large potential and are in development. These are catalytic dehydrogenation in CO_2, catalytic oxidative dehydrogenation and the combined catalytic dehydrogenation of ethane and ethylbenzene (SNOW process). The theory, applied catalysts, development status and best results are described in this chapter.

1.1 Styrene

The styrene molecule (Figure 1.1) is best known for its application in expanded polystyrene ('piepschuim' in Dutch). It has many more applications, like styrene-butadiene rubber (SBR), latex (SBL), resins, as a copolymer, or for adhesives. This list and all its markets are still growing. Styrene owes its popularity to the easily reacting double bond that can undergo polymerisation reactions with itself or other monomers. The demand of styrene is still growing every year, roughly following the world economic growth. It is no surprise that the upcoming economies are the main drivers for these increasing demands. In 2010 about 27 million tons of styrene monomer were produced.[2] This makes it the 4th largest bulk monomer in production amounts. An overview of other important bulk monomers is shown in Table 1.1. The reported prices of styrene fluctuate constantly, due to difference in production and demand and overcapacity in the market due to new plants that are built every couple of years. The cost of benzene is the largest cost factor in the process. The main licensors of styrene production processes are Badger, Lummus, LyondellBasell, Shell, DOW and BASF.

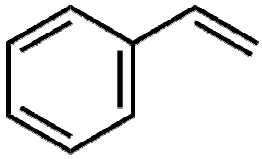

Figure 1.1: Styrene monomer.

All styrene is produced from ethylbenzene (EB). Therefore, a styrene (ST) production process is always built in combination with an ethylbenzene production process. Ethylbenzene is produced by the alkylation of benzene with ethene. This process is very efficient with extremely high selectivities (>98-99%).[3] As a result it is not worthwhile to try to improve that process further.

Since the development of the catalytic dehydrogenation reaction of ethylbenzene to styrene over potassium promoted iron oxide catalysts and its commercialization, much effort has been put into improving the process and its catalyst.[3, 4] This is a result of the importance of the product styrene, that has become a chemical commodity. On the production scale of 27 million tons, one can imagine that even a small improvement of catalyst performance will have an impact on the process energy requirements and overall costs.

Table 1.1: Overview of the most important bulk monomers.[1, 2]

Monomer	World demand Mt/a	Selective dehydrogenation?	Catalyst
Ethene	123	No	
Propene	77	Yes	$Pt(Sn)/Al_2O_3$ or Cr/Al_2O_3
Butene	19	Yes	
Butadiene	11	Yes	
Styrene	27	Yes	K-Fe
Terephthalic acid	42	No	

Most of the styrene is produced *via* dehydrogenation (Eq. 1.1). A fraction, ca. 15%, is produced *via* the SMPO or POSM process (Eq. 1.2) that also produces propene oxide (SM = styrene monomer, PO = propene oxide). Depending on the company that operates it, the most important product is named first. The main drawback of a SMPO process is its limited product flexibility. Styrene and propene oxide are always produced together in a mass ratio of around 2.1 (SM:PO, the molar ratio is ~1), while the market demand is often different. Recently, technology was successfully commercialised that produces PO without a hydrocarbon byproduct, the HPPO process (DOW/BASF technology). Therefore, expansion of the ST production by the construction of new SMPO plants is not expected, whereas for PO this might not be the case.

Because the dehydrogenation process is very energy and capital intensive, other production processes are also being developed. Some already up to pilot plant scale, others still in research laboratories. Examples are the oxidative dehydrogenation with oxygen, enhanced dehydrogenation in CO_2 and the SNOW process that uses a reactor/regenerator system. These and the standard dehydrogenation in steam, will be discussed in detail in the next paragraphs of this chapter.

$$C_8H_{10} \rightleftarrows C_8H_8 + H_2 \qquad 1.1$$

$$C_8H_{10} + C_3H_6 + O_2 \rightarrow \ldots \rightarrow C_8H_{10} + C_3H_6O + H_2O \qquad 1.2$$

1.2 Dehydrogenation in steam

The direct dehydrogenation of ethylbenzene to styrene (Eq. 1.1) is a highly endothermic reaction (125 kJ/mol). A large excess of steam is fed to the reactor together with ethylbenzene. The molar ratio of steam to EB varies from 7-12, depending on the exact catalyst formulation and type of process used (isothermal or adiabatic). Directly after the reactor, the whole product stream is cooled down rapidly to prevent styrene polymerisation reactions. The products and diluent undergo a phase transition from vapour to liquid. Heat recovery from the product stream is difficult. This, together with the reaction endotherm, makes the process very energy intensive. After separation, the water is recycled and the hydrocarbon product stream is further separated into unconverted EB that is also recycled, ST product, H_2, benzene and toluene byproducts. A small amount of waste (tars, gaseous hydrocarbons) is left after separation. A simplified process scheme is shown in Figure 1.2.

The conversion of EB into ST is equilibrium limited and therefore, operated at high temperature and an EB partial pressure as low as practically possible, also by dilution with H_2O. Usually two reactors are used in series with additional heating in be-

tween to increase the conversion, which is typically around 60-65%. Selectivity to styrene is high, 96%. The byproducts in this process are hydrogen, benzene, toluene, CO_2 and traces of methane and ethane. Benzene can be recycled to the alkylation process to make ethylbenzene and toluene can be sold for a byproduct credit. Hydrogen can also be removed from the product stream and sold, if it can be used in the near-by area. Otherwise, its heating value can be used for the process itself.

The steam diluent is an essential and elegant part of this process as it serves several functions: delivers heat for the reaction; improves conversion by dilution; keeps the catalyst in the appropriate oxidation state; and prevents deactivation by coke formation. Besides this, a large advantage is that water or steam is also easily available and abundant in most parts of the world. Consequently, steam generation and associated energy costs are an important factor in the production of styrene with this process.[5] The steam itself is not participating in the dehydrogenation reaction, it acts only as a diluent for the main reaction and could be replaced by other inert gases if it was not needed for its other functions as mentioned above.[6]

In this process a potassium promoted iron catalyst is used that contains several other promoters. The typical catalyst lifetime is 2 years, after which the whole catalyst bed is replaced.[5] Catalyst deactivation is due to loss of promoters and poisoning by halogen impurities in the feed. The latter one has become less of a problem since the $AlCl_3$ catalyst of the alkylation process was replaced with zeolites (ZSM-5). The dehydrogenation catalyst also suffers from deactivation by coke formation, but this is reversible and can be counteracted by varying the steam to EB ratio. Due to the small vapour pressure of potassium hydroxide, the potassium in the catalyst migrates to the cooler regions in two directions: (1) towards the centre of the catalyst particles and (2) to the exit of the reactor. This causes irreversible deactivation of the catalyst. The cata-

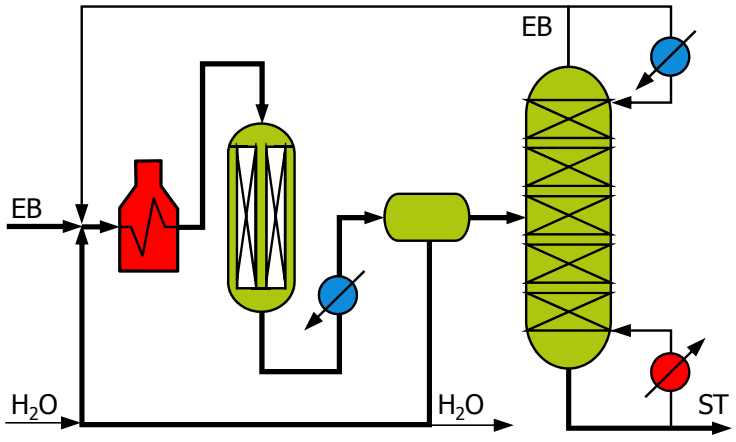

Figure 1.2: A very simplified scheme of the EB to ST dehydrogenation process with H_2O.

lyst shell has much lower activity due to the lack of potassium and deactivation by coke and the catalyst core has lower activity due to an excess of potassium. This means that only a small part of the catalyst particle is still active. The addition of potassium to the process helps only slightly, as it cannot prevent the redistribution of potassium inside the catalyst particles. Due to potassium loss, the aged catalyst particles have a higher surface area and pore volume.[5]

The potassium promoted catalyst contains up to 5 wt% potassium. This amount has increased over years of catalyst development to above 10 wt%, probably to improve the catalyst lifetime and decrease the S/O ratios (mass ratio Steam/Oil (= ethylbenzene)).[7] Other alkali metals than potassium, such as rubidium and cesium, also work well or even slightly better, but potassium is cheaper and is therefore, preferred.[5] The catalyst also contains many promotors, such as Cr that acts as a structural stabilizer for the iron oxide. Many patents and papers can be found that claim higher selectivities with different promotors, but usually at the expense of activity. This is due to the fact that the formation of styrene is limited by thermodynamic equilibrium, but the formation of benzene and toluene are not. The reaction proceeds so fast over the catalyst, that the reaction rates are limited by internal diffusion of ethylbenzene and styrene in the catalyst particles. These internal diffusion limitations have an influence on the selectivity. For high selectivity, macro-porosity and very low surface areas of only 2-5 m^2/g are desired. This is obtained by high temperature calcination of unsupported catalysts around 900-950 °C. Calcium binders are often used to obtain improved strength and when used in small amounts, there is no significant effect on catalyst performance.

Understanding the promoting effect of potassium has been the goal of many researchers. Potassium can have an effect on the electron transfer,[5] on the catalyst/promotor interface[8], or by an effect on the reduction of the oxidation state of iron oxide.[7] Based on their work there is now, more or less, consensus about the active site of the potassium promoted catalyst. It is identified to be a ternary phase of iron, oxygen and potassium by XRD measurements. Spent catalysts that were measured by *ex-situ* XRD only showed Fe_3O_4 and K_2CO_3, however, a steam treated catalyst that had higher activity showed an additional phase, $KFeO_2$. Therefore, this $KFeO_2$ was suggested to be the active phase.[9] Later on, *in-situ* XRD measurements confirmed that it was the active phase.[6] The reason that this phase was not detected by *ex-situ* XRD on spent catalysts is its metastable nature. After two days exposure to ambient air the $KFeO_2$ XRD signal could not be detected anymore.[6] The catalyst transformations during the process are presented in the scheme in Figure 1.3. Under reaction conditions, the active phase $KFeO_2$ is formed from its precursors, $K_2Fe_{22}O_{34}$ and Fe_2O_3. The catalyst deactivates by the deep reduction into KOH and Fe_3O_4 that is irreversible. Carbon deposition also takes place, but this deactivation mechanism is counteracted by an *in-situ* regeneration by

steam. A reaction mechanism of the dehydrogenation over this catalyst is not found in the literature. Sometimes it is assumed to be Mars-van Krevelen with Fe_2O_3 and Fe_3O_4 where steam is the oxidant,[10] but this does not correspond with the active site $KFeO_2$ that was identified,[6, 7] or the fact that steam has no influence on the dehydrogenation reaction.[6]

During the initial stage, or line-in period, of the catalyst testing, the activity increased gradually and reaches steady state in about 20 h. This time is required to bring the catalyst to its appropriate oxidation state.[7] A pre-reduction of the catalyst with hydrogen or ammonia reduces this initial period.[5]

The role of the carbon deposits on this catalyst is not completely clear. Coke deposition causes deactivation of the catalyst, but Hirano *et al.* found that the more active catalysts contained more carbon deposits. This was, however, in the range of 0.024-0.050 wt%. They concluded that carbon deposits might not exist on the active sites to inhibit the activities.[7]

When small amounts of CO_2 were added to the feed stream, deactivation of the

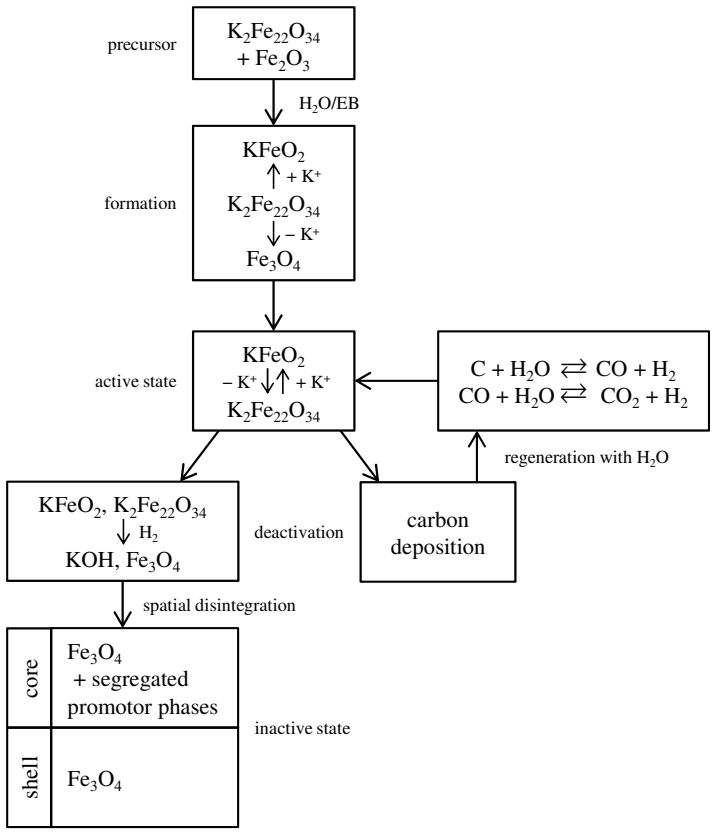

Figure 1.3: Schematic life cycle of a prototype catalyst without any promotor additives.[6]

catalyst was observed, see Figure 1.4. Carbon dioxide inhibited the formation of styrene, benzene and toluene. Upon removal of the CO_2 in the feed, the catalyst gradually recovered to its original activity. It is suspected that active potassium species react to form potassium carbonate. In the presence of steam it can go back to its active species.[7] Further research by Muhler *et al.*[11] showed that the addition of CO_2 did not increase the amounts of KCO_3 as detected by *in-situ* XPS. Only higher amounts of coke were observed after the addition of CO_2. The deactivating effect could be explained by the competitive adsorption between CO_2 and ethylbenzene on the active sites. Also CO_2 could suppress the coke gasification activity, giving the increased coke amounts.[11] The claimed active phase of the dehydrogenation catalyst, $KFeO_2$, is also the active material in catalysed coal gasification.[11, 12]

When ethylbenzene was removed from the feed for a few hours and then fed again, a steam treatment of the catalyst, an increase in the activity for the formation of styrene, toluene and benzene was observed for a short while, resulting in a slightly lower styrene selectivity. This is shown in Figure 1.5. The system's activity gradually decreased to steady-state (st.st.) levels with time on stream, styrene selectivity increased to st.st. levels with time on stream. Similarly, initially a steam treatment followed by CO_2 treatment, gave a small increase in styrene selectivity, but decreased the activity of the catalyst, like with the CO_2 addition.[7, 9] In both cases it is believed that the active phase is influenced, either increasing or decreasing the activity. Steam treatment is known to remove carbon deposits, but in both cases the amount of carbon was so low that it should not have influenced the activity.[9]

Concluding, one can state that the direct dehydrogenation process suffers from several disadvantages. The dehydrogenation reaction is equilibrium limited, giving large reactant recycle streams, it is a highly endothermic reaction (125 kJ/mol), large steam-to-hydrocarbon ratios are required to counteract the reversible deactivation by coke and

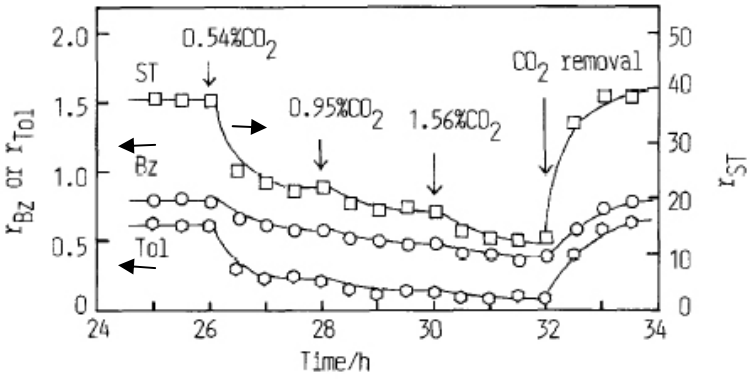

Figure 1.4: The influence of CO_2 addition to the feed upon the rates (10^5 mol g^{-1} min^{-1}) of styrene (□, *right axis*), benzene (○, *left axis*) and toluene (○, *left axis*) formation over 72Fe-28K at 600 °C.[7]

the catalyst also suffers from irreversible deactivation.[5]

It is clear that the direct dehydrogenation process can and should be improved in many aspects. Here several strategies for improvement come to mind. Further catalyst development for the steam-aided process, reducing the amount of steam required, improving the selectivity of the reaction, or making a catalyst with an even longer life time. This strategy has been followed mainly in the past time and has yielded some good results. The current catalyst consists of a mixture of metal oxides (Fe, K, Mg, Ce, Cr, Mo, V, Ca, Al) which operates at a steam-to-hydrocarbon ration as low as 6 mol/mol with good activity and selectivity.[4] Much more improvement is not to be expected from this route. Another strategy is to shift the equilibrium by removing hydrogen. This can be done either directly through membranes, or indirectly by a coupled reaction. If the coupling reaction is exothermic it could even deliver some of the heat of reaction, for instance the selective oxidation of hydrogen with oxygen that is done in the Lummus SMART Styrene technology. Other options besides oxidation with O_2 are N_2O decomposition, nitrobenzene hydrogenation, CO_2 methanation and CO_2 reverse-water-gas-shift.[4, 13-15] The use of oxygen or CO_2 have been pointed out to be the best, as these molecules are abundant and do not make the process dependent on the prices of another byproduct (PO) that has to be sold.

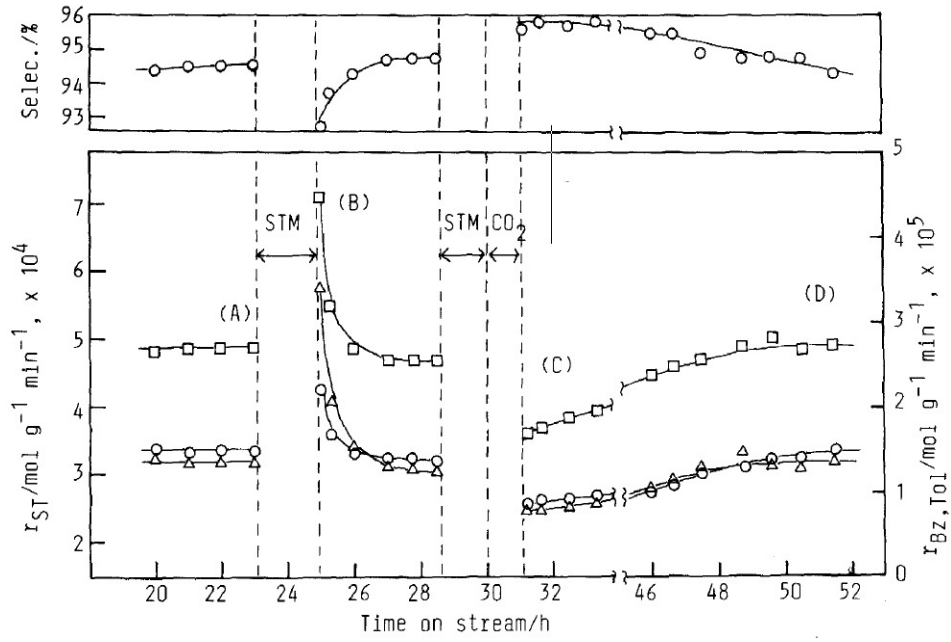

Figure 1.5: Effects of steam and CO_2 treatments on the styrene selectivity (*top*) and rates of styrene (□, *left axis*), benzene (○, *right axis*) and toluene (△, *right axis*) formation over potassium promoted iron oxide catalyst at 620 °C; STM: steam treatment; CO_2: CO_2 treatment.[9]

1.3 Dehydrogenation in carbon dioxide

In the dehydrogenation reaction of ethylbenzene to styrene in CO_2, many functions are ascribed to the use of CO_2:[13, 14, 16]

- Acts as a diluent, shifting the equilibrium conversion
- Enhancing the equilibrium conversion even more by H_2 removal through the RWGS reaction
- Remove coke from the catalyst surface by the reverse Boudouard reaction
- Improve selectivity
- Keep the active phase in the right oxidation state
- Better heat delivery due to high heat capacity

Simply said, CO_2 can perform the same actions as steam, with the large advantage that the RWGS reaction increases the EB conversion. It addresses most of the major issues with the conventional process, like the low conversions, large reactant recycles and the large energy losses due to the phase transitions of water. Despite all the advantages that CO_2 can bring, the use of CO_2 also has a negative side effect. From a thermodynamic point of view the process does not become more attractive, the reaction becomes even more endothermic. Also it is not clear yet if CO_2 can live up to the expectations.

The general accepted reactions and side reactions taking place during ethylbenzene dehydrogenation are the following:[4]

Direct reactions:

ethylbenzene $\rightleftarrows$ styrene + H_2	(dehydrogenation)
ethylbenzene $\rightarrow$ benzene + C_2H_4	(cracking)
ethylbenzene + H_2 $\rightarrow$ toluene + CH_4	(hydrogenolysis/hydrocracking)
ethylbenzene + CO_2 $\rightarrow$ CO + H_2	(dry reforming)

Consecutive reactions

H_2 + CO_2 $\rightleftarrows$ H_2O + CO	(reverse water-gas-shift)
styrene $\rightarrow$ precursors of coke	(oligomerization, polymerization, condensation)
precursors of coke $\rightarrow$ coke + H_2	(dehydrogenation)
(precursors of) coke + CO_2 $\rightleftarrows$ CO	(reverse Boudouard)

Using thermodynamic equilibrium calculations,[14] the effect of diluent and RWGS reaction coupling can be well visualized. This is shown in Figure 1.6. At 600 °C, the equilibrium ST yield with a 10:1 diluent to EB molar feed ratio is 71%. Taking into account the RWGS when CO_2 is used as a diluent, equilibrium ST yield reaches 90% at 600 °C, or for the same equilibrium ST yield the reaction temperature can be reduced

with more than 50 °C. The 1-step and 2-step mechanisms are further explained in 1.3.2.

Of course industrial reactors will not operate at equilibrium conditions, as enormous reactors will be required and selectivity issues will come into play because the (unwanted) side products, benzene and toluene, are not equilibrium limited. For the same reasons as with steam, the ratio of CO_2:EB should be kept as low as practically possible. However, a change of the feed ratio will count double, as it will have an effect on the diluent effect as well as on the RWGS, which is also an equilibrium limited reaction. The RWGS equilibrium product distribution (CO/H_2) as a function of the ST yield is shown in Figure 1.7. In all these cases the CO/H_2 ratio is larger than 1, meaning that

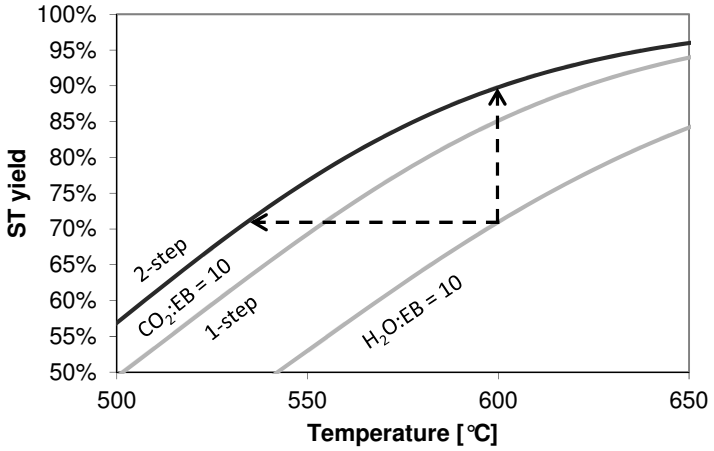

Figure 1.6: Thermodynamic equilibrium ST yields for the dehydrogenation of EB to ST in CO_2 (1- or 2-step) or H_2O with a 10:1 molar feed ratio with EB.

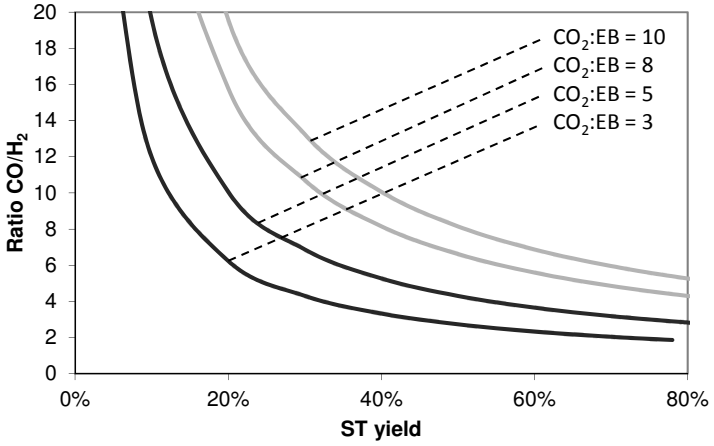

Figure 1.7: Thermodynamic equilibrium ratios of CO and H_2 by-products as a function of the ST yield from the dehydrogenation of EB to ST in CO_2 with different CO_2:EB molar feed ratios.

CO and water will be the main by-products of the CO_2 coupled ethylbenzene dehydrogenation. The CO/H_2 ratio will decrease with higher ST yields and lower CO_2:EB feed ratios.

In the CO_2 oxidative dehydrogenation process there will be much less hydrogen present in the reaction mixture compared to the current process. This can have a positive effect on the selectivity of the reaction, as hydrocracking of ethylbenzene will have a lower reaction rate with lower hydrogen amounts.[17, 18] A lower reaction temperature will also reduce the amount of byproducts that are formed.

At the temperatures used for dehydrogenation of ethylbenzene to styrene, carbon dioxide can be considered to be a mild oxidant.[13] At low temperatures CO_2 is regarded as unreactive, but it is also known that the RWGS reaction is active at temperatures well below 600 °C. In the gasification of coke the oxidizing power of several molecules is of the following order: O_2 (103) > H_2O (3) > CO_2 (1) > H_2 (0.003).[13] Looking just at counteracting the reversible deactivation by coke on the catalyst, this means that the catalyst of the new CO_2 process has to be about three times more effective. This should be possible, looking at past accomplishments in catalyst development for the conventional process.

In order for the CO_2 based process to become successful, it is not even necessary to fulfil all the ascribed functions. Even for similar catalyst performance compared to the steam-aided process, like stability, selectivity and activity, the overall process could be a winner as the use of steam is avoided. Any increase in conversion will result in even less energy required for the separation and smaller recycle streams. The energy required for this process is estimated to be 2.5 GJ/t-styrene, compared to 6.3 GJ/t-styrene for the current process, saving about 60% of the energy.[19-22]

Possible disadvantages are the availability of CO_2 that needs to be separated from a CO_2 rich stream like flue gas that needs to be close by. For the CO_2 recycle in the process, an additional CO_2 separator is needed and a costly gas compressor. Lastly, the CO byproduct should be put to good use. One can use a WGS unit and make H_2, or perhaps its heating value can be used in the process itself. Working with CO involves increased risks due to its toxicity.

1.3.1 Catalyst development

A good catalyst for the CO_2 oxidative dehydrogenation process has to be multifunctional: both dehydrogenation and RWGS reactions have to take place on its surface. The present molecules are quite different from each other and need different catalytic functionalities. Ethylbenzene has to be dehydrogenated, which usually proceeds through a redox-mechanism on a metal oxide surface. It is also a slightly basic molecule, so adsorption of EB is enhanced by the acidity of the surface. Carbon dioxide on the other

hand is acidic and needs basic sites to be activated. The RWGS reaction is also catalysed by a metal-oxide surface. With this we already have three requirements: acid sites, basic sites and redox sites.[16, 17, 23-26] The challenge is to find the optimum balance of these properties, resulting in a good catalytic system.

So far, many catalysts have been tested for this reaction. Already during the development of the catalyst for the current dehydrogenation process, CO_2 was tested as a possibly suitable diluent for the process. Over the K-Fe catalyst, carbon dioxide gave lower conversion, but a better selectivity. In the early seventies, carbon dioxide was identified to be, next to a diluent, an effective oxidant in dehydrogenation and coke removal. The best claimed catalysts of these studies were Cr/Al_2O_3, V/Al_2O_3 and activated carbon.[27] Decoking using CO_2 was not very effective, hydrocarbons in the system seemed to inhibit the decoking reaction. Too much CO_2 deactivated the catalyst, too small amounts of CO_2 resulted in rapid coking deactivation.[27]

After this publication in the 70's there seems to be a period of silence on this topic, to be picked up again in the late eighties and nineties. The catalysts that are being tested over time shift from metal oxides supported on activated carbon,[14, 16, 20, 28, 29] to metal oxides supported on alumina,[17, 18, 25, 26, 30-33] to unsupported mixed metal oxides[34-44] and hydrotalcite-like materials,[45-48] to mixed oxides supported on mesoporous materials.[42, 49-51] Already quite soon there seemed to be a relationship between activity and specific surface areas.[16] Activated carbon, mesoporous supports and alumina as a more practical alternative were therefore, the logical choices as they have large surface areas. Unsupported mixed metal oxides and hydrotalcite-like materials are also interesting candidates because of their acid, base and redox properties. Comparing the catalyst data from literature is not straightforward, as catalyst contact times, reaction times, dilutions and CO_2:HC ratios are almost never the same. However, some trends can be observed.

Activated carbon support is active for the dehydrogenation reaction and its activity and selectivity can be improved by most transition metal oxides (V, Cr, Fe, Mn, Mo,…) and lanthanides (La, Ce). Addition of basic metal oxides (Li, Na, K, Mg, Ca) and lanthanides has a good effect on the catalyst performance. In all cases, catalyst deactivation due to coking could not be prevented.[14, 16, 20, 28, 29]

Alumina catalyst support is very similar. Also active itself[17] and the same metal oxides (transition, lanthanide, alkali) have a positive effect on catalyst performance. Here, in almost all cases catalyst deactivation due to coking could not be prevented.[14, 15, 22, 23, 27-30] The only catalyst that showed stable operation in time was antimony promoted vanadium oxide on alumina. This system was developed further and patented. The authors ascribe the stability effect to the enhanced redox behaviour of vanadia due to the antimony. Preventing the deep reduction of the vanadia species and lowering of the alumina surface acidity with MgO modification reduces the coke formation.[26, 30]

Hydrotalcite-like catalysts were based on Mg, together with either V or Fe and other transition metals. These were all active in the dehydrogenation process, with some small differences between the different (metal) mixtures. However, all these catalysts were measured under high dilution and all suffered from deactivation due to coking.[45-48]

The unsupported mixed metal oxide catalysts were mostly based on zirconia, with a minor amount of other metal oxides. In this way a catalyst is made with a higher surface area than its single metal oxide equivalent, making these catalysts more active but still very selective. Unfortunately again the deactivation due to coking could not be prevented.[34-44]

Some recent papers successfully tried to apply mesoporous materials as the catalyst support. Due to the large surface areas their activity is very high, but also here deactivation is still an issue.[42, 49-51]

From this summation it can be concluded that many catalysts are found to be active and selective in the dehydrogenation reaction with CO_2. This is also shown in Figure 1.8. The problem of deactivation due to coking has still to be addressed. The catalyst deactivation can be delayed, but not prevented. The only catalyst showing stable operation consists of vanadium and antimony oxides (VSbO) on a magnesium modified Al_2O_3 support.[26, 30] Also, no catalyst has been found yet to be an order of magnitude more active like in the steam-aided dehydrogenation process.

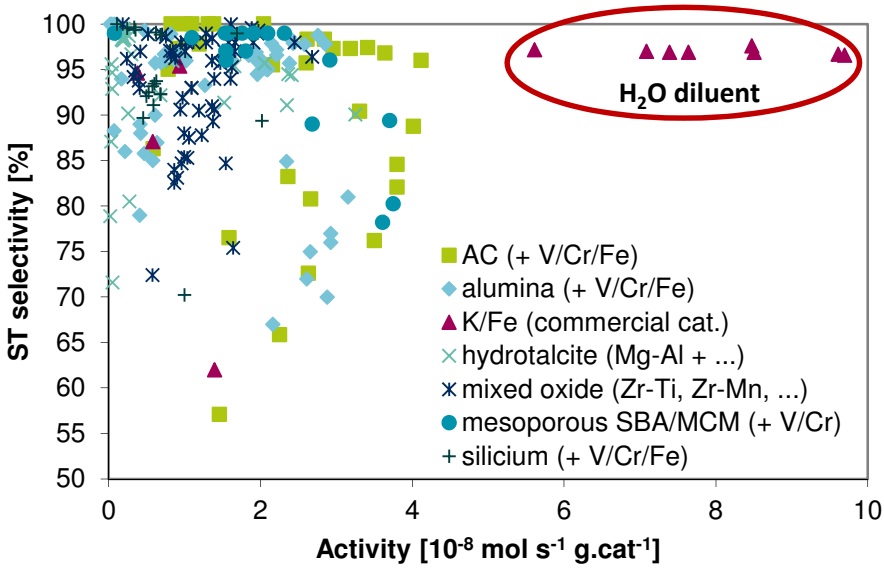

Figure 1.8: Overview of the catalyst selectivities as a function of their activity for the dehydrogenation of EB to ST in CO_2. All these catalysts are not stable with *TOS*. For comparison, data of the steam-aided process is also included. This catalyst is stable with *TOS*.

1.3.2 Reaction mechanism

In literature, several ideas of possible reaction mechanisms have been written down.[14, 17, 20] One of the easiest ways to describe the reaction is by a one, or two-step reaction path.

Two-step:

Ethylbenzene $\rightleftarrows$ styrene + H_2

$H_2 + CO_2 \rightleftarrows H_2O + CO$

One-step:

Ethylbenzene + $CO_2 \rightleftarrows$ styrene + H_2O + CO

Does the CO_2 oxidative dehydrogenation really consist of two separate, independent reactions that only influence each other's equilibrium conversions, or is it possible that ethylbenzene reacts directly with carbon dioxide? The equilibrium calculations for the combined dehydrogenation and RWGS show that higher CO_2-to-EB ratios will give higher CO/H_2 product ratios. Also lower conversion of the dehydrogenation reaction gives a higher CO/H_2 ratio. The observations of Mimura that above a CO_2/EB ratio of 8, the one-step pathway is the main route can be explained by this as well.

From a molecular point of view, the one-step pathway can exist. When CO_2 is adsorbed on the surface, a more acidic site is created that can attract an ethylbenzene molecule. The CO_2 becomes a carbonate, which is hydrogenated by ethylbenzene to give styrene, water and carbon monoxide, which all should desorb. There is also another possibility related to a redox type mechanism, where ethylbenzene reduces the redox site producing ethylbenzene and CO_2 oxidizes the redox site by dissociation into carbon monoxide and one oxygen atom. This redox site could also be of a carbonate nature that can be reduced by hydrogen, or ethylbenzene. The desorption of CO from the surface, or the dehydrogenation of ethylbenzene on the surface are two possible rate limiting steps.

Some groups did test the RWGS activity of the catalysts as well,[14, 17] showing that the catalysts are quite active for this reaction. This, combined with the results from the equilibrium calculations, make the two-step pathway the more likely one. From the available data it is difficult, maybe even impossible, to prove this unambiguously.

1.3.3 Catalyst coking

Deactivation of the catalyst due to excessive coking is the biggest concern in the catalyst development for CO_2 oxidative dehydrogenation. One of the reasons that the

catalyst performance data in most literature references is given after a time on stream of only 2-6 h is because of the fast deactivation of the catalysts. Data from later contact times would not be representative of the catalyst properties. The deactivation can amount up to more than 20% in just 4 h. However, this deactivation of the catalyst by coke is reversible. Removing the coke with an oxygen treatment (regeneration) will allow the catalyst to perform same as before.

Looking back to the past developments in steam-aided dehydrogenation of ethylbenzene to styrene, the deactivation of the catalyst by coke also was a main issue. It was only by the discovery of the potassium-iron catalyst system combined with the steam diluent that this problem was resolved. The catalyst lifetime is now determined by the rate of potassium loss and other irreversible deactivation processes.[4, 5] A similar trajectory might be envisaged for the CO_2 oxidative dehydrogenation process. The issue of preventing the excessive coking has been a starting point to develop new, coke resistant, catalysts.

The K-Fe catalyst of the current steam-aided dehydrogenation process is not completely coke-free. A stationary amount of coke is present on the catalyst surface.[52-54] The coke makes the reddish iron oxide catalyst look black once it is used. This blackening can also be an effect of the formation of Fe_3O_4-phase[5], but thermo-gravimetric studies clearly show the presence of coke. The amount depends on the exact catalyst composition and reaction conditions, but more active catalysts seem to have a larger amount of coke present.[7] The role of this stationary amount of coke is a reason for a debate. The active phase of the K-Fe catalyst is generally believed to be $KFeO_2$, which is formed in the presence of steam.[7, 9] Some research groups, however, think that coke might also play a role in the reaction mechanism.[54-56] Although coke is usually perceived as being malign, in some cases coke has a beneficial effect.[57] One such example is very closely related, namely the oxidative dehydrogenation of ethylbenzene to styrene using molecular oxygen. The most active and selective catalysts for oxidative dehydrogenation are carbon molecular sieves. A redox mechanism of quinine/hydroxyl groups is presumed to be the active center.[4] But even if coke has a positive effect on the reaction, the excessive formation of coke remains a problem to solve for the dehydrogenation in CO_2.

1.4 Oxidative dehydrogenation

The second alternative is the oxidative dehydrogenation process and is well reviewed by Cavani and Trifiro.[4] A short overview will be given based on this paper and references therein. The oxidative dehydrogenation (ODH) reaction, Eq. 1.3, is exothermic, producing 129 kJ/mol EB converted. The main advantage of this reaction is that it is not reversible and potentially higher yields can be obtained. Compared with the

commercial dehydrogenation process, another advantage is that the use of steam is avoided. Also the reaction temperatures are much lower, 400-500 °C, reducing the amount of cracking products. But with the use of oxygen, CO and CO_2 can be formed easily (Eqs. 1.4 and 1.5), these are also the main byproducts in an ODH process. This process also has a potential risk of explosion. Therefore, the concentrations of EB and O_2 are both 5 vol% or lower by dilution with helium in most public and patent literature.[4, 59]

$$C_8H_{10} + ½O_2 \rightarrow C_8H_8 + H_2O \quad 1.3$$

$$C_8H_{10} + 10½O_2 \rightarrow 8CO_2 + 5H_2O \quad 1.4$$

$$C_8H_{10} + 6½O_2 \rightarrow 8CO + 5H_2O \quad 1.5$$

The most promising catalysts are metal oxides and metal phosphates that have moderate acidity, or carbon materials. Actually the real catalyst is the carbonaceous deposit (coke) that is formed on these catalysts and not the catalyst itself. The catalytic sites on this coke are the quinone/hydroquinone groups on the surface of the coke.[58, 61-63] Ethylbenzene conversions of 70-80% with a ST selectivity of >90% are claimed (Table 1.2). A nice reaction mechanism has been formed by Emig and Hofman,[58] this is shown in Figure 1.9. In this mechanism, coke is formed from styrene, oxygen forms the catalytically active sites on the coke and CO_X are mainly formed by the oxidation of coke with oxygen. Most catalysts are quite stable with time on stream and show very repro-

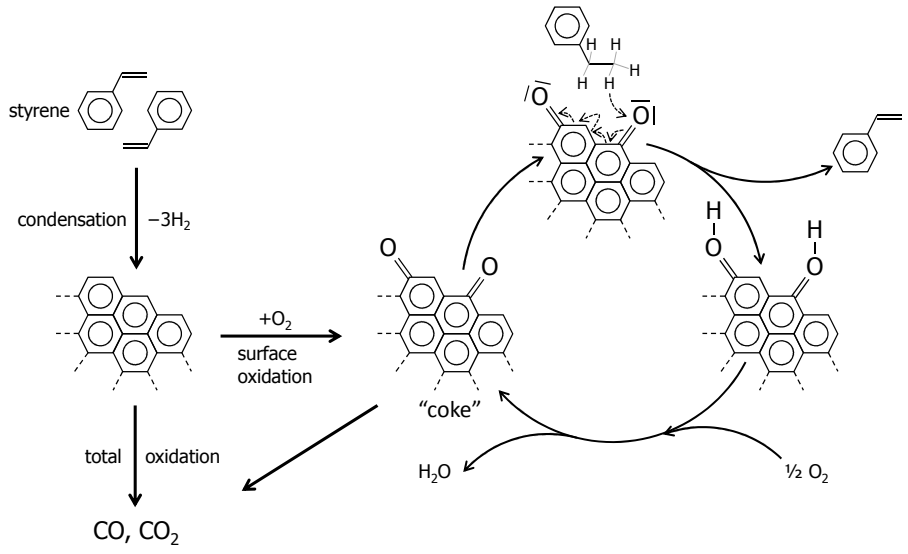

Figure 1.9: Simplified mechanism for the oxidative dehydrogenation reaction.[58]

Table 1.2: Catalyst performance of some catalysts in the ODH of EB to ST.

Catalyst	T	O_2:EB	EB conv.	ST sel.
Al_2O_3 [58]	450	1.2	59	79
Ce-P[59]	605	1.1	76	90
Mg-P[59]	530	1	71	93
P/SiO_2[59]	530	1	65	89
Carbon molsieve CMS AX 21[60]	350	2	80	90

ducible results after regenerations.[58, 59, 64] Despite these promising research results, the oxidative dehydrogenation process has not been applied on a commercial scale. The more recent literature on oxidative dehydrogenation focusses on the development of stable structured carbon materials as catalysts.[65-70]

1.5 The SNOW process / Advanced Styrene Monomer

In the attempt to completely redesign the styrene production process and make it more economical, the companies Snamprogretti and DOW teamed up and developed the SNOW process. A block scheme of the process is shown in Figure 1.10 and consists of an EB production process, dehydrogenation section and separation section. Ethane is fed to the dehydrogenation section, the ethene and ethane are recycled to the EB process where it reacts with benzene to form EB. The EB, unconverted C_2 and fresh ethane are co-fed to the dehydrogenation section. Styrene leaves the process after purification. The main advantages are that the process does not require a steam cracker to make ethane, it does not require steam diluent (in fact, ethane functions as diluent) and it has a more efficient heat delivery system. Especially because of the cheaper raw materials, this process can save up to 8% on the economics, compared to the conventional process.[65]

The SNOW process utilizes a FCC-type riser reactor with regenerator that is fed with ethane and ethylbenzene (Figure 1.11). These are dehydrogenated simultaneously in the riser reactor to form ethene and styrene at a temperature between 590-700 °C. The hydrocarbon partial pressures do not have to be lowered for improved lifetime or selectivity like in the conventional process. The produced ethene goes to the alkylation process to produce ethylbenzene. This alkylation unit together with the dehydrogenation section forms the SNOW process. Both dehydrogenation reactions are still equilibrium

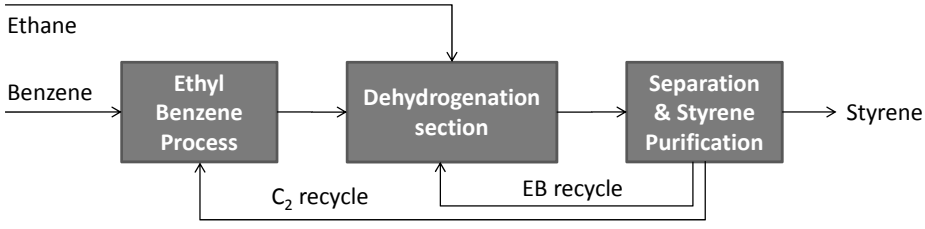

Figure 1.10: Block scheme of the SNOW process.[65]

limited. The ethane is more difficult to dehydrogenate, so the amount of ethane feed has to be adjusted to match the requirements of the alkylation process. The residence time of ethane and ethylbenzene can also be different by separate feeding points. This also allows a better temperature fit for the two dehydrogenation reactions. Unconverted ethylbenzene and ethane are recycled.[71]

The catalyst is a promoted gallium system and is very active, the reaction only need a couple of seconds and therefore, suitable to perform in a riser reactor. The selectivity is so high that steam dilution is not required.[65] Some results from a K-Pt-Ga-Si oxides (0.4 wt% - 75 ppm – 2.33 wt% – 1.56 wt%) on Al_2O_3 (mixed δ, θ and α phase) that was tested in a fixed bed reactor are given in Table 1.3.[72]

A small amount of coke is formed on the catalyst system. This is burnt in the catalyst regenerator, maintaining the high activity of the catalyst. The heat that is generated by combustion heats up the solid catalyst to deliver the heat to the endothermic dehydrogenation reactions in the reactor. To meet the energy requirements of the reactions, additional fuel has to be burnt in the regenerator. This can be the hydrogen by-product that is produced, additionally it reduces the CO_2 emissions of the process. Because of the catalytic combustion at relatively low temperature, CO and NO_X emissions are low.[71]

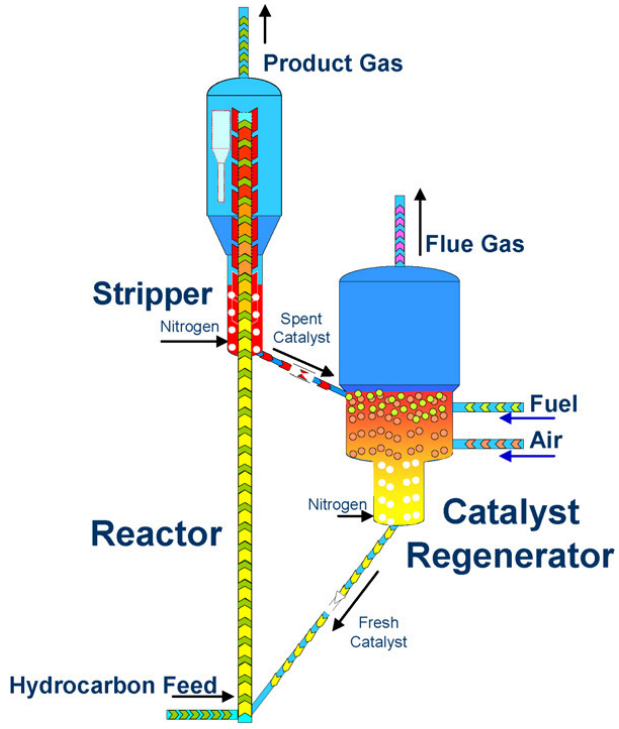

Figure 1.11: The SNOW reaction section.[71]

Table 1.3: Catalyst test results for the SNOW process.[72]

EB Vol%	C_2H_6 Vol%	Temp. [°C]	Press. Atm	*WHSV* EB kg/h/kg	SV h^{-1}	EB conv. %	C_2H_6 conv. %	ST sel. %	C_2H_4 sel. %	C_2H_4/ST mol/mol
9	91	600	1.1	0.2	587	57.9	12	94.0	95	2.12
19.1	80.9	600	1.1	0.43	596	50	8.5	94.0	95	0.73
28.8	71.2	600	1.1	0.64	595	45.4	7.1	94.1	95	0.39

The SNOW process was tested successfully up to pilot-scale, also catalyst production was scaled up successfully. Besides the 'ethane option', an 'ethene option' was also investigated in case a steam cracker is available. This 'ethene option' is also economically interesting because of the efficient heat delivery system and absence of steam diluent. The SNOW process is flexible and can handle both options. It has been commercialised under the name Advanced Styrene Monomer technology.

1.6 Conclusions

There are many ways to produce styrene, but even despite the disadvantages of the conventional steam-aided dehydrogenation process and the SMPO process, these are the only commercially operating processes. Dehydrogenation in CO_2, or dehydrogenation with O_2 are interesting alternatives because of their increased styrene yields, lower operating temperatures, avoiding steam as a diluent and avoiding a large amount of co-product formation. For both new processes, large improvements need to be made by catalyst development and optimisation, to be able to compete with the conventional process and its extremely high styrene selectivity (>96%). For dehydrogenation in CO_2, catalyst stability is the largest issue to solve. For the oxidative dehydrogenation process the styrene selectivity has to be increased. The SNOW process is a nice alternative that can be competitive in areas where ethene is difficult to obtain.

1.7 Goal of the thesis

Considering the continuing growth in styrene demand and the disadvantages of the conventional steam-aided dehydrogenation process, it is very worthwhile to investigate new process options for the production of styrene *via* dehydrogenation. Such dehydrogenation processes are unilaterally catalysed with heterogeneous catalysts. The success of such a catalyst largely determines the viability of these processes. The development of these catalysts is the main goal of this thesis. This includes catalyst preparation, characterisation, testing and reaction kinetics. The first part, preparation and characterisation, is the responsibility of our project partners at the University of Groningen. The catalyst testing and reaction kinetics were done in Delft.

The promising results on CO_2 oxidative dehydrogenation using a VSb-Mg/Al catalyst from the KRICT research group from Korea were the trigger to start this research. Initially the validation and further development of a catalyst for the CO_2 dehydrogenation process was targeted. However, on the official start of the project (> 1.5 years after my start) the topic changed to the oxidative dehydrogenation process with molecular oxygen, because the economic potential of this process exceeds that of the CO_2 process. This means that, together with some reference work on steam-aided dehydrogenation, I have worked on all relevant catalytic dehydrogenation processes. A second goal of this thesis is therefore, also to provide an overview and good insight into these three catalytic dehydrogenation processes.

The bulk of the work that was carried out was exploratory research, where possible, when time allowed it and with willingness of the equipment, I tried to extend the scope beyond the exploratory phase. This resulted in a few very nice studies that allowed this research to be placed into a wider context.

1.8 Outline of the thesis

An overview of the existing styrene production processes and the new catalytic dehydrogenation processes is presented in **Chapter 1**. Next, the steam-aided dehydrogenation process and catalyst are shortly explored in **Chapter 2**. This chapter also provides the reference data and defines the boundary conditions of the following chapters.

With **Chapter 3** the topic changes to the catalytic dehydrogenation in CO_2. It describes how Al_2O_3 is transformed into an active and highly selective catalyst for dehydrogenation in CO_2 or N_2 by deposition of coke on the catalyst. This coke is the actual active phase for the dehydrogenation reaction of ethylbenzene to styrene. **Chapter 4** focuses on the effect of CO_2 and the reverse water-gas shift (RWGS) reaction on the dehydrogenation reaction. In the presence of CO_2, more styrene is produced, but this effect is only temporary due to deactivation by excessive coking. The reaction mechanisms of the RWGS reaction and the dehydrogenation in CO_2 are investigated. The presence of coke enhances the RWGS activity by hydrogen spill-over. **Chapter 5** concludes the topic of dehydrogenation in CO_2. It describes some efforts to improve the catalyst stability by the addition of potassium promoter and the addition of steam diluent and their effects on the CO_2 dehydrogenation reaction.

In **Chapter 6** a start is made in the exploratory research for the oxidative dehydrogenation reaction with the screening of many catalysts, according to a testing protocol that consists of 10 conditions with different temperatures, O_2:EB feed ratios and CO_2 and/or N_2 diluent. The goal was to find a catalyst that showed a positive effect of CO_2 on the ODH reaction. This was not found. It did result in a couple of leads for further

research. In **Chapter 7** one of these leads is investigated, the loading of phosphorous on a SiO_2 support is optimised. In **Chapter 8** another lead is further developed, the high temperature calcination of γ-Al_2O_3 support shows a positive effect on the EB conversion and ST selectivity. The type and coverage of coke are responsible for part of this improvement, the improvement of pore accessibility also plays a role in the improvement. In **Chapter 9** it is proven that the ODH reaction can benefit a lot from a low O_2 concentration by the cross-feeding (stage-wise) of this reactant. The EB conversion can be increased without a significant decrease in ST selectivity that is the case when the EB and O_2 reactant are co-fed. The CO_X formation reactions have a higher reaction order for O_2 than the ST formation reaction. In **Chapter 10** the dynamics of the coke formation on ODH catalysts is investigated in detail by a TEOM-GC setup. It appears that the initial coke coverage and styrene yield are directly correlated and that a slow, but positive build-up of coke takes place continuously, causing the catalyst to slowly deactivate.

In the final chapter, **Chapter 11**, the whole project is discussed and evaluated, including the three catalytic dehydrogenation reactions: in H_2O, in CO_2 and with O_2. A new reaction mechanism is proposed for the steam-aided dehydrogenation reaction with an important role for the coke deposits on the catalyst.

Some of the introductory parts of the chapters contain duplicate information as these have been written as separate articles.

References

[1] J.A. Moulijn, M. Makkee, A.E. Van Diepen, Chemical Process Technology, Wiley, 2001.
[2] http://www.sriconsulting.com/WP/Public/PurchasingOptions.html, 27/5/2011.
[3] D.H. James, W.M. Castor, in: Ullmann's Encyclopedia of Industrial Chemistry, Wiley-VCH Verlag GmbH & Co. KGaA, 2002, Styrene.
[4] F. Cavani, F. Trifiro, Appl. Catal. A: Gen. 133 (1995) 219-239.
[5] E.H. Lee, Cat. Rev. - Sci. Eng. 8 (1973) 285-305.
[6] M. Muhler, J. Schütze, M. Wesemann, T. Rayment, A. Dent, R. Schlögl, G. Ertl, J. Catal. 126 (1990) 339-360.
[7] T. Hirano, Appl. Catal. 26 (1986) 65-79.
[8] A.K. Vijh, J. Chim. Phys. Phys.- Chim. Biol. 72 (1975) 5-8.
[9] T. Hirano, Appl. Catal. 26 (1986) 81-90.
[10] C.H. Bartholomew, R.J. Farrauto, Fundamentals of industrial catalytic processes,second ed., John Wiley & Sons, Inc., Hoboken, New Jersey, 2005, Ch. 7: Hydrogenation and Dehydrogenation of Organic Compounds, p.
[11] M. Muhler, R. Schlögl, G. Ertl, J. Catal. 138 (1992) 413-444.
[12] J. Carrazza, W.T. Tysoe, H. Heinemann, G.A. Somorjai, J. Catal. 96 (1985) 234-241.

[13] S.E. Park, S.C. Han, J. Ind. Eng. Chem. 10 (2004) 1257-1269.
[14] A.L. Sun, Z.F. Qin, J.G. Wang, Appl. Catal. A: Gen. 234 (2002) 179-189.
[15] S.B. Wang, Z.H. Zhu, Energy & Fuels. 18 (2004) 1126-1139.
[16] Y. Sakurai, T. Suzaki, N. Ikenaga, T. Suzuki, Appl. Catal. A: Gen. 192 (2000) 281-288.
[17] S. Sato, M. Ohhara, T. Sodesawa, F. Nozaki, Appl. Catal. 37 (1988) 207-215.
[18] G.I. Fedorov, S.G. Sibgatullin, N.L. Solodova, R.I. Izmailov, Pet. Chem. 16 (1976) 157-162.
[19] N. Mimura, M. Saito, Appl. Organomet. Chem. 14 (2000) 773-777.
[20] N. Mimura, M. Saito, Catal. Today. 55 (2000) 173-178.
[21] N. Mimura, M. Saito, Catal. Lett. 58 (1999) 59-62.
[22] G. Towler, S. Lynn, Chem. Eng. Sci. 49 (1994) 2585-2591.
[23] O.V. Krylov, A.K. Mamedov, S.R. Mirzabekova, Ind. Eng. Chem. Res. 34 (1995) 474-482.
[24] O.V. Krylov, A.K. Mamedov, S.R. Mirzabekova, Catal. Today. 24 (1995) 371-375.
[25] A.L. Sun, Z.F. Qin, S.W. Chen, J.G. Wang, J. Mol. Catal. A: Chem. 210 (2004) 189-195.
[26] J.S. Chang, D.Y. Hong, V.P. Vislovskiy, S.E. Park, Catal. Surv. Asia. 11 (2007) 59-69.
[27] D.B. Fox, M.H. Rei, E.H. Lee, Ind. Eng. Chem. Prod. Res. Dev. 11 (1972) 444-446.
[28] M.O. Sugino, H. Shimada, T. Turuda, H. Miura, N. Ikenaga, T. Suzuki, Appl. Catal. A: Gen. 121 (1995) 125-137.
[29] N. Ikenaga, T. Tsuruda, K. Senma, T. Yamaguchi, Y. Sakurai, T. Suzuki, Ind. Eng. Chem. Res. 39 (2000) 1228-1234.
[30] V.P. Vislovskiy, J.S. Chang, M.S. Park, S.E. Park, Catal. Commun. 3 (2002) 227-231.
[31] X.N. Ye, W.M. Hua, Y.H. Yue, W.L. Dai, C.X. Miao, Z.K. Xie, Z. Gao, New J. Chem. 28 (2004) 373-378.
[32] X.N. Ye, Y.H. Yue, C.X. Miao, Z.K. Xie, W.M. Hua, Z. Gao, Green Chem. 7 (2005) 524-528.
[33] S.W. Chen, Z.F. Qin, X.F. Xu, J.G. Wang, Appl. Catal. A: Gen. 302 (2006) 185-192.
[34] J.N. Park, J. Noh, J.S. Chang, S.E. Park, Catal. Lett. 65 (2000) 75-78.
[35] J. Noh, J.S. Chang, J.N. Park, K.Y. Lee, S.E. Park, Appl. Organomet. Chem. 14 (2000) 815-818.
[36] J. Ren, W.Y. Li, K.C. Xie, Catal. Lett. 93 (2004) 31-35.
[37] D.R. Burri, K.M. Choi, D.S. Han, J.B. Koo, S.E. Park, Catal. Today. 115 (2006) 242-247.
[38] D.R. Burri, K.M. Choi, S.C. Han, A. Burri, S.E. Park, J. Mol. Catal. A: Chem. 269 (2007) 58-63.
[39] D.R. Burri, K.M. Choi, S.E. Park, Adv. Nanomater. Proc., Pts 1-2. 124-126 (2007) 1737-1740.
[40] D.R. Burri, K.M. Choi, D.S. Han, Sujandi, N. Jiang, A. Burri, S.E. Park, Catal. Today. 131 (2008) 173-178.
[41] B.M. Reddy, H. Jin, D.S. Han, S.E. Park, Catal. Lett. 124 (2008) 357-363.
[42] B.M. Reddy, D.S. Han, N. Jiang, S.E. Park, Catal. Surv. Asia. 12 (2008) 56-69.
[43] B.M. Reddy, S.-C. Lee, D.-S. Han, S.-E. Park, Appl. Catal. B: Env. 87 (2009) 230-238.

[44] H.Y. Li, Y.H. Yue, C.K. Miao, Z.K. Xie, W.M. Hua, Z. Gao, Catal. Commun. 8 (2007) 1317-1322.
[45] Y. Sakurai, T. Suzaki, K. Nakagawa, N. Ikenaga, H. Aota, T. Suzuki, J. Catal. 209 (2002) 16-24.
[46] N. Mimura, I. Takahara, M. Saito, Y. Sasaki, K. Murata, Catal. Lett. 78 (2002) 125-128.
[47] G. Carja, R. Nakamura, T. Aida, H. Niiyama, J. Catal. 218 (2003) 104-110.
[48] X.N. Ye, N. Ma, W.M. Hua, Y.H. Yue, C.X. Miao, Z.K. Xie, Z. Gao, J. Mol. Catal. A: Chem. 217 (2004) 103-108.
[49] D.R. Burri, K.M. Choi, J.H. Lee, D.S. Han, S.E. Park, Catal. Commun. 8 (2007) 43-48.
[50] B.S. Liu, G. Rui, R.Z. Chang, C.T. Au, Appl. Catal. A: Gen. 335 (2008) 88-94.
[51] Y.Y. Qiao, C.X. Miao, Y.H. Yue, Z.K. Xie, W.M. Yang, W.M. Hua, Z. Gao, Microp. Mesop. Mater. 119 (2009) 150-157.
[52] G.R. Meima, P.G. Menon, Appl. Catal. A: Gen. 212 (2001) 239-245.
[53] B.D. Herzog, H.F. Rase, Ind. Eng. Chem. Prod. Res. Dev. 23 (1984) 187-196.
[54] K.R. Devoldere, G.F. Froment, Ind. Eng. Chem. Res. 38 (1999) 2626-2633.
[55] G.F. Froment, Catal. Rev. - Sci. Eng. 50 (2008) 1-18.
[56] W.J. Lee, G.F. Froment, Ind. Eng. Chem. Res. 47 (2008) 9183-9194.
[57] P.G. Menon, J. Mol. Catal. A: Chem. 59 (1990) 207-220.
[58] G. Emig, H. Hofmann, J. Catal. 84 (1983) 15-26.
[59] G.E. Vrieland, J. Catal. 111 (1988) 1-13.
[60] G.C. Grunewald, R.S. Drago, J. Mol. Catal. 58 (1990) 227-233.
[61] L.E. Cadus, O.F. Gorriz, J.B. Rivarola, Ind. Eng. Chem. Res. 29 (1990) 1143-1146.
[62] M.F.R. Pereira, J.J.M. Orfao, J.L. Figueiredo, Appl. Catal. A: Gen. 184 (1999) 153-160.
[63] A. Schraut, G. Emig, H.G. Sockel, Appl. Catal. 29 (1987) 311-326.
[64] L.E. Cadus, L.A. Arrua, O.F. Gorriz, J.B. Rivarola, Ind. Eng. Chem. Res. 27 (1988) 2241-2246.
[65] J.J. Delgado, X. Chen, J.P. Tessonnier, M.E. Schuster, E. Del Rio, R. Schlögl, D.S. Su, Catal. Today. 150 (2010) 49-54.
[66] J.J. Delgado, X.W. Chen, D.S. Su, S.B.A. Hamid, R. Schlögl, J. Nanosc. Nanotech. 7 (2007) 3495-3501.
[67] J.J. Delgado, R. Vieira, G. Rebmann, D.S. Su, N. Keller, M.J. Ledoux, R. Schlögl, Carbon. 44 (2006) 809-812.
[68] N. Keller, N.I. Maksimova, V.V. Roddatis, M. Schur, G. Mestl, Y.V. Butenko, V.L. Kuznetsov, R. Schlögl, Angew. Chem., Int. Ed. 41 (2002) 1885-1888.
[69] D.S. Su, J.J. Delgado, X. Liu, D. Wang, R. Schlögl, L.F. Wang, Z. Zhang, Z.C. Shan, F.S. Xiao, Chem. As. J. 4 (2009) 1108-1113.
[70] D.S. Su, N.I. Maksimova, G. Mestl, V.L. Kuznetsov, V. Keller, R. Schlögl, N. Keller, Carbon. 45 (2007) 2145-2151.
[71] D. Sanfilippo, G. Capone, A. Cipelli, R. Pierce, H. Clark, M. Pretz, Natural Gas Conversion VIII, Proceedings of the 8th Natural Gas Conversion Symposium. 167 (2007) 505-510.
[72] F. Buonomo, G. Donati, E. Micheli, L. Tagliabue, Process for the production of styrene, 2000, U.S. patent 6031143.

2

Performance of the steam dehydrogenation catalyst

Abstract

A commercial catalyst sample for the dehydrogenation of ethylbenzene to styrene in steam was used as the reference to verify the functionality of our catalyst testing setup and will be used as the basis for comparison with the new processes that are under investigation: dehydrogenation in CO_2 and oxidative dehydrogenation. With a total diluent:EB molar feed ratio of 20 (of which H_2O:EB is 10) a styrene selectivity of 98% with 50% EB conversion at 575 °C was measured. We believe that 96% selectivity at 60% EB conversion should be possible in a commercial plant that uses a total diluent:EB molar feed ratio of 7-12 (all H_2O). The new process should give at least 80% EB conversion at similar or higher ST selectivity (96%) in the commercial process. The BASF catalyst deactivates in the presence of CO_2 and is not selective in the oxidative dehydrogenation process conditions. Different types of catalysts have to be developed for these processes.

2.1 Steam dehydrogenation catalyst

In this research work the target was to develop a catalyst for a new oxidative dehydrogenation process that would be able to compete in performance with the conventional steam dehydrogenation process and catalyst system. For a good comparison it is necessary to have good data on the reference material, the potassium promoted iron oxide catalyst. At the same time it is also an essential part of the commissioning of our testing setup to evaluate if we are able to obtain good and reliable data that is in line with the available data on this process.

In the literature and patents, many recipes can be found to synthesize a potassium promoted iron oxide catalyst.[1-5] Usually the solid catalyst precursors plus promotors are well mixed together and calcined for several hours at temperatures between 900-950 °C. This results in an unsupported catalyst system with low specific surface area (2-5 m^2/g) containing mainly macro pores. Instead of trying to master this art ourselves, we chose to obtain a commercial catalyst sample.

The commercial steam dehydrogenation catalyst sample was obtained from BASF (type S6-38). It was supplied as extrudates, with 3 mm in diameter and 0.5-1 cm in length. For the catalyst testing, these particles were grinded and sieved to 212-425 μm size. Several experiments were done with this catalyst. First of all in steam, to have the reference for the functionality of the setup and of course a reference of its performance to compare to other catalysts and processes. Out of curiosity, this catalyst was also tested for dehydrogenation in CO_2 and for oxidative dehydrogenation. The results will be described and discussed in the following paragraphs.

2.2 Experimental

The ethylbenzene dehydrogenation catalyst S6-38 was obtained from the BASF. The catalyst was supplied as 3 mm extrudates. These were crushed and sieved. The sieve fraction of 212-425 μm was used for testing.

A quartz reactor tube of 4 mm inner diameter was loaded with 1.0 gram of catalyst. The catalyst bed height was 12 cm. The bed was held in position by quartz wool plugs. Above the catalyst bed there was 5 cm of SiC (250 μm) for reactant preheating and mixing. This reactor tube was loaded in the reactor furnace. Our reactor furnace consists of 6 heating zones. These were all set to the desired reaction temperature. The whole furnace has an isothermal zone of 20 cm, +/– 0.5 °C of the setpoint.

During reaction, liquid water (0.9 g/h = 18 Nml-vap/min) and liquid ethylbenzene (0.5 g/h = 1.8 Nml-vap/min) were fed to an evaporator at 150 °C. In the evaporator, water and ethylbenzene vapours were mixed with nitrogen gas (18 Nml/min). This re-

sulted in a H_2O:EB molar feed ratio of 10 and a total diluent:EB feed ratio of 20. The pressure at the end of the reactor was 1.3 bara. This was as low as practically possible.

An online GC system was used for products analysis. The GC has two channels. (1) TCD (columns: 0.3m Hayesep Q 80-100 mesh with back-flush, 25 m × 0.53 mm Porabond Q and 15 m × 0.53 mm molsieve 5A with bypass for CO_2 and H_2O, all in series) for permanent gas analysis (CO_2, H_2, N_2, O_2, CO). (2) FID (column: 30 m × 0.5 3mm, D_f = 3μm, RTX-1) for the hydrocarbons analysis (methane, ethane, ethene, benzene, toluene, ethylbenzene, styrene, heavy condensates). A sample was taken every 15 minutes to follow the catalyst performance over time on stream.

2.3 Dehydrogenation in steam

Several experimental runs were done for steam dehydrogenation. It was not successful directly, due to problems with the water evaporation, analysis, deactivated catalyst and having not enough catalyst. The goal was not to optimize the conditions of this system. We only wanted to obtain reasonable conversion levels and high selectivity to verify our setup and analysis and to get some experience with dehydrogenation reactions in general.

The BASF catalyst was tested at three different temperatures: 575 °C (0-20 h), 600 °C (20-30 h) and 625 °C (30-40 h). The results in time are shown in Figure 2.1. After a short induction period of 5 h the catalyst showed good stability and performance. At 575 °C, the EB conversion is 50% with a styrene selectivity of 98%. At 600 °C, the EB conversion increases to 69% with a styrene selectivity of 97%. At the highest tested temperature of 625 °C, the EB conversion reached 82% while the styrene selectivity slightly decreased to 95%. Under all conditions, toluene is the main byproduct, followed by benzene and methane. The coupled byproducts benzene/ethane (cracking) and toluene/methane (hydrocracking) are not detected in equimolar amounts. More hydrogen than styrene product is formed in the dehydrogenation reaction. The coke gasification by steam results in low amounts of carbon dioxide. Only at the highest temperature (625 °C), trace amounts of carbon monoxide could be detected as a second coke gasification product.

The TGA analysis in air of a spent BASF catalyst sample (Figure 2.2) first shows a small release of water and volatile hydrocarbons (100-200 °C). Between 200-400 °C the catalyst gains 1.2 wt%, possibly by the oxidation of Fe^{2+} to Fe^{3+}. Above 400 °C the sample loses 1.4 wt% of its mass, possibly due to the oxidation of coke on the catalyst. When the same analysis is done in helium instead of air, the peak between 200-400 °C disappears, but the peak above 400 °C remains and is also 1.4 wt%. With the high (bound) oxygen content of the catalyst it is possible that the lattice oxygen reacts with

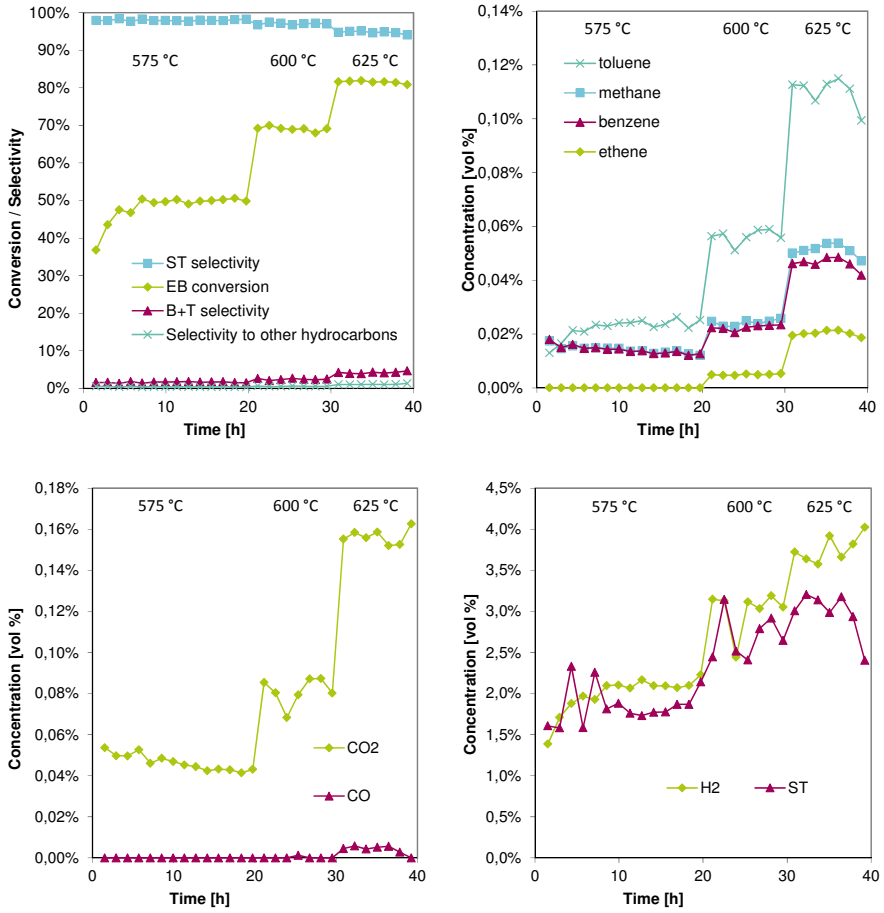

Figure 2.1: Results from the dehydrogenation experiment with the BASF catalyst with time on stream, showing EB conversion, ST selectivity, benzene + toluene selectivity and selectivity to other hydrocarbons (top left); concentrations of toluene, methane, benzene and ethene (top right); concentrations of CO and CO_2 (bottom left); concentrations of styrene and hydrogen (bottom right).

coke, removing oxygen and coke together from the catalyst.

As it was expected from the equilibrium of the endothermic dehydrogenation reaction, the conversion increases with higher temperatures. Equilibrium was not reached in the experiments. Cracking and hydrocracking rates increase with increasing temperature. Also the higher production of styrene yields more hydrogen in the product stream and this can also give higher hydrocracking rates. This results in lower selectivity to styrene at higher temperatures. The coke gasification function of the potassium promoted iron oxide catalyst works well. The catalyst displays stable performance in time. The coke gasification rates increase with higher temperatures. From the available data it is not clear if coke formation is also faster at higher temperatures. This could be true, then

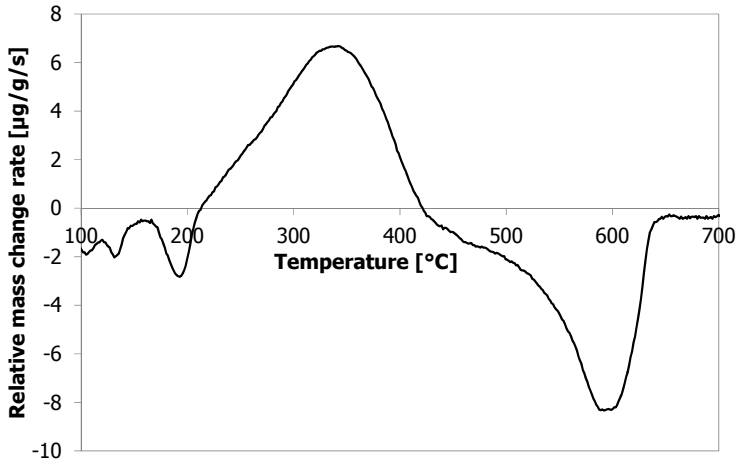

Figure 2.2: The mass change rate as a function of the oxidation temperature from thermo gravimetric analysis in air of a spent K-Fe catalyst sample at a ramp of 3 °C/min.

the CO_2 formation should be constant in time and also an increase in the surplus of H_2 is observed at higher temperatures. This H_2 surplus could be originating from coke formation and coke gasification with steam (Eqs. 2.1 and 2.2).

$$C_8H_{10} \rightarrow 8C + 5H_2 \qquad 2.1$$

$$C + 2H_2O \rightarrow CO_2 + 2H_2 \qquad 2.2$$

These results have quite some consequences for the new processes that we want to develop further. Because of the high total dilution (diluent:EB = 20 mol/mol) the conversion might be a little higher than in commercial plants that operate under vacuum and around a 7-12 molar diluent ratio due to a shift in the equilibrium. Equilibrium was not reached. The styrene selectivity could also be a little higher because of the high dilution, but most side-reactions are not thermodynamically equilibrium limited and therefore, the selectivity will be very close to that of a commercial plant. To our opinion, a single pass EB conversion of 60% at a ST selectivity of 96% could be achieved in a commercial unit for steam-aided dehydrogenation. In addition to this high selectivity, a large part of the by-products (benzene, toluene and hydrogen) still have a high value and can be sold for a by-product credit for the process, after a simple separation.

A competing technology will have to show a large improvement in the single pass EB conversion, for instance 80% or higher, while matching the same high ST selectivity of 96%. This will reduce the separation and recycle costs. If additionally the reactor temperature can be lowered and the use of H_2O as a diluent can be limited or avoided, even larger energy reductions can be realized. However, thinking about the alternatives, the by-product spectrum will shift a lot. By using CO_2 a lot of CO will be produced

instead of H_2 that can be converted into H_2 again, but this requires an additional water-gas-shift (WGS) unit. In the oxidative dehydrogenation process the main byproduct will become CO_2, that has no value at all, but the process becomes exothermal and possibly this can generate added value.

These results have also proven the functionality of our setup and analysis. The evaporation of ethylbenzene and water was very stable in time. The online GC analysis of the hydrocarbons and permanent gases works well, nearly all products are measured and the byproduct distributions match with the expectations.

Additionally, a couple of other materials were tested for their performance in the dehydrogenation with H_2O. These materials are used as catalyst diluent (SiC), catalyst (ZrO_2 and Al_2O_3), or support (Al_2O_3) in the other dehydrogenation reactions as well. An overview of these results is shown in Table 2.1.

Table 2.1: Results from the dehydrogenation experiments in H_2O at different temperatures.

Sample	Amount [g]	Temp. *TOS*	575 °C 0-20 h	600 °C 20-30 h	625 °C 30-40 h
KFe (BASF)	1.0	ST sel.[%]	98.1	97.2	95.0
		EB conv. [%]	49.9	69.1	81.6
γ-Al_2O_3	0.50	ST sel. [%]	48.3	49.5	56.9
		EB conv. [%]	1.0	2.1	5.2
ZrO_2	0.91	ST sel. [%]	78.3	76.1	75.4
		EB conv. [%]	1.2	4.0	13.1
SiC		ST sel. [%]	73.7	71.5	69.2
		EB conv. [%]	0.7	2.0	6.3

2.4 Dehydrogenation in H_2O and CO_2

Similar to the work of Hirano *et al.*[3], we wanted to observe the effect of CO_2 on the commercial steam dehydrogenation catalyst from BASF. This type of catalyst is claimed to be ineffective in the dehydrogenation with CO_2. The presence of CO_2 should poison this catalyst reversibly.

For this experiment, the reactor was loaded with 2.0 g of catalyst. The flow of EB was 1 g/h (3.5 Nml-vap/min), with a H_2O feed rate of 1.2 g/h (25 Nml-vap/min) and a N_2 flow of 25 Nml/min. This results in feed ratios of H_2O:EB = 7 and diluent:EB = 14. The reactor temperature was 580 °C. CO_2 was added after 35 h *TOS* in a CO_2:EB feed ratio of 1, at 50 h *TOS* this was increased to 5 and after 58 h *TOS* the CO_2 feed was closed.

The results of this experiment are shown in Figure 2.3. When CO_2 is added to the feed after 35 h *TOS*, the EB conversion plummets immediately from about 65% to barely 10%. Just after the CO_2 addition, the ST selectivity decreases only a little from 96%

to 94%, after which it increases with *TOS* up to 98%. The EB conversion also increases a little with the *TOS* from 8 to 10%. Adding more CO_2 does not change the catalyst performance. When CO_2 is removed from the feed, the catalyst system recovers, going back to a ST selectivity of about 96%. The EB conversion does not recover completely to about 65%, it increases to about 55%. Under the applied conditions, the BASF catalyst deactivates slowly with *TOS*. It loses about 5% EB conversion in 100 h *TOS* (not shown). Selectivity to ST remains stable at 96%.

Clearly, the presence of CO_2 deactivates the catalyst. In the presence of such large amounts of CO_2 (tiny amounts of CO_2 are present due to the coke gasification) the potassium in the catalyst forms stable carbonates and the active phase of the catalyst ($KFeO_2$) cannot be formed anymore. Surprisingly, the selectivity does not change much and even increases a little with *TOS*. Upon removal of CO_2 from the feed, the reversible nature of its poisoning effect becomes visible. The carbonates slowly dissociate and the active phase is slowly restored, although its activity was lower. Another effect that might explain the deactivation and recovery is the fast formation of coke and its slow removal by coke gasification (potassium catalysed) when CO_2 is removed from the feed.

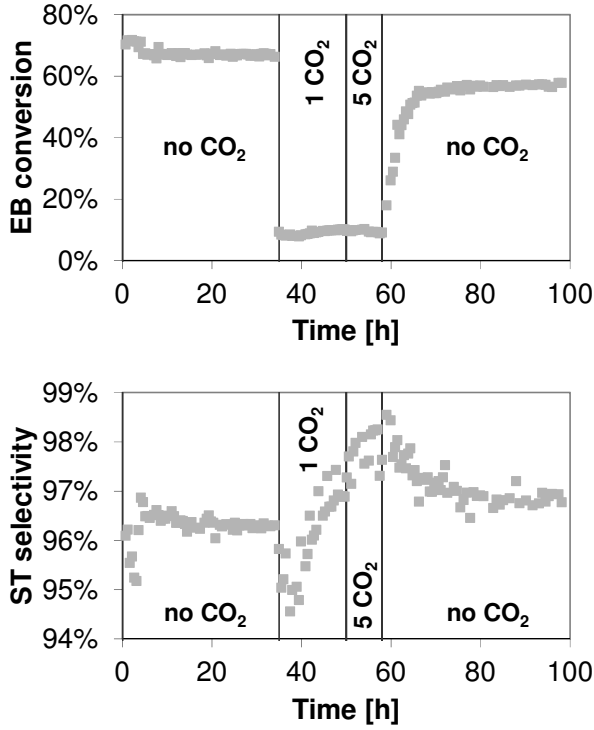

Figure 2.3: EB conversion and ST selectivity in time over the BASF catalyst in H_2O and with CO_2 co-feeding. The molar CO_2:EB feed ratio is indicated.

In this single example the deactivation was not completely reversible, contrary to the results presented by Hirano *et al.*[3] This can have several reasons, as this test was done under different conditions, with a different catalyst and the longer exposure to CO_2.

2.5 Oxidative dehydrogenation

To complete the circle of the three dehydrogenation reactions that are of interest, the BASF catalyst was also tested for its activity in the oxidative dehydrogenation reaction, according to the testing protocol that is described in Chapter 8. The result is shown in Figure 2.4. The BASF catalyst proves to be an excellent oxidation catalyst, with some of the highest selectivities to CO_X of 50-70% and a selectivity to ST of only 20-50%. The EB conversion is low, 12%, decreasing to 5% at lower temperatures. Selectivity to benzene and toluene is low, about 1%. The O_2 conversion was 100%. The BASF catalyst is a poor selective oxidative dehydrogenation catalyst, but it was designed for steam-aided dehydrogenation.

2.6 Conclusions

Our own tests with a commercial steam dehydrogenation catalyst from BASF nicely outline the challenge that lies ahead. The highest measured styrene selectivity was

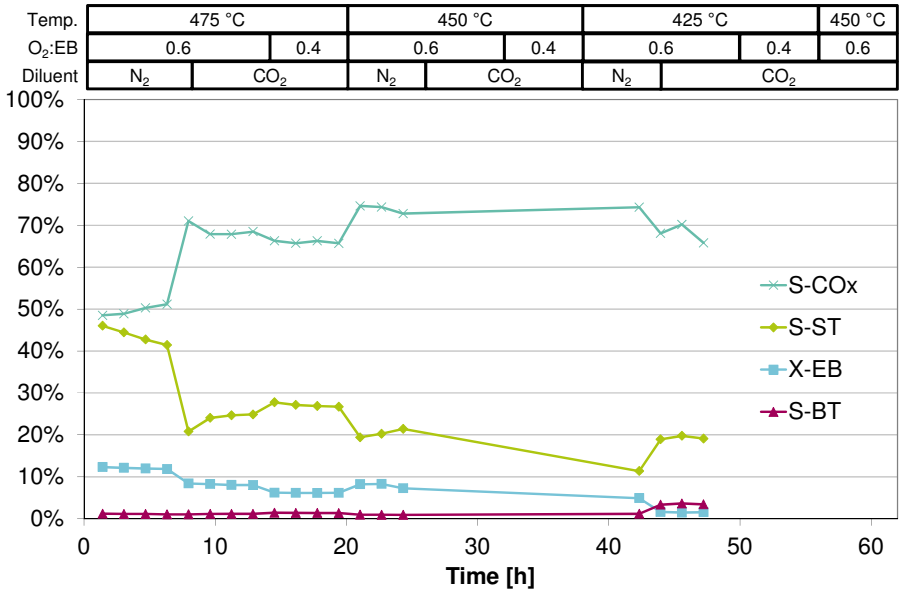

Figure 2.4: Testing results of the BASF catalyst in oxidative dehydrogenation.

98% at an EB conversion of 50% and at a temperature of 575 °C. The new process should achieve at least 96% selectivity at 80% conversion per single pass to be competitive. The current catalyst is useless in the presence of CO_2 or in oxidative dehydrogenation. Our catalyst testing setup proved to deliver very nice results that give confidence in the results that are presented in the following chapters.

References

[1] E.H. Lee, Cat. Rev. - Sci. Eng. 8 (1973) 285-305.
[2] M. Muhler, J. Schutze, M. Wesemann, T. Rayment, A. Dent, R. Schlögl, G. Ertl, J. Catal. 126 (1990) 339-360.
[3] T. Hirano, Appl. Catal. 26 (1986) 65-79.
[4] G.H. Riesser, Dehydrogenation Catalyst, 1979, U.S. patent 4144197.
[5] M. Baier, O. Hofstadt, W.J. Pöpel, H. Petersen, Catalyst for dehydrogenating ethyl benzene to produce styrene, 2003, U.S. patent 6551958 B1.

3

Catalysed ethylbenzene dehydrogenation in CO_2 and N_2 - Carbon deposits as the active phase

Abstract

Bare alumina support transforms into an active catalyst for the dehydrogenation of ethylbenzene to styrene in CO_2 or N_2. During the first 15 h time on stream in CO_2, or the first 10 h time on stream in N_2, the alumina shows an increase in ethylbenzene conversion and styrene selectivity from 15% to 60% and from 60% to 92%, respectively, under industrially relevant conditions of 600 °C and 10 vol% ethylbenzene. Thereafter, the system slowly deactivates, but remains highly selective. TGA analysis shows an increase in coke content. The specific surface area and pore volume show a decrease with time on stream. TEM-imaging reveals that the spent catalyst surface is completely covered by several layers of coke. These results combined suggest that the carbon deposits on the alumina are responsible for the increase in activity and selectivity and also are the cause of deactivation once a monolayer of carbon is deposited on the support surface. Similar trends are observed for zirconia support. Supported vanadium and chromium oxides on alumina all give similar results, but after a faster activity development. Also for these supported catalysts and even carbon samples, deposited coke is the active and selective phase.

This chapter has been published:
C. Nederlof, F. Kapteijn, M. Makkee, Appl. Catal. A: Gen. 417-418 (2011) 163-173

3.1 Introduction

Styrene monomer is one of the largest bulk monomers at this moment and will probably be in this position for a long time to come. In industry it is mainly produced by steam-aided dehydrogenation of ethylbenzene over a promoted potassium-iron catalyst. This process suffers from high energy requirements and low perpass conversions due to its endothermic nature and equilibrium limitations. A large part of the energy is lost in the steam condensation, which cannot be recovered due to practical reasons.[1, 2]

To overcome these issues, oxidative dehydrogenation with pure oxygen has been explored. This solves the issues related to the endothermic nature of dehydrogenation and its equilibrium limitations, but brings its own issues. It has a poor selectivity due to secondary oxidation, safety issues like risk of explosion and may lead to hot-spots in the catalyst bed due to the highly exothermic nature of this type of reaction. Due to these issues and the higher operating costs oxidative dehydrogenation has not been commercialised yet.[2]

CO_2 has been investigated as an alternative oxidant for this process. The use of CO_2 is safer than using oxygen and at the used temperatures CO_2 is considered to be a mild oxidant that relaxes the equilibrium limitations of the current steam-aided dehydrogenation process. Also the energy losses due to steam condensation can be circumvented, making the overall process energy saving.[3-7]

The CO_2 oxidative dehydrogenation (ODH) process is, however, still equilibrium limited.[4] The equilibrium conversion at 600 °C and 1:10 ratio of EB:CO_2 is 91%, compared to 76% for the steam-aided dehydrogenation process under the same conditions. The CO_2 oxidative dehydrogenation reaction 3.3 is a result of a two-step mechanism consisting of direct dehydrogenation 3.1 followed by the reverse water-gas-shift (RWGS) 3.2 that removes the hydrogen.[4, 8]

$$C_8H_{10} \rightleftarrows C_8H_8 + H_2 \qquad 3.1$$

$$CO_2 + H_2 \rightleftarrows CO + H_2O \qquad 3.2$$

$$C_8H_{10} + CO_2 \rightleftarrows C_8H_8 + CO + H_2O \qquad 3.3$$

A lot of research effort has already been put into the development of a CO_2 ODH process for styrene production. Many catalysts have been tested, using many types of supports and quite active and selective catalysts have been claimed.[4-7, 9-35] An often used catalyst support is alumina.[6, 7, 12-17] The overview in Table 3.1 shows some examples of alumina supported catalysts with chromium or vanadium. Most of the recent publications on alumina supported catalysts reported that the alumina support itself had a poor

Table 3.1: Overview of performance and conditions of supported Al_2O_3 catalysts with chromium or vanadium.

Source	[mmol/g] catalyst	*X* [%]	*S* [%]	*T* [°C]	*CO_2:EB*	*Wt* [g]	*WHSV* [g/g/h]
Fedorov, 1976 [7]	0.65 Cr	24	79	550	1	10	0.65
Ye, 2004 [13]	2.6 Cr	76.9	98.6	550	19	0.10	0.42
Sakurai, 2000 [5]	1 V	59	84.9	550	50	0.10	1.5
Vislovski, 2002 [12]	2.2 V	74.8	94.5	595	1	1.0	1.0
Sun, 2004 [14]	0.57 V	45.5	97.8	550	11	0.20	2.16
Chen, 2006 [16]	1.5 V	67.4	96	550	20	0.30	0.58

Table 3.2: Overview of reported Al_2O_3 data.[6, 7, 11, 16]

Source	*X* [%]	*S* [%]	*T* [°C]	*CO_2:EB*	*Wt* [g]	*WHSV* [h^{-1}]
Fedorov, 1976 [7]	1	100	550	1	10	0.65
Sato, 1988 [6]	58	72	610	3.4	2	1.72
Mimura, 2000 [11]	7^a / 11^b	80^a / 87^b	550	11	1.4	2.26
Chen, 2006 [16]	5	88	550	20	0.3	0.58

X = conversion; *S* = selectivity; *T* = reaction temperature; EB = ethylbenzene; *Wt* = catalyst weight; *WHSV* = [(g EB)/(g cat)/h]; [a]0.42 h reaction time; [b]6 h reaction time;

activity. Additional metal oxides were required to make a good catalyst. Only Sato *et al.* found alumina and sodium on alumina to be active under slightly different conditions, but with a low selectivity. An overview of reported alumina performances and applied conditions is presented in Table 3.2.

Generally, the CO_2 oxidative dehydrogenation is believed to proceed through a redox type mechanism over a transition metal oxide.[4, 5, 8-35] Sato *et al.*[6] attributed the activity of alumina to the combined action of acid and basic sites on the surface of the alumina. Ethylbenzene preferably adsorbs on the acidic sites and carbon dioxide on the basic sites. The dehydrogenation could then proceed *via* acidic protolysis, or directly by the reaction with carbon dioxide. The activity of the alumina was improved by adding alkaline metals, increasing also the conversion of hydrogen with CO_2 *via* the RWGS reaction.

The major issue with CO_2 ODH is the deactivation of the catalysts due to excessive coking.[36] Vislovskiy *et al.*[12] compared conversion data from 1 h and 4 h time on stream at 595 °C, where up to 46% of activity was lost. Chen *et al.*[16] compared conversion data at 1 h and 20 h operation at 550 °C, where up to 21% of the activity was lost. In all cases a large amount of coke is found on the spent catalysts, the cause of this deactivation. In the steam-aided process one of the functions of steam is to counteract this reversible deactivation by coke gasification 3.4. A similar role is envisaged for CO_2 through a reverse Boudouard reaction 3.5, but this has not been proven successful yet.

$$C + H_2O \rightarrow CO + H_2 \qquad 3.4$$

$$C + CO_2 \rightarrow 2CO \qquad 3.5$$

In this paper we demonstrate the transformation of gamma-alumina and zirconia into a very active and selective CO_2 ODH catalyst by deposition of coke under reaction conditions. The activity and selectivity are attributed to this coke.

3.2 Experimental

3.2.1 Catalyst preparation

The γ-Al_2O_3 (Engelhard Al-3972 P, 222 m^2/g, 0.53 ml/g), ZrO_2 (AlfaAesar 043815, 104 m^2/g, 0.38 ml/g), activated coal (Norit RB-II, 691 m^2/g, 1.06 ml/g), carbon nanotubes (Hyperion Catalysis CS-02C-063-XD, 425 m^2/g, 1.02 ml/g) and SiC (120 μm) samples were crushed if needed and sieved, the fraction between 40 and 90 μm was used for the dehydrogenation experiments without any further pre-treatment.

Six supported catalysts were made by co-impregnation using the incipient wetness method, using the same γ-Al_2O_3 support as above. Three had vanadium oxide as the main component (1 mmol/g loading), promoted by potassium oxide (0.5 mmol/g loading) or magnesium oxide (0.5 mmol/g loading). These will be denoted by V, KV and MgV. The other three were a similar series of chromium oxide, denoted by Cr, KCr and MgCr. The support was dried at 120 °C before impregnation. The required amounts of $Cr(NO_3)_3{\cdot}9H_2O$, $Mg(NO_3)_2{\cdot}6H_2O$, KNO_3 or NH_4VO_3 + $2C_2H_2O_4{\cdot}2H_2O$ were dissolved in demineralised water, after which the gamma-alumina support was impregnated with the solution. The wetted support was shaken until a homogeneous colour was obtained visually. The wetted support was then dried at 120 °C in air for four hours, followed by calcination in air at 600 °C for four hours in a static air calcination oven.

Additional experiments with CO_2 and N_2 were performed with another γ-Al_2O_3 sample (Ketjen CK300-000-1.5E, 270 m^2/g, 0.65 ml/g). These extrudates were crushed and sieved, the fraction between 212 and 425 μm was used for the dehydrogenation experiments without any further pre-treatment.

3.2.2 Catalyst testing

The dehydrogenation experiments were carried out in a quartz fixed bed reactor with inner diameter of 8 mm. The reaction temperature was 600 °C and the pressure at the reactor outlet was atmospheric. In a typical experiment 400 mg of catalyst was used. On top of the catalyst bed was a 1cm layer of SiC to preheat the feed. The catalyst bed and SiC were fixed in the quartz tube by quartz wool plugs. Carbon dioxide was fed through a mass-flow controller set at 15 ml (NTP)/min (20 °C, 1 atm). Ethylbenzene (EB) was fed to the reactor by passing the gas feed over an ethylbenzene saturator vessel at a temperature of 85 °C. This resulted in feed mixture of ethylbenzene and CO_2

with a molar ratio of 1:10, as confirmed by gas chromatography (GC). The ethylbenzene weight hourly space velocity (*WHSV*) was 1 g/g/h (wt EB/wt cat). The total *GHSV* was 1500 l/l/h (vol. gas/vol. cat/h). These conditions are representative for industrial operation. Before starting the experiment the reactor would be heated up with 10 °C/min and allowed to stabilize at reaction temperature for half an hour under CO_2 atmosphere. The experiment was started by feeding ethylbenzene to the reactor.

For the comparative experiments with CO_2 and N_2, a parallel flow reactor setup was used with quartz fixed bed reactors with inner diameter of 4 mm. In a typical experiment 1000 mg of catalyst was used. Carbon dioxide and ethylbenzene flow were adjusted accordingly (36 ml CO_2 (NTP)/min and 1.00 g EB/h) to reach the same ethylbenzene weight hourly space velocity (*WHSV*) of 1 g/g/h (wt EB/wt cat). Other reaction conditions and the reactor loading procedure were the same.

The concentrations in the reactor effluent were measured online by a two channel gas chromatograph with a TCD (columns: 0.3 m Hayesep Q 80-100 mesh with backflush option, 25 m × 0.53 mm Porabond Q and 15 m × 0.53 mm molsieve 5A with bypass option for CO_2 and H_2O, all in series) for permanent gas analysis (CO_2, H_2, N_2, O_2, CO) and a FID (column: 30m × 0.53 mm, D_f = 3μ, RTX-1) for the hydrocarbons analysis (methane, ethane, ethene, benzene, toluene, ethylbenzene, styrene and tars). A sample was analysed every 15 minutes in order to follow the catalyst performance over time. A constant flow of nitrogen was used as internal standard. Conversions and selectivities are based on moles of ethylbenzene and calculated according to Eqs. (6) and (7). Conversion of CO_2 was calculated according to Eq. 3.8. The overall carbon balance is >99%, only carbon that was deposited on the catalyst as coke is lacking from the carbon balance by GC.

$$EB\ conversion = \frac{ethylbenzene_{in} - ethylbenzene_{out}}{ethylbenzene_{in}} \qquad 3.6$$

$$ST\ selectivity = \frac{styrene_{out}}{ethylbenzene_{in} - ethylbenzene_{out}} \qquad 3.7$$

$$CO_2\ conversion = \frac{CO_{2,in} - CO_{2,out}}{CO_{2,in}} \qquad 3.8$$

3.2.3 Catalyst characterization

After an experiment, a sample of the catalyst was analysed to determine the amount of coke by a TGA (MettlerToledo TGA/SDTA851[e], 20 mg sample of spent catalyst, 100 ml/min air, 50 ml/min He flow) using a ramp of 3 °C/min from RT to 723 °C. Surface area, pore volume and pore size distribution were determined of both fresh and spent catalyst samples by N_2 adsorption at -196 °C (BET-method, Quantachrome Autosorb 6B). The samples were pre-treated in nitrogen at 250 °C. In Raman spectroscopy, the fresh and spent catalyst samples were analysed without any pre-treatment. Spectra were recorded using a Renishaw Raman Imaging Microscope, system 2000, using a green 514 nm laser of 20 mW. A Leica DMLM optical microscope with a 50× objective lens was used to determine the analysed part of the sample. The Ramascope was calibrated using a silicon wafer. The power output of the laser was set at 20% to avoid influencing the sample.

Transmission electron microscopy (TEM) was performed using a FEI Tecnai TF20 electron microscope with a field-emission gun as the source of electrons operated at 200 kV. Samples were mounted on Quantifoil® carbon polymer supported on a copper grid by placing a few droplets of a suspension of ground sample in ethanol on the grid, followed by drying at ambient conditions.

3.3 Results

3.3.1 Catalyst performance

All alumina supported catalysts (V, KV, MgV and Cr, KCr, MgCr) showed a very similar performance. The ethylbenzene conversion, styrene selectivity and CO_2 conversion in the CO_2 ODH of ethylbenzene to styrene over these six catalysts is shown in Fig. 3.1. Under the applied conditions the ethylbenzene conversion starts between 92-85% but decreases to 53-56% in 20 h. Selectivity starts below 80% and increases to a steady value of 92% for all catalysts after about 10 h. Similar to the ethylbenzene conversion, the CO_2 conversion (Fig. 3.1-C) starts high at 10-19% and is reduced to 2-5% in 20 h. The increase in styrene selectivity is due to a decrease of cracking products (benzene, toluene) and a decrease of the surplus hydrogen and CO. The surplus of hydrogen and CO is the amount of these products that is above the expected amount based on the

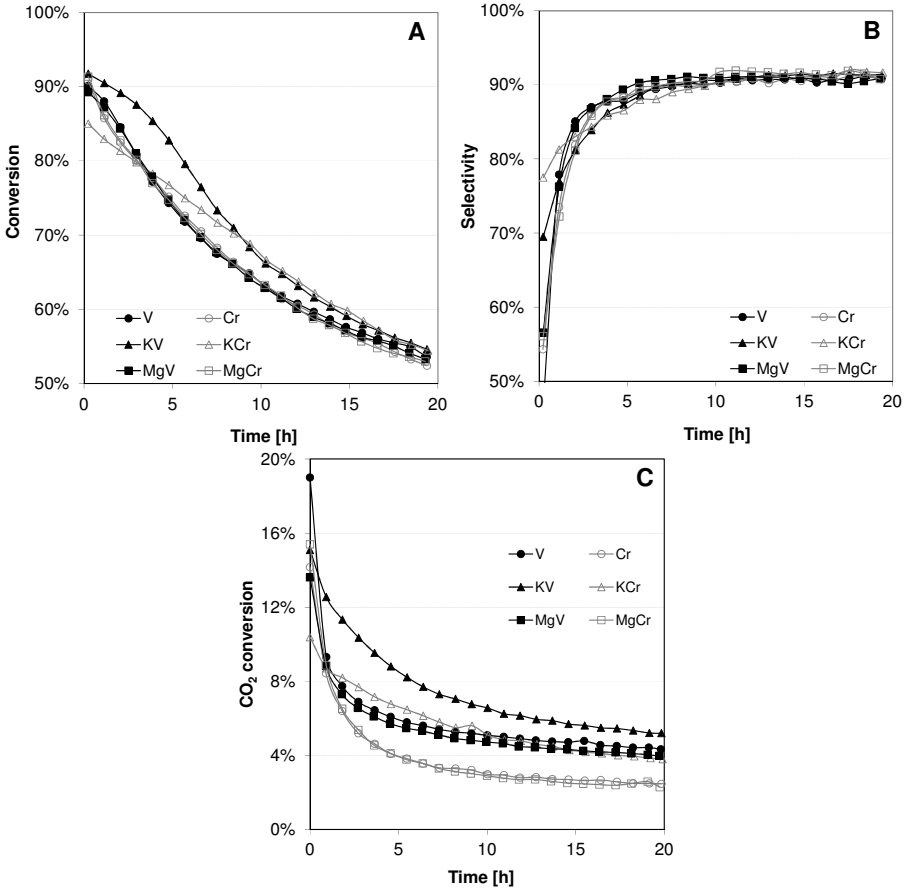

Fig. 3.1: Ethylbenzene conversion (A), styrene selectivity (B) and CO_2 conversion (C) as a function of time on stream with CO_2 as diluent for six Al_2O_3 supported catalysts: V (●), KV (▲), MgV (■), Cr (○), KCr (△), MgCr (□).

dehydrogenation coupled with the RWGS reaction. Differences between the catalysts are small and disappear with time on stream. The initial differences in ethylbenzene conversion are related to the CO_2 conversion. The potassium promoted vanadium catalyst (KV) has the highest initial conversion of ethylbenzene and CO_2.

Five other bare samples were tested under CO_2 oxidative dehydrogenation conditions: γ-alumina (Al_2O_3), high surface area zirconia (ZrO_2), activated carbon (AC), carbon nanotubes (CNT) and the silicon carbide (SiC) that was used as diluent material. The conversion and selectivity data for these samples are presented in Fig. 3.2 for 20 h time on stream. The SiC diluent material showed a constant 3% conversion and 60-70% selectivity during the 20 h time on stream. Therefore, silicon carbide is considered to be inert in this reaction. The alumina sample started at 20% conversion and 70% selectivity, but both increased steadily over time. After 10 h on stream the conversion and selectivity increase levelled off, the conversion stabilised around 60% with a selectivity of

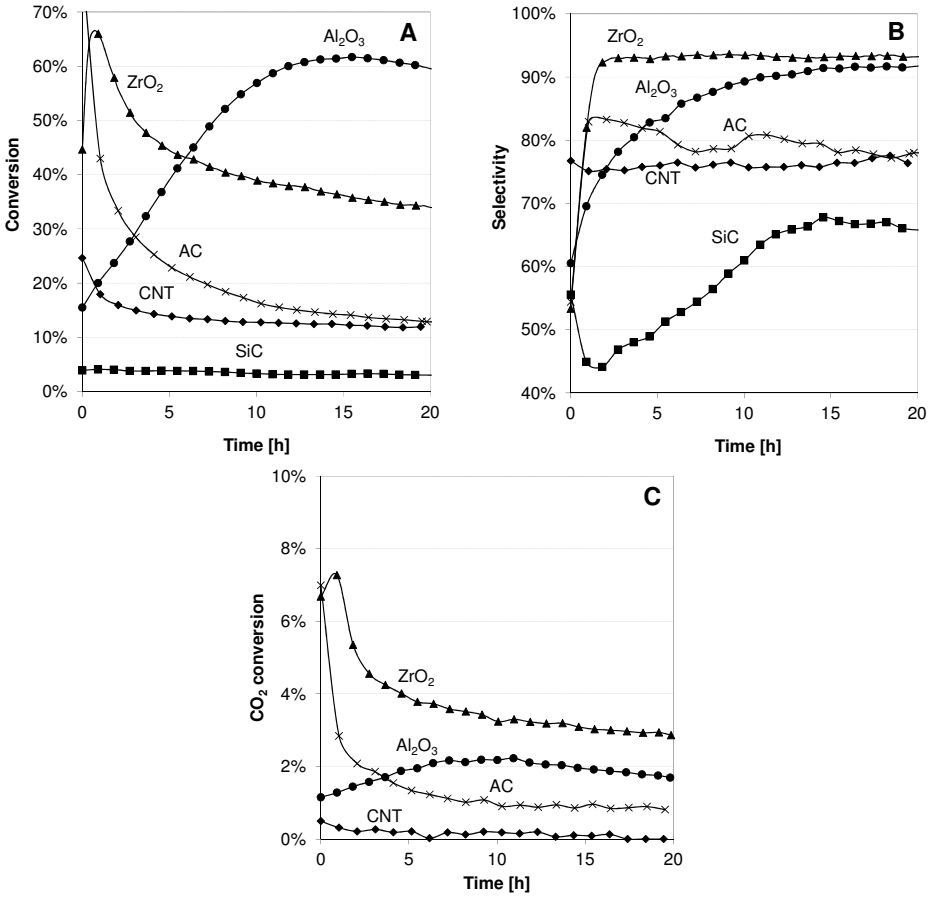

Fig. 3.2: Ethylbenzene conversion (A), styrene selectivity (B) and CO_2 conversion (C) as a function of time on stream with CO_2 as diluent for five bare samples: ZrO_2 (▲), Al_2O_3 (●), activated carbon (✕), carbon nanotubes (◆), SiC (■).

92%. Zirconia was initially more active than alumina. ZrO_2 shows an optimum after two hours and then deactivates. The selectivity to styrene over zirconia increased initially, until reaching a stationary value of 92%. The selectivity plateau was reached at the same time as the maximum conversion was reached. The CNT sample behaved differently from alumina and zirconia. It deactivated at first, after which the conversion stabilised around 13%. Its selectivity was constant during 20 h of reaction at 76%. The activated carbon material was initially very active, but it also deactivated very fast to end up at a conversion of 13% after 20 h. The initial selectivity of activated carbon was poor, but very quickly increased to its highest value of 83% after 2 h. After this optimum the styrene selectivity slowly decreased to 78% after 20 h on stream at 13% conversion. The conversion of CO_2 is much lower for the bare samples than for the alumina supported samples. Over alumina just 2% is reached, over the AC sample it stabilizes around 1%, whilst the CNT sample displays almost no CO_2 conversion. Only ZrO_2 exhibits somewhat higher CO_2 conversions, decreasing from 7% to 3% in 20 h.

In order to see if alumina reached an optimum in performance or a stable performance after 20 h, a longer time on stream was evaluated. The results are shown in Fig. 3.3 (*left*), together with data on coke loadings. An optimum in activity was obtained after 15 h, with a conversion of 62% and with 92% selectivity, after which the catalyst started deactivating. The deactivation progressed at an almost constant rate until around 80 h. After this time the catalyst seemed to deactivate at a slower rate. The selectivity to styrene increased in the first 15 h, after which it reached a stationary level of 92%. This experiment with alumina shows large similarity with zirconia (Fig. 3.3, *right*). For both samples a selectivity plateau was reached at the same time as the maximum conversion was reached and for both supports these levels were nearly identical. However, the ZrO_2

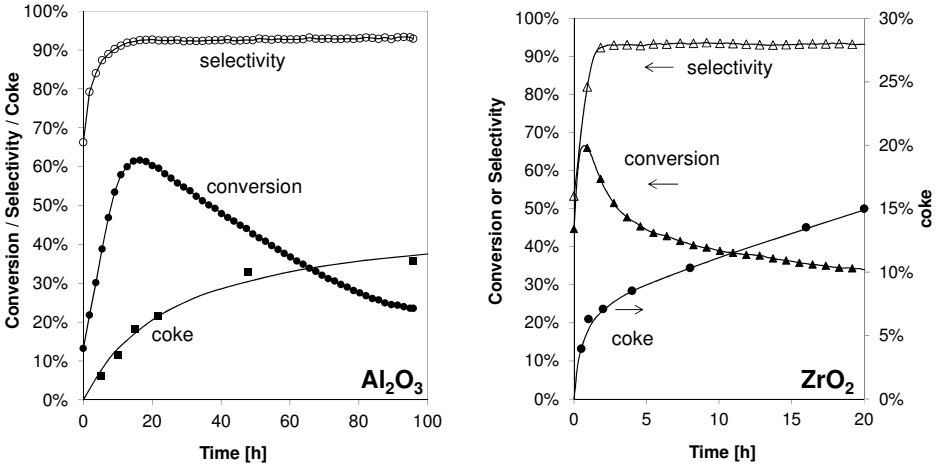

Fig. 3.3: Styrene selectivity, ethylbenzene conversion and coke deposited as a function of time with CO_2 as diluent using Al_2O_3 (*left*) or ZrO_2 (*right*).

sample is activated and deactivated about ten times faster than the Al_2O_3 sample.

Comparative experiments with alumina and CO_2 or N_2 were done to observe if carbon dioxide could have an effect on the formation of coke and the rate thereof, or on the activity of the deposited coke. The comparative performance data in Fig. 3.4 shows that the alumina in N_2 becomes active faster and selective faster than in CO_2. In N_2 the optimal performance is reached after 10 h, where 15 h are required in CO_2. Also the coke build-up under nitrogen atmosphere is faster than in CO_2. When comparing the data for N_2 after 10 h and for CO_2 after 15 h, the ethylbenzene conversion, styrene selectivity and coke build-up are identical. The distribution of by-products during these experiments is shown in Fig. 3.5. The main byproducts are benzene and toluene, followed by the surplus of CO + H_2. Tars are produced the least. The toluene formation follows the same trend as the EB conversion, whilst benzene is formed in an earlier stage of time on stream, indicating a decreasing cracking severity with increasing coke deposition.

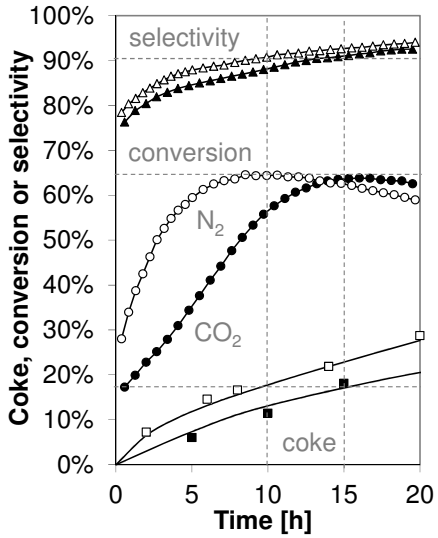

Fig. 3.4: ST selectivity (▲△), EB conversion (●○) and coke build-up (■□) as a function of time on stream for Al_2O_3 under CO_2 (▲●■) or N_2 (△○□) atmosphere.

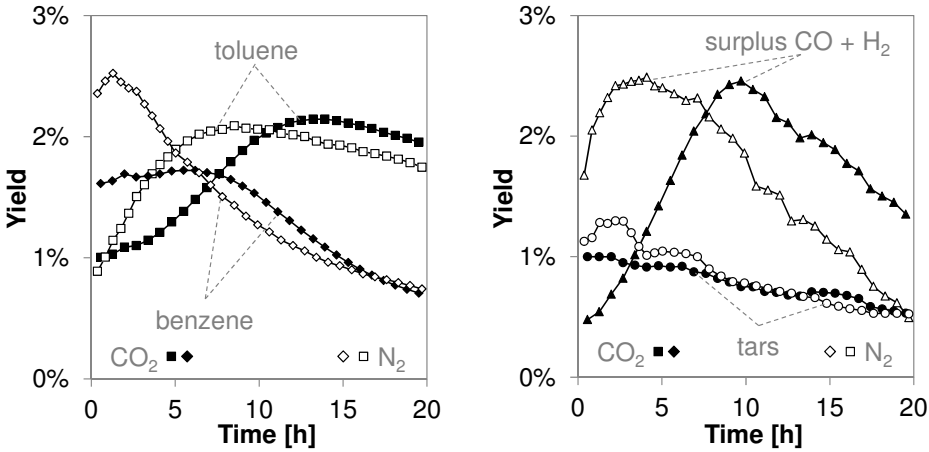

Fig. 3.5: Selectivities of benzene (◆◇), toluene (■□), surplus CO + H_2 (▲△) and tars (●○) as a function of time on stream for Al_2O_3 under CO_2 (▲●■◆) or N_2 (△○□◇) atmosphere.

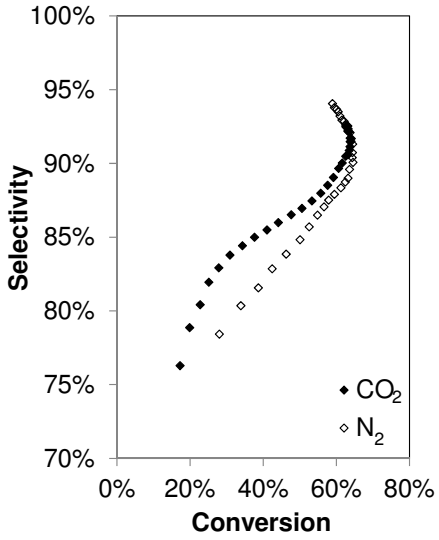

Fig. 3.6: Styrene selectivity at different ethylbenzene conversions over bare Al_2O_3 in CO_2 or N_2 as diluent.

The styrene selectivity increases with ethylbenzene conversion in these experiments (Fig. 3.6, using the same data as Fig. 3.4) indicating that an improved selectivity is not due to a decreasing activity, as would be the case for consecutive reactions, but should be attributed to the development of a more selective system. The performance for both cases is identical for styrene selectivities above 90%.

To check if the selected diluent really did not have any effect on the performance of the alumina samples, the other diluent was fed over the reactor, a few hours after their optimal performance in either CO_2 or N_2 flow. The results are presented in Fig. 3.7. Switching from CO_2 to N_2 diluent after 20 h gives almost an almost identical performance with the CO_2 experiment. Similarly, switching from N_2 to CO_2 diluent after 15 h gives an almost identical performance with the N_2 experiment. The minor differences can be attributed to the dilution ratio that was measured to be a little higher for N_2 than for CO_2 (10.3 and 9.9), having a small effect on the conversion.

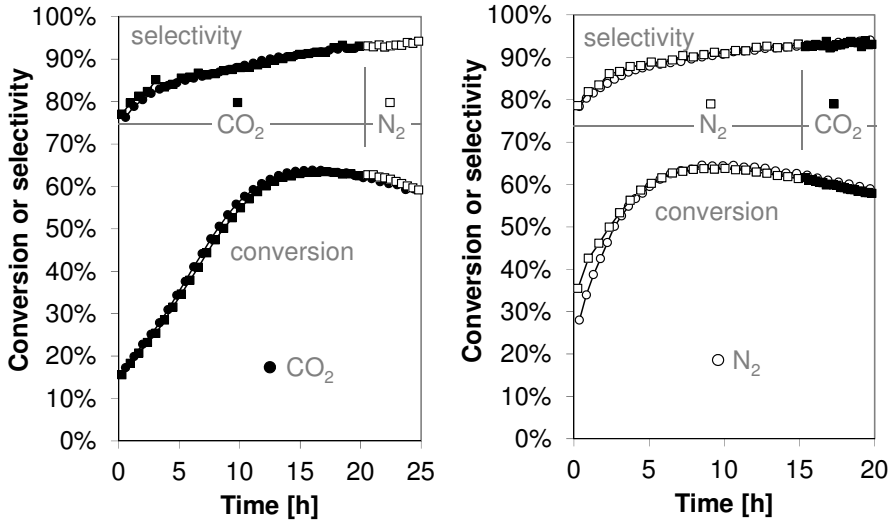

Fig. 3.7: Performance of the Al_2O_3 sample, switching from CO_2 to N_2 (left) and from N_2 to CO_2 (right), compared with the performance in CO_2 (left) or N_2 diluent (right).

3.3.2 Catalyst characterization

In replicated experiments with alumina and zirconia, catalyst samples were produced after different hours on stream for further characterization. All these experiments showed the same characteristic changes in selectivity and conversion as the experiments shown in Fig. 3.3 (*left*) and Fig. 3.4 for alumina and in Fig. 3.3 (*right*) for zirconia. Thermo gravimetric analysis (TGA) of the samples in air showed an increase in the amount of coke on the catalyst with time, reaching 36 wt% of coke after 96 h with alumina and 13.5 wt% coke after 16 h with zirconia. The TGA profiles of CNT, AC, Al_2O_3 and zirconia samples are presented in Fig. 3.8.

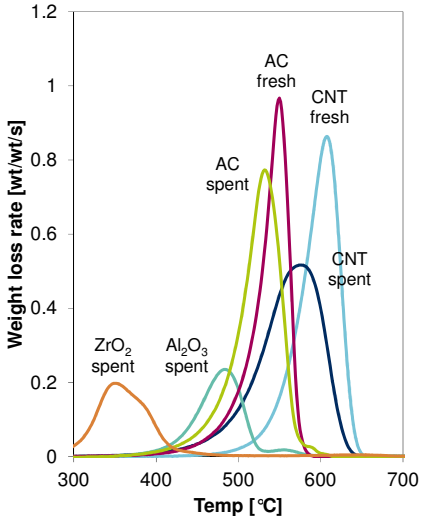

Fig. 3.8: Weight loss rate for the oxidation in air of the fresh and spent CNT and AC samples compared with spent Al_2O_3 and ZrO_2 samples as a function of temperature.

The oxidation profiles of spent CNT and AC samples are shifted to lower temperatures than those of the pristine carbon material. Coke oxidised the easiest on zirconia, followed by alumina, AC and CNT, in that order.

An overview of the characterisation data is given in Table 3.3. The six supported vanadia and chromia catalysts all showed high loadings of coke in TG analysis. The promoted samples had slightly reduced coke loadings. The KV sample had the highest CO_2 conversion and RWGS activity. From the other samples, only ZrO_2 showed some RWGS activity. All samples exhibited a large drop in surface area and pore volume due to the coke build-up. The coke loading on alumina used in nitrogen is higher than the coke loading on alumina used in carbon dioxide. The characterisation data for the duplicated experiments are given in Table 3.4-3.6 for alumina in CO_2, alumina in N_2 and zirconia, respectively. These analyses show that initially there is a fast drop in surface area and pore volume, for longer times the changes are smaller. Coke build-up is also

Table 3.3: Characterisation data the catalyst samples (after 20 h time on stream).

Sample		V	KV	MgV	Cr	KCr	MgCr	Al_2O_3	ZrO_2	AC	CNT	Al_2O_3-N_2
Coke [wt%]		28.5	25.7	25.5	26.3	22.2	25.0	20.8	13.5	93.4	96.7	24.6
S_A [m^2/g]	F	202	201	193	205	199	202	222	104	691	425*	n.d.
	S	96	95	89	98	110	94	142	68	n.d.	317	n.d.
V_p [ml/g]	F	0.47	0.46	0.46	0.47	0.45	0.46	0.53	0.31	0.52	1.02*	n.d.
	S	0.15	0.15	0.14	0.15	0.18	0.15	0.25	0.18	n.d.	1.06	n.d.

F = fresh samples; S = spent sample; A_S = specific surface area from BET analysis; V_p = pore volume from BET analysis. *Data from the manufacturer.

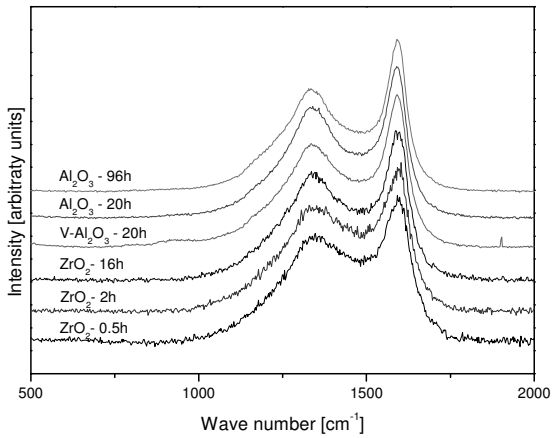

Fig. 3.9: Raman spectra of several spent samples obtained after different times on stream.

fast initially and slows down at longer times on stream.

Raman spectra from several of the spent catalysts (Fig. 3.9) showed the same peaks with the same intensity ratio between 1330 cm^{-1} (amorphous carbon[37]) and 1590 cm^{-1} (graphitic carbon[37]). These normalised spectra show no qualitative differences between the different catalysts, including the supported catalysts, or the different times on stream.

HR-TEM micrographs in Fig. 3.10 and Fig. 3.11 show both fresh and spent cata-

Table 3.4: Characterisation data of the duplicated Al_2O_3 experiments in CO_2 after different times on stream (*TOS*).

TOS [h]	0	5	10	15	22	48	96
S_A [m^2/g]	222	178	174	155	142	80	41
V_p [ml/g]	0.53	0.42	0.37	0.30	0.25	0.12	0.07
Coke [wt%]	-	6.0	11.4	18.1	21.6	32.8	35.7

Table 3.5: Characterisation data of the duplicated Al_2O_3 experiments in N_2 after different times on stream (*TOS*).

TOS [h]	0	2	6	8	14	20
S_A [m^2/g]	270	237	223	209	178	152
V_p [ml/g]	0.65	0.58	0.47	0.43	0.34	0.27
Coke [wt%]	-	6.2	13.6	15.8	21.0	28.0

Table 3.6: Characterisation data of the duplicated ZrO_2 experiments in CO_2 after different times on stream (*TOS*).

TOS [h]	0	0.5	1	2	4	8	16
S_A [m^2/g]	101	70	72	70	71	71	72
V_p [ml/g]	0.29	0.24	0.23	0.23	0.21	0.21	0.18
Coke [wt%]	-	4.0	6.3	7.1	8.5	10.3	13.5

lysts. The pristine ZrO_2 support samples have a clear structure of crystalline spheres (Fig. 3.10) whilst crystalline plates are visible for Al_2O_3 (Fig. 3.11). The spent samples in Fig. 3.10-B and Fig. 3.11-B show the presence of irregular, layered structures of coke that are deposited on the external surface of the particles. At least three layers of carbon are present after 20 h on stream on both supports. In the highly deactivated and coked Al_2O_3 sample in Fig. 3.11-C, all voids between the crystalline structures are completely filled with coke. Eight and even more layers of carbon can be counted. The structure of the parent material remains unchanged in the spent catalyst samples.

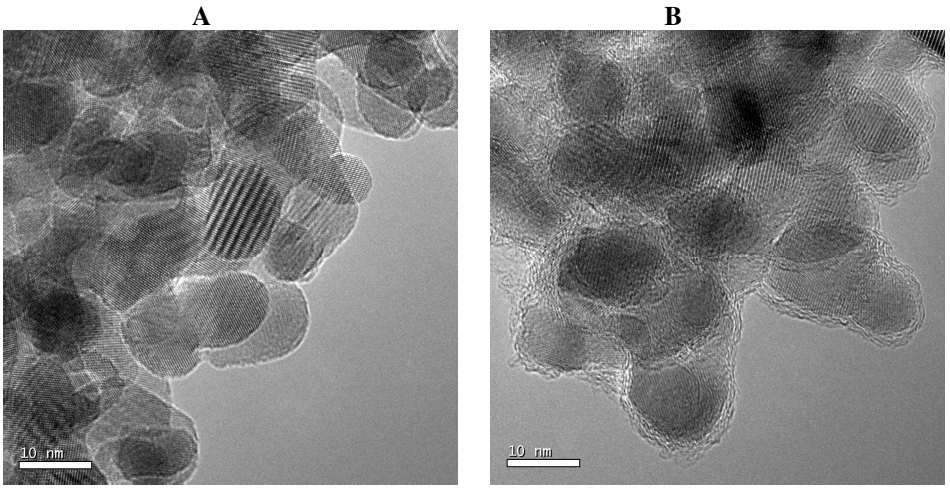

Fig. 3.10: HR-TEM micrographs of ZrO_2: A – fresh, B – spent 20 h.

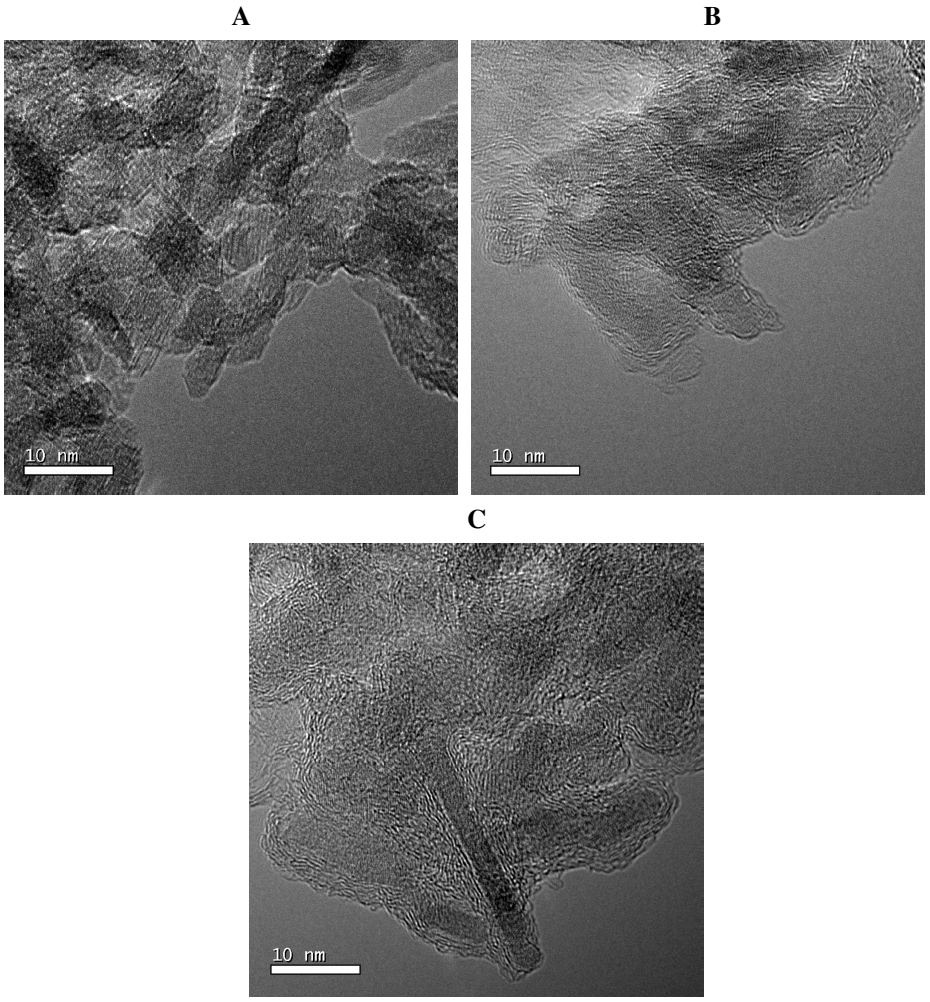

Fig. 3.11: HR-TEM micrographs of Al_2O_3: A – fresh, B – spent 22 h, C – spent 96 h.

3.4 Discussion

All six supported catalysts (V, KV, MgV and Cr, KCr, MgCr) show a very similar behaviour in time (Fig. 3.1). They are initially very active, but unselective. Selectivities rise to a steady, high value of 92% after 5 h, whilst conversion continuously decreases. A possible explanation for the increasing selectivity in the first hours is that the catalyst is reduced to the appropriate oxidation state and the most acidic sites on the catalyst are changed or have become inaccessible. Cracking of ethylbenzene into benzene or toluene is reduced, as well as the surplus of hydrogen and CO. Highly active and unselective sites disappear by coke coverage, first forming on the non-selective sites, decreasing activity but increasing the selectivity at the same time. The formation of coke does not stop when there are no non-selective sites left, but it continues, deactivating the catalysts further. The catalysts become less accessible by this fouling and differences disappear as the original catalyst surface is no longer accessible. Coke initially has a positive influence on the selectivity, but later a negative effect on the activity. With decreasing dehydrogenation activity, the CO_2 conversion also decreases (Fig. 3.1-C). These seem to be directly related to each other.

The observed activity of alumina in the CO_2 ODH of ethylbenzene is consistent with previous literature reports.[6, 7, 11, 16] Apparent discrepancies can be attributed to differences in the time on stream, molar ratio of CO_2 and ethylbenzene, ethylbenzene partial pressure and space velocity of the reported activity data. For short times on stream the EB conversion over alumina is below 20%, representing a poor activity, but for longer times on stream conversion may develop to above 60%, which represents a reasonable activity and is similar to the maximum conversion of ZrO_2 under the same conditions (Fig. 3.2). These examples clearly show that initial catalyst performance data, at short times on stream, are a wrong performance indicator. In the presented case, dehydrogenation experiments should be run for at least 20 h in order to get a good and relevant impression of the catalyst performance in terms of conversion, selectivity and stability. The experiment with alumina is a prime example, since at 20 h on stream the catalyst has barely started to deactivate even though >20 wt% coke has been deposited. This indicates that some catalysts like alumina have to run longer (*e.g.* for 96 h, Fig. 3.3) to fully appreciate their performance.

The combined information on Al_2O_3 from TGA, N_2-adsorption and HR-TEM micrographs (Fig. 3.11), confirm that a growing, irregular layer of coke is being deposited on the catalyst surface. At first this increases both activity and selectivity. Secondly, with increasing time, the coke is filling up the catalyst pores, decreasing the specific surface area and pore volume (Table 3.4 and 3.5). After about 15 h in CO_2 diluent or 10 h in N_2 diluent, the loss of available surface area causes activity to decrease, but the catalytic system remains highly selective. Only selective poisoning of unselective active

sites, that would increase selectivity, as is the case with the supported catalysts samples, does not apply here. The EB dehydrogenation activity of alumina increases as well. Coke clearly contributes to the catalyst activity and selectivity and is likely to be a catalytic species.

Similar reasoning can be followed for the case of ZrO_2. A fast initial coke build-up in the first 2 h is observed by TG analysis, as is displayed in Fig. 3.3, whilst conversion and selectivity are also both rising quickly. Zirconia has been reported active in the CO_2 oxidative dehydrogenation.[18] The active site was identified to be tetragonal phase zirconia.[18] As this phase is not present in alumina and both supports exhibit a very similar EB dehydrogenation behaviour, this points to another active site that both materials have in common, *viz.* the carbon deposits. The formation of coke proceeds over acidic sites.[38] Zirconia is a much more acidic support than alumina [39], hence the formation of coke and its activation for dehydrogenation is also much faster.

Interestingly, the amount of coke at which these systems reach their optimum conversion and selectivity, corresponds with the amount of a theoretical monolayer of coke on the surface. Calculated from the unit cell dimensions, graphitic carbon has a single side surface area of about 1300 m^2/g. The fresh γ-Al_2O_3 has a surface area of 222 m^2/g, so 0.17 g/g (15 wt%) of graphitic carbon is needed to cover the surface with a single layer. For ZrO_2 with a specific surface area of 104 m^2/g this amounts to 0.08 g/g (7.5 wt%). Monolayer coverage of the initial material appears to be the optimal coke loading.

Proper analysis of the gas stream by GC is an important aspect of this work. Besides the common side products such as benzene and toluene, we were also able to detect many higher aromatics (naphthalenes, biphenyl, benzylbenzene, stilbene and many more unidentified) that we named tars and surplus of hydrogen/carbon monoxide. For instance for catalyst KV, omitting the selectivity to tars (4%) and surplus H_2 and CO (1.5%), would give a selectivity to styrene of 97.5%. This clearly shows the importance of taking these side products into account. The molar balance for surplus hydrogen, based on the formation of coke and hydrogen from ethylbenzene, is approximated by applying equation 3.9. Hydrogen is easily converted into CO by the RWGS reaction, so these were always taken into account together. It is assumed that the carbon from this reaction ends up as coke on the catalyst. By integrating the amount of coke from the surplus of H_2 and CO, we obtain the same order of magnitude of coke as what is determined by TGA. This demonstrates that the carbon balance in this study seems well closed.

$$C_8H_{10} \rightarrow 8C + 5H_2 \qquad 3.9$$

Assuming that coke is the active species of the catalyst, other carbon materials could also exhibit a good performance, from the initial stage onwards. The experiments with carbon based materials such as AC and CNT, shown in Fig. 3.2, also point in the direction that carbon is responsible for the dehydrogenation activity and selectivity. Although AC and CNT deactivate much faster than Al_2O_3 or ZrO_2, they show a constant high selectivity right from the start. The difference in selectivity between samples might be explained as the result of impurities in these materials, that were used as received. The reason for faster deactivation is, however, unclear, as the measured specific surface area of the spent samples is still high. The BET surface area, however, is not a measure for the accessible surface area for ethylbenzene due to the presence of microporosity. The large difference between the surface areas and pore volumes of fresh and first spent sample for the alumina and zirconia series in Table 3.4-6, is attributed to easy blockage of the micropores by the initial coke deposition and thereby becoming inaccessible.

The TGA profiles of the carbon materials in Fig. 3.8 show a clear change in reactivity, showing that the type of carbon material deposited is more reactive. The amount of material removed by TGA in case of AC was 90.5% and 93.4% for the fresh and spent material, respectively. This indicates that more carbon material was present on the spent sample. With the CNT samples there was no significant change in weight loss, the ash content is very low. Also the spent CNT is more reactive in TGA, indicating large coke deposits.

The behaviour of the carbon deposits on alumina in CO_2 and N_2 diluent shows similarities with oxidative dehydrogenation catalysts that use molecular oxygen. In the presence of oxygen, carbon deposits and other forms of structured carbons like carbon nanotubes and onion-like carbon have been identified as active materials. The actual catalytic site under molecular oxygen conditions is believed to be oxygen-surface groups like quinones and hydroxyls.[2, 40-51] However, it is reasoned that in the absence of molecular oxygen these groups cannot be formed and that hence coke cannot be the active phase.[2] This reasoning seems to break down as we clearly see a catalytic effect of the carbon deposits under CO_2 and N_2 flow (Fig. 3.4), although a higher temperature is required. Even in the absence of any oxidant, as the N_2-experiment shows, carbon deposits catalyse the ethylbenzene dehydrogenation reaction.

More examples of the beneficial effects of coke deposition in catalysed reactions exist, including butane skeletal isomerisation, alkylation of toluene with methanol to form xylenes, catalytic cracking, hydrotreating and aromatization.[38, 52-55] Even other direct dehydrogenation reactions are known to proceed over carbon deposits, like with cyclohexene[56] and butane.[57] Going back even further in time also direct ethylbenzene dehydrogenation was already known to be catalysed by coke.[58-62] Sato *et al.*[6] published comparable results showing increasing conversion and selectivity with time on stream,

but carbon was not identified as the key in the performance.

As to the active site or mechanism of dehydrogenation on carbon deposits, this is still not resolved. Good characterisation of the carbon deposits is a challenge. Also the characterizations presented in this paper do not provide a unambiguous explanation of the catalytic activity. The Raman spectra do not provide any indication (Fig. 3.9). The ratio between the 'graphitic' carbon (~1600 cm^{-1}) and the 'amorphous' carbon (~1350 cm^{-1}) is apparently not a measure. In the range of 100-2000 cm^{-1} no other peaks were observed than those attributed to carbon deposits, even though vanadium oxides and zirconia have very distinct peaks in this region of Raman spectroscopy. Electron spin resonance and THz-time domain spectroscopy have been used to characterize the carbon,[57, 58, 61] but information from these techniques is also limited. The intensity of the signal increases with carbon content and activity of the catalyst, leading to believe that unpaired electrons play a role in the dehydrogenation reaction. This is also observed with oxidative dehydrogenation.[48] Such free radicals can perform hydrogen atom abstraction and successive hydrogen atom abstraction will lead to dehydrogenation.[56-59, 61] The difference between direct dehydrogenation, CO_2 oxidative dehydrogenation and oxidative dehydrogenation may be only limited by the way of hydrogen radical removal: by formation of dihydrogen, or water formation *via* RWGS, or oxidation, respectively. In the case of CO_2, a less acidic support can improve adsorption properties and, thereby, RWGS reactions and increase dehydrogenation activity, as was reported by Sato.[6]

The results with alumina and the use of nitrogen as diluent learns that carbon dioxide, or another oxidant, is not necessary to achieve a good dehydrogenation performance. Only a certain amount of carbon deposit, enough to create a surface monolayer, seems to be required. Oxygen groups on the coke surface are also not necessary. Defects and edges of the coke deposits are more likely to be part of the active site. Differences in the initial performance development (the first 10-15 h on stream, up to the optimum) between CO_2 and N_2 diluent can be explained by competitive adsorption in the case of CO_2. Here CO_2 could block sites that otherwise participate in the formation of coke or other side reactions. This causes slower coke formation in CO_2 and as coke (below monolayer) makes the catalyst more active and more selective, the reduction of by-product formation is also slower. In the experiment where we switched from CO_2 to N_2 diluent or the other way around during dehydrogenation (Fig. 3.7), the conversion and selectivity are identical after initial monolayer coke laydown. This shows that the coke is active and of similar composition, indifferent from the used diluent.

From the perspective of CO_2 ODH, where the RWGS reaction is used to elevate the equilibrium conversion, carbon and bare alumina samples exhibit hardly any RWGS activity. From the bare supports, only ZrO_2 shows some RWGS activity, because of its

redox properties.[63] These redox properties are also not active enough to reach the conversion levels that would make this process commercially interesting. The (formed) carbon is inactive for the RWGS reaction. The six supported catalysts show a better RWGS activity, the best is KV with a CO_2 conversion of 15%, decreasing to 5% as stability is an issue with these catalysts. Carbon dioxide is fed in large excess. Initial CO_2 conversions are higher than those expected due to high hydrogen formation rates from the coking reaction 3.9. A redox function on the catalyst is needed for RWGS activity, but this function will also influence the coke formation and, thereby, the catalyst deactivation.

The gasification of coke with CO_2, the reverse Boudouard reaction, was not observed in our experiments. The carbon monoxide product that was measured can be explained by the RWGS alone, where hydrogen is produced from dehydrogenation or coke formation. A simple TGA experiment with a coked sample such as a spent alumina support and CO_2 as the oxidant showed that temperatures higher than 650 °C are required for gasification of the coke by CO_2.

The selective dehydrogenation activity of a catalyst under CO_2 or N_2 atmosphere is clearly correlated to the formation of carbon deposits on alumina and zirconia. The actual activity of the catalyst is a result of the sensitive balance between the amount of coke, the characteristics of the parent material and to a lesser extent the available pore volume and surface area. For a stabilised catalyst system, a stationary amount of coke has to be present. This can be achieved by avoiding the excessive formation of coke, preferably by reducing the rate of formation or otherwise by promoted coke removal/gasification. The latter could be possible by addition of a more oxidative gas to the reaction mixture, removing excess carbon and creating the radical edge sites needed for the dehydrogenation. The reactivity of the oxidant dictates its concentration and the temperature level on which a stable steady state is reached. Without an activating oxidant mainly thermal activation occurs, but inherently a faster deactivation takes place.

3.5 Conclusion

This study with ZrO_2 and Al_2O_3 supports for the dehydrogenation reaction of ethylbenzene to styrene in CO_2 shows that with both systems carbon deposits are responsible for the activity and selectivity. These bare catalysts show an optimal activity after 1 h and 15 h of time on stream respectively, which coincide with reaching a stable styrene selectivity plateau of 92%. Also with Al_2O_3 support and N_2 as diluent the same phenomenon is observed. The optimum performance in this case is at 10 h of time on stream. Characterizations of the Al_2O_3 samples after different times on stream show a clear correlation between the formed coke and the activity and selectivity.

The vanadium and chromium supported catalysts act in the same manner as the bare Al_2O_3 and ZrO_2 supports, only the rates of activation and deactivation are higher. The amounts of coke on these catalysts support that carbon deposits are the active and selective ingredient in those catalyst formulations. The advantage of the supported catalysts is their RWGS activity that gives a minor increase in styrene yield.

The coke that is initially formed during reaction is responsible for the increased activity and selectivity for the dehydrogenation reaction. After a certain point in time the increase in the amount of coke, however, reduces the activity due to a loss in available surface area. Oxygen groups on the coke seem not essential for dehydrogenation, but rather defects and edges of the carbon deposits play a role in the reaction mechanism. The overall activity and selectivity of the catalyst depends on its amount of coke, parent material and accessible surface area.

References

[1] D.H. James, W.M. Castor, Ullmann's Encyclopedia of Industrial Chemistry, Wiley-VCH Verlag GmbH & Co. KGaA, 2002.
[2] F. Cavani, F. Trifiro, Appl. Catal. A: Gen. 133 (1995) 219-239.
[3] S.E. Park, S.C. Han, J. Ind. Eng. Chem. 10 (2004) 1257-1269.
[4] A.L. Sun, Z.F. Qin, J.G. Wang, Appl. Catal. A: Gen. 234 (2002) 179-189.
[5] Y. Sakurai, T. Suzaki, N. Ikenaga, T. Suzuki, Appl. Catal. A: Gen. 192 (2000) 281-288.
[6] S. Sato, M. Ohhara, T. Sodesawa, F. Nozaki, Appl. Catal. 37 (1988) 207-215.
[7] G.I. Fedorov, S.G. Sibgatullin, N.L. Solodova, R.I. Izmailov, Pet. Chem. 16 (1976) 157-162.
[8] S.B. Wang, Z.H. Zhu, Energy & Fuels. 18 (2004) 1126-1139.
[9] M.O. Sugino, H. Shimada, T. Turuda, H. Miura, N. Ikenaga, T. Suzuki, Appl. Catal. A: Gen. 121 (1995) 125-137.
[10] N. Ikenaga, T. Tsuruda, K. Senma, T. Yamaguchi, Y. Sakurai, T. Suzuki, Ind. Eng. Chem. Res. 39 (2000) 1228-1234.
[11] N. Mimura, M. Saito, Catal. Today. 55 (2000) 173-178.
[12] V.P. Vislovskiy, J.S. Chang, M.S. Park, S.E. Park, Catal. Commun. 3 (2002) 227-231.
[13] X.N. Ye, W.M. Hua, Y.H. Yue, W.L. Dai, C.X. Miao, Z.K. Xie, Z. Gao, New J. Chem. 28 (2004) 373-378.
[14] A.L. Sun, Z.F. Qin, S.W. Chen, J.G. Wang, J. Mol. Catal. A: Chem. 210 (2004) 189-195.
[15] X.N. Ye, Y.H. Yue, C.X. Miao, Z.K. Xie, W.M. Hua, Z. Gao, Green Chem. 7 (2005) 524-528.
[16] S.W. Chen, Z.F. Qin, X.F. Xu, J.G. Wang, Appl. Catal. A: Gen. 302 (2006) 185-192.
[17] J.S. Chang, D.Y. Hong, V.P. Vislovskiy, S.E. Park, Catal. Surv. Asia. 11 (2007) 59-69.
[18] J.N. Park, J. Noh, J.S. Chang, S.E. Park, Catal. Lett. 65 (2000) 75-78.

[19] J. Noh, J.S. Chang, J.N. Park, K.Y. Lee, S.E. Park, Appl. Organomet. Chem. 14 (2000) 815-818.
[20] J. Ren, W.Y. Li, K.C. Xie, Catal. Lett. 93 (2004) 31-35.
[21] D.R. Burri, K.M. Choi, D.S. Han, J.B. Koo, S.E. Park, Catal. Today. 115 (2006) 242-247.
[22] D.R. Burri, K.M. Choi, S.C. Han, A. Burri, S.E. Park, J. Mol. Catal. A: Chem. 269 (2007) 58-63.
[23] D.R. Burri, K.M. Choi, S.E. Park, Adv. Nanomater. Proc., Pts 1-2. 124-126 (2007) 1737-1740.
[24] D.R. Burri, K.M. Choi, D.S. Han, Sujandi, N. Jiang, A. Burri, S.E. Park, Catal. Today. 131 (2008) 173-178.
[25] B.M. Reddy, H. Jin, D.S. Han, S.E. Park, Catal. Lett. 124 (2008) 357-363.
[26] B.M. Reddy, D.S. Han, N. Jiang, S.E. Park, Catal. Surv. Asia. 12 (2008) 56-69.
[27] B.M. Reddy, S.-C. Lee, D.-S. Han, S.-E. Park, Appl. Catal. B: Env. 87 (2009) 230-238.
[28] H.Y. Li, Y.H. Yue, C.K. Miao, Z.K. Xie, W.M. Hua, Z. Gao, Catal. Commun. 8 (2007) 1317-1322.
[29] Y. Sakurai, T. Suzaki, K. Nakagawa, N. Ikenaga, H. Aota, T. Suzuki, J. Catal. 209 (2002) 16-24.
[30] N. Mimura, I. Takahara, M. Saito, Y. Sasaki, K. Murata, Catal. Lett. 78 (2002) 125-128.
[31] G. Carja, R. Nakamura, T. Aida, H. Niiyama, J. Catal. 218 (2003) 104-110.
[32] X.N. Ye, N. Ma, W.M. Hua, Y.H. Yue, C.X. Miao, Z.K. Xie, Z. Gao, J. Mol. Catal. A: Chem. 217 (2004) 103-108.
[33] D.R. Burri, K.M. Choi, J.H. Lee, D.S. Han, S.E. Park, Catal. Commun. 8 (2007) 43-48.
[34] B.S. Liu, G. Rui, R.Z. Chang, C.T. Au, Appl. Catal. A: Gen. 335 (2008) 88-94.
[35] Y.Y. Qiao, C.X. Miao, Y.H. Yue, Z.K. Xie, W.M. Yang, W.M. Hua, Z. Gao, Microp. Mesop. Mater. 119 (2009) 150-157.
[36] G.R. Meima, P.G. Menon, Appl. Catal. A: Gen. 212 (2001) 239-245.
[37] D. Espinat, H. Dexpert, E. Freund, G. Martino, M. Couzi, P. Lespade, F. Cruege, Appl. Catal. 16 (1985) 343-354.
[38] P.G. Menon, J. Mol. Catal. A: Chem. 59 (1990) 207-220.
[39] T. Klimova, M.L. Rojas, P. Castillo, R. Cuevas, J. Ramirez, Microp. Mesop. Mater. 20 (1998) 293-306.
[40] A. Schraut, G. Emig, H.G. Sockel, Appl. Catal. 29 (1987) 311-326.
[41] G. Mestl, N.I. Maksimova, N. Keller, V.V. Roddatis, R. Schlögl, Angew. Chem., Int. Ed. 40 (2001) 2066-2068.
[42] J.J. Delgado, R. Vieira, G. Rebmann, D.S. Su, N. Keller, M.J. Ledoux, R. Schlögl, Carbon. 44 (2006) 809-812.
[43] J.J. Delgado, D.S. Su, G. Rebmann, N. Keller, A. Gajovic, R. Schlögl, J. Catal. 244 (2006) 126-129.
[44] D.S. Su, N. Maksimova, J.J. Delgado, N. Keller, G. Mestl, M.J. Ledoux, R. Schlögl, Catal. Today. 102 (2005) 110-114.
[45] D.S. Su, N.I. Maksimova, G. Mestl, V.L. Kuznetsov, V. Keller, R. Schlögl, N. Keller, Carbon. 45 (2007) 2145-2151.
[46] N. Keller, N.I. Maksimova, V.V. Roddatis, M. Schur, G. Mestl, Y.V. Butenko, V.L. Kuznetsov, R. Schlögl, Angew. Chem., Int. Ed. 41 (2002) 1885-1888.

[47] A.E. Lisovskii, C. Aharoni, Catalysis Reviews: Science and Engineering. 36 (1994) 25-74.
[48] R. Fiedorow, W. Przystajko, M. Sopa, J. Catal. 68 (1981) 33-41.
[49] L.E. Cadus, L.A. Arrua, O.F. Gorriz, J.B. Rivarola, Ind. Eng. Chem. Res. 27 (1988) 2241-2246.
[50] L.E. Cadus, O.F. Gorriz, J.B. Rivarola, React. Kinet. Catal. Lett. 42 (1990) 101-106.
[51] L.E. Cadus, O.F. Gorriz, J.B. Rivarola, Ind. Eng. Chem. Res. 29 (1990) 1143-1146.
[52] R. Le Van Mao, L.A. Dufresne, J.H. Yao, Y.L. Yu, Appl. Catal. A: Gen. 164 (1997) 81-89.
[53] G.C. Bond, Appl. Catal. A: Gen. 149 (1997) 3-25.
[54] S. van Donk, J.H. Bitter, K.P. de Jong, Appl. Catal. A: Gen. 212 (2001) 97-116.
[55] C. Glasson, C. Geantet, M. Lacroix, F. Labruyere, P. Dufresne, J. Catal. 212 (2002) 76-85.
[56] H. Amano, S. Sato, R. Takahashi, T. Sodesawa, PCCP. 3 (2001) 873-879.
[57] J. McGregor, Z.Y. Huang, E.P.J. Parrott, J.A. Zeitler, K.L. Nguyen, J.M. Rawson, A. Carley, T.W. Hansen, J.P. Tessonnier, D.S. Su, D. Teschner, E.M. Vass, A. Knop-Gericke, R. Schlögl, L.F. Gladden, J. Catal. 269 (2010) 329-339.
[58] P.A. Berger, J.F. Roth, J. Phys. Chem. 72 (1968) 3186-3193.
[59] J.B. Donnet, Carbon. 6 (1968) 161-176.
[60] J.F. Roth, A.R. Schaefer, Catalyst and Catalytic Process, 1969, United States patent 3446865.
[61] J.F. Roth, J.B. Abell, L.W. Fannin, A.R. Schaefer, Adv. Chem. Ser. (1970) 193-203.
[62] J.F. Roth, J.B. Abell, L.W. Fannin, A.R. Schaefer, Abstracts of Papers of the American Chemical Society (1969) 90.
[63] K. Tanabe, Mater. Chem. Phys. 13 (1985) 347-364.

4

The role of RWGS in the dehydrogenation of ethylbenzene to styrene in CO_2

Abstract

The addition of CO_2 to the dehydrogenation of ethylbenzene (EB) to styrene over promoted and un-promoted vanadia, iron and chromia catalysts on alumina improves the yield of styrene, in comparison with the use of N_2 as diluent. Depending on the catalyst, EB conversion increases 5-10%, while selectivity does not change significantly. The potassium promoted vanadium catalyst shows the highest CO_2 conversion for dehydrogenation with the largest increase in EB conversion. The activity of these catalysts in the reverse water-gas-shift (RWGS) reaction, in the presence and absence of the dehydrogenation, is very different. Vanadium catalysts exhibit the lowest CO_2 RWGS activity. The presence of coke on the catalyst supresses the RWGS reaction over chromium and iron catalysts, but improves the activity of the vanadium catalyst. This is attributed to hydrogen spill-over from the coke to the metal catalyst. A two-step mechanism with a hydrogen spill-over is proposed for the EB dehydrogenation in CO_2. Step-response experiments show that the redox mechanism for the RWGS and the two-step pathway for dehydrogenation in CO_2 are the dominant routes. A slight RWGS activity of the bare alumina support is attributed to an associative mechanism.

This chapter has been published:
C. Nederlof, G. Talay, F. Kapteijn, M. Makkee, Appl. Catal. A: Gen. 423-424 (2012) 59-68.

4.1 Introduction

The dehydrogenation of ethylbenzene to styrene with CO_2 is an alternative process option for the styrene production. It has several advantages over the normal production route *via* the steam-aided dehydrogenation. This new process has an improved conversion, higher selectivity, is safer and is less energy consuming.[1-6]

The steam-aided dehydrogenation process is responsible for about 85% of the worldwide production of styrene. This process uses a potassium promoted iron oxide catalyst and requires a high molar ratio of steam to ethylbenzene of 7-10. Steam is an essential part of the process. Several functions have been attributed to H_2O in the process:[7, 8]

- provides the energy for the endothermic dehydrogenation reaction (125 kJ/mol at 600 °C)
- acts as a diluent, improving the equilibrium conversion of the reaction
- brings the catalyst to the right active oxidation state
- cleans the catalyst from coke deposits by coke gasification
- provides easy separation of diluent and product stream.

Carbon dioxide is believed to act in a similar way, with some additional advantages. Its heat capacity is higher, requiring less diluent from an energetic point of view. Under the dehydrogenation conditions, CO_2 is considered to be a mild oxidant like steam and is able to re-oxidize the catalyst. It is claimed that coke can be removed by the reverse Boudouard reaction. Carbon dioxide is a permanent gas, making the separation of the product stream easier. And most importantly, CO_2 can react with the formed H_2 *via* the reverse water-gas-shift (RWGS) reaction and, thereby, shifting the equilibrium conversion to higher values. [1-6]

The RWGS reaction is a mildly endothermic reaction (36 kJ/mol at 600 °C) and makes the process more endothermic, but the increased conversion per pass easily makes up for those additional costs.[2] The RWGS reaction and its counterpart, the water-gas-shift (WGS) reaction, are well known and widely practiced. The WGS reaction is used in hydrogen production *e.g.* for the ammonia production, the methanol synthesis and the Fischer-Tropsch synthesis. For the WGS reaction there is a high temperature and a low temperature process with different catalysts. The low temperature WGS process (210-240 °C) is most favourable for H_2 production, a copper based catalyst ($Cu/ZnO/Al_2O_3$) is used here.[9] A low temperature does not always match with the desired process conditions and as copper is not stable at high temperatures another catalyst is required.[10] The high temperature (300-500 °C) WGS process uses an iron oxide based catalyst (Fe_2O_3/Cr_2O_3), but the conversions are lower because of the equilibrium limitations.[9]

The mechanism of (R)WGS can be either an associative or redox type.[9] In the associative mechanism, the reactants adsorb, form an intermediate, break into the products and desorb.[11, 12] The redox mechanism consists of adsorption, reduction of the catalyst by H_2 or CO and oxidation of the catalyst by CO_2 or H_2O and desorption.[12-16] In the associative mechanism, CO can only be formed in the presence of hydrogen. With the redox mechanism, the CO production or H_2O production should be observed without the presence of the other reactant.

The dehydrogenation process in CO_2 can be considered as two consecutive reactions: a dehydrogenation (4.1) followed by the RWGS (4.2); or as a direct dehydrogenation by CO_2 (4.3).[2, 6, 17] These two variations are comparable to the associative and redox mechanism in (R)WGS. Carbon dioxide will oxidize the catalyst, or form a reactive intermediate. Ethylbenzene, or hydrogen for that matter, will reduce the catalyst, or it reacts with the intermediate species on the catalyst. Both pathways are discussed in literature and both seem to be possible. The two-step pathway, where both hydrogen and CO are produced is most favourable from a thermodynamic point of view and will give the highest theoretical styrene yield.

$$C_8H_{10} \rightleftarrows C_8H_8 + H_2 \qquad 4.1$$

$$H_2 + CO_2 \rightleftarrows H_2O + CO \qquad 4.2$$

$$C_8H_{10} + CO_2 \rightleftarrows C_8H_8 + H_2O + CO \qquad 4.3$$

The role of the RWGS reaction has already been subject of previous research. [2, 6, 17] However, the RWGS experiments were often done under different reaction conditions, making good comparison with the dehydrogenation results cumbersome. Sun *et al.*[17] compared the CO_2 conversions of the different catalysts in the presence and absence of dehydrogenation (Figure 4.1). Catalysts, containing iron or chromium, were quite active for the RWGS alone, but the vanadium containing catalysts performed much better in combination with the dehydrogenation reaction. Vanadium catalysts in the dehydrogenation yield higher CO_2 conversions than the iron or chromium catalysts. This was explained by a difference in mechanism for vanadium and other catalysts. Vanadium would follow more the one-step pathway with the involvement of atomic hydrogen; whereas the other catalysts would follow more the two-step pathway with molecular hydrogen (Figure 4.2). Conditions in those experiments were not exactly the same for dehydrogenation and RWGS: the contact time was doubled for dehydrogenation experiments and EB was never completely converted making the amount of hydrogen produced deficient compared to the RWGS reaction conditions. An absolute comparison of

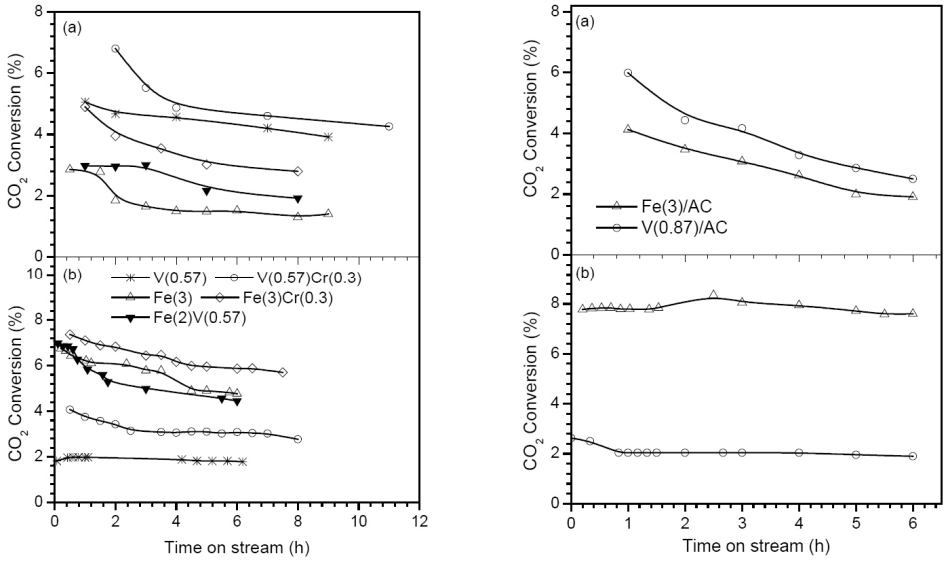

Figure 4.1: Comparison of CO_2 conversions in the (*a*) coupled EB dehydrogenation and (*b*) single RWGS for catalysts supported on Al_2O_3 (*left*) and activated carbon (AC) (*right*). RWGS conditions: 550°C, 0.1 MPa, CO_2/H_2 = 11, *W/F* = 2.04 g-cat h/mol. EB dehydrogenation conditions: 550°C, 0.1 MPa, CO_2/EB = 11, *W/F* = 4.07 g-cat h/mol. The figure is taken from Sun at al.[17]

the CO_2 conversions is therefore, extremely difficult.[17]

The goal of this study is to investigate the role of the RWGS reaction in the dehydrogenation in CO_2. This systematic study applies the most used catalysts in the dehydrogenation: iron, vanadium and chromium, supported on alumina; un-promoted and promoted with potassium or magnesium. RWGS experiments are done in the presence and absence of the dehydrogenation under comparable conditions for good comparison. Based on our recent insights into dehydrogenation catalysis (Ch. 3), also coked catalysts and support are included. Based on the results, the reaction pathway of the dehydrogenation in CO_2 and the mechanism of RWGS is discussed.

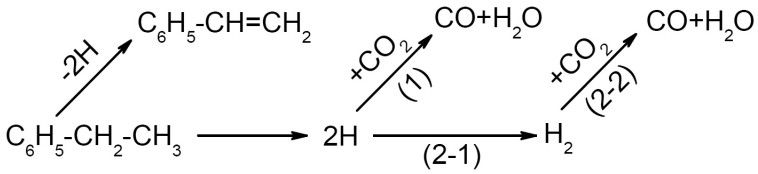

Figure 4.2: Role of CO_2 in the coupled EB dehydrogenation in the presence of CO_2. The routes of the one-step (1) and two-step pathways (2-1 / 2-2) are indicated. The figure is taken from Sun at al.[17]

4.2 Experimental

4.2.1 Catalyst preparation

The γ-Al_2O_3 support (Ketjen 000-3P, 0.63 ml/g, 303 m^2/g) was crushed and sieved to 150-300 μm and dried at 120 °C overnight. The active metals were introduced by co-impregnation using the incipient wetness method. The required amounts of $Cr(NO_3)_3 \cdot 9H_2O$, $Fe(NO_3)_3 \cdot 9H_2O$, $Mg(NO_3)_2 \cdot 6H_2O$, KNO_3 or NH_4VO_3 together with $2C_2H_2O_4 \cdot 2H_2O$ were dissolved in demi-water, after which the γ-Al_2O_3 support was impregnated with the solution. The impregnated support was put in a ceramic cup, dried at 120 °C in air for four hours, followed by calcination in a static air calcination oven at 600 °C for four hours (heating ramp of 10 °C/min). The chosen loadings are 1 mmol/g for vanadia (V), iron (Fe) and chromia (Cr) and 0.5 mmol/g for the promotors potassium (K) and magnesium (Mg). This should result in coverage of the catalyst support that is around 25-50% of that of a monolayer[18] (coverage is ~2 atoms/nm^2 for Cr, V, Fe). Short names are used for the catalysts, *e.g.* KV will mean potassium promoted vanadium on alumina catalyst. The coked catalyst samples were produced by testing the fresh catalysts in dehydrogenation in CO_2 diluent for 20 h, according to the conditions described below.

4.2.2 Catalyst testing

4.2.2.1 RWGS studies, dehydrogenation of EB in CO_2

These experiments were carried out under steady-state conditions in a quartz fixed bed reactor with an inner diameter of 8 mm. The reaction temperature was 600 °C and the pressure at the reactor outlet was atmospheric. In a typical experiment 400 mg of catalyst was used. On top of the catalyst bed was a 1 cm layer of SiC to preheat the feed. The catalyst bed and SiC were fixed in the quartz tube by quartz wool plugs. Gaseous carbon dioxide was fed through a mass-flow controller set at 15 ml (NTP)/min (NTP = 20 °C, 1 atm). The total *GHSV* was 1500 l/l/h (vol. gas/vol. cat). Before starting the experiment the reactor would be heated up with 10 °C/min and allowed to stabilize at reaction temperature for half an hour under only a CO_2 flow. The experiment was started by feeding hydrogen to the reactor. The flow of CO_2 was kept constant, the flow of hydrogen was set at 1.5 (9% H_2), 1.15 (7% H_2), or 0.8 (5% H_2) ml (NTP)/min by a mass-flow controller (Brooks). The RWGS experiment started with a CO_2 to H_2 ratio of 18 for 12 h, followed by a ratio of 13 for 4 h and a ratio of 10 for another 4 h.

4.2.2.2 Step-response experiments

The step-response experiments, where the feed of each of the reactants could be switched on or off within a couple of seconds, were performed using the same equip-

ment as the RWGS studies and under the same temperature and pressure. In a typical experiment 100 mg of catalyst was used. Hydrogen and/or carbon dioxide mass-flow controllers could be turned on or off and were set at a flow of 1 ml (NTP) /min, in a continuous flow of argon of 100 ml (NTP) /min. A mass spectrometer (MS-Thermostar, Pfeiffer Vacuum D35614 Asslar) was connected directly to the reactor outlet for a continuous analysis. A typical experiment consisted of six time intervals. Before and after these periods only argon is flowing over the catalyst. The six periods consist of: only CO_2 feed (a-b), only H_2 feed (c-d), again only CO_2 feed (e-f), CO_2 with H_2 (g-h), CO_2 with a short period of H_2 (i-j-k-l), H_2 with a short period of CO_2 (m-n-o-p).

4.2.2.3 Dehydrogenation of EB in CO_2

The dehydrogenation experiments were performed under the same temperature and pressure as the RWGS studies. The testing was done in a parallel fixed bed setup with six reactors. Each reactor had an independent gas (CO_2 or N_2) feed and liquid feed (ethylbenzene). The temperature and the pressure of all reactors were set at 600 °C and atmospheric pressure. The amount of catalyst loaded was 1000 mg, in a 4 mm inner diameter quartz tube (about 12 cm bed height). The catalyst bed was held between layers of SiC (10 cm), to hold it in position and to preheat the feed. The liquid EB feed flow rate was 1 g/h (3.6 ml/min vapour), the gas flow rate was 36 ml/min, N_2 or CO_2, resulting in a 1:10 molar ratio of ethylbenzene and diluent gas. Ethylbenzene liquid was fed into an α-alumina filled tube, where it was evaporated in a co-current flow with the gas feed.

4.2.2.4 GC analysis

During the dehydrogenation experiments in CO_2 and the RWGS experiments, the concentrations in the reactor effluent were measured online by a two channel gas chromatograph with a TCD (columns: 0.3m Hayesep Q 80-100 mesh with back-flush option, 25m × 0.53mm Porabond Q and 15 m × 0.53mm molsieve 5A with bypass option for CO_2 and H_2O, all in series) for permanent gas analysis (CO_2, H_2, N_2, O_2, CO) and a FID (column: 30m × 0.53mm, D_f = 3μm, RTX-1) for the hydrocarbons analysis (methane, ethane, ethene, benzene, toluene, ethylbenzene, styrene, tars). A sample was analysed every 15 minutes in order to follow the catalyst performance over time. A constant flow of nitrogen was used as an internal standard. Conversions and selectivities are based on the moles of ethylbenzene present in the reactor outlet and calculated according to Eqs. 3.6 and 3.7. The overall carbon balance is >99%, only carbon that was deposited on the catalyst as coke is missing from the carbon balance by the GC. The indicator for RWGS activity that we use, R_{RWGS}, is the ratio between the products and reactants of RWGS, relative to its equilibrium value. It is calculated according to equation 3.8. In case of

reaching RWGS equilibrium, the value is 1 (equilibrium constant K_{eq} = 0.38 at 600 °C). The amount of water is not determined, but calculated from the mole balances as the concentration of styrene minus the concentration of hydrogen.

$$EB\ conversion = \frac{ethylbenzene_{in} - ethylbenzene_{out}}{ethylbenzene_{in}} \quad 4.4$$

$$ST\ selectivity = \frac{styrene_{out}}{ethylbenzene_{in} - ethylbenzene_{out}} \quad 4.5$$

$$R_{RWGS} = \frac{[CO][ST - H_2]}{[CO_2][H_2]} / K_{eq} \quad 4.6$$

4.2.3 Catalyst characterization

After each experiment, a sample of the catalyst was analysed to determine the amount of coke by a TGA (MettlerToledo TGA/SDTA851^e, 20 mg sample of spent catalyst, 100 ml/min air, 50 ml/min He flow) using a ramp of 3 °C/min from RT to 723°C.

BET surface area and pore volume were determined of both fresh and spent catalyst samples by N_2 adsorption at –196 °C (Quantachrome Autosorb 6B). The samples were pre-treated overnight in nitrogen at 250 °C.

Temperature programmed reduction (TPR) was carried out in a fixed bed reactor system connected to a TCD and a MS for monitoring the hydrogen consumption and the methane formation (only detected >650 °C). The heating rate was 5 °C/min, the sample amount was 200 mg for each run. The flows of H_2 and Ar were set to 2.6 and 25.2 ml/min, giving a 9.3 vol% H_2 mixture. The TPR was calibrated with CuO, a one electron change in each of the samples should result in an area of around 200 [mV·K].

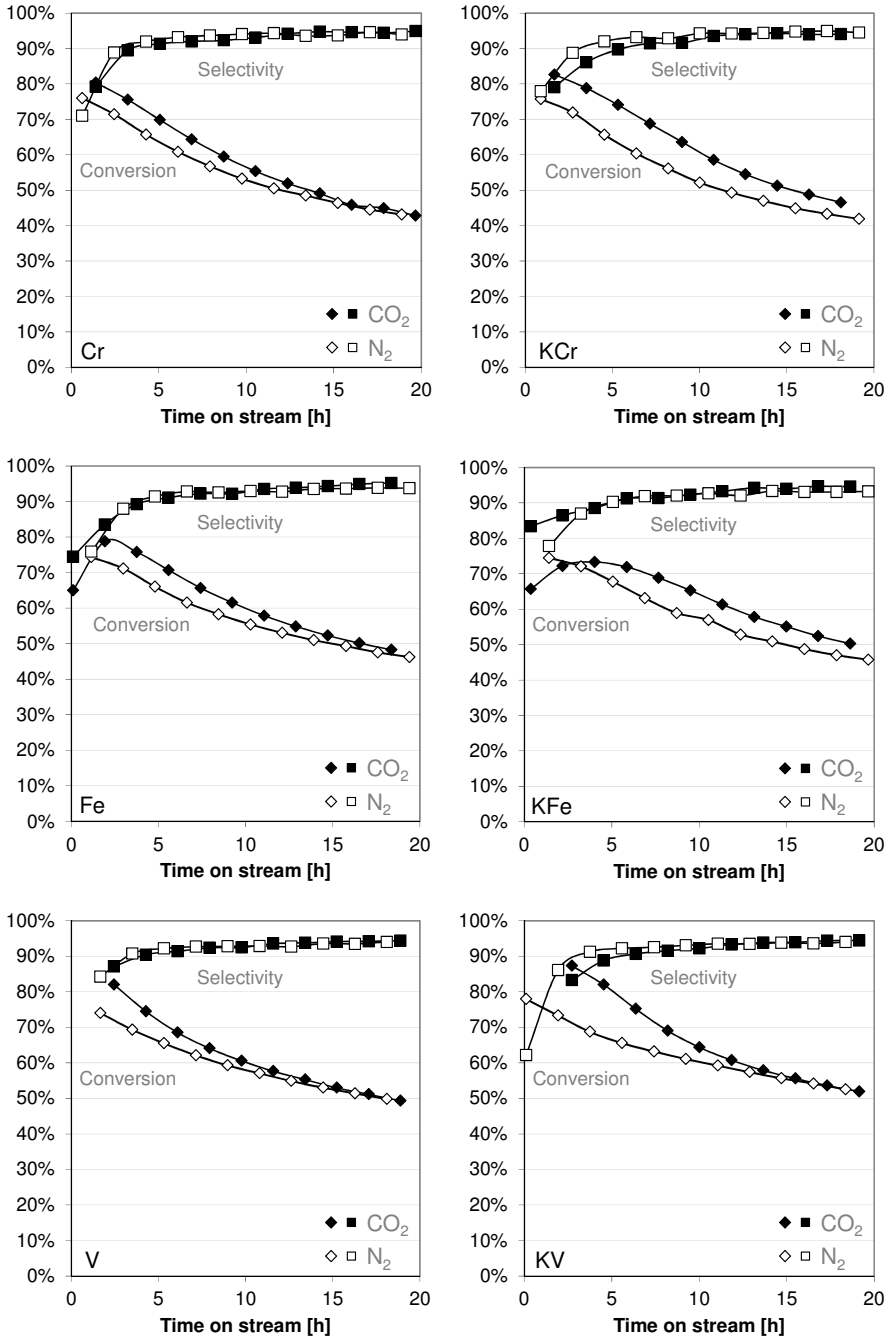

Figure 4.3: Ethylbenzene conversions (◆◇) and styrene selectivities(■□) for six γ-Al_2O_3 supported catalysts (Cr, KCr, Fe, KFe, V, KV) in CO_2 (solid, ◆■) and N_2 (open, □◇) diluent.

4.3 Results

4.3.1 Catalyst testing

4.3.1.1 Ethylbenzene dehydrogenation, with and without CO_2

Six of the nine supported catalyst samples were tested for their performance in the ethylbenzene dehydrogenation, in both carbon dioxide (CO_2) and nitrogen (N_2) diluent. Their ethylbenzene conversion and styrene selectivities are presented in Figure 4.3. All six catalysts initially show a difference in conversion for the CO_2 and N_2 diluent, in favour of the CO_2 diluent. The differences in selectivities are rather small, in CO_2 there is a little more surplus H_2 and CO (than expected from styrene yield). In the first hours, all the selectivities increase to stable and high levels of 92-95%. The differences in the catalyst activity are clearly present, especially for the KV catalyst. In CO_2 diluent the EB conversion is about 10% higher than in N_2. For the Cr catalyst the difference is about 5%, initially. All catalysts show a decreasing conversion, only the iron catalysts in CO_2 exhibit a maximum in the ethylbenzene conversion after 2-4 h time on stream.

With an increase in time on stream, all the catalysts deactivate. The conversions after 20 h time on stream are down to 40-50%, while initially they had an EB conversion between 70-90%. The differences between the experiments using CO_2 and N_2 diluent are also decreasing in time. For most catalysts, the performance in CO_2 or N_2 is almost identical after 15-20 h. The selectivities remain stable and high after about 5 h time on stream. The dehydrogenation results of the Al_2O_3 support in CO_2 and N_2 can be found in detail in Chapter 3.

4.3.1.2 RWGS in the absence and presence of dehydrogenation

All the catalysts, the alumina support and the four coked catalysts were tested for their RWGS performance. In dehydrogenation, a higher styrene yield results in a higher hydrogen production. To simulate different styrene yields, three hydrogen concentrations (5 vol%, 7 vol%, 9 vol%) were tested. Comparing with a 10 vol% EB dehydrogenation experiment, these H_2 concentrations would correspond to 50%, 70% and 90% EB conversion at 100% selectivity. The RWGS results are shown in Figure 4.4, together with the thermodynamic equilibrium conversion.

The chromium catalyst series (Figure 4.4-A) nicely shows that the potassium promoter enhances the RWGS activity. Magnesium has a negligible promoting effect on the RWGS activity, compared to the un-promoted chromium catalyst. The coked KCr catalyst shows that coke has deactivated this catalyst, as CO_2 conversions are more than 25% lower than the fresh catalyst. The iron catalyst series (Figure 4.4-B) are comparable to the chromium series. The potassium promoter enhances the RWGS

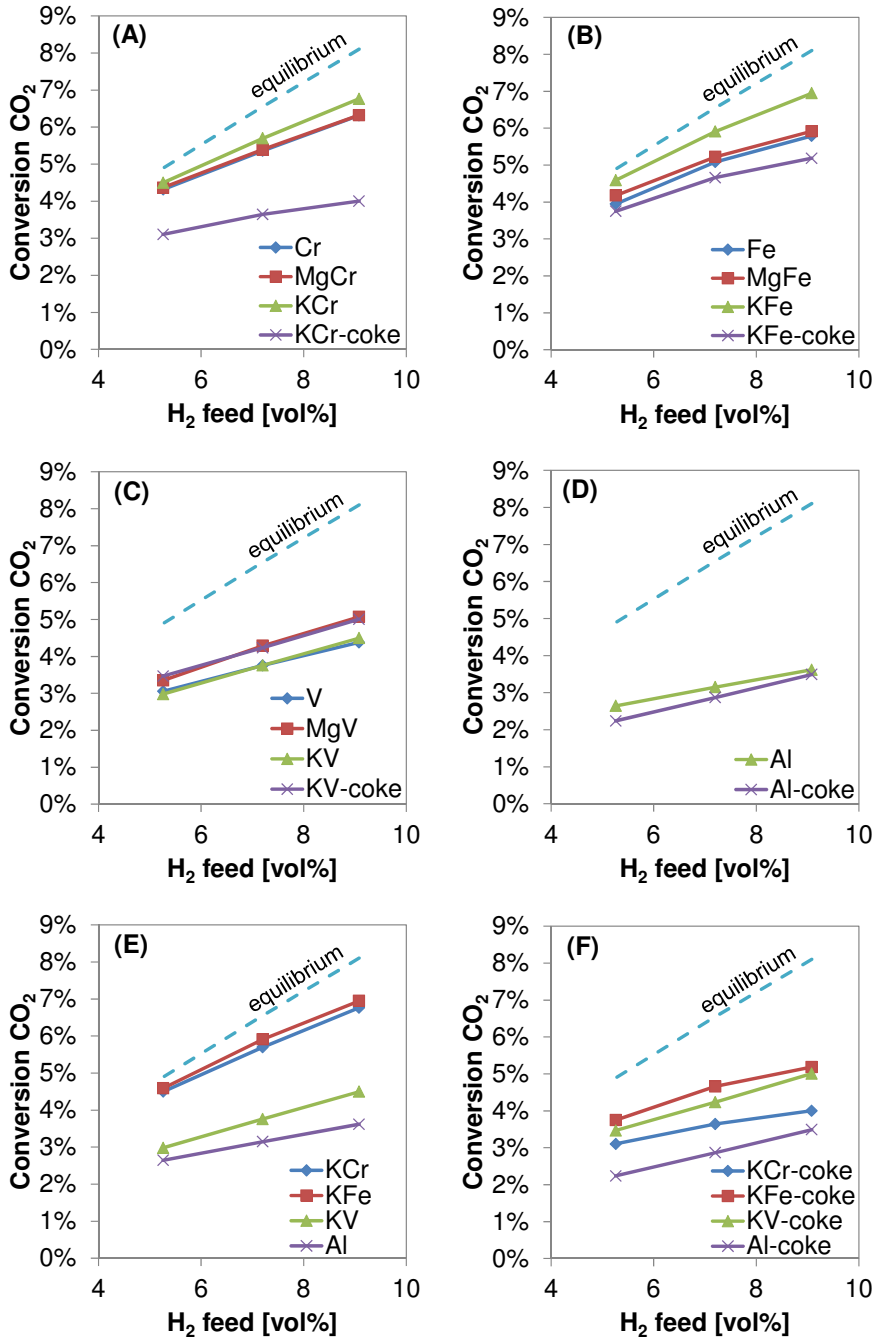

Figure 4.4: Conversion of CO_2 versus the amount of H_2 fed in RWGS experiments for γ-Al_2O_3 supported chromium (A), iron (B), vanadium (C), the γ-Al_2O_3 support (D) and the un-coked (E) and coked (F) samples for comparison. For reference purposes, the equilibrium conversions of CO_2 for the different H_2 feed concentrations are also displayed.

activity, the magnesium promoter only has a small effect on the CO_2 conversion. The coked KFe catalyst shows, again, that the presence of coke deactivates the RWGS reaction. The vanadium series (Figure 4.4-C) shows a different trend. For the vanadium catalyst, magnesium proves to be a better promoter than potassium. The coked KV catalyst does not seem to be deactivated at all for the RWGS reaction. Compared to the other vanadium catalysts, it actually performs slightly better. The alumina support (Figure 4.4-D) does show some CO_2 conversion, 2.5-3.5%, but this is dramatically lower than all the other catalysts. The coke on the alumina sample (Al-coke) clearly deactivated the RWGS reaction even further. Its conversion of CO_2 is lower at all conditions. Comparing the potassium promoted chromium, iron and vanadium catalysts with each other and bare alumina (Figure 4.4-E), it is clear that KCr is the best RWGS catalyst, followed closely by KFe. For both these catalysts, potassium is a good promoter for the RWGS reaction. The KV catalyst or bare alumina are not good RWGS catalysts, much lower CO_2 conversions are obtained than by the KCr and KFe catalyst. Of the coked samples (Figure 4.4-F) the iron catalyst is the most active, followed by the vanadium and chromium catalysts.

The reverse water-gas-shift activity during EB dehydrogenation of the potassium promoted catalysts (KCr, KFe, KV), V catalyst and alumina support, expressed as R_{RWGS} that indicates the approach to equilibrium, is shown in Figure 4.5. The KCr and KFe catalysts show a decrease of the RWGS activity in the first 10 h and then seem to stabilize. The KV catalyst shows a high and constant RWGS activity during the whole experiment, its R_{RWGS} is about 85%, close to the equilibrium value. The R_{RWGS} value of the KCr and KFe catalysts are much lower, 13% and 20%, respectively. The R_{RWGS} value for the bare alumina is very low, 5% and is slowly going down during the experiment. The R_{RWGS} value of the un-promoted V catalyst goes up in the first two hours and then stabilizes around a value of 28%.

The reverse water-gas-shift activities, in the absence of EB dehydrogenation, of the fresh and coked potassium promoted catalysts (KCr, KFe, KV) and the Al_2O_3 support, expressed as R_{RWGS}, are shown in Figure 4.6. The best catalyst, fresh KCr, approaches only half of the equilibrium value. Fresh KFe catalyst starts at about the same activity, but slowly decreases in time, to 35% of the equilibrium value at 20 h time on stream. The fresh KV catalyst has a much lower activity, attaining only 15% of the equilibrium value, slowly decreasing in time. The ratio of CO_2 and H_2 was changed after 12 and 16 h time on stream, but the R_{RWGS} did not change with a different gas composition. All the coked catalysts have a stable RWGS activity. The differences between the coked catalysts are much smaller than between the fresh catalysts.

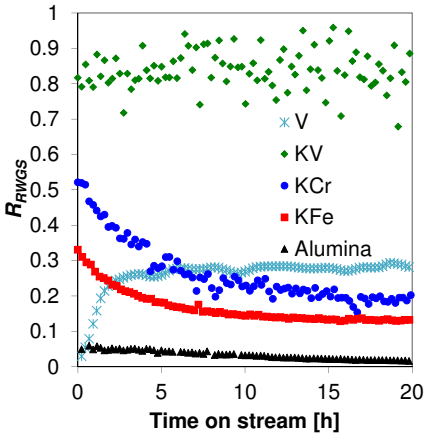

Figure 4.5: The RWGS approach to equilibrium versus time on stream for dehydrogenation experiments in CO_2 over Al_2O_3-based catalysts

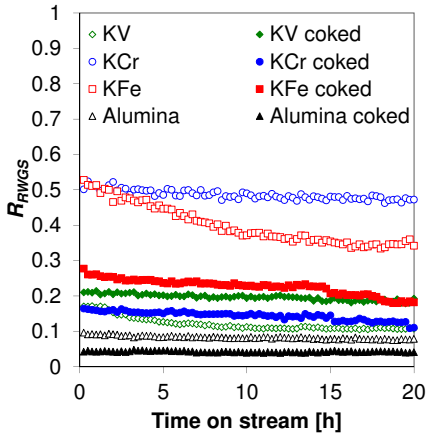

Figure 4.6: The RWGS approach to equilibrium versus time on stream for RWGS experiments with fresh and coked Al_2O_3-based catalyst samples.

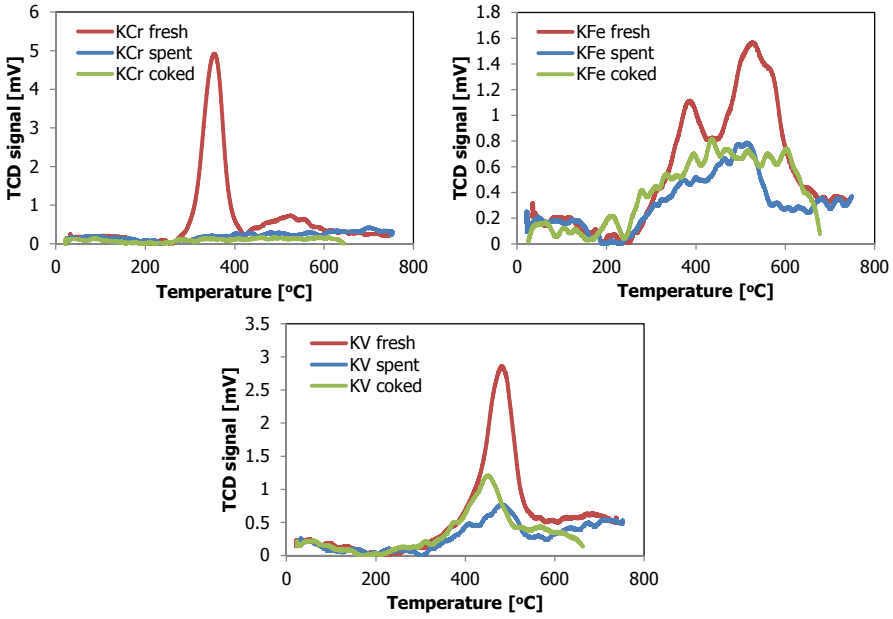

Figure 4.7: TPR profiles of fresh (red), spent (after RWGS, blue) and coked (after dehydrogenation, green) Al_2O_3-based catalysts of KCr (top left), KFe (top right) and KV (bottom).

Table 4.1: Quantification of the TPR results. Step 1: KCr = 230-420 °C, KFe = 230-430 °C, KV = 230-640 °C. Step 2: KCr = 420-640 °C , KFe = 430-640 °C. Linear baseline correction is applied.

Sample	Area step 1	Area step 2
KCr-fresh	251	64
KCr-spent	0	21
KCr-coked	13	24
KFe-fresh	61	176
KFe-spent	35	75
KFe-coked	46	92
KV-fresh	206	
KV-spent	48	
KV-coked	93	

4.3.2 Catalyst characterization

The TPR results of the KCr, KFe and KV catalysts in fresh, spent (after RWGS) and coked (after dehydrogenation) form, are displayed in Figure 4.7. The areas under these curves have been calculated and are tabulated in Table 4.1.

The fresh KCr sample shows two reduction steps, a large peak around 350 °C and a small one around 500 °C. These steps can be ascribed to the reduction of Cr^{6+} to Cr^{3+} and Cr^{3+} to Cr^{2+}, respectively.[19-21] On the fresh catalyst, almost half of the chromia is present as Cr^{6+}, also Cr^{3+} is already available. The spent and coked catalyst do not show any peaks and are considered to be in the reduced state.

The fresh KFe profile also consists of two reduction steps, around 400 °C and around 550 °C. The first step is assigned to the transformation of Fe_2O_3 to Fe_3O_4, the second step is the reduction of Fe_3O_4 to FeO.[22-25] Within the error of the measurement, the full sample is reduced from Fe^{3+} to Fe^{2+}. The spent KFe catalyst does not show distinct reduction peaks, but the TCD signal is elevated in both reduction regions, therefore some of both iron phases are probably still present. The same holds for the coked KFe sample. These samples are partly reduced under reaction conditions.

In the TPR profiles of the KV samples, only one reduction step is observed around 500 °C, the transformation of V^{5+} to V^{4+}.[26-29] The fresh sample is completely in V^{5+} state. In the spent and coked sample, most vanadium is in V^{4+} oxidation state, but some V^{5+} is still present. These samples are partly reduced under reaction conditions.

With the coked catalyst samples methane can also be formed during TPR analysis. As a result of the methane formation the TCD signal becomes negative, even though H_2 is consumed. Mass spectroscopy showed that methane was only produced above 650 °C. These data are not shown in Figure 4.7.

The amount of coke before and after RWGS testing of the coked catalyst samples is analysed by TGA. Coke is deposited during the EB dehydrogenation in CO_2 over these catalysts, before the RWGS testing. The results in Table 4.2 show that the amount

Table 4.2: Amounts of coke before and after RWGS testing and surface areas of the fresh and spent (coked) KCr, KFe and KV samples.

Catalyst	S_A [m^2/g] fresh	S_A [m^2/g] coked	Coke before [wt%]	Coke after [wt%]
KCr	224	94	24.9	24.2
KFe	230	113	22.4	21.5
KV	224	93	29.9	28.8
Alumina	303	208	22.1	20.1

of carbon hardly changes during the RWGS testing so no substantial coke gasification by hydrogen, steam or carbon dioxide takes place. The specific surface areas of the fresh and coked catalyst samples are determined by N_2 adsorption (Table 4.2). The surface area of a coked catalyst is about half that of a fresh catalyst. Among the fresh or coked catalyst series, the differences are not considered to be significant.

4.3.3 Step-response experiments

Data from the mass spectrometer (MS) on CO_2 (m/e = 44), H_2 (m/e = 2), CO (m/e = 28) and H_2O (m/e = 18) were recorded during the step-response experiments and are displayed in Figure 4.8 for the bare alumina and in Figure 4.9 for the V catalyst. Each experiment took more than 4 h in total. The y-axes are arbitrary, the MS signals of CO and CO_2 are on the same scale, but the orders of magnitude are different from H_2 and from H_2O. The data can only be compared qualitatively. The ratio of CO to CO_2 signal is also given on the right axis, this is about 1.2 when only CO_2 is fed and no reaction takes place. When this ratio is higher than 1.2, it indicates that CO is produced. In between each period, argon is flowing over the catalyst to flush the system and reach steady-state (base-line) MS signals.

A short description of each of the six periods:

1. In the first period (a-b) with CO_2 only, nothing special is observed from the MS data, the catalysts are unaffected.
2. The second period (c-d) with only H_2, on both samples some CO is produced (the CO/CO_2 ratio is larger than 1.2) together with H_2O. The bare alumina produced more CO and is known to adsorb and/or form carbonates easily.[30] The peak of water (c) and delay in H_2 appearance indicates a reduction of the vanadium catalyst. This is not observed over the Al_2O_3.
3. The third period (e-f), with only CO_2, has no effect on the Al_2O_3. Some CO is produced on the vanadium catalyst (e) without production of H_2O, indicating the (re)oxidation of the vanadium.
4. During the fourth period (g-h) with H_2 and CO_2 feed, RWGS occurs on both catalysts. Conversion on vanadium catalyst is much higher, as is shown by the

ratio CO to CO_2. The initial peak of the CO/CO_2 ratio at (g) is due to the interaction of CO_2 with the catalysts (adsorption and chemisorption) that delays the breakthrough of CO_2 compared to that of CO. This effect is stronger on bare Al_2O_3. No initial peak of CO production is observed.

5. The fifth period (i-j-k-l) is very comparable to the third and fourth period combined. On the V catalyst some CO is formed when CO_2 feeding starts (i). When H_2 is fed together with CO_2 (j-k), RWGS is observed on Al_2O_3 and V catalyst. The CO_2 signal clearly drops during the RWGS reaction (j-k). Over Al_2O_3, the CO production peaks initially, then evolves to its steady-state value. At (k) the CO signal from Al_2O_3 drops instantaneous. The CO signal from the V catalyst shows a delay, indicating again the (re)oxidation of the vanadium.
6. The sixth period (m-n-o-p) shows a combination of the second and fourth period. Some CO is produced over both catalysts when only H_2 is fed (m-n), with both feeds RWGS is clearly observed (n-o). The H_2 signal clearly drops when CO_2 is fed (n-o). When the CO_2 feed is stopped (o), the RWGS reaction still continues, its rate decreasing quickly. The CO_2 signal decreases much faster than the CO signal, giving a ratio above 1.2.

Step-response experiments were also done with Cr and Fe catalysts; these gave comparable results as with the V catalyst.

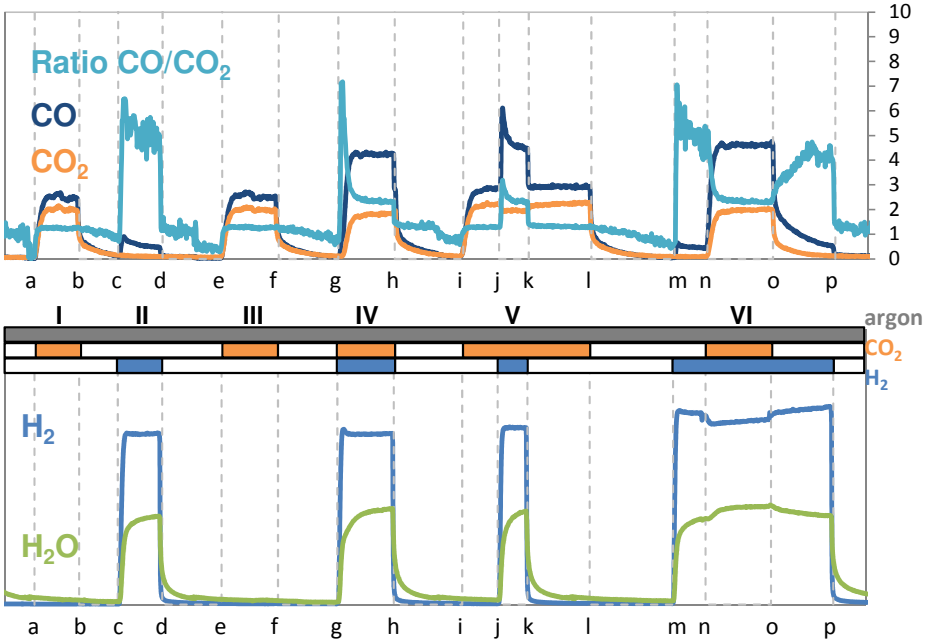

Figure 4.8: Mass spectrometry results from step-response experiments on bare alumina support. The bars (grey for argon, orange for CO_2 and blue for H_2) indicate which gas is fed over the catalyst.

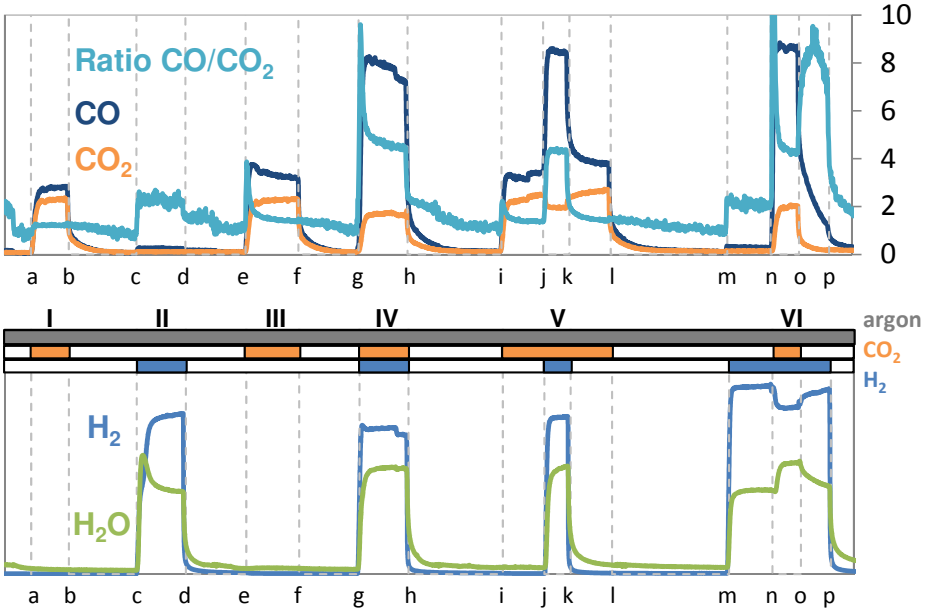

Figure 4.9: Mass spectrometry results from step-response experiments on V catalyst. The bars (grey for argon, orange for CO_2 and blue for H_2) indicate which gas is fed over the catalyst.

4.4 Discussion

The dehydrogenation experiments clearly show the advantage of using CO_2 as a diluent. All catalysts show higher EB conversions in dehydrogenation in CO_2 than in N_2 as diluent. In the presence of CO_2, the produced hydrogen can be removed by the RWGS reaction, increasing the equilibrium conversion of EB. In N_2 diluent the H_2 product cannot react. Adding a potassium promoter to these catalysts improves the EB conversion in CO_2 even more, compared to the un-promoted catalysts. The KV catalyst shows the highest RWGS activity and the largest difference between the CO_2 and N_2 diluent. This R_{RWGS} value indicates an approach of 85% of the value at equilibrium. The other catalysts have much lower activities and also have smaller differences between the CO_2 and N_2 diluent. A high RWGS activity is necessary for an improved dehydrogenation performance in CO_2. A medium or low RWGS activity will not influence the dehydrogenation conversion.

The RWGS experiments show a clear trend that chromium is the best catalyst, followed by iron. Vanadium is a poor RWGS catalyst. A comparison based on R_{RWGS} values is a better measure, because of the reversible nature of the (R)WGS reaction. Chromium is easily reduced to Cr^{3+} as shown in the TPR profile in Figure 4.7 and has stable activity during the experiment, as the R_{RWGS} parameter shows in Figure 4.5. Iron is partially reduced during the experiment, all oxidised states seem to be present in the spent catalyst. During the experiment, R_{RWGS} is going down, indicating that the catalyst deactivates. A slow transformation of the iron species into inactive Fe^{2+} could be responsible for the deactivation.[31] Vanadium shows the lowest R_{RWGS} values. Both V^{5+} and V^{4+} are present after reaction. Adding a magnesium promoter to the catalysts shows a positive effect for vanadium. The potassium promoter improves the activity of both iron and chromium catalysts. The enhanced adsorption CO_2 of due to the basicity of the potassium and hence a higher intermediate concentration, is thought to be the reason for this improvement. The potassium can also assist in the oxygen transfer to the iron or chromium oxide in the redox mechanism (see below).

Although different catalysts are tested with different promoters, none of them reach the equilibrium conversion under the testing conditions. Even changing the gas composition in the RWGS experiments does not have an effect on R_{RWGS}, even though the hydrogen concentration changes from 5% to 9%. Of course the conversion changes (Figure 4.4), but with a different composition the equilibrium conversion changes as well. For these reasons we compare activities based on the R_{RWGS}. It appears that the change in hydrogen concentration balances the effect of varying the hydrogen contact time with the catalyst, giving equal R_{RWGS} values. A better RWGS catalyst should be made by improving its hydrogen dissociation and CO_2 oxidation properties. This can possibly be achieved by introducing noble metals and by introducing more and stronger

basic sites.

The fact that none of the catalysts have a R_{RWGS} value larger than one (CO concentrations higher than expected from equilibrium conversion) suggests that the two-step pathway with RWGS and dehydrogenation is most likely. In case of the one-step pathway, much more CO product would be expected, giving R_{RWGS} values larger than one. Sun *et al.*[17] analyses the one-step and two-step mechanism slightly different, the one-step pathway being the reaction of CO_2 with adsorbed hydrogen from the dehydrogenation reaction and the two-step pathway would be the reaction between molecular hydrogen and CO_2. This will however both give the same end result (both H_2 and CO can be produced) and does not differentiate one pathway from the other. The difference between the one- and two-step pathway is sometimes also simplified by assigning all the CO_2 converted to the one-step pathway and all the formed H_2 to the two-step pathway.[2] This ignores the fact that in the two-step pathway both H_2 and CO are formed.

The step-response experiments give mechanistic information on the RWGS reaction. Both the alumina supported vanadia catalyst and the bare alumina show RWGS activity. The activity being the highest for the V catalyst. Carbon dioxide is easily transformed into carbonate on the alumina support surface and is converted into CO and H_2O when H_2 is fed *(associative mechanism)*. On the V catalyst, part of the alumina surface is not covered with vanadia. Some carbonates are still formed, but less than on the bare support, leading to lower amounts of CO with the V catalyst in the period (c-d). Hydrogen does not appear to adsorb, as no RWGS is observed at (e-f) over both catalysts. Hydrogen does, however, reduce the vanadium in the period (c-d) *(redox mechanism)*. When CO_2 is fed after the reduction, it is initially converted into CO by oxidizing the vanadium (e-f) until the vanadium cannot be oxidised further *(redox mechanism)*. These experiments show the clear differences between the two mechanisms proposed in the literature, the redox and associative mechanism.[9] A simplified reaction scheme is shown in Figure 4.10. On the support only the associative RWGS mechanism takes place and on the metal oxide catalyst the redox mechanism. On a supported metal oxide catalyst

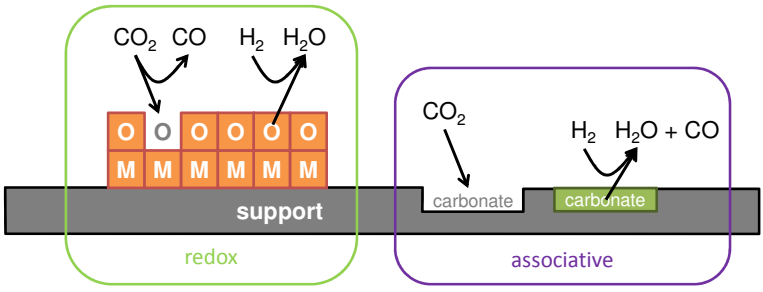

Figure 4.10: Simplified scheme for the redox and associative mechanism of RWGS (only showing the forward reaction).

both mechanisms have to take place, because the catalyst loading is below monolayer coverage. As the activity of the supported catalyst is much higher than of the support alone, the redox mechanism has the largest contribution to the RWGS activity.

The dehydrogenation experiments also show a large challenge that needs to be (re)solved: the catalyst deactivation by the excessive coke formation. All the tested catalysts deactivate. When the catalysts deactivate, the beneficial effect of CO_2 disappears. Coke is not active for the RWGS reaction, but a limited amount of coke needs to be present for selective dehydrogenation (Ch. 3). Therefore the coked catalysts from the dehydrogenation reaction are also tested for their RWGS activity without dehydrogenation (Figure 4.6). This should give a more realistic view on the role of the RWGS in the EB dehydrogenation because the catalyst composition is closer to the actual catalyst during dehydrogenation in CO_2. The iron and chromium catalysts are clearly deactivated due to the presence of coke on the catalyst surface that can block the active RWGS sites, but the vanadium catalyst shows the opposite. The presence of coke enhances the RWGS activity of the vanadium catalyst, although the coke itself does not show RWGS activity. The differences in the R_{RWGS} (Figure 4.6) between the coked catalysts are much smaller than for the fresh catalysts.

Comparing the R_{RWGS} values from the fresh catalysts in dehydrogenation (Figure 4.5) and in RWGS experiments (Figure 4.6), there seems to be no correlation. The poorest catalyst for RWGS, KV, is the best catalyst for dehydrogenation in CO_2 with the highest CO_2 conversion. This is consistent with other literature results.[17] Fresh KCr and KFe catalysts start with similar activities for the RWGS and dehydrogenation, but deactivate during the process of the dehydrogenation due to the coke formation and possibly over-reduction of the metal oxide as in case of KFe. The increase in RWGS activity under dehydrogenation conditions of the KV catalyst is striking. As a plausible explanation it is speculated that the coke, where the dehydrogenation takes place and the hydrogen is generated, functions as a hydrogen supply to the RWGS catalyst. The hydrogen spills over from the coke to the metal sites. This system shows the typical characteristics of spillover, where the sum (CO_2 conversion during the dehydrogenation in CO_2) is much larger than the separate parts (CO_2 conversion during RWGS).[32-35] The RWGS activity over the alumina support is low, as is also the case for the V and KV catalysts. Coke has a positive effect on the RWGS activity (and CO_2 conversion) of the KV catalyst, but when adsorbed hydrogen is produced from the dehydrogenation the CO_2 conversion is much higher (and the associated RWGS activity). In this case it is not necessary that molecular hydrogen dissociates, as the hydrogen atoms are already provided by the dehydrogenation reaction. This can explain the similar activities of all the coked catalysts, where hydrogen spill-over is the rate determining step in RWGS. Without coke and dehydrogenation, hydrogen dissociation is very likely the rate-limiting step on

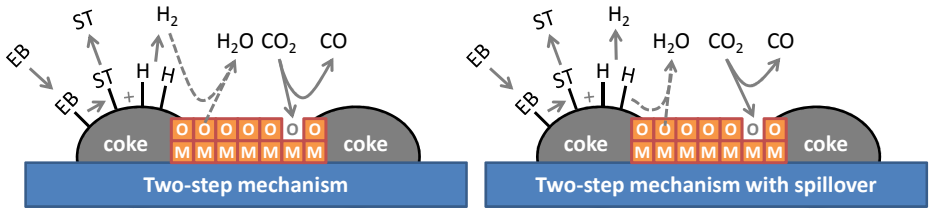

Figure 4.11: Schematic with the original two-step mechanism (*left*) and the proposed two-step mechanism with spillover of hydrogen (*right*).

the vanadium catalyst.

The observations also have its consequences for the mechanism of dehydrogenation in CO_2. Returning to the proposed pathways by Sun *et al.* (Figure 4.2), step 2-2 seems to be of minor importance. Their "one-step" mechanism is already constituted of a dehydrogenation, a hydrogen spill-over and a RWGS step. During the dehydrogenation in CO_2, coke is always present. All the coked catalysts yield similar CO_2 conversions in RWGS, even though the fresh catalysts have very different and higher RWGS activities. The RWGS activity of the catalysts in the presence of dehydrogenation in CO_2 is not changing, the responsible sites for (R)WGS are still accessible despite the large amounts of coke. The conversion of CO_2 during dehydrogenation shows no correlation with CO_2 conversions in RWGS experiments. Proof of a real one-step mechanism, where di-hydrogen is unable to form, has not been observed. During all the dehydrogenation experiments in CO_2, more hydrogen is measured than would be expected from the RWGS equilibrium. It is also not strictly a two-step mechanism, but a two-step approach with a hydrogen spill-over describes the system best. Figure 4.11 shows two simplified reaction schemes for the original two-step mechanism and the proposed two-step mechanism. In the proposed mechanism the adsorbed hydrogen, formed on the coke by dehydrogenation of EB (step 1), spills over from the coke to the metal oxide, where it reduces the metal and forms water (step 2); part of the adsorbed hydrogen forms molecular hydrogen and desorbs. Carbon dioxide oxidizes the reduced metal site again. It is also possible that the associative RWGS takes place simultaneously on the catalyst support, giving a slightly different two-step mechanism where carbonates react with adsorbed hydrogen. However, as was demonstrated with RWGS over the bare alumina, the associative mechanism has a much lower activity on the catalysts.

4.5 Conclusions

The reverse water-gas-shift reaction is an important part of dehydrogenation in CO_2. However, a direct correlation between the catalytic RWGS activity in the absence and presence of dehydrogenation was not found. The presence of coke and the combina-

tion with a dehydrogenation reaction have a different influence on the catalytic RWGS reaction, depending on the catalyst. Hydrogen for the RWGS reaction originates from adsorbed hydrogen, generated in the dehydrogenation, that spills over from the coke to the RWGS catalyst. A new mechanism, including the hydrogen spill-over, is proposed. RWGS activity in the presence and absence of dehydrogenation cannot be compared. The RWGS activity of the KV catalyst is even enhanced. The dominant routes are the redox mechanism for the RWGS reaction and the two-step pathway for the dehydrogenation in CO_2.

References

[1] G.I. Fedorov, S.G. Sibgatullin, N.L. Solodova, R.I. Izmailov, Pet. Chem. 16 (1976) 157-162.
[2] S. Sato, M. Ohhara, T. Sodesawa, F. Nozaki, Appl. Catal. 37 (1988) 207-215.
[3] S.E. Park, S.C. Han, J. Ind. Eng. Chem. 10 (2004) 1257-1269.
[4] A.L. Sun, Z.F. Qin, J.G. Wang, Appl. Catal. A: Gen. 234 (2002) 179-189.
[5] Y. Sakurai, T. Suzaki, N. Ikenaga, T. Suzuki, Appl. Catal. A: Gen. 192 (2000) 281-288.
[6] N. Mimura, M. Saito, Catal. Today. 55 (2000) 173-178.
[7] D.H. James, W.M. Castor, Ullmann's Encyclopedia of Industrial Chemistry, Wiley-VCH Verlag GmbH & Co. KGaA, 2002.
[8] F. Cavani, F. Trifiro, Appl. Catal. A: Gen. 133 (1995) 219-239.
[9] C. Rhodes, G.J. Hutchings, A.M. Ward, Catal. Today. 23 (1995) 43-58.
[10] O.S. Joo, K.D. Jung, Bull. Korean Chem. Soc. 24 (2003) 86-90.
[11] C.S. Chen, W.H. Cheng, S.S. Lin, Catal. Lett. 68 (2000) 45-48.
[12] C.S. Chen, W.H. Cheng, Catal. Lett. 83 (2002) 121-126.
[13] K.H. Ernst, C.T. Campbell, G. Moretti, J. Catal. 134 (1992) 66-74.
[14] S. Fujita, M. Usui, N. Takezawa, J. Catal. 134 (1992) 220-225.
[15] Y. Lei, N.W. Cant, D.L. Trimm, J. Catal. 239 (2006) 227-236.
[16] M.J.L. Gines, A.J. Marchi, C.R. Apesteguia, Appl. Catal. A-Gen. 154 (1997) 155-171.
[17] A.L. Sun, Z.F. Qin, S.W. Chen, J.G. Wang, J. Mol. Catal. A: Chem. 210 (2004) 189-195.
[18] *I.E.* Wachs, Catal. Today. 27 (1996) 437-455.
[19] S.D. Yim, I.S. Nam, J. Catal. 221 (2004) 601-611.
[20] Z. Sarbak, W. Jozwiak, J. Therm. Anal. Calorim. 85 (2006) 335-337.
[21] S.M.K. Airaksinen, A.O.I. Krause, J. Sainio, J. Lahtinen, K.J. Chao, M.O. Guerrero-Perez, M.A. Banares, PCCP. 5 (2003) 4371-4377.
[22] H.J. Wan, B.S. Wu, C.H. Zhang, H.W. Xiang, Y.W. Li, B.F. Xu, F. Yi, Catal. Commun. 8 (2007) 1538-1545.
[23] X.T. Gao, J.Y. Shen, Y.F. Hsia, Y. Chen, J Chem Soc Faraday T. 89 (1993) 1079-1084.
[24] D.B. Bukur, C. Sivaraj, Appl. Catal. A: Gen. 231 (2002) 201-214.
[25] J.Y. Park, Y.J. Lee, P.K. Khanna, K.W. Jun, J.W. Bae, Y.H. Kim, J. Mol. Catal. A: Chem. 323 (2010) 84-90.

[26] E.P. Reddy, R.S. Varma, J. Catal. 221 (2004) 93-101.
[27] K.V.R. Chary, G. Kishan, C.P. Kumar, G.V. Sagar, Appl. Catal. A: Gen. 246 (2003) 335-350.
[28] M.M. Koranne, J.G. Goodwin, G. Marcelin, J. Catal. 148 (1994) 369-377.
[29] S.W. Chen, Z.F. Qin, X.F. Xu, J.G. Wang, Appl. Catal. A: Gen. 302 (2006) 185-192.
[30] J.C. Lavalley, Catal. Today. 27 (1996) 377-401.
[31] G.R. Meima, P.G. Menon, Appl. Catal. A: Gen. 212 (2001) 239-245.
[32] W.C. Conner, J.L. Falconer, Chem. Rev. 95 (1995) 759-788.
[33] P.C.H. Mitchell, A.J. Ramirez-Cuesta, S.F. Parker, J. Tomkinson, J. Mol. Struct. 651 (2003) 781-785.
[34] G.M. Pajonk, Appl. Catal. A: Gen. 202 (2000) 157-169.
[35] J.A. Menendez, L.R. Radovic, B. Xia, J. Phillips, J. Phys. Chem. 100 (1996) 17243-17248.

5

Catalyst stability – Effect of CO_2

Abstract

A series of potassium on γ-Al_2O_3 catalysts were prepared in order to see the effect on the catalyst stability for the ethylbenzene dehydrogenation in CO_2. Besides CO_2 also H_2O was added as a second oxidant for the coke gasification. In both cases a stable catalyst was not found under the applied conditions. The addition of potassium (0.1-2.0 mmol/g Al_2O_3) had a positive effect on the rate of activation, styrene selectivity, RWGS activity and rate of deactivation. Low loadings of potassium decreased the rate of activation, high loadings showed an increased rate of activation and deactivation. The cracking selectivity was decreased with all potassium catalysts. The addition of steam inhibits the RWGS reaction and diminishes the advantage of the use of CO_2 in dehydrogenation. The sample with 1.5 mmol/g potassium was stable for the dehydrogenation in nitrogen-steam diluent in the absence of CO_2.

5.1 Introduction

This chapter discusses a few experiments that were exploited to see if the stability of the alumina based catalysts could be improved for the dehydrogenation in CO_2. Bare γ-Al_2O_3 becomes active and selective for the dehydrogenation reactions, but CO_2 has no effect on the activity or selectivity (Ch. 3). It is envisaged for the dehydrogenation process in CO_2 that CO_2 reacts with H_2 and elevates the thermodynamic equilibrium and that CO_2 should remove any excess coke that is on the catalyst. The stability of the catalysts is largely determined by the amounts of coke that are being formed under reaction conditions. Some of this coke is needed to catalyse the dehydrogenation reaction (Chapters 3 and 4), but too much coke will reduce the available catalytic surface and make the catalyst inefficient. The problem of too much coke can be addressed from two directions: either form less coke during reaction or remove coke under reaction conditions.

For the initial catalyst stability testing experiments, the performance of γ-Al_2O_3 was compared with catalysts containing 1 mmol/g of K, Mg, or V. These promotors were added to reduce the acidity, or improve the redox properties of the γ-Al_2O_3 catalyst. These results (Figure 5.1) showed that the addition of potassium to the alumina improves the overall performance. It showed the highest selectivity during these experiments. The V promoted catalyst initially has the highest conversion, but also deactivates the fastest. Magnesium on alumina takes much longer to become active and selective and cannot compete with the other catalysts. These initial experiments give the

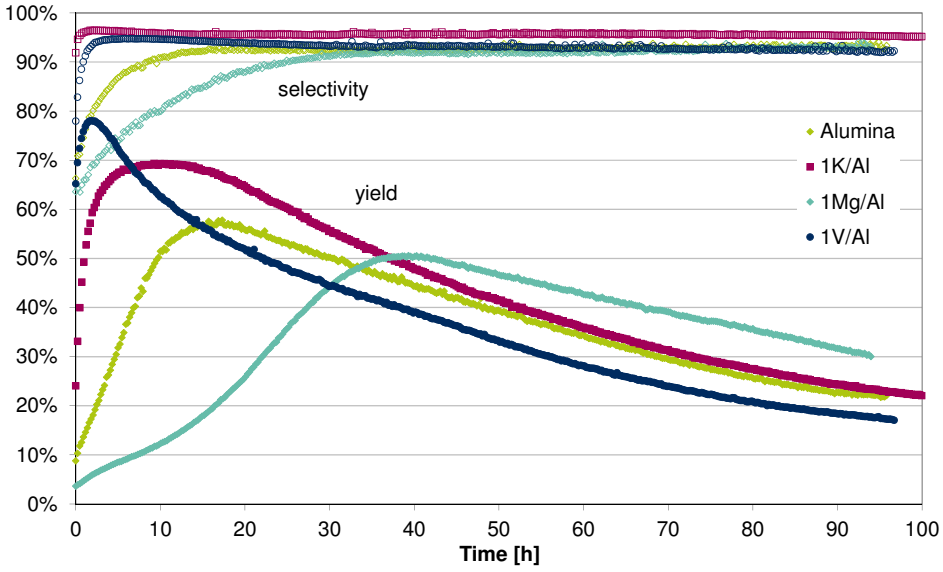

Figure 5.1: Styrene yield and selectivity for alumina supported Mg, K, V and bare alumina for the dehydrogenation of EB to ST in CO_2 at 600 °C and an CO_2:EB feed ratio of 10.

impetus to focus on potassium addition and optimize its loading. Potassium improves the RWGS activity, ST selectivity and ST yield.

The catalytic coal gasification studies with steam show that the alkali metals have a good gasification activity. They are also good catalysts for carbon gasification with CO_2. There appears to be a correlation between the ionisation potential and the catalytic activity: Cs > K > Na > Li.[1] However, the conditions of catalysed carbon gasification (~700-800 °C and a molar H_2O/C ratio of 1.2) are very different from the conditions of the dehydrogenation in CO_2 (600 °C and some H_2O from RWGS). Actually, many gases have been tested and showed a gasification activity. The (temperature dependent) gasification activity of the different oxidants in the coal gasification with potassium is in the following order: $O_2 > N_2O > NO > H_2O > CO_2$, all with about an order of magnitude difference.[2-4] For the catalytic carbon gasification specifically, four gases show a gasification potential: H_2, CO_2, O_2, H_2O.[5] The carbon gasification studies also show the significance of a good contact between the catalyst and the carbon, possible mobility of the catalyst and the spill-over of the oxygen from the catalyst to carbon.[2, 5] The addition of alkali to the alumina will also have an effect on the acidity of the catalyst. The formation of coke proceeds over the acidic centres on the surface. Reduction of the acidic sites can also help to improve the catalyst stability.

Another option to improve the catalyst stability is to utilize a mixture of gasification agents. Steam is a logic choice, this is already present in the product stream, although in small quantities. Steam is ~3 times more reactive than CO_2. Allowing a small amount of H_2O in the feed mixture, combined with a good gasification catalyst could result in a stable process. This has been proven to work in oxidative dehydrogenation of butane, although high steam:butane ratios (> 20) were applied.[6] However, the feeding of too much steam will give the same disadvantage as the current steam-aided dehydrogenation: large energy losses due to fast quenching of the product stream that does not allow a good heat recovery.

For this study, a series of six potassium loaded aluminas were prepared. The loading was varied between 0.1 and 2.0 mmol/g. These samples will be subjected to the different diluents (CO_2, N_2 and H_2O) and mixtures of these diluents to find the best conditions and K-loading for a good performing catalyst with high ST yield, high CO_2 conversion and good stability.

5.2 Experimental

5.2.1 Catalyst preparation

The γ-Al_2O_3 support (Ketjen CK300-000-1.5P, 0.52 ml/g, 190 m^2/g) was crushed and sieved to 212-425 μm and dried at 120 °C overnight. The potassium was introduced by impregnation using the incipient wetness method. The required amounts of KNO_3 were dissolved in demineralized-water, after which the γ-alumina support was impregnated with the solution. The impregnated support was then dried at 120 °C in air for four hours, followed by calcination in a static air calcination oven at 600 °C for four hours. The chosen loadings are 0.1, 0.25, 0.5, 1.0, 1.5 and 2.0 mmol/g. Short names for the catalysts are used in this chapter. The name 1.5K/Al means a potassium loading of 1.5 mmol/g on alumina.

5.2.2 Catalyst testing CO_2 ODH of EB

The dehydrogenation experiments were performed in a parallel fixed bed setup with six reactors. Each reactor had independent gas (CO_2 or N_2) and liquid feed (ethylbenzene and/or H_2O). The temperature and pressure of the reactors were equal and set at 600 °C and atmospheric pressure, respectively. The amount of catalyst loaded was 1000 mg, in a 4 mm inner diameter quartz tube. On top of the catalyst bed was a 5 cm layer of SiC to preheat the feed. The catalyst bed and SiC were fixed in the quartz tube by quartz wool plugs. The liquid feed flow rate was 1 g/h EB (3.5 Nml/min vapour), the diluent gas flow rate was 31.5 ml/min, N_2 or CO_2. This gives a 1:9 molar ratio of ethylbenzene and CO_2 or N_2. Normally a liquid feed flow rate of 1 g/h H_2O is used for the experiments with steam (21.4 Nml/min vapour), giving a H_2O:EB feed ratio of about 6. Also feed ratios of 10 (1.7 g/h H_2O) and 1.5 (0.25 g/h H_2O) were used. Before starting the experiment the reactor is heated up with 10 °C/min and allowed to stabilize at the reaction temperature for half an hour under a CO_2 or N_2 flow. The experiment was started by feeding the ethylbenzene to the reactor.

During the dehydrogenation experiments, the concentrations in the reactor effluent were measured online by a two channel gas chromatograph with a TCD (columns: 0.3m Hayesep Q 80-100 mesh with back-flush option, 25 m × 0.53 mm Porabond Q and 15 m × 0.53 mm molsieve 5A with bypass option for CO_2 and H_2O, all in series) for permanent gas analysis (CO_2, H_2, N_2, O_2, CO) and a FID (column: 30 m × 0.53 mm, D_f = 3 μm, RTX-1) for the hydrocarbons analysis (methane, ethane, ethene, benzene, toluene, ethylbenzene, styrene, heavy aromatics). One analysis, from start to start, takes 15 minutes. Six reactors and one reference gas analysis gives that each reactor was analysed every 1¾ h in order to follow the catalyst performance over time. A constant flow of nitrogen was used as internal standard. The internal standard was fed just before the

GC. Conversions, selectivities and yields are based on moles of ethylbenzene and calculated according to the equations 3.6, 3.7 and 5.3. The overall carbon balance is > 99%, only carbon that was deposited on the catalyst as coke is missing from the carbon balance by GC. The R_{RWGS} that is used as an indicator for RWGS activity is calculated according to equation 3.8 for dehydrogenation in only CO_2 diluent. When water is fed, equation 5.5 is used. In case of the RWGS equilibrium, R_{RWGS} reaches 100% (equilibrium constant $K_{eq} = 0.38$).

$$conversion = \frac{ethylbenzene_{in} - ethylbenzene_{out}}{ethylbenzene_{in}} \quad 5.1$$

$$selectivity = \frac{styrene_{out}}{ethylbenzene_{in} - ethylbenzene_{out}} \quad 5.2$$

$$yield = selectivity \times conversion \quad 5.3$$

$$R_{RWGS,CO_2only} = \frac{[CO][ST - H_2]}{[CO_2][H_2]} / K_{eq} \times 100\% \quad 5.4$$

$$R_{RWGS} = \frac{[CO][H_2O]}{[CO_2][H_2]} / K_{eq} \times 100\% \quad 5.5$$

5.3 Results

5.3.1 Dehydrogenation in CO_2

The performance of the potassium loaded aluminas in CO_2 diluent is presented in Figure 5.2. For comparison purposes the bare alumina performance is also shown. Low loadings of the potassium (0.1, 0.25, 0.5) give a delay in the catalyst activation and the coke formation. The optimum in the yield shifts in time from 15 h (0) to 30 h (0.1), to 50 h (0.25 and 0.5) for these samples. The optimum yield is comparable with bare alumina. The 1K/Al sample shows a 10% improvement of the optimum yield at 15 h. The samples of 1.5K/Al and 2K/Al both show a 20% improvement of the optimum yield at 5 h. These two samples (1.5 and 2.0) deactivate faster than the other samples. After a little more than 10 h, the 1K/Al sample has a better yield. All these samples show an optimum in the yield with time, after which they deactivate.

By the addition of potassium, the ST selectivity of the alumina is improved from 92% up to 96%. Less cracking products (benzene, toluene) are observed. Small amounts of the potassium already show an improvement. The 1.5K/Al sample shows the highest selectivity to styrene, but the differences are very small between the 1.0, 1.5 and 2.0 loadings. The optimal selectivity and optimum ST yield are reached at the same time for each catalyst, although the time on stream of this event varies for the different catalysts. The selectivity *versus* time of 1K/Al shows a deviating trend in the first 10 hours, when the yield is increasing. During this period, the moles of CO and H_2 are lower than the moles of styrene, probably due to the GC detection limit of H_2 under these conditions. The R_{RWGS} values also show erratic behaviour in this period, probably due to the deviating CO and H_2 amounts.

The reverse water-gas-shift (RWGS) activities of all samples are also shown in Figure 5.2. The more potassium is loaded on alumina, the higher the activity of the RWGS and as a consequence the conversion of CO_2. The highest RWGS activity, of 2K/Al, approaches 50-60% of equilibrium. The R_{RWGS} values are not constant. The values decrease when the catalyst deactivates.

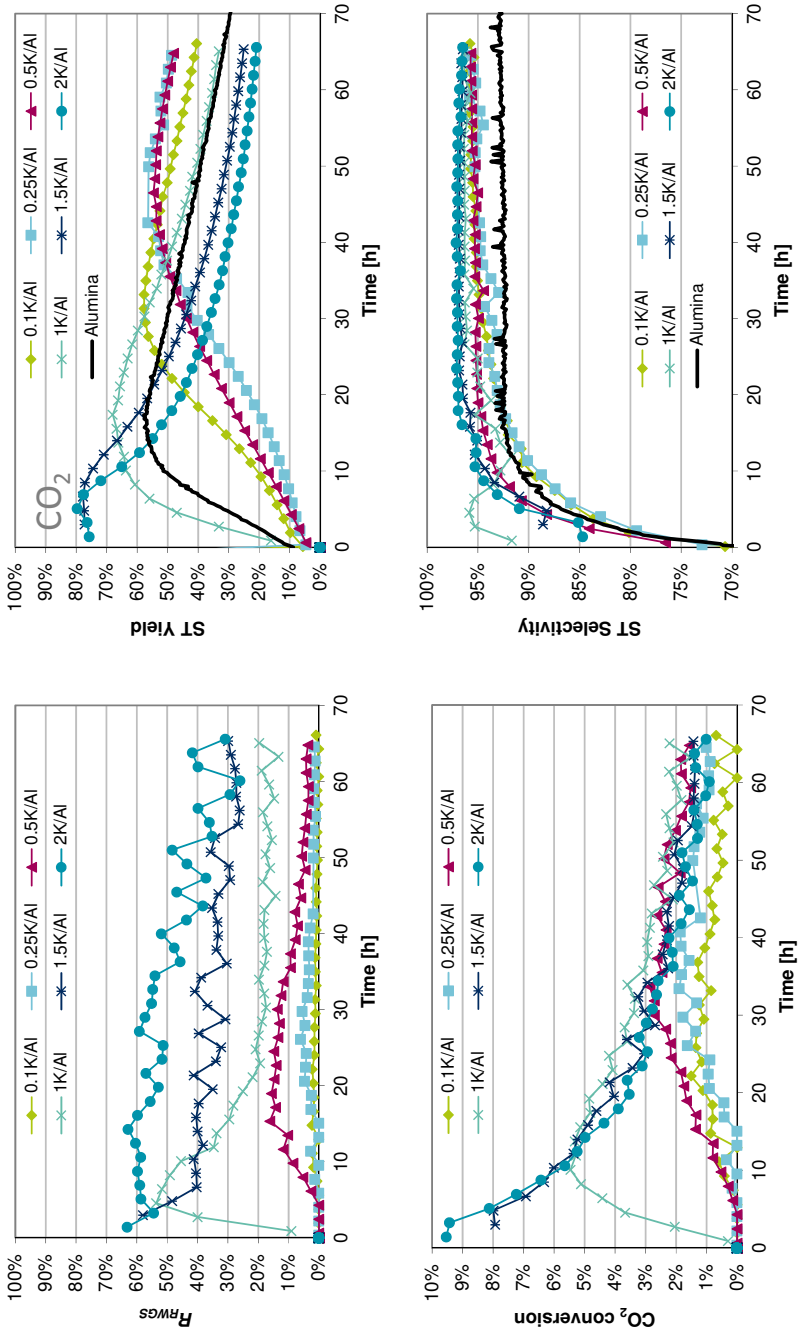

Figure 5.2: Styrene yield (top left), styrene selectivity (top right), R_{RWGS} (bottom left) and CO_2 conversion (bottom right) at 600 °C in CO_2 diluent for potassium modified alumina catalysts with different loadings (given in mmol/g).

5.3.2 Dehydrogenation in N_2, CO_2/H_2O and N_2/H_2O

This series of potassium on alumina samples were tested with different diluents. In between the experiments, the samples were regenerated with diluted air (6 vol% O_2) for 10 h. The evolving amounts of CO and CO_2 were negligible after 5 h. Regeneration had no effect on the catalyst performance. The same activation coupled with selectivity increase was observed.

In Figure 5.3, the yields of the samples are shown in the different diluents. The top graph is copied from Figure 5.2, for an easier comparison. The middle graph shows the yield in the nitrogen diluent. The bottom graph shows a mixture of CO_2 and H_2O for the first 50 h *TOS (time on stream)*, where after N_2 replaced CO_2 for another 15 h *TOS*. In the nitrogen diluent (Figure 5.3, *middle*), some of the samples are less active than of the bare alumina (0.1K/Al, 1K/Al), or do not become active at all (0.25K/Al, 0.5K/Al). The highest two loadings of potassium (1.5K/Al, 2K/Al) have a higher yield than those of the bare alumina initially, but only up to 10 h *TOS*. Compared with the CO_2 experiments (Figure 5.3, *top*), the yields of the K series in the N_2 diluent are at least 10% lower. The bare alumina has initially a little higher yield than the bare alumina in CO_2. The selectivities of the 0.1K/Al, 1.5K/Al and 2K/Al samples were comparable to the selectivities in CO_2. The other samples did not become active and selective.

When CO_2 is combined with H_2O (Figure 5.3, *bottom*), the catalysts need much more time to become active, or do not show any activity. Only the highest two potassium loadings (1.5K/Al and 2K/Al) show a reasonable yield of 70% after 20 h *TOS* for 2K/Al and 50% for 1.5K/Al after 45 h. It seemed that the 2K/Al sample was stable after 20 h *TOS*, but after 35 h *TOS* it started to deactivate. The 1.5K/Al sample did not reach a stable yield in 50 h *TOS* in CO_2 and H_2O, the yield was still slowly increasing as a function of *TOS*. After 50 h *TOS*, the CO_2 was replaced by N_2. The 2K/Al sample continued to deactivate, but the 1.5K/Al sample stabilised at a 60% styrene yield under these conditions. The selectivity of the 1.5K/Al and 2K/Al samples was comparable to the selectivity in CO_2. The other samples did not become active and selective. The yield in this experiment with H_2O is about 10% lower than for the similar experiment in CO_2 (Figure 5.3, *top*). The conversion in CO_2 in combination with H_2O was also lower. The presence of H_2O has a large effect on the net CO_2 conversion as is shown in Figure 5.4. The maximum CO_2 conversion decreased from 10% to 5%. Due to the high concentration of H_2O, the R_{RWGS} value appears to be a little higher, 80% *versus* 60% without H_2O feed.

An additional experiment with vanadium, iron and chromium catalysts was done to evaluate the effect of H_2O on the RWGS reaction over these catalysts. The R_{RWGS} values and CO_2 conversions are shown in Figure 5.5. A small amount of water reduces the CO_2 conversion. Adding more water, the CO_2 conversion become almost negligible.

The effect of H_2O on the RWGS activity appears to be small, comparing with the data from Chapter 4 (Figure 4.5). The RWGS reaction deactivates together with the DH reaction. The addition of water in these experiments could not prevent the catalyst deactivation.

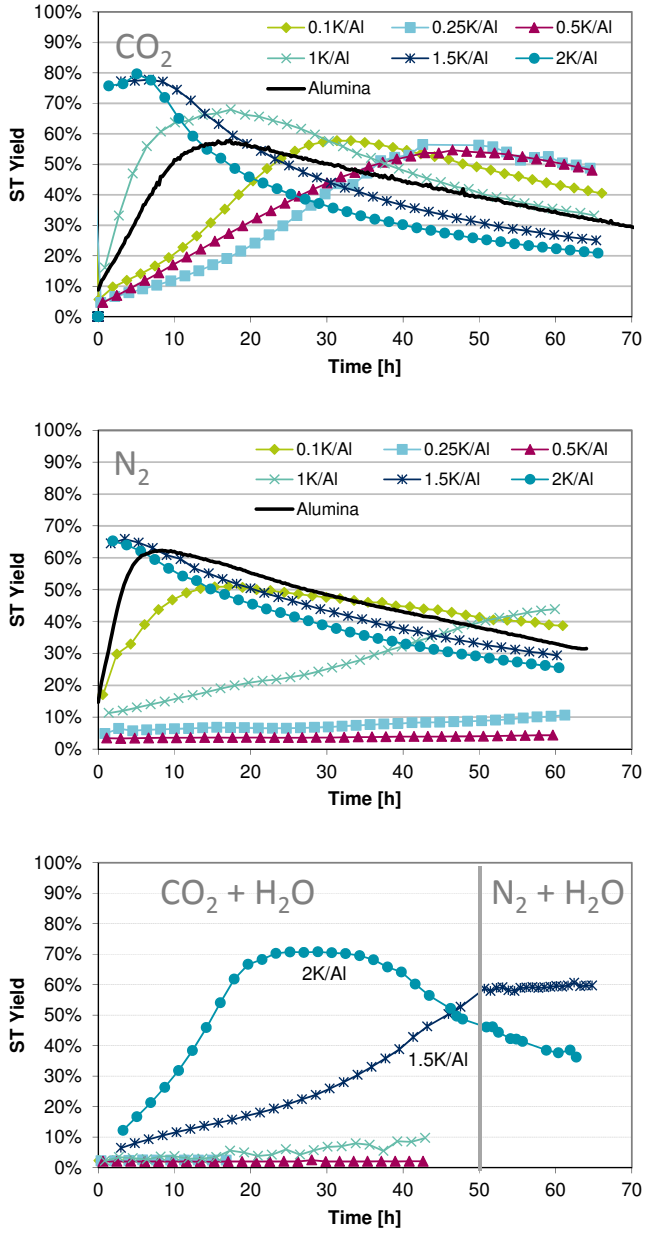

Figure 5.3: Styrene yields in CO_2 diluent (top), N_2 diluent (middle) and CO_2 or N_2 with H_2O (bottom) at 600 °C for potassium modified alumina catalysts with different loadings (given in mmol/g). (CO_2 or N_2):EB feed ratio of 9, H_2O:EB feed ratio of 6.

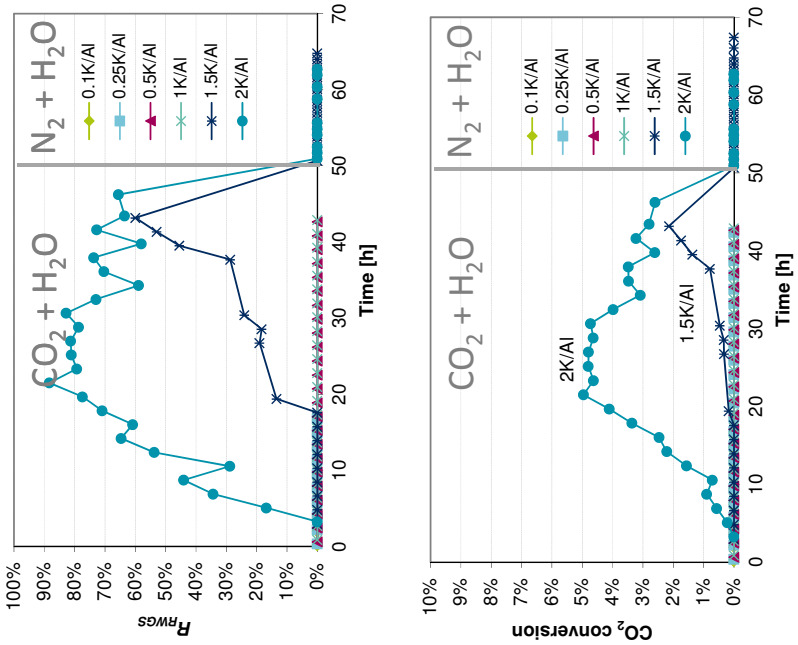

Figure 5.4: The activity of the RWGS reaction as R_{RWGS} (left) and CO_2 conversion (right) in time for the mixed diluents experiment at 600 °C. (CO_2 or N_2):EB feed ratio of 9, H_2O:EB feed ratio of 6.

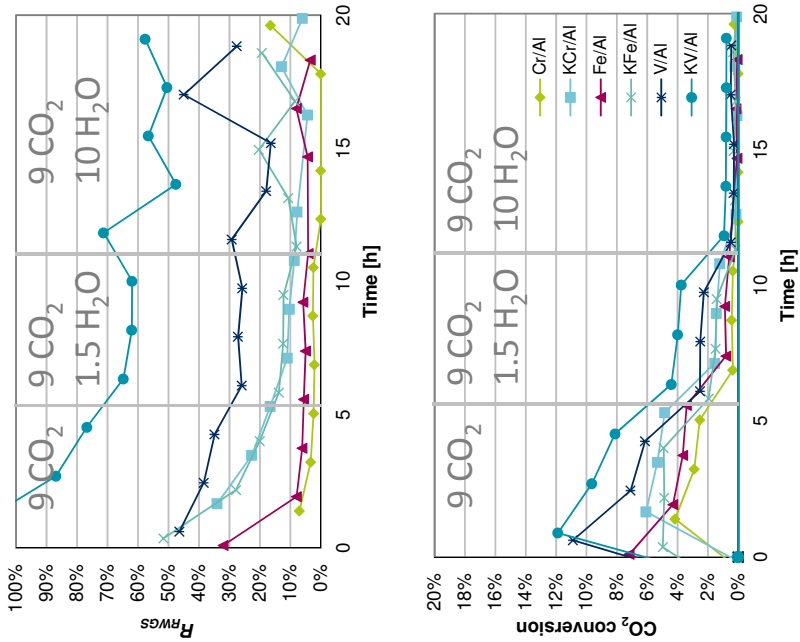

Figure 5.5: The activity of Fe, V, Cr catalysts in the RWGS reaction with different amounts of CO_2 and H_2O at 600 °C in terms of R_{RWGS} and CO_2 conversion as a function of time.

5.4 Discussion

5.4.1 Dehydrogenation in CO_2

By varying the potassium loading in the alumina catalysts we observed samples that activate faster, or slower and become more selective than the bare alumina, but a stable catalyst was not found. The K addition is envisaged as an acid site titration of alumina. Plotting the ST yield around 6 h *TOS* versus the potassium loading (Figure 5.6) shows a minimum ST yield around 0.25 mmol K / g Al_2O_3. The samples around this minimum have such a low number of acid sites and low site density that it is very hard to form the active coke that catalyses the dehydrogenation reaction.[5] The lower number of acid sites due to K addition is also reflected in the selectivity. Especially the cracking to benzene and toluene, that are acid catalysed reactions, is reduced. Similar to the 1Mg/Al sample (Figure 5.1) of the initial exploratory results, these samples become active and selective, but it takes much longer. This has no effect on the relatively poor stability. Initially the coke formation of the samples around the minimum is slower, but the formation of multilayer coke is not affected. Multilayer coke is responsible for the catalyst deactivation. The deactivation rates of the samples are very similar. The samples with higher potassium loadings exhibit a faster activation, but also a faster deactivation. Because of the high RWGS activity, these samples also show higher styrene yields. Like we concluded before (Ch. 4), the reverse Boudouard reaction, *i.e.* gasification, hardly takes place and cannot match with the coke formation rate, even though potassium is a catalyst for CO_2 gasification.[2] The temperature should be increased to start coke gasification by CO_2 at a reasonable rate,[2] but that will be at the cost of styrene selectivity due to increased cracking to mainly benzene and toluene.

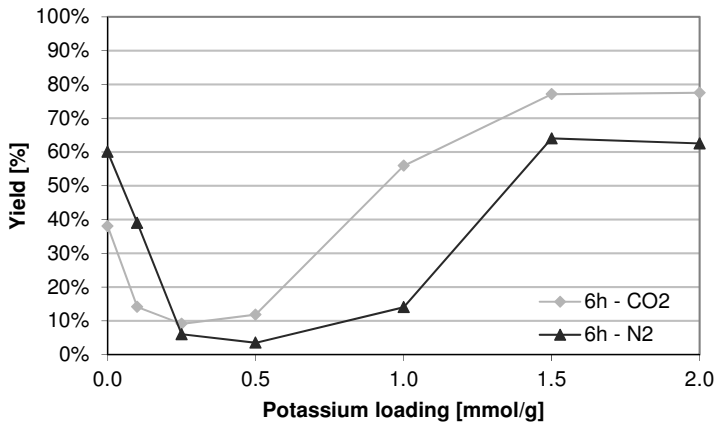

Figure 5.6: Styrene yield versus potassium loading on alumina after six hours on stream in N_2 or CO_2 diluent in the EB dehydrogenation at 600 °C.

5.4.2 Dehydrogenation in N_2, CO_2/H_2O and N_2/H_2O

In nitrogen as diluent, the effect of the acid sites neutralisation by potassium is even larger. Two of the samples do not become active at all, as coke is probably not being formed. Looking at the differences between CO_2 and N_2 diluent, it almost seems like CO_2 also has an effect on the coke formation. This could be by adsorptive effects, creating acidic sites such as carbonates that participate in either or both coke formation and dehydrogenation in a one-step mechanism as discussed in Chapter 4.

With the CO_2 - H_2O diluent mixture, only the samples with the highest potassium loading seem to be able to form coke and become active and selective. This is possibly due to the enhanced coke gasification by the steam. Although the gasification is enhanced by steam addition, it is not able to completely stabilize the catalyst in the presence of CO_2. Replacing the CO_2 by N_2, the 1.5K/Al sample seems stable and the 2.0K/Al sample seems to be too far in the deactivation by coke or K has be partly lost by volatilization.[7]

Another effect of the steam addition is a reduced effect of the RWGS reaction, because the feed is already closer to equilibrium as steam is a product of this reaction. Indeed lower CO_2 conversions are observed and therefore, lower styrene yields. The experiment with the Fe, Cr and V catalysts shows that water inhibits the RWGS reaction. A small amount of H_2O has a large effect on the CO_2 conversion. This diminishes the advantage of CO_2 for the dehydrogenation reaction. An improvement of the stability has to come through another way than the steam addition. It had been shown before that steam gasification is inhibited by CO_2, H_2 and CO,[2] and all are present in the reaction mixture.

The performance of the high potassium loaded alumina's in N_2 plus H_2O shows similarities to the commercial catalyst. It shows stable and high yields, but without the presence of iron oxide (the main part of the commercial catalyst formulation). A similar active phase of coke in both systems is therefore, very likely. The potassium stabilizes the amount of coke by gasification with the steam. The role of iron oxide could be to function as a binder that prevents the potassium volatilisation in the steam environment.[5]

The gasification of coke should be possible under the dehydrogenation conditions. The gasification agents like hydrogen, carbon dioxide and water are all present, but also influence each other. Improving the spillover of hydrogen or oxygen atoms from the catalyst may improve the coke gasification. Adding another promoter to the K/Al sample could be an interesting start, examples could be antimony[8] or rhodium.[9]

A final comment has to be made on the comparisons in this chapter: the experiments were done with different γ-Al_2O_3 sources. The reference alumina (Engelhard) used in this thesis is other than the γ-Al_2O_3 for the K-series (Ketjen CK300) and also

different from the Cr, Fe, V series (Ketjen 000-3P). Impurities and characteristics like surface area and acidity are slightly different and can influence the rate of activation and the overall selectivity. However, quite similar trends are observed on all three alumina samples. Although their performances are not exactly the same it does not change the observations or conclusions.

5.5 Conclusions

The addition of potassium to alumina does not result in a stable catalyst for the EB dehydrogenation in CO_2. At the applied reaction conditions (600 °C), the catalysed coke gasification does not take place. The addition of steam to CO_2 had a detrimental effect on CO_2 conversion and dehydrogenation activity and did not yield a stable catalyst performance either. Using only steam with N_2, in the absence of CO_2, the 1.5K/Al catalyst showed stable performance. Coke gasification activity in CO_2 should be a priority for further catalysts development for the process of dehydrogenation in CO_2.

References

[1] F. Kapteijn, G. Abbel, J.A. Moulijn, Fuel. 63 (1984) 1036-1042.
[2] R. Meijer, F. Kapteijn, J.A. Moulijn, Fuel. 73 (1994) 723-730.
[3] J.A. Moulijn, F. Kapteijn, Carbon. 33 (1995) 1155-1165.
[4] R. Meijer, B. Van der Linden, F. Kapteijn, J.A. Moulijn, Fuel. 70 (1991) 205-214.
[5] D.L. Trimm, Appl. Catal. 5 (1983) 263-290.
[6] J.C. Jung, H. Kim, Y.S. Kim, Y.M. Chung, T.J. Kim, S.J. Lee, S.H. Oh, I.K. Song, Appl. Catal. A: Gen. 317 (2007) 244-249.
[7] G.R. Meima, P.G. Menon, Appl. Catal. A: Gen. 212 (2001) 239-245.
[8] V.P. Vislovskiy, J.S. Chang, M.S. Park, S.E. Park, Catal. Commun. 3 (2002) 227-231.
[9] W.C. Conner, J.L. Falconer, Chem. Rev. 95 (1995) 759-788.

6

Screening I: Effect of CO_2 on the oxidative dehydrogenation of ethylbenzene to styrene

Abstract

A wide range of alumina based catalysts are screened for their performance in the oxidative dehydrogenation reaction. The coke on the catalyst is the active phase. A temperature of 450 °C is found to be optimal for EB conversion and ST selectivity, since above this temperature cracking becomes significant and below this temperature much more heavy condensates are formed, both giving a lower ST selectivity. A lower O_2:EB ratio gives a lower EB conversion, but a higher ST selectivity because of a lower CO_X production. The effect of CO_2 on the ODH reaction was of special interest, but a significant effect is not found. Within the screened catalysts, P, K, or B containing samples showed an improvement in the ODH performance. A 150 h stability test showed that this improvement is only temporary. After 70 h time on stream all samples perform equal or less compared with the reference catalyst γ-Al_2O_3 (Albemarle). Samples that contain noble metals or transition metals have a poor performance because of high CO_X production. A comparison of the styrene yields after about 30 h and 60 h time on stream learns that the reference γ-Al_2O_3 has the best stability, only 5% of the styrene yield is lost. The catalysts deactivate due to excessive coke formation.

6.1 Introduction

The oxidative dehydrogenation (ODH) reaction is a strongly exothermic reaction. This reaction is of large interest because it does not suffer from equilibrium limitations. The reaction stoichiometry shows that only 0.5 moles of oxygen are needed per mole of ethylbenzene, but higher ratios of 1.0 or even larger are often used to achieve high ethylbenzene (EB) conversions in laboratory studies. The process styrene (ST) selectivity suffers mainly from the reactant combustion forming CO_2 that requires 10.5 moles of O_2. The temperatures that are used vary from 300 °C to 600 °C. The highest EB conversions that are reported are 70-80% at a ST selectivity of 90%. These performances are obtained by using metal phosphates or carbon molecular sieves as catalysts.[1-3]

Other issues with ODH are safety related, because of O_2 feeding and catalyst stability due to severe coking. The addition of CO_2 has been shown to improve catalyst selectivity and activity in ODH of propane and butane[4-7]. Mainly dehydrogenation selectivity is improved from low to moderate levels. A short overview is given in Table 6.1. It will be part of this work to explore the possibilities of CO_2 co-feeding in the ODH of EB in order to improve ST selectivity and catalyst stability.

A wide range of catalyst samples has been tested for several reasons: activated carbons, as coke and other carbon materials are active for ODH[8-12]; Mesoporous aluminosilicate because it shows interesting improvement in other applications; Several aluminas for selecting the best starting material for the promoted aluminas in this chapter; Promotors such as P, B as they are known to improve the ODH performance[2-4]; just like K[13, 14]; and various metal bromides such as MnBr[15], additionally bromides are radical scavengers and can prevent radical reactions and coke deposition[8]; Mo shows a beneficial effect on CO_2 addition[7]; The VPO catalyst shows a CO_2 effect in the selective oxidation of butane to maleic anhydride[16, 17]; The BASF (FeK) catalyst is included to benchmark the dehydrogenation performance of the commercial steam dehydrogenation catalyst in ODH; The promotors Pd, Pt, Ru, Re are of interest for an increased coke gasification activity and lower steady-state amounts of coke.

The main goal of this chapter is to identify any general trends in the ODH reaction, including possible trends in and between, the catalyst series that are screened. For a

Table 6.1: Overview of CO_2 effects on oxidative dehydrogenation reactions.

Source	Reactant	Catalyst	CO_2 effect
Urlan *et al.*[4]	n-butane	TiP_2O_7	Upon CO_2 addition: conversion from 25% to 20%, dehydrogenation selectivity from 56% to 83%. Less cracking products.
Ge *et al.*[5]	n-butane	V-Mg-O	Upon CO_2 addition: conversion from 20% to 18%, dehydrogenation selectivity from 65% to 75%. Less CO_X production.
Bi *et al.*[6]	isobutane	$LaBaSmO_X$	Upon CO_2 addition: conversion from 4% to 7%, isobutene selectivity from 30% to 55%. Less cracking and CO_X production.
Zhaorigetu *et al.*[7]	propane	$Nb/PrVO_4$	Increase of yield and selectivity

good comparison of all the samples, we want to achieve full oxygen conversion under all conditions. In the results and discussion part, the catalyst performances (EB conversion, ST selectivity and stability) will be compared relative to that of bare alumina, a reference sample for oxidative dehydrogenation of EB to ST.

6.2 Experimental

6.2.1 Catalyst preparation

The γ-Al_2O_3 support (Albemarle, 0.83 ml/g, 272 m^2/g) is crushed and sieved to 212-425 μm and dried at 150 °C in vacuum for four hours. This γ-Al_2O_3 is the reference system to which all other samples will be compared in this chapter. The promotors are introduced to the γ-Al_2O_3 by impregnation using the incipient wetness method with a 5% excess of the pore volume. The required amounts of metal salts are dissolved in demineralised water, after which the γ-Al_2O_3 support is impregnated with the solution. The wetted support is shaken vigorously with an automatic shaker to homogenize the impregnated support. Next it is dried at 70 °C in air overnight, followed by calcination in a static air calcination oven at 500 °C for eight hours. The heating rate is set at 4 °C /min. A list with all samples that were prepared by impregnation is shown in Table 6.2.

Table 6.2: List of samples that were prepared by impregnation.

		Loading		Calcination		
Name	**Precursor**	**wt% M**	**Steps**	**[°C]**	**Gas**	**support**
0.1Mo/Al	$(NH_4)Mo_7O_{24}$	0.1	1	500	Air	γ-Al_2O_3
0.1Pd/Al	$Pd(NO_3)_2 \cdot H_2O$	0.1	1	500	Air	γ-Al_2O_3
0.1Pt/Al	$Pt(NH_3)_4Cl_2 \cdot H_2O$	0.1	1	500	Air	γ-Al_2O_3
0.1Re/Al	NH_4ReO_4	0.1	1	500	Air	γ-Al_2O_3
0.1Ru/Al	$RuCl_3 \cdot H_2O$	0.1	1	500	Air	γ-Al_2O_3
0.25K/Al	KNO_3	0.25	1	500	Air	γ-Al_2O_3
0.5K/Al	KNO_3	0.5	1	500	Air	γ-Al_2O_3
1B/Al	H_3BO_3	1	1	500	Air	γ-Al_2O_3
2B/Al	H_3BO_3	2	2	500	Air	γ-Al_2O_3
3B/Al	H_3BO_3	3	3	500	Air	γ-Al_2O_3
1CaBr$_2$/Al	$CaBr_2$	1	1	500	Air	γ-Al_2O_3
3CaBr$_2$/Al	$CaBr_2$	3	1	500	Air	γ-Al_2O_3
1KBr/Al	KBr	1	1	500	Air	γ-Al_2O_3
3KBr/Al	KBr	3	1	500	Air	γ-Al_2O_3
1NaBr/Al	NaBr	1	1	500	Air	γ-Al_2O_3
3NaBr/Al	NaBr	3	1	500	Air	γ-Al_2O_3
3Mn/Al	$Mn(CH_3CO_2)_2 \cdot 4H_2O$	3	1	500	Air	γ-Al_2O_3
9P/Al-300C-air	H_3PO_4	9	3	300	Air	γ-Al_2O_3
9P/Al-300C-N$_2$	H_3PO_4	9	3	300	N_2	γ-Al_2O_3
9P/Al-400C-air	H_3PO_4	9	3	400	Air	γ-Al_2O_3
9P/Al-400C-N$_2$	H_3PO_4	9	3	400	N_2	γ-Al_2O_3
9P/Al-450C-air	H_3PO_4	9	3	450	Air	γ-Al_2O_3
9P/Al-450C-N$_2$	H_3PO_4	9	3	450	N_2	γ-Al_2O_3
9P/Al-500C-N$_2$	H_3PO_4	9	3	500	N_2	γ-Al_2O_3
9P/Al-dried	H_3PO_4	9	3			γ-Al_2O_3
9P/Al-new	H_3PO_4	9	3	500	Air	γ-Al_2O_3
9P/Si-500C-air	H_3PO_4	9	3	500	Air	SiO_2

Table 6.3: List of samples that are used as received.

Name	S_A [m^2/g]	V_P [ml/g]	Other details
AC Norit ROX0.8	959	0.609	Norit
AC Norit CNR 115	1417	0.989	Norit
Al-MSU-F	605	2.03	SigmaAldrich mesoporous aluminosilicate, $(SiO_2)_{0.9875}(Al_2O_3)_{0.0125}\cdot xH_2O$
γ-Al_2O_3 (CK300)	190	0.57	Ketjen
γ-Al_2O_3 (000-3P)	303	0.56	Ketjen
γ-Al_2O_3 (Albemarle)	272	0.83	Albemarle
α-Al_2O_3	~10	0.5	Engelhard Al-4196E 1/12
VPO			Activated, commercially available
BASF			Commercial FeK catalyst for EB dehydrogenation

For one sample (9P/Si-500C-air) silica extrudates were used (Silica NorPro SS61138, 257 m^2/g, 1.00 ml/g). The silica were crushed and sieved. The sieve fraction of 212-425 μm was used for impregnation.

Other catalysts that are used are only crushed and sieved without any further (pre-) treatment. These are listed in Table 6.3.

6.2.2 Catalyst screening

The oxidative dehydrogenation experiments are performed in a parallel fixed bed reactor setup with six quartz reactors with an inner diameter of 4 mm, in down-flow operation. In a typical experiment a catalyst bed height of 65 mm is used (0.80 ml). The reactors are loaded-from top to bottom-with a quartz wool plug, 10cm glass pearls (0.5 mm diameter), the catalyst, 10 cm glass pearls (0.5 mm diameter) and a quartz wool plug. The catalyst bed is positioned within the 20 cm isothermal zone of the reactor. The reactor gas feed is a mixture that can consist of CO_2, N_2 and air. To each reactor, the gas flow rate is 36 ml/min, the liquid EB feed flow rate is 1 g/h (3.6 ml/min vapour), resulting in a 1:10 molar ratio of ethylbenzene and gas. The ethylbenzene liquid is fed into a heated α-alumina filled tube, where it is evaporated in a co-current flow with the gas feed. This evaporator is located in an oven, where also the reactor furnace is installed.

The reactors are heated up under nitrogen flow with 5 °C/min. The temperature is allowed to stabilize for another 15 minutes when the reaction temperature is reached. The EB flow is started first (1-5 minutes earlier), before any oxygen is added to the gas mixture, to prevent any pre-oxidation of the catalyst samples. The reaction starts when oxygen is added to the reactors. The pressure at the setup outlet is atmospheric, the pressure before the reactors is typically about 1.2-1.3 bara.

A testing protocol of 10 conditions is used to test the catalyst samples. This testing protocol was developed based on preliminary tests with γ-Al_2O_3 that showed optimal performance at 450 °C and a O_2:EB ratio of 0.6. It was also recognized that other cata-

Table 6.4: The catalyst testing protocol.

Condition	Time on stream [h]	Temp. [°C]	O_2:EB	CO_2:EB
1.	0-8	475	0.6	0
2.	8-14	475	0.6	5
3.	14-20	475	0.4 (0.2)	5
4.	20-26	450	0.6	0
5.	26-32	450	0.6	5
6.	32-38	450	0.4 (0.2)	5
7.	38-44	425	0.6	0
8.	44-50	425	0.6	5
9.	50-56	425	0.4 (0.2)	5
10.	56-62	450	0.6	5

lysts could have different optimal operating conditions, allowing for higher and lower temperatures and a lower O_2:EB feed ratios. The protocol consists of three temperatures, going from high to low, because this is the fastest for activating the catalyst (a break-in period is required for the initial coking of the catalyst under reaction conditions). Two O_2:EB feed ratios are used and two CO_2:EB feed ratios to see the effect of these gases on the reaction. One condition is tested twice to see the aging effect of the catalyst (the 5^{th} and 10^{th} condition). An experiment, from start to start, takes 3 days. This includes ending the experiment and starting a new one (cooling down of the reactors, replace reactor tubes, leak testing, heating up, *etc.*). The testing protocol is given in Table 6.4.

During the ODH experiments, the concentrations in the reactor effluent are measured online by a two channel gas chromatograph with a TCD (columns: 0.3m Hayesep Q 80-100 mesh with back-flush option, 25m × 0.53mm Porabond Q and 15 m × 0.53mm molsieve 5A with bypass option for CO_2 and H_2O, all in series) for permanent gas analysis (CO_2, H_2, N_2, O_2, CO) and a FID (column: 30m × 0.53mm, D_f = 3µm, RTX-1) for the hydrocarbons analysis (methane, ethane, ethene, benzene, toluene, ethylbenzene, styrene, heavy aromatics). One analysis, from start to start, takes 15 minutes. Six reactors and one reference gas analysis gives that each reactor is analysed every 1¾h in order to follow the catalyst performance with time on stream. A constant flow of nitrogen is used as the internal standard. The internal standard was fed just before the GC. The lines from the reactor to the GC are heat-traced at 175 °C to prevent condensation of the vapours. The EB conversion, selectivities and yields are based on moles of ethylbenzene and calculated according to Eqs 3.6 and 3.7. The overall carbon balance is >99%, only the carbon that is deposited on the catalyst as coke is missing from the carbon balance by the GC analysis.

$$EB\ conversion = \frac{ethylbenzene_{in} - ethylbenzene_{out}}{ethylbenzene_{in}} \qquad 6.1$$

$$ST\ selectivity = \frac{styrene_{out}}{ethylbenzene_{in} - ethylbenzene_{out}} \quad 6.2$$

$$ST\ yield = EB\ conversion \times ST\ selectivity \quad 6.3$$

6.3 Results

6.3.1 Catalyst screening

The reference experiment in Figure 6.1 with γ-Al_2O_3 (Albemarle) shows almost identical data for all six reactors. It took about 4 hours before the catalysts were active and selective. The CO_2 diluent had no significant effect. At a lower O_2:EB ratio of 0.2 instead of 0.6 (at 450 °C) the EB conversion went down from 35% to 16% and the ST selectivity went up from 83% to 88%. At the same time the CO_X selectivity went down from 17% to 10%. The reaction temperature did not have a large effect on the EB conversion or ST selectivity. At a O_2:EB ratio of 0.6 and a temperature of 475, 450 and 425 °C, the EB conversion was 33%, 35%, 34% and the ST selectivity was 81%, 82%, 81% and the CO_X selectivity was 18%, 17%, 17%, respectively. These small changes in the performance gave an optimum temperature of 450 °C. The selectivity to cracking products (benzene and toluene) went down with decreasing temperature. The selectivity to heavy condensates went up with decreasing temperature, especially at 425 °C there was a large increase in heavy condensates. The last condition (56-62 h) at 450 °C / 0.6 O_2:EB showed a decrease, compared with the earlier performance under the same conditions (26-32 h). The EB conversion decreased from 35% to 33%, the ST selectivity decreased from 82% to 81%, but CO_X selectivity increased from 17 to 18%. The testing setup showed remarkable reproducibility among the reactors. During the two years that the catalysts were screened, this experiment was repeated several times with identical outcome.

Three different γ-Al_2O_3 samples and one α-Al_2O_3 sample were tested (Figure 6.2). One γ-Al_2O_3 sample was produced by Albemarle, the other two by Ketjen (CK300 and 000-3P). The Albemarle and CK300 samples had very similar performance in the ODH reaction. The γ-Al_2O_3 (Albemarle) sample is used as the reference catalyst throughout this chapter. The 000-3P sample performed slightly less, 1-2% points difference in both EB conversion and ST selectivity compared with the other two γ-Al_2O_3 samples. An analysis by XRF showed a high amount of silica impurities (18.7 wt%) in this sample. The α-Al_2O_3 sample had a much lower surface area (~10 m^2/g) therefore, double the amount of catalyst sample volume was loaded (13 cm). With the increasing time-on-stream (*TOS*) and decreasing temperature, the EB conversion and ST selectivity improved for the α-Al_2O_3. The 10^{th} condition showed deactivation of the sample.

Figure 6.3 shows the performance of two activated carbon samples (CNR115 and ROX0.8) and a mesoporous aluminosilicate (Al-MSU-F), compared to the γ-Al_2O_3 (Albemarle) reference. The results from the two AC samples were very different. The ROX0.8 sample performed worst for the ODH reaction. The EB conversion and ST selectivity were lower than for γ-Al_2O_3. After 58 h the EB conversion and ST selectivity were lost due to the complete gasification of the starting material (activated carbon). Compared with the γ-Al_2O_3, the other AC sample (CNR115) initially performed better (at 475 °C). Later on, at 450 °C it was similar and at 425 °C it became less. This was most likely due to the temperature, as the performance at the 10th condition was the same as the 5th. A visual inspection of the reactor tube showed that some of the starting material was lost due to gasification during the testing protocol. The mesoporous aluminosilicate (Al-MSU-F) was the more favourable sample in this series. It takes longer to become active (8 h *vs.* 4 h), but initially its EB conversion (44% *vs.* 35%) and ST selectivity (84% *vs.* 81%) were higher than for the alumina at 475 °C and 0.6 O_2:EB. After 40 h and at 425 °C the difference was gone and it did not return when increasing the temperature again (10th condition).

Several samples were tested with a 9 wt% phosphorous (P) loading that were prepared by the addition of phosphoric acid on a γ-Al_2O_3 (2×) and a silica support (Figure 6.4). The two 9P/Al samples were nearly identical. At 475 °C and 450 °C, both P/Al samples did better than the bare alumina, the EB conversion increased 8% and 4% points and the ST selectivity increased 3% and 2% points, respectively. At 425 °C the bare alumina performed better. The ODH performance at the 10th condition was lower than at the 5th, these phosphorous samples deactivated from an EB conversion of 38% to 30%. The 9P/Si catalyst showed very good ST selectivity, > 90% at an O_2:EB feed ratio of 0.6. Its EB conversion was the lowest in this series (< 30%), the 9P/Si catalyst did not reach full O_2 conversion (below 50% at an O_2:EB of 0.6). The ST yield at the 10th condition was higher than at the 5th, 22% versus 20%, even though ST selectivity decreased from 90% to 88.5%. The O_2 conversion increased from 40% to 48%.

Three different loadings of boron (B) on alumina were tested and compared with bare alumina (Figure 6.5). Initially a higher loading of boron gave a higher EB conversion (EB conversion of 40%, 42% and 44%), but after 14 h there was no more difference between the boron loaded samples. At 425 °C, only the 1B/Al sample was a little better (1-2% points of EB conversion) than the bare alumina, the 2B/Al and 3B/Al sample performed worse than the bare alumina. This was also true for the 10th condition. The boron samples deactivated during testing, the 3B/Al sample deactivated most. All boron samples had a little higher ST selectivity than of the bare alumina, but differences between the boron samples were not significant at 475 °C and 450 °C. Deactivation of the samples had a clear effect on ST selectivity, it went down while deactivating.

Among the samples that were tested, not all were successful for the selective dehydrogenation of EB to ST. Three of these samples are shown in Figure 6.6 in comparison with alumina. The catalyst for steam-aided dehydrogenation from BASF (potassium promoted iron oxide catalyst) performed the worst, with a ST selectivity of 45% and lower, it hardly produced any styrene. Almost all the oxygen was used for the complete oxidation of ethylbenzene. This was similar for the 3Mn/Al (a ST selectivity of 78%) and VPO (a ST selectivity of 55%) catalysts, although less extreme than for the BASF catalyst. The data for the BASF and VPO samples are missing between 25-40 h *TOS* due to a temporary malfunction of the gas chromatograph system.

Several 9 wt% P samples were prepared with different calcination pre-treatments. These results are presented in Figure 6.7. All these samples showed very similar behaviour. Initially the P/Al samples showed improved performance compared with bare alumina, up to 8% points increase in EB conversion and up to 3% points increase in ST selectivity and they all deactivated more strongly with *TOS*. The EB conversions after 40 h showed larger differences, but these cannot be attributed to the calcination temperature or calcination gas. There was no clear trend observed. Also, the performance after 40 h was less than of the reference γ-Al_2O_3.

A series of samples with a low noble metal loading of 0.1 wt% were prepared and tested. Their performances are shown in Figure 6.8. The Ru loaded sample produced some hydrogen. This also resulted in a higher toluene selectivity (not shown). Of this series, the Ru sample performed the worst in the ODH reaction. The EB conversion (15-20%) and ST selectivity (55-65%) were the lowest in the series. The Pt and Pd samples had a lower EB conversion and ST selectivity at high O_2:EB ratios, but at low O_2:EB ratios their performance was similar to that of the alumina reference. The low loading of Re or Mo had no effect on the catalyst performance.

Two different potassium loaded aluminas were tested. Their results, together with the bare alumina reference, are shown in Figure 6.9. Initially a higher loading of K gave a higher EB conversion (+ 7% / + 9% points) and ST selectivity (+ 3% / + 4% points). The 0.5K/Al sample deactivated fast, at 450 °C it performed less than of the 0.25K/Al sample and at 425 °C it became less than of the alumina too. The 0.5K/Al sample performed clearly less in the 10^{th} condition than in the 5^{th} condition. The 0.25K/Al sample also deactivated. Initially, it did a better job than the alumina, but after 40 h its performance was similar to the bare alumina.

Three different bromide salts were deposited on alumina, each with two different loadings. The EB conversion and ST selectivity of these six samples, together with the alumina reference are presented in Figure 6.10. All samples needed more time than the alumina to become active and selective for the ODH reaction or did not become that active and selective at all. The samples with a high (3 wt%) bromide salt loading per-

formed the worst. These samples were not able to convert all the O_2 under all the applied conditions. The 3KBr/Al sample became active and selective at 475 °C and 450 °C, but it deactivated at 425 °C. Also with the low loadings, KBr was the best in respect to the Na and Ca salts. The samples with a low (1 wt%) bromide salt loading became active and selective, but had a lower performance than the alumina.

6.3.2 Catalyst stability

A 150 h stability test was done with the reference γ-Al_2O_3 (Albemarle) and the samples that showed improved performance over the reference (9P/Al, 1B/Al, Al-MSU). The results are shown in Figure 6.11. The Al-MSU sample needed 20 h to reach its optimum conversion (41%), the optimum selectivity (86%) was reached in a couple of hours. The other samples reached their optimum in activity and selectivity within a couple of hours. The 9P/Al sample and 1B/Al samples initially showed a very similar EB conversion and ST selectivity, 40% and 85% respectively, compared with 35% and 83% for the alumina. Both these samples deactivated much faster than the alumina. The performance of the 9P/Al sample became less than of the alumina after 40 h, for the 1B/Al sample this occured after 70 h. The Al-MSU sample showed an optimum performance that was comparable to 9P/Al and 1B/Al. It also deactivated and after 70 h there was no significant difference between the alumina and Al-MSU. All samples showed a decreasing selectivity to styrene with the time on stream due to the increasing production of CO and CO_2, probably due to the excessive formation of coke.

The 5^{th} and 10^{th} condition in the testing protocol are identical and can be used to investigate the stability of the samples. Figure 6.12 shows the averaged styrene yields of the 5^{th} and 10^{th} condition and the ratio of these two. Two samples, AC-CNR115 and 0.1Pd/Al, did not deactivate in the 30 h between the two conditions. The γ-Al_2O_3 samples, Albemarle, CK300 and 000-3P, lost about 5% of the ST yield at 26 h. The 9P/Al samples lost about 20% of their ST yield.

Similarly for the 150 h stability test, the maximum yields of the catalyst samples were compared with their yields after 150 h. The 9P/Al-400C-air had the highest styrene yield of 36%, about the same for the 1B/Al and Al-MSU-F samples. The maximum styrene yield of γ-Al_2O_3 was almost 30%. After 150 h, 72% of this yield remained for the γ-Al_2O_3. For the Al-MSU-F sample only 63% of the maximum yield remained, this was the same styrene yield as the γ-Al_2O_3. The 1B/Al and 9P/Al-400C-air sample resulted in less yield in 150 h.

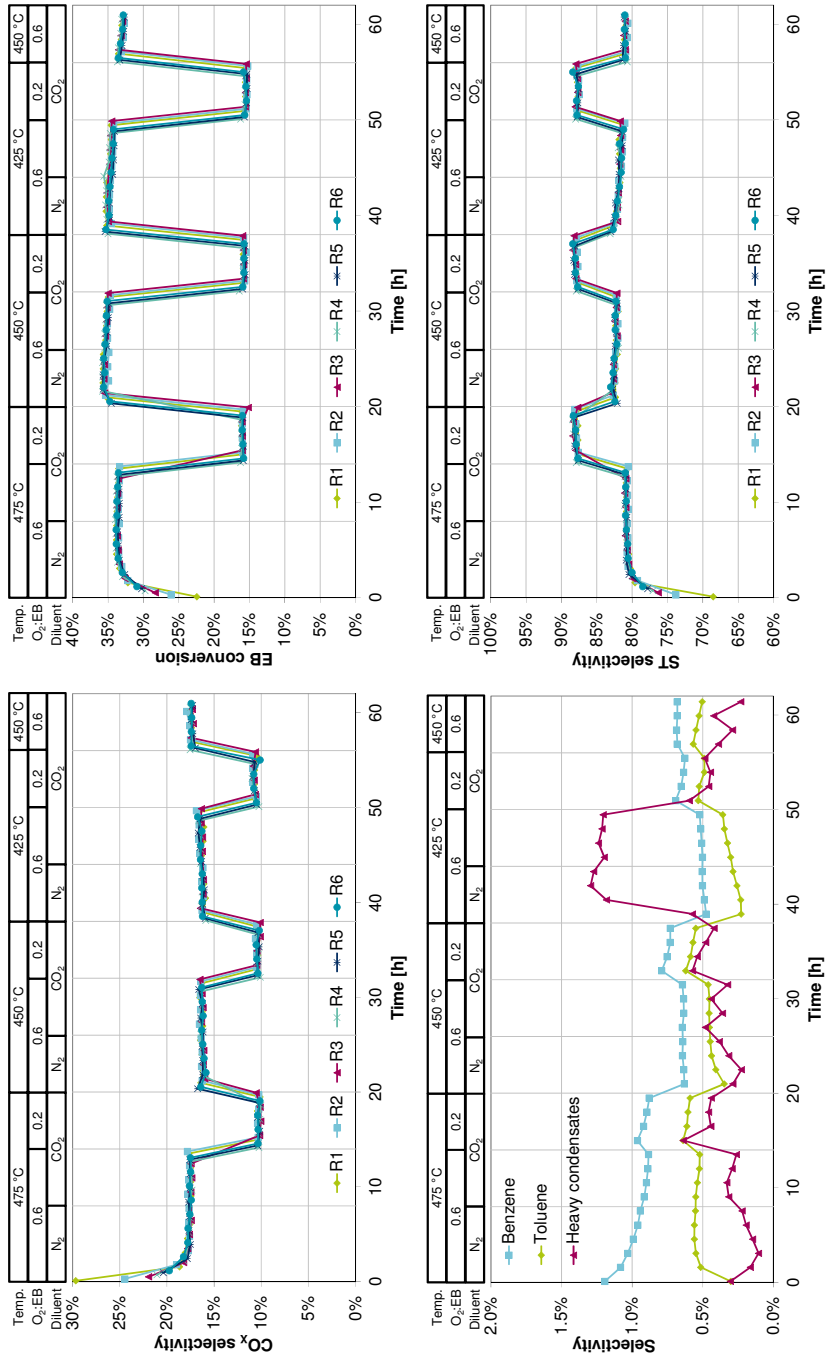

Figure 6.1: Ethylbenzene conversion (top left), styrene selectivity (top right) and CO_X selectivity (bottom left) for the six parallel reactors and selectivity to benzene, toluene and heavy condensates for reactor 1 (bottom right, the other reactors give similar selectivities to by-products), each reactor loaded with 500 mg γ-Al_2O_3 (CK300).

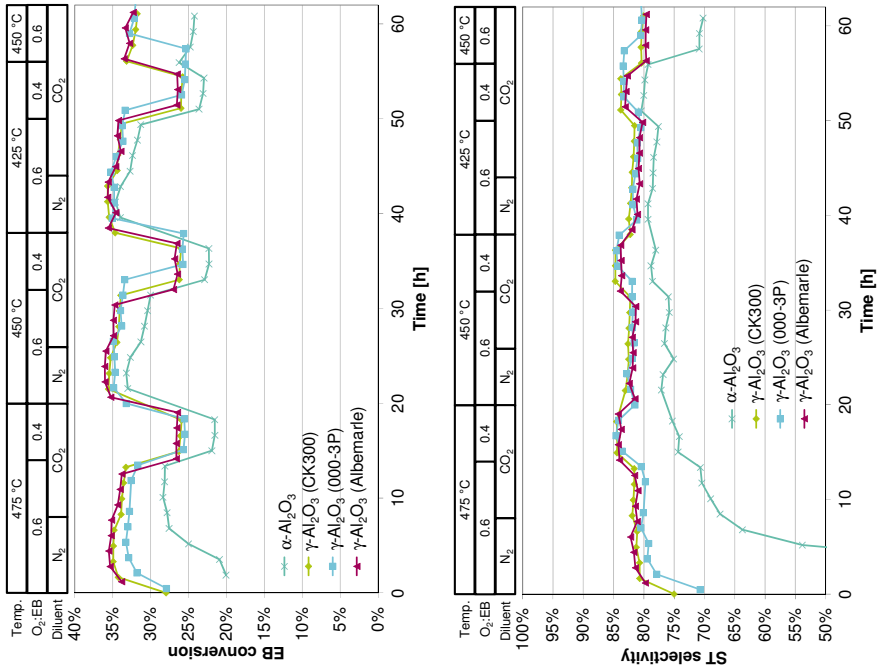

Figure 6.2: EB conversion (left) and ST selectivity (right) for different aluminas.

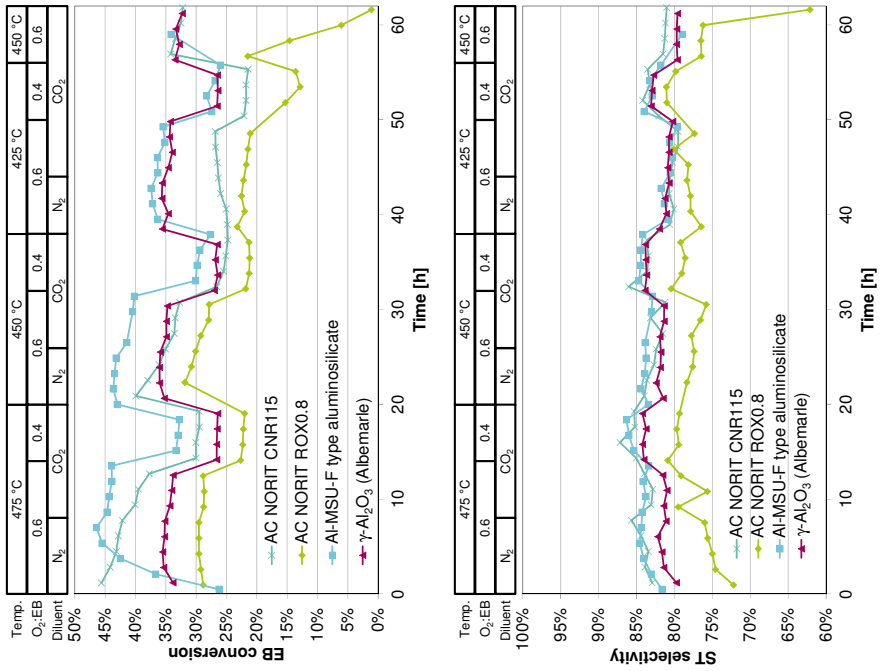

Figure 6.3: EB conversion (left) and ST selectivity (right) for two activated carbons, mesoporous aluminosilicate and γ-Al_2O_3 (Albemarle) for reference.

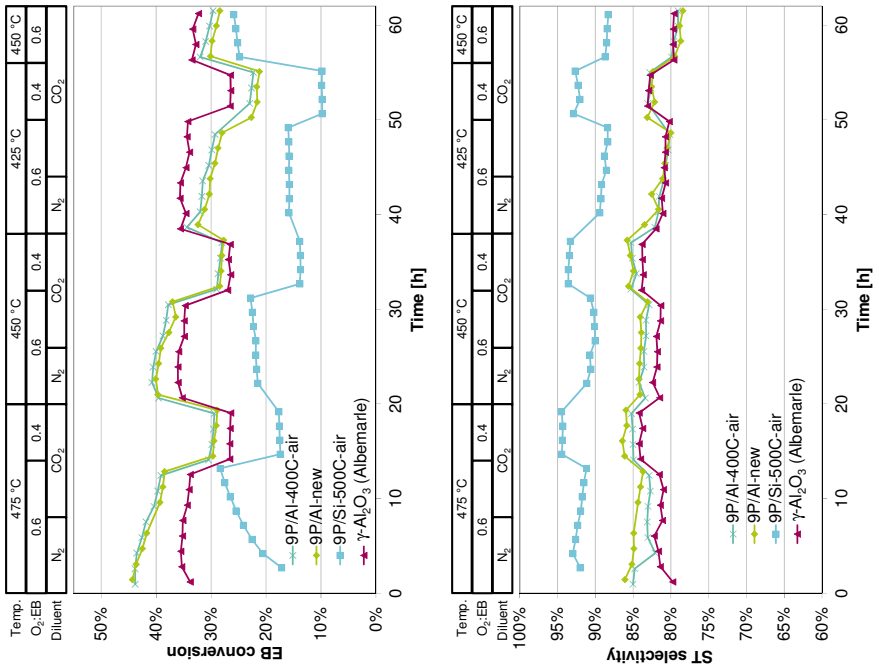

Figure 6.4: EB conversion (left) and ST selectivity (right) for 9 wt% phosphor loaded samples.

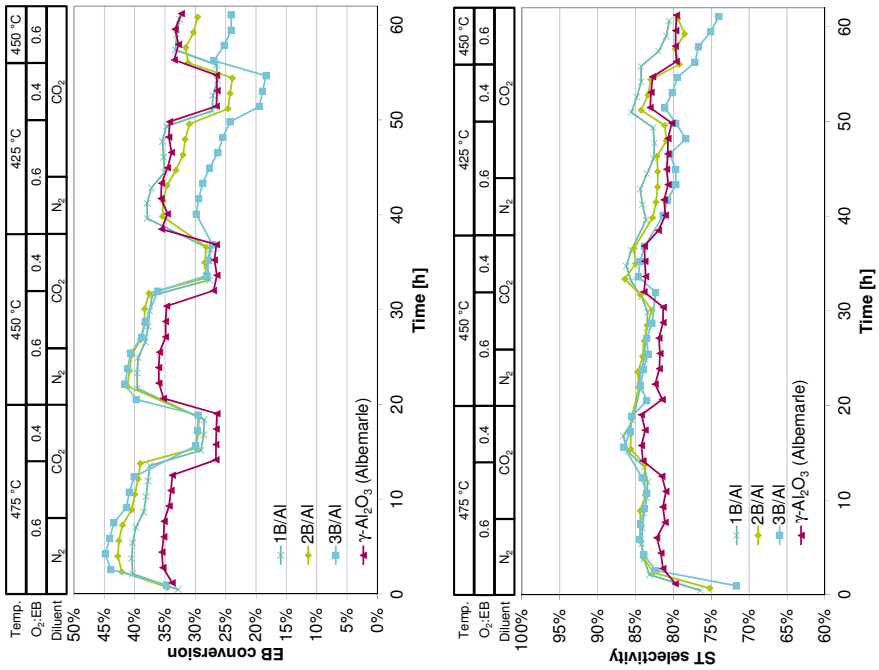

Figure 6.5: EB conversion (left) and ST selectivity (right) for different loadings of boron.

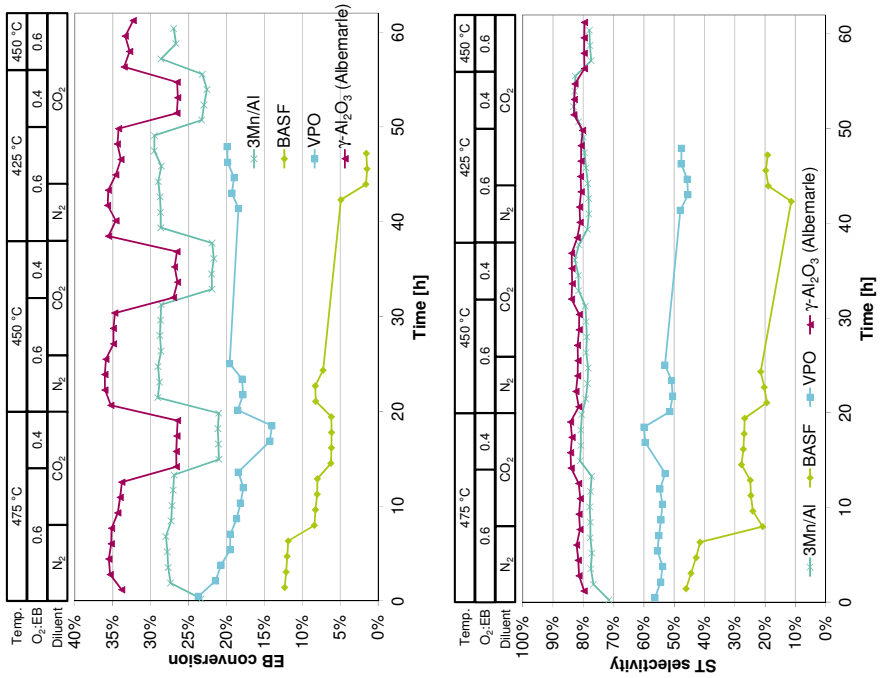

Figure 6.6: EB conversion (left) and ST selectivity (right) for poor catalysts.

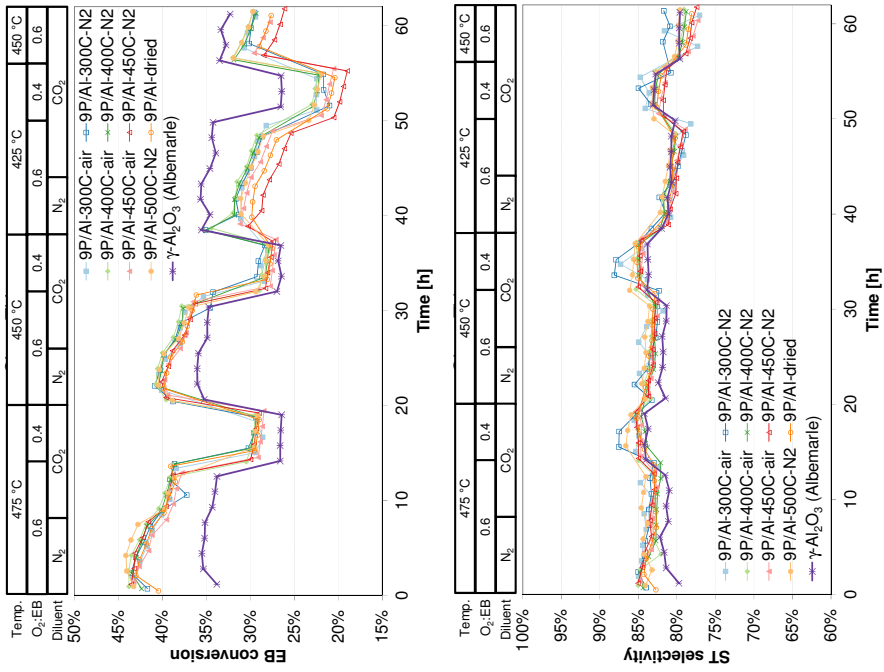

Figure 6.7: EB conversion (left) and ST selectivity (right) for 9P/Al catalysts with different pre-treatments.

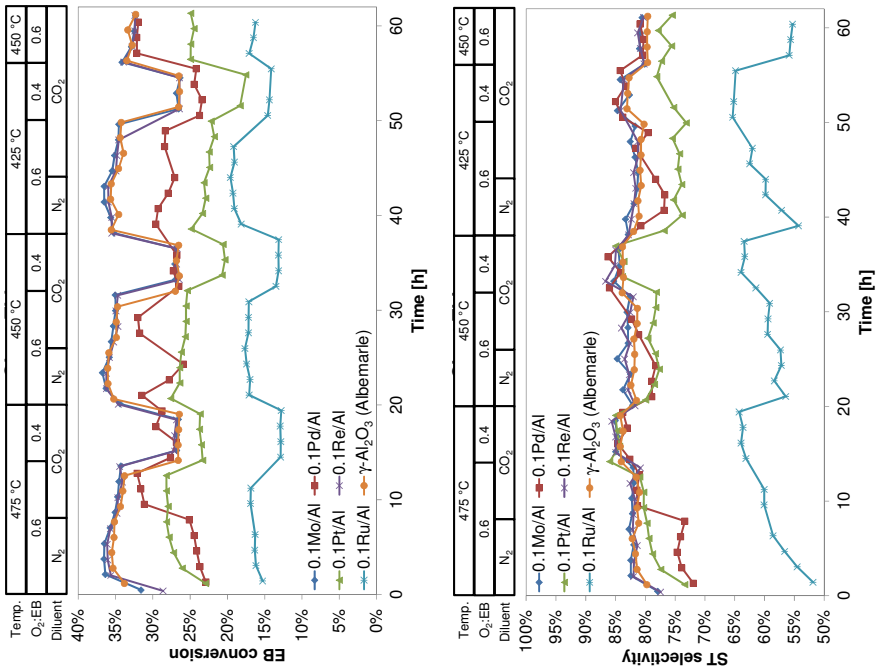

Figure 6.8: EB conversion (left) and ST selectivity (right) for samples with low metal loadings.

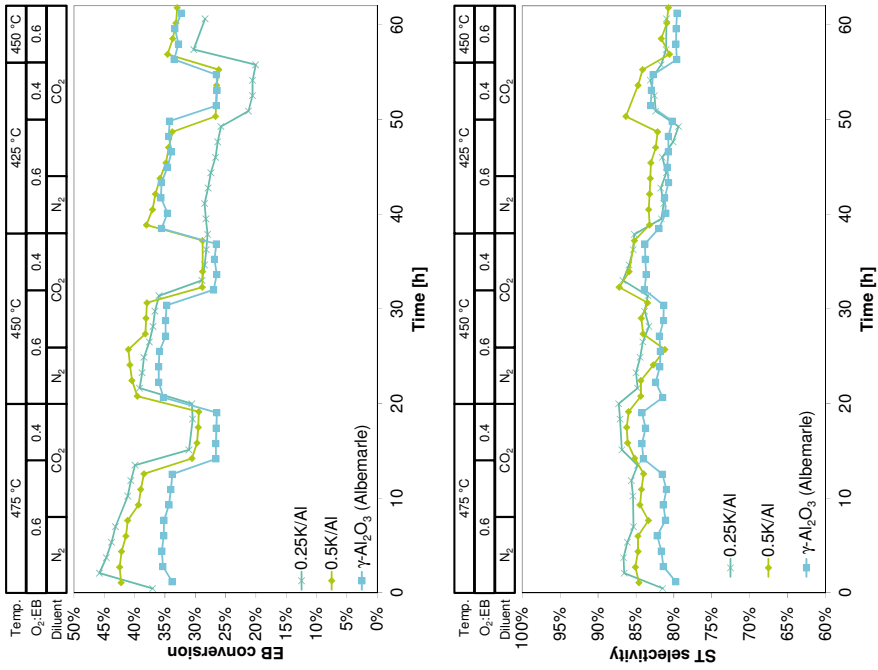

Figure 6.9: EB conversion (left) and ST selectivity (right) for potassium loaded samples.

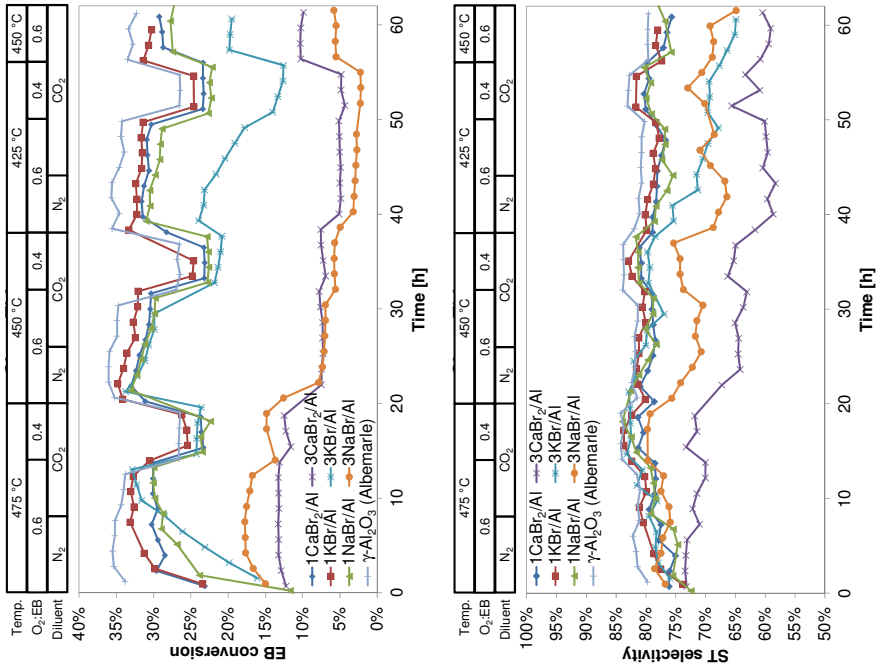

Figure 6.10: EB conversion (left) and ST selectivity (right) for samples with bromide salts.

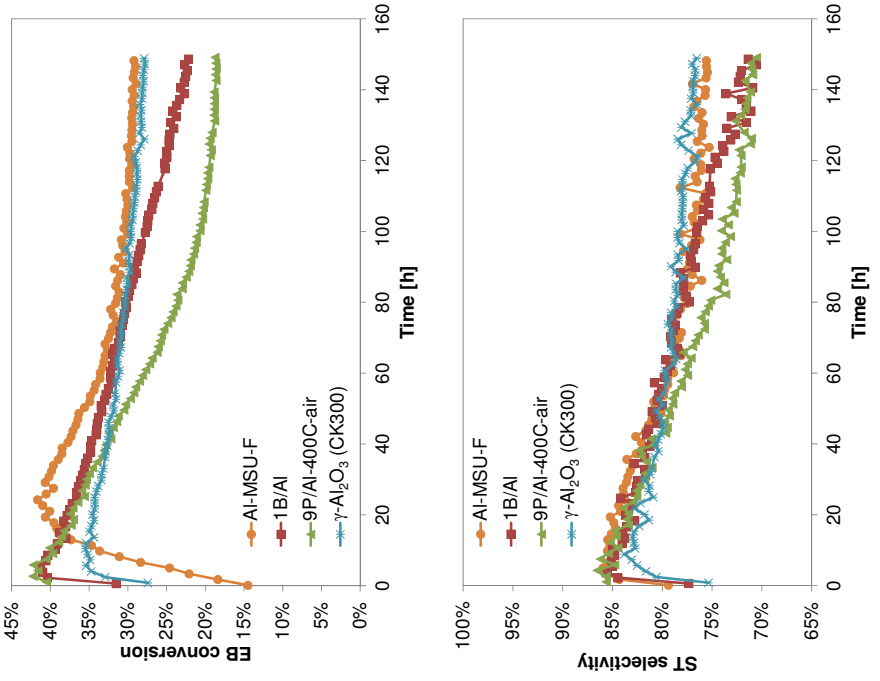

Figure 6.11: EB conversion (left) and ST selectivity (right) for selected samples in the stability test at 450 °C and a 0.6 O_2:EB ratio.

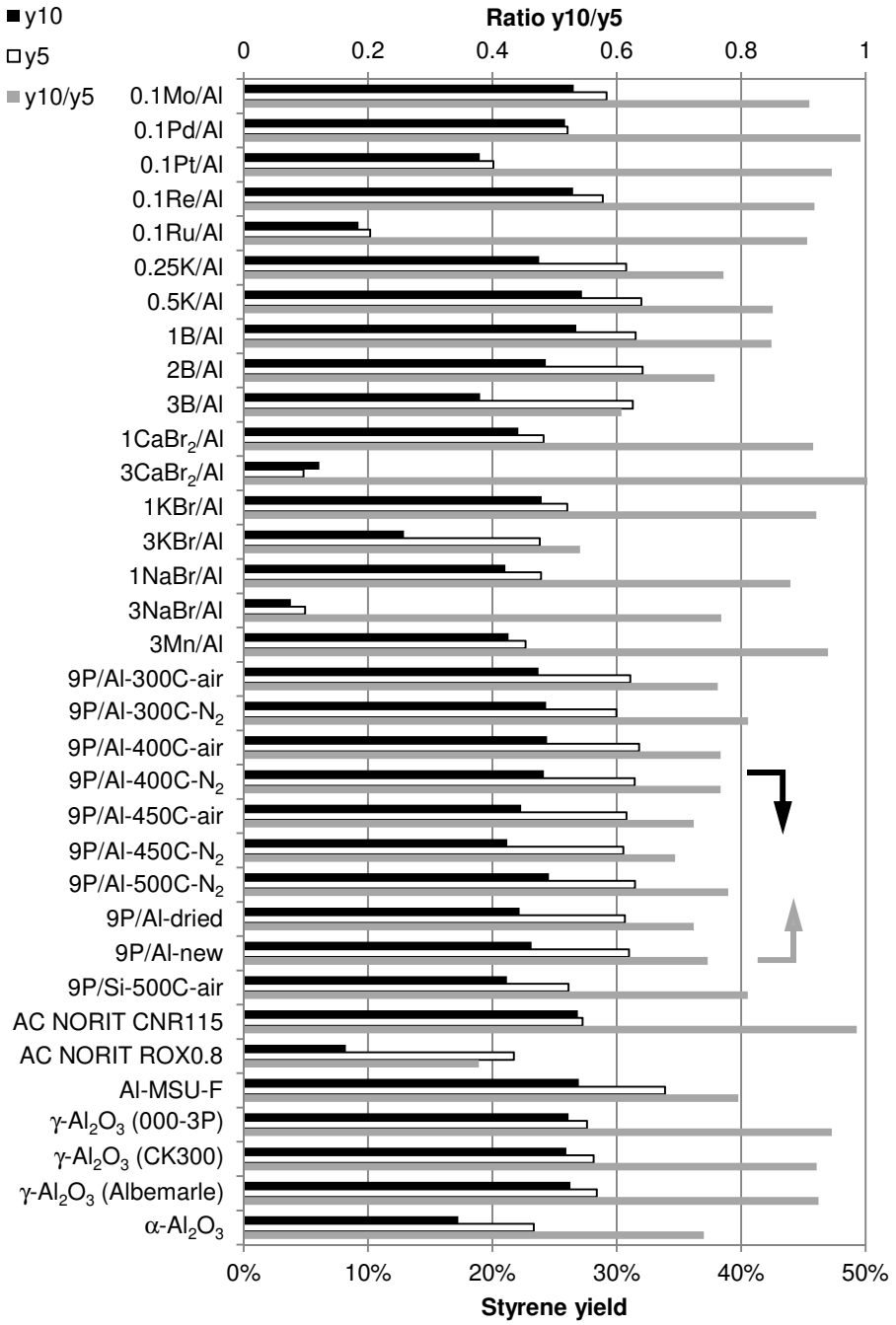

Figure 6.12: Averaged ST yields of the 5th (open) and 10th condition (black) (both at 450 °C and a 0.6 O_2:EB ratio) and the ratio of 10th/5th (gray).

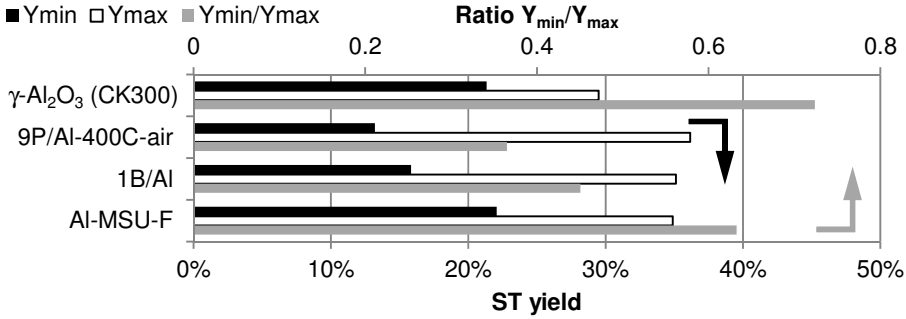

Figure 6.13: Maximum yields (open), yields after 150 h (black) and the ratio of these yields (grey) for the 150 h stability experiment.

6.4 Discussion

Many different materials were tested for their performance in the oxidative dehydrogenation reaction. Throughout this chapter, γ-Al_2O_3 (Albemarle) is used as a reference material, as it is a cheap and easy material that shows extremely reproducible and very reasonable performance. An improvement therefore, has to be significant compared with this reference sample to be of interest.

It is well documented in the literature on the oxidative dehydrogenation reaction that the true catalyst is not the starting material, but the coke that is being formed during the reaction.[1] A carbon containing starting material can already be active and selective from the start, as is also shown in Figure 6.3. As a consequence, a sample will not be active and selective as long as there is insufficient or no coke present on the surface of the carrier. The formation of sufficient coke can be accomplished in about 4 h for γ-Al_2O_3 (Figure 6.1), going up to about 10 h for Al-MSU-F (Figure 6.3). This is also a temperature dependent process. For Al-MSU-F it takes about 10 h at 475 °C (Figure 6.3) and about 20 h at 450 °C (Figure 6.11). Therefore, the testing protocol was designed to go from high to low temperature, minimizing the break-in period.

Within the tested sample pool, there are many unselective and inactive samples that were not able to form sufficient coke and reach full oxygen conversion with a high selectivity towards CO_X. These are the VPO (selective oxidation of butane to maleic anhydride), BASF (steam-aided EB to ST dehydrogenation), Ru/Al, 3NaBr/Al and 3CaBr/Al samples. Another special case is the AC-ROX0.8. This sample was slowly gasified during the experiment until there was insufficient coke or carbon available to catalyse the oxidative dehydrogenation reaction.

With the bromide salt loaded samples, it is most likely that only the effect of the counter-ion (Ca, Na, K) is observed. These counter-ions can neutralize the acidic sites on the support that cause the coke formation and activation of the samples. Although the

pure metal bromide salts are stable up to very high temperatures, it can react with the water from the dehydrogenation reaction to form HBr. In the other studies using bromides, it is usually supplied with the feed.[8, 12] The KBr/Al samples are thus similar to the K/Al samples, although their loading is much higher and giving a worse ODH performance compared with the low loading K/Al samples. The action of bromide as a potential radical scavenger was not demonstrated.

The samples that showed improved dehydrogenation performance (B/Al, P/Al, K/Al, Al-MSU-F) usually showed the lowest selectivity to CO and CO_2 (CO_X) production. This is probably due to a lower activity for the complete oxidation reaction over these starting materials (uncoked). Another possibility that explains their improvement could be that less coke is formed on these samples. With less coke, there is also less CO_X formation.[2] Or the reactivity of the coke could be different.

The 9P/SiO_2-500C-air catalyst showed a very good ST selectivity. The O_2 conversion at a 0.6 O_2:EB molar feed ratio is below 50%, leading to low EB conversions. The ST selectivity is high, despite these low O_2 conversions. The testing conditions need to be optimised to see the full potential of this catalyst type. Similar samples will be studied further, it is one of the more promising leads from this screening study (Chapter 7).

Most of the samples show a deactivation with time on stream due to the excessive coke formation, combined with an increase in CO_X production. When a sample deactivates in the oxidative dehydrogenation reaction, the EB conversion and ST selectivity go down, the CO_X selectivity increases, maintaining a 100% O_2 conversion. The selectivity decreases due to a shift towards the complete oxidation reaction (CO_X formation). As a result, less oxygen is available for the ODH reaction and the EB conversion also decreases. When more coke is present it appears easier to gasify this coke. The surface area that is accessible on the sample to oxygen is higher than for ethylbenzene due to the fact that their molecular sizes are different (EB is 0.7 nm, O_2 is 0.35 nm).[18, 19] The complete oxidation and coke gasification reactions are coupled for selective catalysts, according to the proposed reaction mechanisms for oxidative dehydrogenation.[1, 18-20]

The idea that a better catalyst is more inert can work in several ways. Firstly, less coke is being formed and therefore, also less CO_X is produced. Secondly, a more inert sample can also be less active for the coke gasification reaction. A good catalyst is foremost a stable catalyst. For the oxidative dehydrogenation reaction this means that the coke formation and gasification should be in balance once a sufficient amount of coke is formed. The alumina is the most stable sample, but it has more than sufficient coke and too much CO_X production. The formation of coke on the catalysts will be investigated further (Chapter 10).

6.4.1 Oxygen balance

The oxygen is one of the two reactants that are required for the oxidative dehydrogenation reaction. This work aimed at having a complete oxygen conversion. Only during the break-in period of the Al-MSU sample and the 3 wt% bromide salt samples the oxygen conversion was not complete. The oxygen balance is based on three main reactions, Eqs. 1.3, 1.4 and 1.5. This includes the series reaction of the EB to coke and finally CO_X. Two product concentrations are unknown. The concentration of H_2O was not measured and the concentration of CO_2 was obscured because it is also used as a diluent. These two concentrations can be calculated by solving the oxygen balance, Eqs. 6.7 and 6.8. For simplicity it is assumed that other byproducts do not contain any oxygen. In reality some byproducts may contain oxygen, but their concentrations are so low that they hardly make a difference to the oxygen balance.

$$C_8H_{10} + \tfrac{1}{2}O_2 \rightarrow C_8H_8 + H_2O \qquad 6.4$$

$$C_8H_{10} + 10\tfrac{1}{2}O_2 \rightarrow 8CO_2 + 5H_2O \qquad 6.5$$

$$C_8H_{10} + 6\tfrac{1}{2}O_2 \rightarrow 8CO + 5H_2O \qquad 6.6$$

$$[CO_2] = \frac{16}{21}\left([N_2]\frac{21\%}{79\%} - \frac{1}{2}[C_8H_8] - \frac{13}{16}[CO] - [O_2]\right) \qquad 6.7$$

$$[H_2O] = \tfrac{8}{5}[CO_2] + \tfrac{8}{5}[CO] + \tfrac{1}{2}[C_8H_8] \qquad 6.8$$

6.4.2 CO_2 effect

The intention of this screening work was to identify the catalysts that have improved EB conversion or ST selectivity in the presence of CO_2. In the testing protocol the performance of each sample is tested at three temperatures, with and without the CO_2 diluent at a O_2 to EB ratio of 0.6 (conditions 1, 2, 4, 5, 7, 8). As can be seen in Figure 6.1-Figure 6.10, there are hardly any differences observable in either EB conversion or ST selectivity between the conditions with or without CO_2. Sometimes the EB conversion is a little bit lower with CO_2, but this can have several causes, like the deactivation (the testing conditions without CO_2 are tested before the testing conditions with CO_2), or small variations in O_2:EB ratios when changing the conditions (gas compositions). Even for the catalyst sample (Mo) that is similar to the ones that were claimed to have a CO_2 effect in the oxidative dehydrogenation reaction of propane and butanes[4-7, 21], a CO_2 effect was not observed. Just like N_2 it behaves like an inert diluent under the oxidative dehydrogenation conditions over the studied catalyst samples. A closer look

into the literature that describes a CO_2 effect shows that this effect is mostly an increase in the poor dehydrogenation selectivity due to a decrease in cracking activity. The explanation is based on competitive adsorption between O_2, CO_2 and the propane or butane, giving a decrease in cracking products.[4-7] In the ODH of EB to ST, the selectivity is much higher compared with the propane or butane systems and the cracking products are not the main byproducts of the reaction here.

6.4.3 Temperature effect

All samples were tested at three different temperatures, because it is unknown beforehand what the optimal temperature would be for that specific sample. Typically, the temperature does not have a large role in the ODH reaction. The main effect of the temperature that was observed is the changing rate of the cracking reaction to benzene and toluene. For instance with the alumina reference experiment (Figure 6.1) the lower ST selectivity at 475 °C can be attributed to the higher production of these cracking products. At the lower temperatures it is observed that more heavy condensates are formed. For the alumina this results in an optimal temperature of 450 °C, where the selectivity to byproducts is minimal. The overall temperature effect on the EB conversion and ST selectivity is only 1-2% points.

Because of the design of the testing protocol, it can look like the lower temperatures are less active. However, this is usually the effect of the catalyst deactivation and not because of the temperature. Good examples, on the one hand, are the 9P/Al samples in Figure 6.7, around 30 h and around 60 h. A fresh catalyst gives a higher EB conversion at 450 °C and a 0.6 O_2:EB ratio, as is shown in Figure 6.11. On the other hand, based on the (limited) available data it cannot be excluded completely. As the true catalyst is the formed coke, it can happen that at a high temperature there is sufficient coke to convert all the oxygen, while at a lower temperature this amount of coke is not sufficient because of the lower reaction rates. The samples that show this temperature effect, with incomplete O_2-conversion, are mainly the more inert samples (P/Al, 3MBr/Al, Al-MSU-F) and AC.

6.4.4 O_2:EB effect

All samples were tested at two different O_2 to EB ratios at each temperature in the CO_2 diluent. Based on the reaction stoichiometry, a O_2:EB ratio of 0.5 should be sufficient. However, oxygen is also consumed by the side reactions that take place, especially the reactions towards CO_X. Even when oxygen is fed in excess (0.6 O_2:EB), not all ethylbenzene is converted, but all O_2 is consumed. Typically an EB conversion of 35-

40% is obtained with a 0.6 O_2:EB ratio. With a lower ratio of 0.4, the general trend is that the samples become more selective to styrene combined with a drop in the EB conversion. The improvement in the ST selectivity can be assigned completely to the decreased production of CO_X. From a kinetics perspective, the complete oxidation (or coke gasification) reaction is more dependent on the oxygen concentration than the oxidative dehydrogenation reaction. A low O_2 partial pressure is preferable for this selective ODH reaction. More on the effects of O_2 partial pressure is shown and discussed in Chapter 9.

6.4.5 Stability (5th *vs.* 10th condition and 150 h test)

Catalyst stability is very important, especially in reactions like dehydrogenations that are inextricably bound up with coke formation for continuous industrial applications. Therefore, there are the two identical conditions in the testing protocol, during a *TOS* of 26-32 h (condition 5) and of 56-62 h (condition 10), that can give an indication of the catalyst deactivation and stability. The yields at these conditions are shown and compared in Figure 6.12. This has proven to be very useful in this work, where a lower activity of a sample can have many reasons. Surprisingly, the reference alumina deactivated the least of all samples. The yield at the 10th condition is 95% of that at the 5th condition. The AC-CNR115 sample also shows very good stability in EB conversion, but this sample was partly gasified and is therefore, not considered stable.[12]

Depositing any material on the alumina has a negative effect on its stability. The additional 150 h stability test clearly shows this (Figure 6.11). The Al-MSU-F sample ends up at a similar EB conversion and ST selectivity, but initially has a slightly better performance and has deactivated (relatively) more than the reference alumina. Possibly, the mesoporous nature of the Al-MSU-F sample prevents the sample from deactivating as much as the 1B/Al or 9P/Al samples that also show a temporary improvement of the ODH performance compared to the bare alumina.

One concern that this screening work has shown is that it is very hard to achieve an overall (activity, selectivity and stability) improvement of the catalyst performance so that it can compete with the industrial dehydrogenation process (>80 % EB conversion and >96% ST selectivity required). Therefore, detailed characterisation of these catalyst samples will not give more insight in how a good ODH catalyst works. Some catalyst samples initially show an improvement in EB conversion and ST selectivity relative to the bare alumina, but have a problem in stability due to excessive coke formation. The oxidative dehydrogenation reaction is quite complex. The real catalyst is formed during the reaction, the starting material has to control the formation and gasification of coke, while also side reactions have to be suppressed. The samples that initially show improved performance have lower coke gasification, but as a result they cannot

prevent catalyst deactivation as a function of *TOS*. It appears to be some kind of "holy grail" to find a starting material that comprises all necessary functions.

6.5 Conclusions

An effect of CO_2 diluent on the selectivity and/or activity of the catalyst was not found, even for comparable samples in the literature. Carbon dioxide is just as inert as nitrogen for the tested samples. Samples that contain P, K, or B deposited on alumina did show improved EB conversion and ST selectivity, but displayed less stability than bare alumina. The targets on the desired catalyst performance were not met. Deactivation is due to excessive coke formation. A stable catalyst requires a balance between the coke formation and coke gasification. This is not found for the tested catalyst samples. Addition of noble metals or transition metals to alumina gives samples that are more active in oxidation, resulting in decreased selectivity to styrene and increased CO_X production. A lower O_2:EB ratio shows in increase in ST selectivity but results in a lower EB conversion.

References

[1] F. Cavani, F. Trifiro, Appl. Catal. A: Gen. 133 (1995) 219-239.
[2] A.E. Lisovskii, C. Aharoni, Catal. Rev. - Sci. Eng. 36 (1994) 25-74.
[3] G.E. Vrieland, J. Catal. 111 (1988) 1-13.
[4] F. Urlan, I.C. Marcu, I. Sandulescu, Catal. Commun. 9 (2008) 2403-2406.
[5] S.H. Ge, C.H. Liu, S.C. Zhang, Z.H. Li, Chem. Eng. J. 94 (2003) 121-126.
[6] Y.L. Bi, K.J. Zhen, R.X. Valenzuela, M.J. Jia, V.C. Corberan, Catal. Today. 61 (2000) 369-375.
[7] B. Zhaorigetu, R. Kieffer, J.P. Hindermann, Stud Surf Sci Catal. 101 (1996) 1049-1058.
[8] R.S. Drago, K. Jurczyk, Appl. Catal. A: Gen. 112 (1994) 117-124.
[9] G.C. Grunewald, R.S. Drago, J. Mol. Catal. 58 (1990) 227-233.
[10] M.F.R. Pereira, J.J.M. Orfao, J.L. Figueiredo, Appl. Catal. A: Gen. 184 (1999) 153-160.
[11] M.F.R. Pereira, J.J.M. Orfao, J.L. Figueiredo, Appl. Catal. A: Gen. 196 (2000) 43-54.
[12] M.F.R. Pereira, J.J.M. Orfao, J.L. Figueiredo, Appl. Catal. A: Gen. 218 (2001) 307-318.
[13] D.R. Burri, K.M. Choi, S.C. Han, A. Burri, S.E. Park, J. Mol. Catal. A: Chem. 269 (2007) 58-63.
[14] S. Geisler, I. Vauthey, D. Farusseng, H. Zanthoff, M. Muhler, Catal. Today. 81 (2003) 413-424.
[15] L. Bajars, Oxidative dehydrogenation process, 1967, United States patent 3,308,187.

[16] E.Z. Xue, J.R.H. Ross, R. Mallada, M. Menendez, J. Santamaria, J. Perregard, P.E.H. Nielsen, Appl. Catal. A: Gen. 210 (2001) 271-274.
[17] R. Mallada, M. Menendez, J. Santamaria, Appl. Catal. A: Gen. 231 (2002) 109-116.
[18] L.E. Cadus, L.A. Arrua, O.F. Gorriz, J.B. Rivarola, Ind. Eng. Chem. Res. 27 (1988) 2241-2246.
[19] G. Emig, H. Hofmann, J. Catal. 84 (1983) 15-26.
[20] G.E. Vrieland, J. Catal. 111 (1988) 14-22.
[21] I.C. Marcu, I. Sandulescu, J.M.M. Millet, Appl. Catal. A: Gen. 227 (2002) 309-320.

7

Screening II: Variation of P loading on SiO_2

7.1 Introduction

The first test of a phosphorous on SiO_2 (P/Si) catalyst showed a very promising selectivity, but the O_2 conversion was below 50% and the resulting EB conversion was low as well, below 30%. This seemed to be contradictory, as an incomplete O_2 conversion usually leads to poor ST selectivity (Ch. 6). Clearly this type of catalyst deserved more attention, for instance to optimize the testing conditions (temperature, O_2:EB feed ratio) and the catalyst loading to see its full potential for oxidative dehydrogenation of EB to ST. A series of samples were made with different P loadings to determine the optimum in the P loading for the ODH performance.

7.2 Experimental

The silica extrudates (Silica NorPro SS61138) were crushed and sieved. The sieve fraction of 212-425 μm was used for impregnation. The required amounts of H_3PO_4 were dissolved in demineralised water. The incipient wetness method was used for impregnation at RT, 105% of the pore volume was used that was determined by the wetting of the support. The support was pre-treated at 150 °C under vacuum for 4 h. The impregnated support was slowly dried overnight at 70 °C and then calcined at 500 °C

Table 7.1: The list with P/SiO_2 samples.

Sample	Impregnation steps	Loading [wt% P]	Loading [wt% P_2O_5]	Test mass [mg]
1P/Si	1	1	2.3	412.6
2P/Si	1	2	4.6	377.4
3P/Si	1	3	6.9	435.2
4P/Si	1	4	9.2	387.4
5P/Si	1	5	11.5	480.0
6P/Si	2	6	13.7	456.8
9P/Si	3	9	20.6	481.2
15P/Si	3	15	34.4	562.8

for 8 h in static air. The heating rate was set at 4 °C/min. An overview of the catalyst samples is given in Table 7.1.

The samples were tested according to the testing protocol that is described in detail in Chapter 6. Most samples were also tested using a similar testing protocol, but with a 25 °C higher temperature, starting at 500 °C.

7.3 Results

The bare SiO_2 support material displayed very low EB conversion (3%) and low styrene selectivity (50%) at 475 °C. For the comparison of the phosphorous loaded catalysts, the data at 475 °C is used with both the 0.2 and 0.6 O_2:EB feed ratio (8-14 h and 14-20 h *TOS*, respectively). The ODH performance data are shown in Figure 7.1.

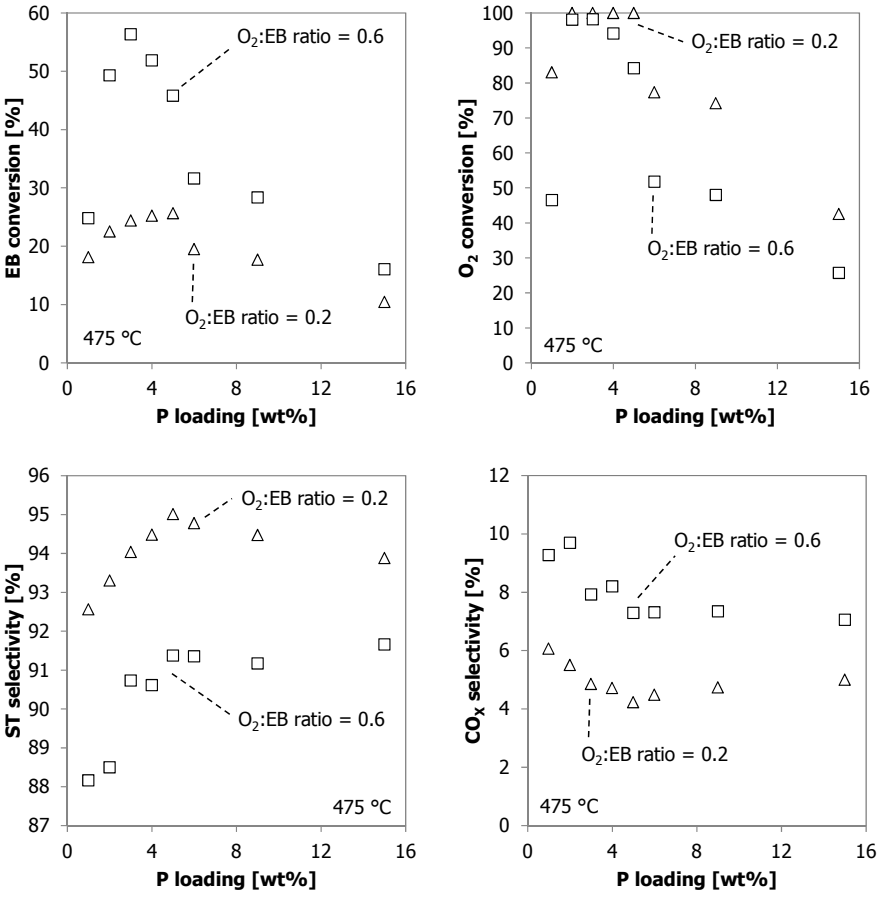

Figure 7.1: EB conversion, O_2 conversion, ST selectivity and CO_X selectivity for P/SiO_2 catalysts as a function of the phosphorous loading. Conditions: 475 °C, 8-20 h *TOS*, total *GHSV* of 2700 l/l/h, O_2:EB feed ratio 0.2 (△) and 0.6 (□), CO_2:EB feed ratio 5, 10 vol% EB feed, N_2 gas as balance.

At a 0.6 O_2:EB feed ratio, the 3P/Si sample shows the highest EB conversion of 56% at full O_2 conversion and 90.7% ST selectivity. The 2P/Si sample has a lower EB conversion and a lower ST selectivity (88.5%). Higher P loadings (> 3 wt% P) have a lower EB conversion because the O_2 conversion decreases with the higher loadings. The ST selectivity shows an optimum around 5-6 wt% P loading at 91.3%. The CO_X selectivity has a minimum here. For higher loadings the ST selectivity is about the same, the ST selectivity decreases for lower P loadings (< 5 wt%), due to increasing CO_X formation. Selectivity to other products (mainly benzene, toluene and heavy condensates) is almost constant with the P loading at about 1-1.5%.

At the 0.2 O_2:EB feed ratio, the 5P/Si sample shows the best ODH performance, with 26% EB conversion, 95% ST selectivity and full O_2 conversion. A lower loading gives a lower ST selectivity, lower EB conversion, higher CO_X selectivity and the O_2 conversion is constant at 100% except for the 1P/SiO_2 sample. A higher loading gives a lower O_2 conversion, lower EB conversion, lower ST selectivity and higher CO_X selectivity. Selectivity to other products is almost constant with the P loading at about 0.5-1%.

A few selected catalyst samples were analysed by N_2-adsorption. The results are given in Table 7.2. It shows that the specific surface area and the pore volume decrease with increasing P loading.

Table 7.2: Results from texture analysis for selected samples.

Sample	S_A [m^2/g]	V_P [ml/g]
SiO_2	257	1.00
3P/Si	165	0.77
6P/Si	74	0.68

7.4 Discussion

A comprehensive comparison of the results from the different P loaded catalysts is not easy. For most of the catalyst samples is proved to be difficult to achieve full O_2 conversion under all experimental conditions. Not having a full oxygen conversion has a negative effect on the ST selectivity as the catalysts are not optimally tested. Some scant comfort can be found in the fact that the negative effect of not having a full oxygen conversion is much smaller over these P catalysts than for the Al_2O_3 catalysts (Ch. 6, 8). The ST selectivity decreases only very little and EB conversion decreases almost linearly with the O_2 conversion. With that in mind, the best parameter for comparison is the ST selectivity. More catalyst can be loaded into the reactor to compensate the ODH activity loss, as the ST selectivity is hardly affected. Alternatively the temperature can be increased, the effect of this is shown in Figure 7.2. It has a positive effect on the O_2

conversion, but the effect on the ST selectivity and EB conversion is negative due to higher CO_X formation and EB cracking rates.

Indeed, comparing only the ST selectivities (the CO_X selectivity being a direct negative response to the ST selectivity), the trends at both 0.2 and 0.6 O_2:EB feed ratios are very comparable. The ST selectivity at 0.2 O_2:EB is about 4% points higher at all P loadings than those at 0.6 due to the lower O_2 concentration. The optimum in ST selectivity for both feed ratios is at 5-6 wt% P. A lower P loading yields a lower ST selectivity and a higher P loading has hardly any effect and would be a waste of materials.

The reason for a lower ST selectivity for P loadings below 5 wt% can possibly be found in the type of coke that is perhaps slightly more reactive towards O_2 due to different acidity and coverage of the catalyst. Unfortunately, there is no experimental characterisation data available to confirm this. The reason for the lower EB and O_2 conversion and slightly lower ST selectivity is possibly more straightforward and directly related to the available surface area for the coke formation and the ODH reaction. The limited characterisation data shows a clear trend towards lower specific surface area and pore volume for catalysts with higher P loadings.

It is hypothesised that at a P loading of 5 wt% an optimum dispersion and "Lewis"-acidity of the catalyst is achieved on the SiO_2 support. The largest contribu-

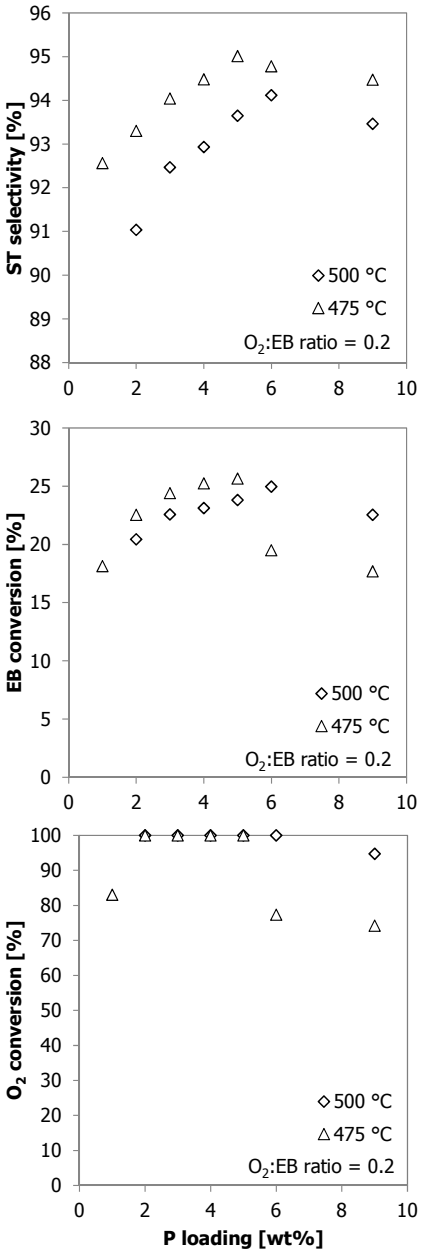

Figure 7.2: ST selectivity, EB conversion and O_2 conversion for P/SiO_2 catalysts as a function of the phosphorous loading. Conditions: 475 °C (△) or 500 °C (◇), 8-20 h *TOS*, total *GHSV* of 2700 l/l/h, O_2:EB feed ratio 0.2, CO_2:EB feed ratio 5, 10 vol% EB feed, N_2 gas as balance.

tion of the P to the ODH reaction is to introduce acid sites on the catalyst that can form coke to perform the selective ODH reaction. The type and amount of acid sites have an effect on the type of coke and the formation rate of coke. At a loading above 5% P, P_2O_5 islands could be formed that are spectators to the reaction and only occupy area and space in the catalyst.

The presented data have been measured between 8 and 20 h *TOS*. This is not necessarily the best performance for these catalysts under the applied conditions. On some catalysts the build-up of coke could have been very slow, as the EB conversion was still increasing with *TOS*, while for other samples coke formation could be that fast that catalyst deactivation was already observed. Typically, these catalysts show their best performance at high temperature and early time on stream. Comparison of the data at the end of the high temperature period seemed like the best option for comparison. Data from staged feeding (Ch. 9) shows that the optimum performance is at 3 h *TOS* for 3wt% and 5 wt% P loading at 500 °C. The presented data have not been corrected in any way for the activation or deactivation effects.

In this work there was no time available to do further analysis and characterization of the samples, for instance to learn more about the deactivation mechanism of these P/Si catalysts. A full and thorough discussion of these results is therefore not possible at this point in time.

7.5 Conclusion

A loading of 5 wt% P (11.5 wt% P_2O_5) on SiO_2 support gives the highest EB conversion (26%) and ST selectivity (95%) at a 0.2 O_2:EB feed ratio at 475 °C. The phosphorous oxides introduce “Lewis”-acid sites onto the otherwise inactive SiO_2 support material and generate an active and selective type of coke for the ODH reaction. Not attaining full oxygen conversion has only a minor effect on the ST selectivity.

8

Oxidative dehydrogenation of ethylbenzene to styrene over alumina: Effect of calcination

Abstract

Commercially available γ-Al_2O_3 was calcined at temperatures between 500 and 1200 °C and tested for its performance in the oxidative dehydrogenation (ODH) under a wide range of industrially-relevant conditions. The original γ-Al_2O_3, as well as η- and α-Al_2O_3, were also tested. A calcination temperature around 1000/1050 °C turned out to be optimal in the ODH performance. The number of acid sites (from 637 to 436 μmol/g) and surface area (from 272 to 119 m^2/g) are reduced by calcination, so the acid site density goes up from 1.4 to 2.4 sites/nm^2. Less coke (from 30.8 wt% to 21.6 wt%) is formed on the Al-1000 sample, but the coke coverage increases. Compared with the γ-Al_2O_3, the EB conversion increased from 36% to 42%, and the ST selectivity increased from 83% to 87%. The ODH performance is improved under all tested reaction conditions. The optimum sample forms enough coke to have full oxygen conversion under the applied conditions, required for optimal selectivity. The type and reactivity of the coke are changed due to higher acid density or presumably due to the strong Lewis acid sites that are formed by the high temperature calcination. This Al-1000 sample and all other investigated catalysts lost ODH activity with time on stream. The loss of selectivity towards more CO_X formation is directly correlated with the amount of coke.

8.1 Introduction

Alumina is a widely used catalyst support in the oxidative dehydrogenation (ODH) of hydrocarbons.[1, 2] Alumina itself is not a selective ODH catalyst, fresh Al_2O_3 shows about 20% ethylbenzene (EB) conversion, with about 70% selectivity to styrene (ST) at a 0.6 O_2:EB ratio and 450 °C. In the first hours of reaction, coke is deposited on the alumina and both EB conversion and ST selectivity increase, up to 36% EB conversion and 83% ST selectivity. The role of the alumina is to enable this coke formation. In the literature there are several studies that have investigated this phenomenon. An overview of the characterization data of several alumina samples in the ODH of EB is given in Table 8.1.

The acidic nature and specific surface area of the alumina play a crucial role in its activity for ODH. The acidic centres on the surface take part in the formation of coke deposits on the surface, that constitutes the actual catalytic phase for the selective ODH. Once a kind of monolayer of coke is deposited on the alumina, the amount of coke stabilizes as well as the yield of styrene and CO_2.[1, 3, 4] Several correlations for alumina were found between the amount of coke and:

- The number of acid sites on alumina
- The amount of CO_2 that is produced.
- The specific surface area and "monolayer" coke amount.

Reducing the acidity by adding KOH to the alumina reduces the amount of coke that is deposited. Also the addition of NH_3 to the feed decreases the formation of coke. Increasing the acidity by adding H_3BO_3 to alumina increases the amount of coke that is deposited. The addition of mineral acids like H_3BO_3 or H_3PO_4 have another side effect, the composition of the coke deposits is changed. This resulted in a more active and selective catalyst.[1]

Another way to change the acidity of the alumina could be by a high temperature calcination. A heat treatment will, first of all, reduce the amount of bound water on the alumina surface. Two OH^- ions on the alumina surface that act as Brönsted acid sites can form a Lewis acid site and one free water molecule. This takes place at temperatures above 300 °C. Two-thirds of the OH^- ions can be removed without affecting the local order, when more OH^- ions are removed oxygen vacancies will occur that behave as strong Lewis acid sites. Even at temperatures as high as 800-1000 °C and under vacuum, still a few tenths of a per cent of OH^- ions exist.[5]

By applying a heat treatment to γ-Al_2O_3, other crystalline phases can be obtained. At a calcination temperature of 900-1000 °C, it is converted into δ- and θ-Al_2O_3 crystalline phases. Above 1100 °C, it changes into α-Al_2O_3. The oxygen packing of γ-Al_2O_3 and η-Al_2O_3 is cubic close packing, which is transformed into hexagonal close packing for α-Al_2O_3. In γ-Al_2O_3 the (110) plane is predominant and in η-Al_2O_3 it is the (111)

Table 8.1: Summary of several characterisation data on Al_2O_3 that was used in the ODH of EB to ST as reported by Lisovskii.[1]

Sample #	Initial material	Calcination temperature [°C]	S_A [m^2/g]	Number of acid centres [µmol/g]	Crystalline structure	Coke* 120 min *TOS* [wt%]	CO_2 yield* [%]	Coke* monolayer amount [wt%]
7	$Al(OH)_3$	1500	1.5	90	α-phase			
1	$AlCl_3$	800	73	299	amorphous	3	0.4	3
9	θ-Al_2O_3	-	73	-	θ-phase	6	1.0	4.5
6	$Al(OH)_3$	1000	120	804	γ-phase, high temperature	11	1.6	6.5
8	γ-Al_2O_3	(commercial)	152	839	γ-phase	15	1.9	8
3	$Al(OH)_3$	600	154	789	γ-phase, low temperature	14	2.0	6
5	$Al(OH)_3$	800	157	810		16	2.1	5.5
4	$Al(OH)_3$	700	160	888		17	2.3	9
2	Al-isopropoxide	700	235	1149	amorphous	22	1.3	12

*** These numbers were not determined at the same ODH conditions.**

plane. The (111) plane has a higher density of Al^{3+} tetrahedral sites, making η-Al_2O_3 more acidic than γ-Al_2O_3.[6] The transformation into α-Al_2O_3 takes place by a nucleation and growth process, whereby the pores rapidly grow in size, especially in the stage from θ to α phase (around 1000 °C).[7, 8]

In this chapter the effect of the calcination temperature on a commercially available γ-Al_2O_3 is reported with regard to the catalyst performance relationships (EB conversion, ST selectivity, stability, coke amount, acidity and surface area) in the ODH reaction of EB to ST. The samples were tested using the screening protocol in Chapter 6, so including two O_2:EB feed ratios and the use of two diluents (CO_2 and N_2).

8.2 Experimental

8.2.1 Catalyst preparation

The γ-Al_2O_3 extrudates (Albemarle, 272 m^2/g, 0.64 ml/g, silica-promoted) were crushed and sieved to 212-425 µm. Each time, 2 g of sample was put in a ceramic cup and calcined for 8 h in a static air calcination oven. The maximum calcination temperature was 1200 °C, the temperature safety limit of this oven. Other calcination temperatures were 500, 600, 700, 800, 900, 1000, 1050, 1100 and 1150 °C. The heating rate was set at 4 °C/min. The suffixes in the names of the samples in this chapter correspond to their calcination temperatures. Other alumina samples that were used in this chapter are mentioned in Table 8.2.

Table 8.2: List of alumina samples that are used as received.

Name	S_A [m^2/g]	V_P [ml/g]	Other details
γ-Al_2O_3 (Albemarle)	272	0.64	Albemarle, silica-promoted
η-Al_2O_3	386	0.20	ETA-EXTRUDATE 1.8/360 Sasol Germany GmbH
α-Al_2O_3	~10	0.5	Engelhard Al-4196E 1/12
Boehmite			Sasol Catapal B alumina (boehmite)

8.2.2 Catalyst testing ODH of EB

The oxidative dehydrogenation experiments are performed in a parallel fixed bed reactor setup with six quartz reactors with an inner diameter of 4 mm, in down-flow operation. In a typical experiment a catalyst bed height of 65 mm is used (0.80 ml). The reactors are loaded – from top to bottom – with a quartz wool plug, 10 cm glass pearls (0.5 mm diameter), the catalyst, 10 cm glass pearls (0.5 mm diameter) and a quartz wool plug. A quartz reactor tube, filled only with glass beads and quartz wool plugs, only showed up to 3% EB conversion under all applied conditions. The catalyst bed is positioned within the 20 cm isothermal zone of the reactor. The reactor gas feed is a mixture that can consist of CO_2, N_2 and air. To each reactor, the gas flow rate is 36 ml (NTP)/min, the liquid EB feed flow rate is 1 g/h (3.6 ml (NTP)/min vapour), resulting in a 1:10 molar ratio of ethylbenzene and gas. The ethylbenzene liquid is fed into a heated α-Al_2O_3 filled tube, where it is evaporated in a co-current flow with the gas feed. This evaporator is located in an oven, where also the reactor furnace is installed.

The reactors are heated up under nitrogen flow with 5 °C/min. The temperature is allowed to stabilize for another 15 minutes when the reaction temperature is reached. The EB flow is started first (1-5 minutes earlier), before any oxygen is added to the gas mixture, to prevent any pre-oxidation of the catalyst samples. The reaction starts when oxygen is added to the reactors. The pressure at the setup outlet is atmospheric, the pressure before the reactors is typically about 1.2-1.3 bara.

A testing protocol of 10 conditions is used to test the catalyst samples. The protocol consists of three temperatures, going from high to low, because this is the optimal way for the activation of the catalyst (initial coking of the catalyst during reaction conditions). Two O_2:EB feed ratios are used and two CO_2:EB feed ratios to see the effect of these gases on the reaction. One condition is tested twice to see the aging effect of the catalyst (the 5^{th} and 10^{th} condition). An experiment, from start to start, takes 3 days. This includes ending the experiment and starting a new one (cooling down of the reactors, replace reactor tubes, leak testing, heating up, *etc.*). The testing protocol is given in Table 8.3.

Table 8.3: The catalyst testing protocol.

Condition	Time on stream [h]	Temp. [°C]	O_2:EB	CO_2:EB
1.	0-8	475	0.6	0
2.	8-14	475	0.6	5
3.	14-20	475	0.4	5
4.	20-26	450	0.6	0
5.	26-32	450	0.6	5
6.	32-38	450	0.4	5
7.	38-44	425	0.6	0
8.	44-50	425	0.6	5
9.	50-56	425	0.4	5
10.	56-62	450	0.6	5

During the ODH experiments, the concentrations of the reactor effluent are measured online by a two channel gas chromatograph with a TCD (columns: 0.3m Hayesep Q 80-100 mesh with back-flush, 25m × 0.53mm Porabond Q and 15 m × 0.53mm molsieve 5A with bypass option for CO_2 and H_2O, all in series) for permanent gas analysis (CO_2, H_2, N_2, O_2, CO) and a FID (column: 30m × 0.53mm, D_f = 3μm, RTX-1) for the hydrocarbons analysis (methane, ethane, ethene, benzene, toluene, ethylbenzene, styrene, heavy aromatics). One analysis, from start to start, takes 15 minutes. Six reactors and one reference gas analysis gives that each reactor is analysed every 1¾h in order to follow the catalyst performance with time on stream. A constant flow of nitrogen is used as the internal standard. The internal standard was fed just before the GC. The lines from the reactor to the GC are heat-traced at 175 °C to prevent condensation of the vapours. The EB conversion, ST selectivity, ST yield and O_2 conversion are based on moles of ethylbenzene and calculated according to Eqs. 8.1-8.4. The overall carbon balance is > 99%, only the carbon that is deposited on the catalyst as coke is missing from the carbon balance by the GC analysis.

$$EB\ conversion = \frac{ethylbenzene_{in} - ethylbenzene_{out}}{ethylbenzene_{in}} \tag{8.1}$$

$$ST\ selectivity = \frac{styrene_{out}}{ethylbenzene_{in} - ethylbenzene_{out}} \tag{8.2}$$

$$ST\ yield = EB\ conversion \times ST\ selectivity \tag{8.3}$$

$$O_2\ conversion = \frac{O_{2,in} - O_{2,out}}{O_{2,in}} \tag{8.4}$$

8.2.3 Catalyst characterization

The amount of coke on the spent catalyst samples was determined by thermo gravimetric analysis (TGA) in synthetic air using a Mettler-Toledo analyzer (TGA/SDTA851e). Alpha alumina crucibles (90 µl) were filled with 5-10 mg of sample and the decomposition of the components was monitored in a flow of air of 100 ml/min. The temperature was increased from room temperature until 900 °C at a rate of 10 °C/min. A blank experiment is performed employing an empty crucible to correct for physical artefacts; this pattern is subtracted from the measured weight automatically. The derivative of the TGA curve was used occasionally to quantify the rate of mass loss.

Nitrogen adsorption was used to determine the porosity characteristics of the catalyst and catalyst supports. Nitrogen adsorption at –196 °C was carried out in a Micromeritics 2420. The samples were pre-treated in N_2 at 250 °C for 10 h for fresh catalyst or catalyst supports while 200 °C was applied for the spent catalysts. No appreciable weight loss was detected. The textural parameters were derived from the BET model.[9] The total pore volume (V_P) is directly measured in the desorption branch at a relatively pressure of ca. 0.987 as recommended by the Micromeritics. The geometrical pore size (D) was calculated as $4V_P/BET$.

NH_3-TPD experiments were carried out in a Micromeritics AutoChem II system equipped with a thermal conductivity detector. The sample (ca. 30 mg) was pre-treated by heating it up to 500 °C in He at 10 °C/min. The sample was cooled to 120 °C at a similar cooling rate and then exposed to 1 vol% NH_3/He (25 ml/min) for 30 min. Subsequently, a flow of He (25 ml/min) was passed through the reactor for 60 min to remove weakly adsorbed NH_3 from the samples' surface. After the baseline stabilization, the desorption of NH_3 was monitored in the range of 120-1000 °C using a heating rate of 10 °C/min.

The crystal structure of some materials was confirmed by powder X-ray diffraction. XRD patterns were recorded in a Philips PW1840 using a Cu-Kα radiation source as an incident beam. The scanning angle was varied from 10-100° with a scanning rate of 0.2° per minute. The identification of the different crystalline phases was performed by the comparison with the corresponding JCPDS diffraction data cards.

8.3 Results

8.3.1 Catalyst characterization

Nitrogen adsorption analysis was done for all fresh samples. Ammonia TPD, XRD and coke amount determination were done for selected fresh samples. Thermo gravimetric analysis was done for all spent samples to determine the amount of coke. The data are given in Table 8.4. These results show that with increasing calcination temperature the surface area, pore volume, acidity and amount of coke decrease. The ODH experiments were done with a constant bed volume of catalyst (0.8 ml). The increasing sample mass reflects therefore, the increasing sample density with increasing calcination temperature.

The TGA profiles of the coked catalyst samples in Figure 8.1 show the maximum in the oxidation rate of coke around 500 °C ('oxidation temperature') for all the samples. Coke on the commercial η-Al_2O_3 is the most reactive with a maximum oxidation rate at 494 °C, coke on the α-Al_2O_3 is the least reactive with a maximum oxidation rate at 555 °C. The amount of coke on the calcined samples ranges from 10.6 wt% for Al-1100 up to 32.7 wt% for Al-500, all measured after 62 h *TOS*. Also a small effect in the temperature of maximum coke combustion is observed for the calcined samples going from 512 °C for Al-500 to 522 °C for Al-1100.

The pore size (Table 8.4) shows a shift to larger pore sizes for the samples with higher calcination temperatures. The most dominant pore diameter shifts from 90-100 Å for the commercial γ-Al_2O_3 to 136 Å for the 900 °C sample. Samples calcined at higher temperatures show a further increase in the pore size, going up to 260 Å for the 1100 °C sample.

The NH_3-TPD measurements show a clear decrease in the amount of NH_3 desorb-

Table 8.4: Characterisation results of the catalyst samples and their mass as used for testing in the ODH reaction. The empty cells represent unavailable data.

Sample name	XRD crystalline phase	Calcination temperature [°C]	Sample mass [mg]	S_A [m^2/g]	V_P [ml/g]	D [Å]	Number of acid sites [µmol/g]	Coke 62 h *TOS* [wt%]	T_{max} TGA [°C]
α-Al_2O_3	α		1432	10	0.50	>1000		37.4	555
boehmite		500	601					24.8	504
η-Al_2O_3	η		590	386	0.20	21		23.5	494
γ-Al_2O_3	γ		487	272	0.64	94	637	30.8	
Al-500	γ	500	532	271	0.65	96	637	32.7	512
Al-600	γ	600	554	255	0.64	100		31.3	512
Al-700	γ	700	506	239	0.64	107		24.9	504
Al-800	γ	800	549	214	0.64	120		29.0	513
Al-900	δ	900	622	179	0.61	136	540	25.8	520
Al-1000	θ	1000	707	119	0.49	165	436	21.6	522
Al-1050	θ	1050	572	101	0.46	182	398	20.8	522
Al-1100		1100	804	54	0.35	260	244	10.6	522
Al-1150		1150	763	20	0.17	340		1.3	
Al-1200		1200	981	16	0.12	300	0	1.1	

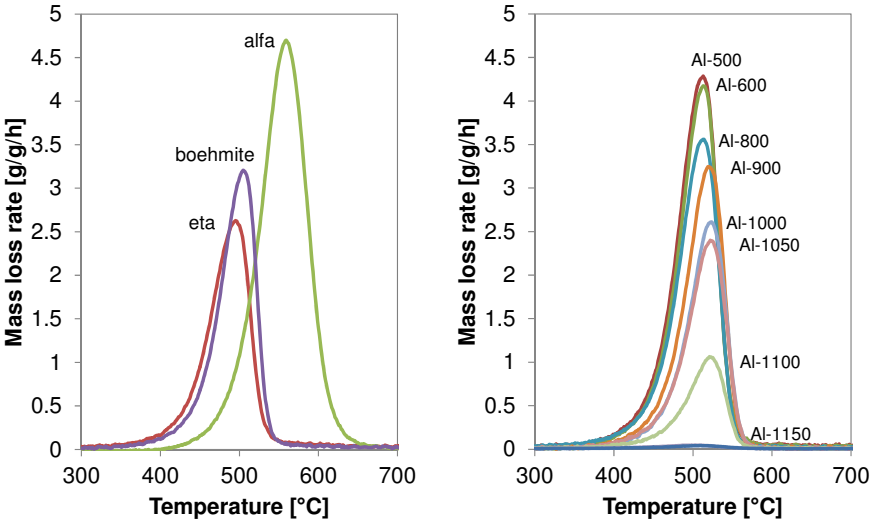

Figure 8.1: TGA profiles of commercial and calcined Al_2O_3.

ing from samples that are calcined at higher temperatures. The shape of the curves is similar, with two desorption steps. One step around 200-350 °C and one step around 500-700 °C. At the same time the acid density or the number of acidic sites increase from 2.34 (μmol/m^2 for bare γ-Al_2O_3) to 4.52 (Al-1100) or 1.4 to 2.4 (sites/nm^2).

Some of the samples were analysed by XRD and agrees well with the expected phases of transitional aluminas.[7, 8]

A few of the spent and coked samples were analysed by N_2 adsorption, these data are shown in Table 8.5, together with the data of the fresh samples. For the commercial γ-Al_2O_3, one third of the surface area and two thirds of the pore volume is lost due to the coke deposition. The specific surface areas of the calcined samples hardly change, but about half of the pore volume is lost to coke deposits on the samples.

Table 8.5: Texture data from N_2 adsorption at –196 °C for selected fresh and spent catalyst samples.

	FRESH		SPENT	
Sample	S_A [m^2/g]	V_P [ml/g]	S_A [m^2/g]	V_P [ml/g]
γ-Al_2O_3	272	0.83	173	0.25
900 °C	179	0.61	152	0.28
1000 °C	119	0.49	119	0.28

8.3.2 ODH experiments

The performance with time on stream of all samples tested according to the screening protocol in the ODH reaction of EB to ST is shown in Figure 8.2 and Figure 8.3. To facilitate a comparison, the performance as a function of the calcination temperature is presented in Figure 8.4. All oxygen was completely converted, unless it is stated otherwise. The role of oxygen is three fold, namely: 1) to create carbon deposits; 2) to perform the oxidative dehydrogenation; and 3) to oxidize the deposited carbon to CO and CO_2.

At 475 °C (0-14 h *TOS*), the samples Al-1100, Al-1050 and Al-1000 have the best performance. Their 42% EB conversion and 86% ST selectivity is an improvement over the 36% EB conversion and 83% ST selectivity for the reference γ-Al_2O_3. At 450 °C (20-32 h *TOS*), the samples Al-1050, Al-1000 and Al-900 have the best performance, similar to the performance at 475 °C. The EB conversion of the Al-1100 sample decreased compared with 475 °C. The available oxygen is not completely converted over the Al-1100 sample anymore. At 425 °C (38-50 h *TOS*), the Al-900 sample has the highest ST yield of 32%, with 38% EB conversion and 83% ST selectivity. Both the EB conversion and O_2 conversion of the samples Al-900, Al-1000 and Al-1050 decreased 5%, 10% and 20%, respectively, compared with 450 °C. The 85% ST selectivity of the Al-1000 and Al-1050 samples is the highest of the series at 425 °C. Full oxygen conversion was not always observed at 425 °C. Samples calcined at a higher temperatures had lower O_2 conversions. The Al-1150 and Al-1200 samples did not reach full oxygen conversion under all investigated reaction conditions. An incomplete oxygen conversion results in a lower selectivity, due to the increased formation of partly oxygenated aromatics (tars) and an increased CO_X formation.

Of the commercial samples in Figure 8.2 and Figure 8.3, the α-Al_2O_3 takes longest (10 h *TOS*) to become active and selective. At 425 °C it reaches its highest EB conversion (34%) and ST selectivity (79%), only a little less than that of γ-Al_2O_3. The γ-Al_2O_3 material is used as source for the calcined samples. The EB conversion (36%) and ST selectivity (82%) of the commercial γ-Al_2O_3 is not significantly different from the Al-500, Al-600 and Al-700 samples. The boehmite sample, a precursor for γ-Al_2O_3, has an EB conversion (34%) and ST selectivity (81%) that is only a little lower than that of the commercial γ-Al_2O_3. The η-Al_2O_3 sample does not become very active or selective, at 450 °C after 20 h *TOS* both its EB conversion (27%) and ST selectivity (77%) are lower than those of the other commercial samples.

The stability of the samples, calculated as the ratio of the yield at the 10^{th} condition (56-62 h *TOS*) and the yield at the 5^{th} condition (26-32 h *TOS*), is shown in Figure 8.5, together with the yields at these conditions. These two reaction conditions are identical and optimal for our reference γ-Al_2O_3 sample: 450 °C, feed ratio O_2:EB = 0.6 and

CO_2:EB = 5. It shows that the calcined γ-Al_2O_3 samples all have a very similar stability, they deactivate about 7% during this period of operation. The η-Al_2O_3 and boehmite samples are less stable and deactivate about 11%. The α-Al_2O_3 sample deactivates the most, the yield decreased 25%. The samples that do not show full oxygen conversion at 450 °C (Al-1150 and Al-1200) show the highest stability and only deactivate 5% or less, although their ST yields are the lowest for the measured catalyst samples.

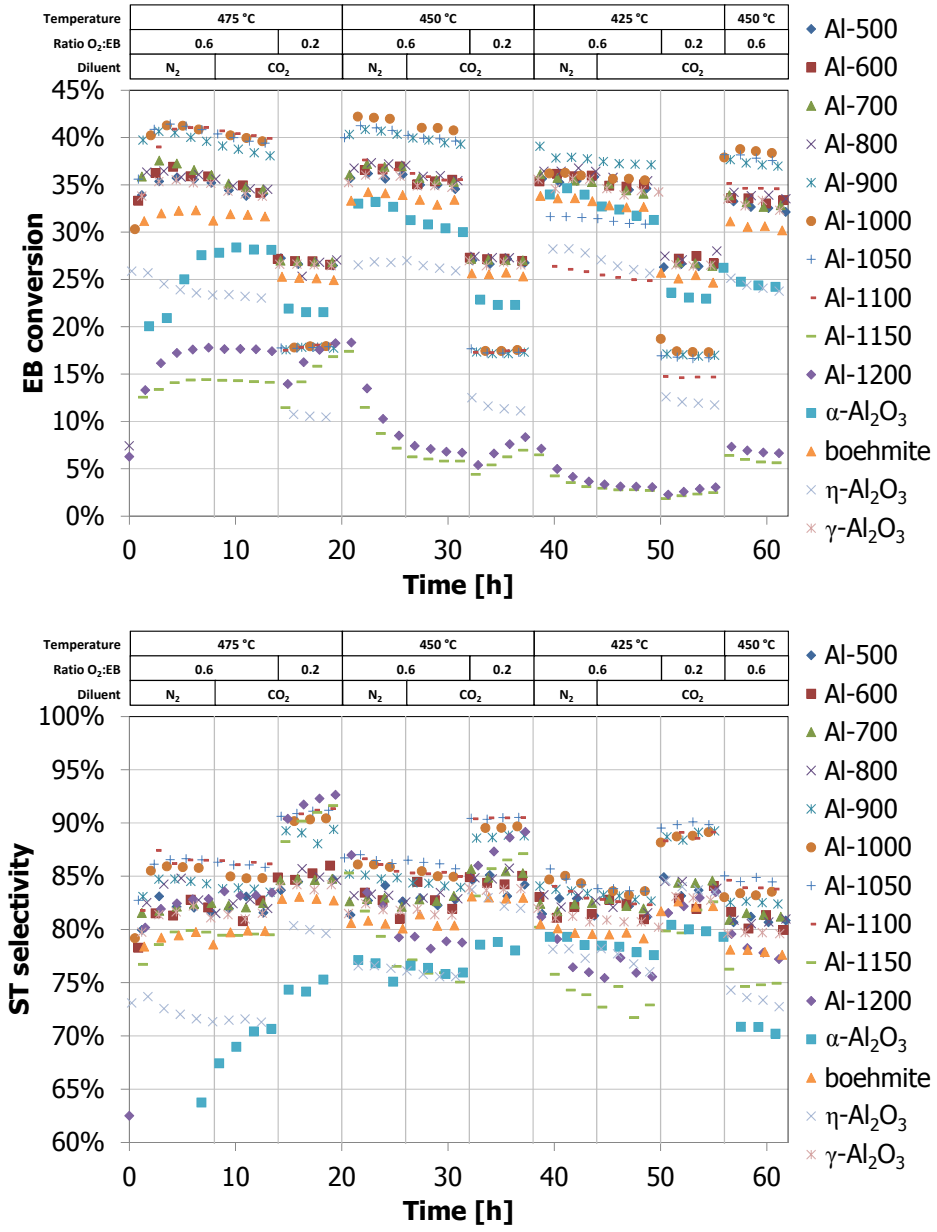

Figure 8.2: Ethylbenzene conversion and styrene selectivity of calcined and commercial alumina samples with time on stream.

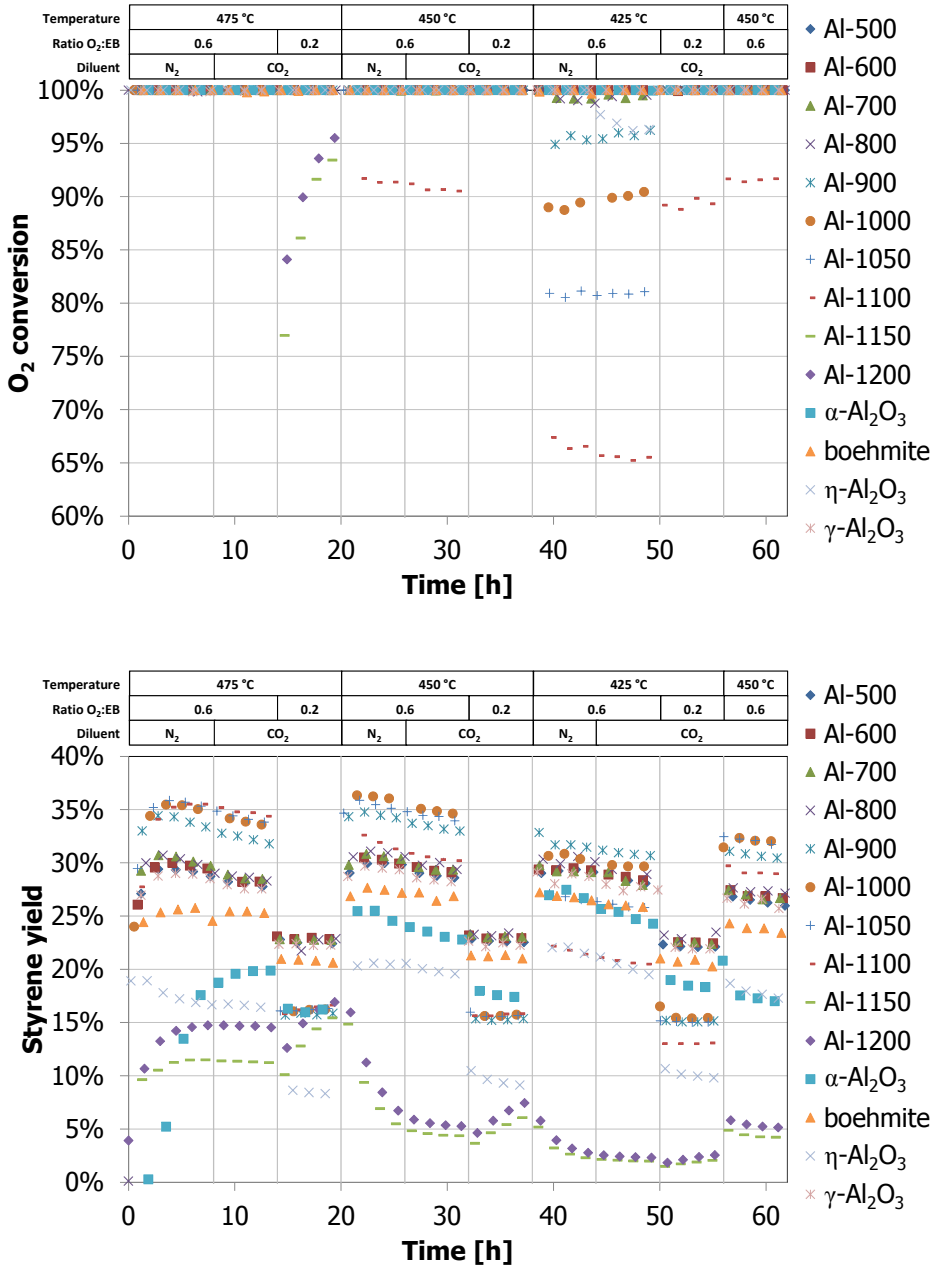

Figure 8.3: Oxygen conversion and styrene yield of calcined and commercial alumina samples with time on stream.

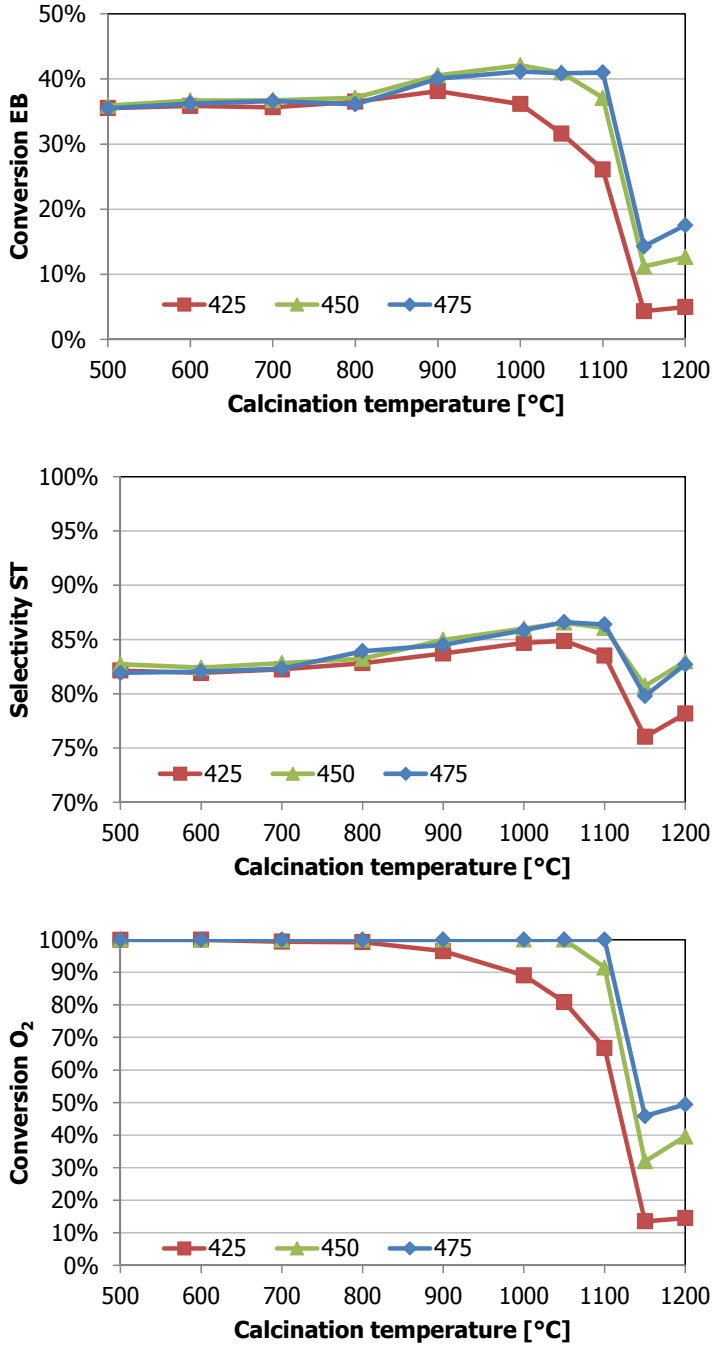

Figure 8.4: Styrene selectivity and conversions of EB and O_2 for the calcined alumina samples at the different operating temperatures. The numbers are averages of conditions 1 (475 °C, 4-8 h *TOS*), 4 (450 °C, 20-26 h *TOS*) and 7 (425 °C, 38-44 h *TOS*). All at a 0.6 O_2:EB feed ratio.

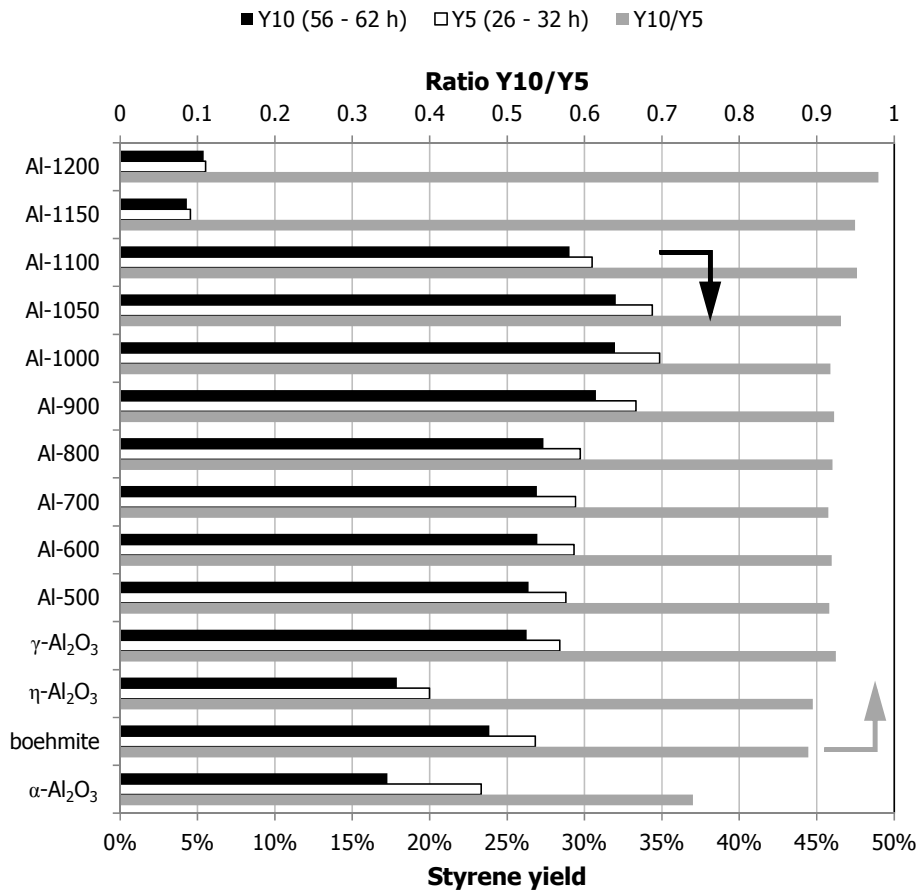

Figure 8.5: Yields and stability (grey) as the ratio of the styrene yield at the 5th (white, 26-32 h *TOS*) and 10th (black, 56-62 h *TOS*) condition, both at 450 °C and a 0.6 O_2:EB feed ratio.

8.4 Discussion

The high temperature calcination of alumina (500-1200 °C) is favourable for both EB conversion and ST selectivity in the oxidative dehydrogenation reaction. Although it is not directly clear what is causing the improvement, it can help in directing the further research to improve the catalyst system and get a better understanding of this complex catalyst system.

By the calcination of γ-Al_2O_3, the samples are dehydrated, the surfaces anneal and they are sintered, while other crystalline phases are being formed. As expected, δ-phase is formed at 900 °C and θ-phase is formed at 1000 °C and higher (Table 8.4). With the increasing calcination temperature, the specific surface area decreases. Also, the mass based acidity, specific surface area and pore volume of the alumina are reduced. The Al_2O_3 density increases by the sintering process and more sample is loaded in the reactor for a constant testing volume. Actually, in this study it appears that these four characterization parameters (pore volume, acidity, surface area and coke) are closely related to each other. As shown in Figure 8.6, these all follow a similar trend. The absolute amounts in the reactor are almost constant for calcination temperatures up to 900 °C. The loss in the weight based properties (Table 8.4) is compensated by the density increase. The pore volume, surface area and the amount of coke on the catalyst decrease between these calcination temperatures. Above 900 °C, there seems to be a tipping point, all of the parameters decrease more pronounced above this temperature. At this point the crystalline phase of the alumina starts to change from δ to θ. Only the decrease of the surface area seems to go a little faster than the other parameters.

As was expected, a less acidic alumina forms less coke deposits,[1] but it also gives a large improvement of the performance in the ODH of EB to ST (Figure 8.4). This can

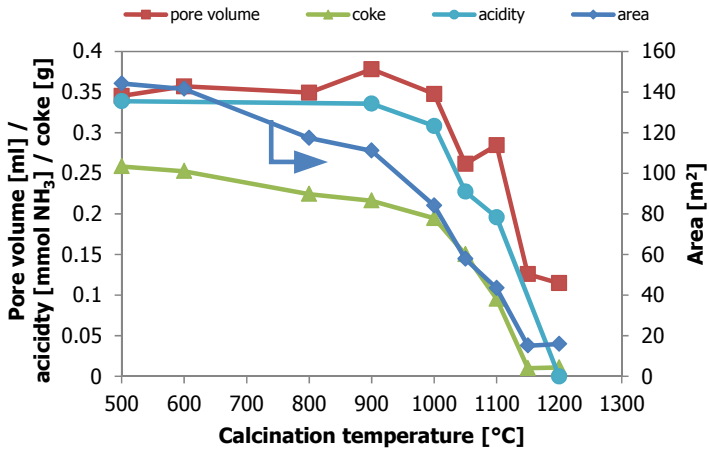

Figure 8.6: The absolute amounts of pore volume (■), acidity (●), coke (▲) and surface area (◆) in the reactor as a function of the calcination temperature of the catalyst samples.

be the result of three effects:

- the type of coke is different and becomes more active for dehydrogenation
- the production of CO_X is proportional to the amount of coke
- the accessibility of the coke is improved

The first effect was also reported when mineral acids (H_3BO_3 and H_3PO_4) were added, the C:H ratio and the C:O ratio of the coke increased, as well as the amount of coke.[1, 10] The type of coke, however, also changes with time on stream and the operating temperature (aging).[1] The TGA profiles of the calcined alumina samples do shift to higher temperatures for higher calcination temperatures (Figure 8.1) and indicate that the reactivity of the coke is slightly different. However, after 62 h and 10 conditions, it will be very hard to explicitly identify which one of these parameters is responsible for a change in the ODH performance.

The second effect is more straight-forward. By lowering the acidity and the surface area, the steady-state amount of coke is reduced. The samples with high surface area and acidity (calcined < 900 °C) form much more coke than is necessary for the dehydrogenation reaction (App. A.1), resulting in relatively more gasification of coke and thus loss of selectivity to CO_X. The samples that have the lowest surface areas have built up about enough coke. This is nicely depicted by the Al-1100 sample in Figure 8.4. At 475 °C it has an almost identical performance as the samples of lower calcination temperature, while at 450 °C and 425 °C its O_2 and EB conversion decrease, as well as its selectivity. The other samples have enough coke to compensate the lower activity due to the decrease in reaction temperature. This will also result in a loss in ST selectivity because of the higher CO_X production. An improvement in the ODH performance for high amounts of a different type of coke cannot be explained by this second effect.

The third effect has been described to explain differences in the ODH performance between several samples with varying pore volume distributions. As a result of the sample properties and the coke deposition, some micropores/mesopores could still be accessible to O_2 only (molecular diameter 0.35 nm) and not to EB (molecular diameter 0.7 nm). The oxidation of coke can continue, deteriorating the ODH performance, until EB has access again.[11, 12] With the calcined alumina series there is also a clear change in the pore volume above 1000 °C. This effect can clearly play a role in the observed ODH performance.

Another phenomenon that is observed in this work is the loss of selectivity at an incomplete oxygen conversion (Figure 8.4). More CO_X and heavy condensates are formed. These are both undesired products that do not represent any value and moreover, the heavy condensates can cause fouling issues downstream and create additional operation costs in the downstream equipment. The residual oxygen can also lead to

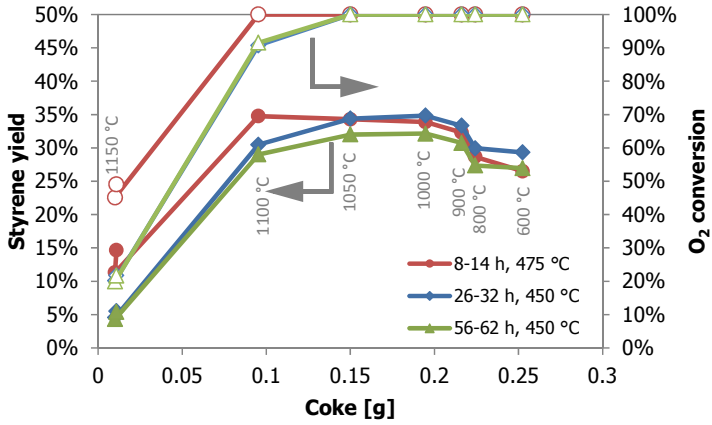

Figure 8.7: Styrene yield (◆▲●) and oxygen conversion (◇△○) as a function of the absolute amount of coke on the catalyst for the final performance at 450 °C / 56-62 h (▲△), at 450 °C / 26-32 h (◆◇) and at 475 °C / 8-14 h (●○). Other conditions: 0.6 O_2: EB feed ratio, 5 CO_2: EB feed ratio.

unwanted process conditions in a commercial operation. This emphasises the need to have a complete oxygen conversion. At full oxygen conversion, the improvements of styrene selectivity and ethylbenzene conversion are coupled. In Figure 8.4 between 800–1100°C, both go up simultaneously as a higher styrene selectivity means that less O_2 is spent on CO_X formation, leaving more O_2 for ethylbenzene conversion into styrene. This was also observed and discussed in Chapter 6.

When the styrene yield is plotted as a function of the amount of coke after 62 h *TOS*, Figure 8.7, these trends become clearer. Note that only the latest performance data (56-62 h) corresponds with the measured amounts of coke. Although the amount of coke is reported to go to a steady-state level[1], this is not what we have observed (Chapter 10). With low amounts of coke in the reactor at 450 °C (below 0.15 g), not all oxygen is converted and styrene yields are lower than was expected. At 475 °C, an amount of 0.10 g of coke is sufficient to convert all the oxygen and the performance is best at this point. At 475 °C, the samples that have higher amounts of coke have a lower styrene yield. With 0.15-0.20 g coke, also all oxygen is converted at 450 °C and this is the optimum in Figure 8.7. In the range of 0.15-0.20 g, the differences are small and this is the optimal region to operate in at the applied conditions. For higher temperatures the range becomes lower, 0.10-0.15 g. Above 0.20 g of coke the loss of yield due to CO_X becomes clearly visible for both temperatures. Figure 8.7 also shows the deactivation of the samples with time on stream. This deactivation can be caused by two effects: increasing amounts of coke, or an aging effect of the coke. This requires more data on coke, with time on stream, to become evident.

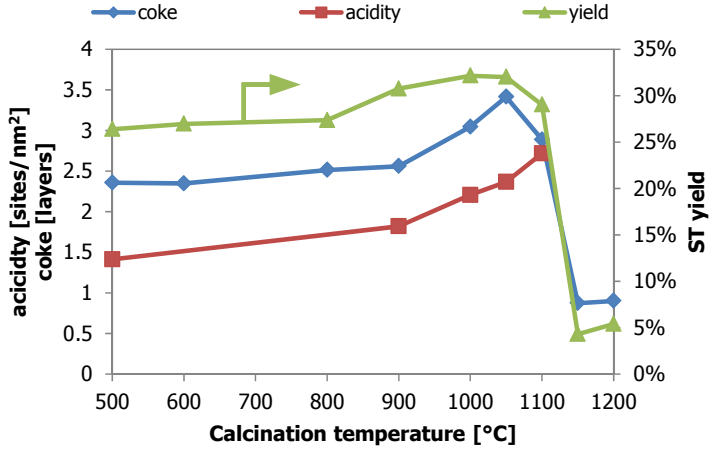

Figure 8.8: The surface acidity, and theoretical number of coke, and ST yield of the calcined aluminas as a function of the calcination temperature.

Another way to look at the available characterization data is to relate it to the specific surface area and see the effect on the ODH performance (Figure 8.8). The number of coke layers are calculated using the theoretical coverage of graphene (0.76 mg/m^2). The acid site density is in the same order of magnitude as determined in the literature (max. 9.3-14.3 sites/nm^2).[13] The amount of coke and the acid site density increase with the calcination temperature, because the surface area decreases faster than the other parameters. It should be noted that the NH_3-TPD quantification should be taken with care as the background level of the TPD profiles does not come back to zero. This reveals that the ST yield goes up with increasing acid site density and coke coverage. The acid site density increases from 1.4 to 2.7 sites/nm^2, coke coverage increases from 2.4 to 3.4 layers. The measured coke coverages are well above the amounts that are reported for a monolayer of coke (0.54-0.76 mg/m^2). Likewise for the column 'coke 120 min *TOS*'[1] in Table 8.1 that corresponds to coverages up to 1.5 layers. The high coke coverages in Figure 8.8 can have the following explanations: (1) the catalysts are deactivated after 62 h *TOS*, possibly due to too high coke coverage, making this coke data is not representative to compare with the ST yield; (2) more of the available catalyst surface is used for the ODH reaction, resulting in a higher coke coverage, the data is the average of the whole catalyst bed; and (3) a higher coke coverage is required for an improved ODH performance.

The η-Al_2O_3 sample should have the highest acidity[6] and therefore, should produce a lot of coke. The TGA analysis shows that the amount of coke after 62 h *TOS* is less than for the γ-Al_2O_3, but in spite of this its ODH performance is worse. It is hardly higher than the performance of uncoked and/or fresh γ-Al_2O_3. Based on the TGA profile, the type of coke is different and is easier to combust (25 °C lower, see Figure 8.1

and Table 8.4). In the ODH reaction this can result in higher selectivity to CO_X and furthermore due to its smaller pores compared to the γ-Al_2O_3. When more coke is formed, but at the same time it is gasified/oxidized faster too in those small pores and it will result in a lower amount of coke, but a higher selectivity to CO_X.

It can be hypothesized that the stronger (Lewis) acid sites or a higher acid site density that are formed by the high temperature calcination[3] are favourable for the selectivity and activity of the coke that is formed. The coke is more difficult to combust, leading to less CO_X and more ST. The coke that forms on the Brönsted and weak Lewis acid sites on the η- and γ-Al_2O_3 surface is more reactive for combustion and therefore, less selective for ST formation. However, the NH_3-TPD measurements do not show a clear change in the strength of the acid sites with the calcination temperature.

The development of a more active and selective catalyst for EB ODH is apparently a complex challenge. Coke is required for activity and selectivity, but there should be an optimum amount. A reduction of the steady-state amount of coke gives a more active and selective catalyst. The activity and the ST selectivity are coupled because of the full oxygen conversion. To enable an improvement in ST selectivity, less O_2 has to be consumed to produce CO_X that is again related to the amount of coke, the type of coke and its accessibility. The reduction of the amount of carbon is limited, however, because sufficient coke is required to achieve the full and selective conversion of oxygen. Stability tests are recommended to get insight on these phenomena.

8.5 Conclusions

The performance of γ-Al_2O_3 in the ODH reaction of EB to ST can be improved by calcining it at high temperature. The acid site density and coke coverage tend to increase with the calcination temperature. The coke becomes less reactive in O_2, more selective for the ODH reaction and is better accessible for both reactants. The mass based acidity, pore volume and surface area are reduced, other crystalline phases are formed and as a consequence, less coke is produced. Full oxygen conversion is required for optimal selectivity, setting the lower limit for the amount of coke. Under the applied conditions, the optimal calcination temperature is around 1000 °C, resulting in about 3 layers of coke on the alumina after 62 h *TOS*. Too much coke results in a loss in ST selectivity and ST yield due to more CO_X formation.

References

[1] A.E. Lisovskii, C. Aharoni, Catal. Rev. - Sci. Eng. 36 (1994) 25-74.
[2] G.E. Vrieland, J. Catal. 111 (1988) 1-13.
[3] F. Cavani, F. Trifiro, Appl. Catal. A: Gen., 1995, 133, 219-239.
[4] G. Emig, H. Hofmann, J. Catal.,1983, 84, 15-26.

[5] B.C. Lippens, J.J. Steggerda, in: B.G. Linsen, J.M.H. Fortuin, C. Okkerse, J.J. Steggerda (Eds.), Physical and Chemical Aspects of Adsorbents and Catalysts, Academic Press Inc., London, 1970, Ch. 4: Active Alumina, p. 171-211.
[6] E.B.M. Doesburg, K.P. De Jong, J.H.C. van Hooff, in: R.A. van Santen, P.W.N.M. van Leeuwen, J.A. Moulijn, B.A. Averill (Eds.), Catalysis: An Integrated Approach,Second, revised and enlarged ed., Elsevier, Amsterdam, 2000, Ch. 9: Preparation of Catalyst Supports, Zeolites and Mesoporous Materials, p. 433-484.
[7] P.A. Badkar, J.E. Bailey, J. Mater. Sci. 11 (1976) 1794-1806.
[8] J.L. Mcardle, G.L. Messing, J. Am. Ceram. Soc. 76 (1993) 214-222.
[9] S. Brunauer, P.H. Emmett, E. Teller, J. Am. Chem. Soc. 60 (1938) 309-319.
[10] R. Fiedorow, W. Przystajko, M. Sopa, J. Catal. 68 (1981) 33-41.
[11] G. Emig, H. Hofmann, J. Catal. 84 (1983) 15-26.
[12] L.E. Cadus, L.A. Arrua, O.F. Gorriz, J.B. Rivarola, Ind. Eng. Chem. Res. 27 (1988) 2241-2246.
[13] H. Knözinger, P. Ratnasamy, Catal. Rev. - Sci. Eng. 17 (1978) 31-70.

9

Oxidative dehydrogenation of ethylbenzene to styrene: Staged O_2 feeding

Abstract

Two catalyst samples, γ-Al_2O_3 and 5P/SiO_2, were applied in the oxidative dehydrogenation with the staged feeding of oxygen. Six isothermal packed bed reactors were used in series with intermediate feeding of O_2, resulting in total O_2:EB feed ratios of 0.2 to 0.6. All EB was fed, diluted with helium or CO_2 (1:5), to the first reactor. Compared with co-feeding at a total O_2:EB feed ratio of 0.6, by staged feeding the EB conversion (+ 15% points for both samples), ST selectivity (+ 4% points for both samples) and O_2 (ST) selectivity (+ 9% points for γ-Al_2O_3 and + 17% points for 5P/SiO_2) improved drastically and the targets for a commercial application are within reach. The production of CO_X was effectively reduced. The ethylbenzene conversion over 5P/SiO_2 can be increased from 18% to 70% by increasing the number of reactors and the total amount of O_2, without the loss of ST selectivity (93%). More catalyst was required to achieve full O_2 conversion in each reactor. For 5P/SiO_2 a higher temperature (500 °C *vs.* 450 °C for Al_2O_3) is required. Staged feeding of O_2 does not solve the existing issues of the stability both in time and catalyst regeneration (5P/SiO_2), or the relatively moderate performance (γ-Al_2O_3).

9.1 Introduction

For many reactions it is favourable to keep one reactant in a low concentration and a second one in a high concentration to reduce the byproduct formation. This works for reactions, where the reaction order of the first reactant in desired reaction is lower *than* in the undesired reaction. An example is the epoxidation reaction of ethylene to ethene oxide (EO), where a high concentration of oxygen and a low concentration of ethene are favourable. This was demonstrated by a membrane reactor setup with distributed feeding of ethene through the membrane tube containing the catalyst and oxygen fed directly to the catalyst bed. The reactant combustion to CO_X was reduced and both the EO product yield and selectivity increased.[1, 2]

In the oxidative dehydrogenation (ODH) process there are two main reactions that use oxygen, the oxidative dehydrogenation reaction 9.1 and the coke gasification reaction 9.2. The dehydrogenation reaction requires much less oxygen for the conversion of one molecule of ethylbenzene (EB) than the total oxidation of EB that is assumed to proceed *via* gasification reaction of the deposited coke. For the coke deposition the presence of oxygen also turned out to be essential (Chapter 11).

$$C_8H_{10} + \tfrac{1}{2}O_2 \rightarrow C_8H_8 + H_2O \qquad 9.1$$

$$C_8H_{10} + 10\tfrac{1}{2}O_2 \rightarrow (coke + O_2) \rightarrow 8CO_2 + 5H_2O \qquad 9.2$$

In the previous single feed experiments for the ODH reaction, both styrene and CO_X production showed a strong dependency on the O_2:EB ratio (Chapter 6-8). Some typical results when using γ-Al_2O_3 or 5P/SiO_2 in the ODH reaction are given in Table 9.1. When more O_2 is fed more ST is produced, but also relatively more CO_X, resulting in a lower ST selectivity and O_2 (ST) selectivity at the higher O_2:EB feed ratio. Therefore, the reaction order of O_2 in the ODH reaction is expected to be lower *than* of the

Table 9.1: Typical ODH results at different O_2:EB ratios for a single feed experiment with 500 mg sample at 450 °C (γ-Al_2O_3) or 500 °C (5P/SiO_2)

Sample	O_2:EB ratio	ST yield	ST[1] selectivity	CO_X yield	CO_X[1] selectivity	O_2 (ST)[2] selectivity
γ-Al_2O_3 (450 °C)	**0.2**	14%	88%	2%	10%	33%
	0.4	22%	84%	4%	14%	26%
	0.6	29%	82%	6%	16%	23%
5P/SiO_2 (500 °C)	**0.2**	23%	94%	1%	5%	55%
	0.6	48%	89%	5%	9%	38%

[1] remaining selectivity to benzene, toluene and heavy condensates.
[2] remaining selectivity to CO_X

gasification reaction and a low concentration of O_2 is desired.

With the staged oxygen feeding an extra degree of freedom is obtained. The local concentration of oxygen can be varied, as well as the total amount that is fed. So, the local concentration of oxygen becomes the additional variable. Moreover, operating the ODH reaction staged-wise will also give better heat control over the exothermal reactions that take place and the process can be operated further away from or outside of the explosive regime. Staged feeding might be an alternative reactor design for the ODH process.

To investigate this staged feeding concept the reference catalyst, γ-Al_2O_3 and the best available catalyst, 5P/SiO_2, identified in Chapter 7 (see Table 9.1) are utilised in this chapter. The staged feeding is realised by placing several reactors in series and distributing the total amount of oxygen over the reactors. The total amount of oxygen and the number of reactors will be varied. The results will be compared with the 'single feed' experiments.

9.2 Experimental

9.2.1 Catalyst preparation

The γ-Al_2O_3 extrudates (Ketjen CK300, 0.57 ml/g, 190 m^2/g) are crushed, sieved to 212-425 μm particles and used as such.

The SiO_2 support (silica NorPro, SS61138, 1.00 ml/g, 257 m^2/g) is crushed and sieved to 212-425 μm and dried at 150 °C in vacuum for four hours. The phosphorous is introduced by impregnation using the incipient wetness method with a 5% excess of the pore volume. The required amounts of H_3PO_4 are mixed with demineralised water, after which the SiO_2 support is impregnated with the solution. The wetted support is shaken vigorously with an automatic shaker to homogenize the impregnated support. Next it is dried at 70 °C in air overnight, followed by calcination in a static air calcination oven at 500 °C for eight hours. The heating rate is set at 4 °C /min.

9.2.2 Catalyst testing

9.2.2.1 Single feed experiments

The oxidative dehydrogenation experiments are performed in a parallel fixed bed reactor setup with 6 quartz reactors with an inner diameter of 4 mm, in down-flow operation. For the single feed experiments, the ethylbenzene (1 g/h liquid, 3.6 Nml/min vapour), oxygen and diluent are fed to each reactor. Typical molar feeding ratios are O_2:EB = 0.6 and (diluent + O_2):EB = 10. The ethylbenzene liquid is fed into a heated α-

Al_2O_3 filled tube, where it is evaporated in a co-current flow with the gas feed. This evaporator is located in an oven, where also the reactor furnace is installed. Each reactor is loaded with 0.80 ml of the catalyst, giving a catalyst bed height of about 65 mm (typically 500 mg catalyst). The reactors are loaded – from top to bottom – with a quartz wool plug, 10cm glass pearls (0.5 mm diameter), the catalyst, 10 cm glass pearls (0.5 mm diameter) and a quartz wool plug. The catalyst bed is positioned within the 20 cm isothermal zone of the reactor. The W/F_{EB} is 212 g-cath/mol, $GHSV_{TOT}$ is 3.000 l/l/h and $WHSV_{EB}$ is 2 g/g/h. The pressure at the setup outlet is atmospheric, the pressure drop over a reactor is about 0.1 bar, giving a typical pressure before a reactor of 1.2-1.3 bara.

The reactors are heated up under nitrogen flow with 5 °C/min. The temperature is allowed to stabilize for another 15 minutes when the reaction temperature is reached. The temperature for the Al_2O_3 experiments was 450 °C, for the $5P/SiO_2$ experiments it was mostly 500 °C, but also 475 and 525 °C were used. The EB flow is started first (1-5 minutes earlier), before any oxygen is added to the gas mixture to prevent any pre-oxidation of the catalyst samples. The reaction starts when oxygen is added to the reactors.

9.2.2.2 Staged feeding experiments

For the staged feeding experiments, the 6 reactors were connected in series. A simplified scheme of the setup is shown in Figure 9.1. All of the 6 quartz reactors were loaded with 500 mg of the catalyst, giving a catalyst bed height of about 65 mm (0.80 ml). The ethylbenzene (1 g/h liquid, 3.6 Nml/min vapour) was fed to the first reactor together with the CO_2 or He diluent (18 ml/min STP (= 1 atm, 20 °C)) for a good evaporation, resulting in an initial 1:5 EB:diluent molar ratio. A mixture of air and nitrogen is fed before the first reactor and as side-feeds in between each reactor. The side-feeds were controlled by individual mass flow controllers. The flow was varied between 1.7

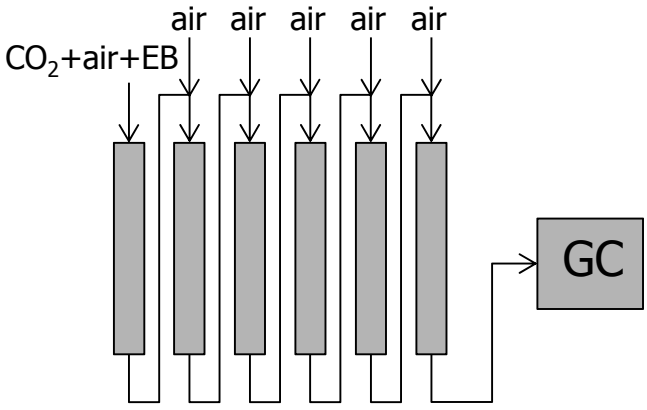

Figure 9.1: Simplified scheme of the modified 6-flow setup.

and 10 ml/min STP. The typical total molar feed flow rates are O_2:EB = 0.6, (diluent + O_2):EB = 8 to 22. The W/F_{EB} is 35 g-cat·h/mol, $GHSV_{TOT}$ is 2,400 to 6,000 l/l/h and $WHSV_{EB}$ is 0.33 g/g/h. The pressure at the setup outlet is atmospheric, the pressure drop over each reactor is about 0.1 bar, giving a typical pressure before the first reactor of 1.7-1.8 bara.

9.2.2.3 Reactor gas analysis

During the ODH experiments, the concentrations in the reactor effluent are measured online by a two channel gas chromatograph with a TCD (columns: 0.3m Hayesep Q 80-100 mesh with back-flush, 25m × 0.53mm Porabond Q and 15 m × 0.53mm molsieve 5A with bypass option for CO_2 and H_2O, all in series) for permanent gas analysis (CO_2, H_2, N_2, O_2, CO) and a FID (column: 30m × 0.53mm, D_f = 3μm, RTX-1) for the hydrocarbons analysis (methane, ethane, ethene, benzene, toluene, ethylbenzene, styrene, heavy condensates). One analysis, from start to start, takes 15 minutes. A constant flow of nitrogen is used as the internal standard. The internal standard was fed just before the GC. The side feed air + N_2 gas mixture was analysed every 7th analysis. This is used as an extra control for the quality of the analysis. The lines from the reactor to the GC are heat-traced at 175 °C to prevent condensation of the vapours. The EB and O_2 conversion, ST and O_2 selectivities and ST yields are based on moles of ethylbenzene and calculated according to Eqs. 9.3-9.7. The overall carbon balance is >99%, only the carbon that is deposited on the catalyst as coke is missing from the carbon balance by the GC analysis.

$$EB\ conversion = \frac{EB_{in} - EB_{out}}{EB_{in}} \tag{9.3}$$

$$ST\ selectivity = \frac{ST_{out}}{EB_{in} - EB_{out}} \tag{9.4}$$

$$ST\ yield = EB\ conversion \times ST\ selectivity \tag{9.5}$$

$$O_2\ conversion = \frac{O_{2,in} - O_{2,out}}{O_{2,in}} \tag{9.6}$$

$$O_2\ selectivity = \frac{ST\ yield \times 0.5}{O_{2,in} / EB_{in} \times O_2\ conversion} \tag{9.7}$$

9.3 Results

9.3.1 The reference γ-Al_2O_3

The staged feeding experiment with alumina was carried out successful. The 6 sequential reactors with 6 oxygen side-feeds and 6 x 500 mg sample give 49% EB conversion and 86% ST selectivity at a 0.68 O_2:EB total feed ratio, compared with 35% EB conversion and 82% ST selectivity at a O_2:EB feed ratio of 0.64 for a single feed reactor with only 500 mg sample. In both cases with full oxygen conversion. The O_2 (ST) selectivity increased from 23% to 32%. By closing the oxygen side-feeds to the reactors, one at a time starting with the last reactor, a linear relationship for the EB conversion and ST and CO_X selectivities as a function of the O_2:EB ratio is obtained, as is shown in Figure 9.2. The EB conversion increases from 10% to 49% by increasing the number of oxygen feeds (and the total amount of O_2 fed). At the same time the ST selectivity only decreases from 88% to 86%, so the ST yield increases nearly proportionally with the O_2 fed. The small ST selectivity change is ascribed completely to the increased CO_X production. The O_2 (ST) selectivity decreases from 39% to 32%. The selectivity to the benzene and toluene byproducts is constant at 3% for all conditions. It appears that the styrene product is stable and does not react in the sequential reactors that have no oxygen feed, or in the last reactor where the hydrocarbon inlet feed is about 1/3 ST and 2/3 EB.

When the total amount of oxygen is lowered from a total O_2:EB ratio of 0.65 to 0.2, but still distributing it in 6 parts to the 6 reactors, the EB conversion decreases from

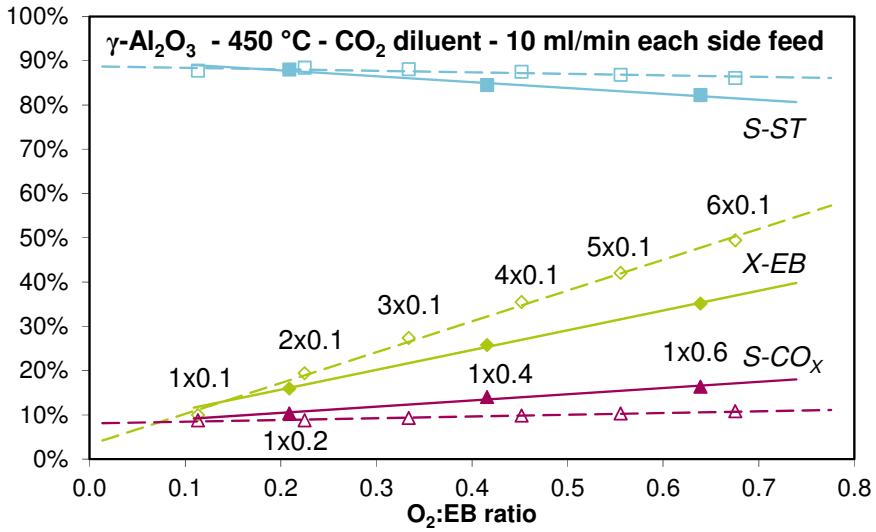

Figure 9.2: Staged feeding using a varying number of side feeds (open symbols) compared to single feeding (closed symbols) over γ-Al_2O_3 as a function of the total O_2:EB_0 feed ratio. Shown are the ST selectivity (*S-ST*), EB conversion (*X-EB*) and CO_X selectivity (*S-CO_X*). 4x0.1 means 4 reactors with each 0.1 O_2:EB_0 feeding.

48% to 21%, whilst the ST selectivity increases from 87% to 91% and the O_2 (ST) selectivity increases from 32% to 48%. This is shown in Figure 9.3. At all three O_2:EB ratios, the staged feeding mode with 6 reactors results in a higher EB conversion and ST selectivity than the single feeding mode, but 6 times more catalyst is used.

9.3.2 The 5P/SiO_2 sample

The EB conversion, ST and CO_X selectivities as a function of the O_2:EB ratio for the 5P/SiO_2 sample in single and staged feeding are shown in Figure 9.4. This staged feeding experiment also shows improved EB conversion and ST selectivity when oxygen is fed stage-wise. Comparing the single feeding with the staged feeding at similar total O_2:EB feed ratios of about 0.6, the EB conversion increases from 55% to 70%, respectively and ST selectivity increases from 89% to 93%, respectively. The O_2 (ST) selectivity increases from 38% to 55%. The O_2 is completely converted under all conditions. The CO_X formation is reduced, thereby improving the EB conversion and ST selectivity. By increasing the number of reactors from 1 to 6 and the total O_2:EB ratio from 0.1 to 0.6, the EB conversion increased from 18% to 70%, whilst maintaining a high ST selectivity of 93%. The yield to benzene and toluene is constant at 1% under all the conditions. Also here it appears that the styrene product is stable and does not react in the sequential reactors that have no oxygen feed. Or in the last reactor where the hydrocarbon inlet feed is about ½ ST and ½ EB.

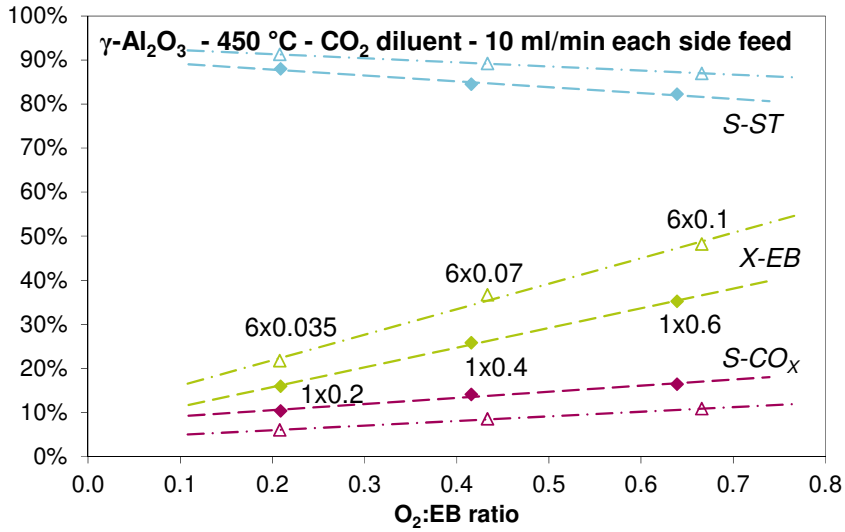

Figure 9.3: Staged feeding with 6 reactors (open symbols) compared to single feeding (closed symbols) over γ-Al_2O_3 as a function of the total O_2:EB_0 feed ratio. Shown are ST selectivity (*S-ST*), EB conversion (*X-EB*) and CO_X selectivity (*S-*CO_X).

A single stability experiment with the reactivated 5P/SiO_2 sample shows that the performance with the time on stream (*TOS*) for the ODH reaction is not constant (Figure 9.5). There is an optimum in the performance after 3 h *TOS*, at the moment that the O_2 conversion reaches 100%. From that point onward the catalyst deactivates and the selectivity to CO_X increases, reducing the ST selectivity, EB conversion and O_2 (ST) selectivity. Ten hours later, at 13 h *TOS*, the EB conversion decreased from 64% to 54%, the ST selectivity from 91% to 89.5% and the O_2 (ST) selectivity from 47% to 40%. After 100 h *TOS*, a 47% EB conversion, 86.5% ST selectivity and a 31% O_2 (ST) selectivity is left. With the *TOS* the conversion fluctuates a little due to tiny variations in the amount of oxygen. The sample had a history of 160 h *TOS* with three regeneration steps before this experiment. The ODH performance optimum of the fresh sample is better than the three times regenerated sample, the maximum EB conversion decreases from 70% to 64%, the corresponding ST selectivity decreases from 93% to 91% and the O_2 (ST) selectivity decreases from 55% to 47%. These 6 reactors with the 5P/SiO_2 sample have been used for almost 900 h *TOS*. The results during this period at 500 °C and a 0.6 O_2:EB total ratio are shown in Figure 9.6. A collection of results, shortly after the (re-) activation is given in Table 9.2. The last (6^{th}) reactivation of the catalysts shows the lowest optimum ODH performance: EB conversion of 62%, ST selectivity of 89% and O_2 (ST) selectivity of 41%.

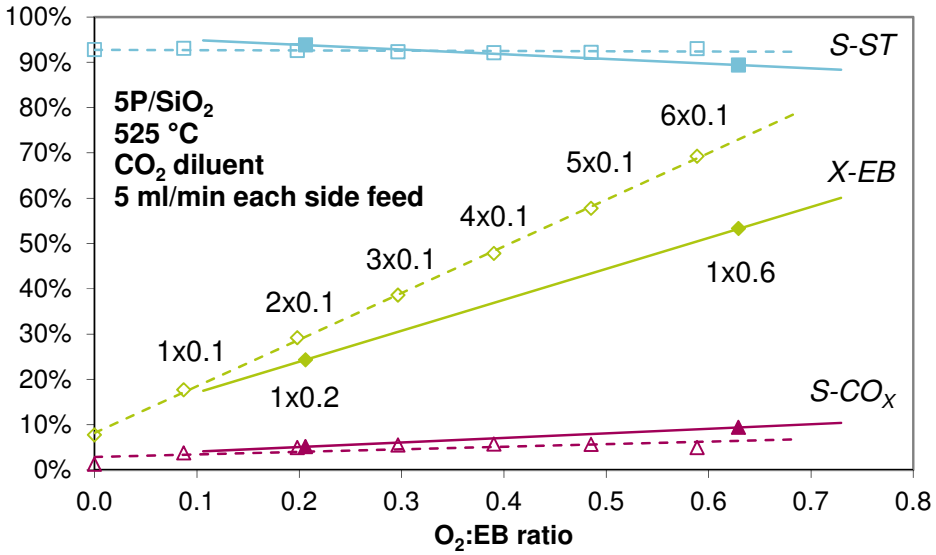

Figure 9.4: ST selectivity (S-ST), EB conversion (X-EB) and CO_X selectivity (S-CO_X) of 5P/SiO_2 in staged feeding using a varying number of side feeds (open symbols) and in single feeding (closed symbols) as a function of the total O_2:EB_0 feed ratio. Conditions: 500 mg sample/reactor, 500 °C, 18 ml/min CO_2, 1 g EB/h (3.6 ml/min EB vapour), 5 ml/min each side feed, 4x0.1 means 4 reactors with each 0.1 O_2:EB_0 feeding.

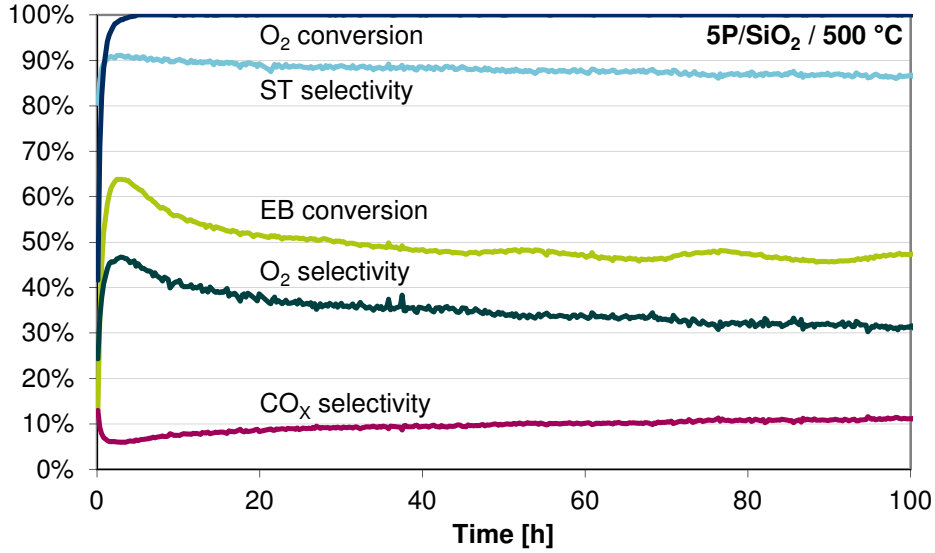

Figure 9.5: Performance versus time on stream after reactivation of the 5P/SiO_2 sample in staged feeding with 6 reactors. Conditions: 500 mg sample/reactor, 500 °C, He diluent, 1 g EB/h (3.6 ml/min EB vapour), 1.7 ml/min air each side feed, 0.6 O_2:EB total feed ratio. The samples have a 160 h *TOS* history.

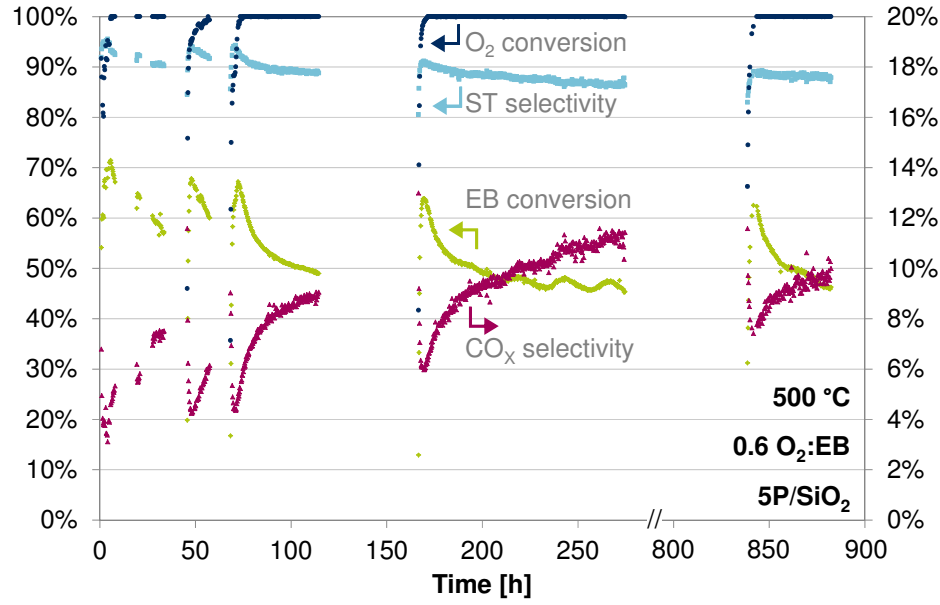

Figure 9.6: Performance during 900 h time on stream of the 5P/SiO_2 sample in staged feeding with 6 reactors. Conditions: 500 mg sample/reactor, 500 °C, He diluent, 1 g EB/h (3.6 ml/min EB vapour), 1.7 ml/min air each side feed, 0.6 O_2:EB total feed ratio.

Table 9.2: Performance data of the 5P/SiO_2 sample at different times on stream.

TOS [h]	*TAA* [h]	Regen. Nr.	Temp. [°C]	ST yield	ST sel.	CO_X sel.	EB conv.	O_2 conv.	O_2 (ST) sel.
2	2	0	475	57%	95%	4%	60%	80%	58%
3	3	0	500	66%	95%	3%	70%	92%	62%
6	6	0	525	65%	93%	5%	70%	100%	55%
48	3	1	500	64%	94%	4%	68%	95%	56%
71	3	2	500	63%	93%	5%	67%	98%	55%
169	3	3	500	58%	91%	6%	64%	99%	47%
842	3	6	500	56%	89%	7%	63%	98%	41%

TOS: time on stream, *TAA*: time after (re)activation, Regen. Nr.: number of regenerations, Temp.: temperature, sel.: selectivity, conv.: conversion.

9.3.3 The effect of diluent

The amount of diluent at the inlet has a small effect on the O_2 and EB conversion, as more diluent results in lower reactant concentrations and total *GHSV*. The same effects are observed on changing the amount of diluent (N_2) in the side feed while maintaining the same amount of oxygen (Figure 9.7). The O_2 conversion decreases from 99% at a side feed flow rate to each reactor of 2 ml/min to 96% at a side feed flow rate of 10 ml/min. Feeding pure air without the addition of nitrogen shows the highest activity. Selectivities do not change when using different amounts of diluent in the applied dilution ratios of diluent:EB between 8.3 and 21.7. The optimum ODH performance of 3P/SiO_2 (58% EB conversion at 92% ST selectivity and 49% O_2 (ST) selectivity) is a little lower than of 5P/SiO_2.

Other experiments with 3P/SiO_2 show that changing the type diluent at the inlet, either CO_2 or He (not shown), has a negligible or no effect at all, similar to what was observed in Ch.6.

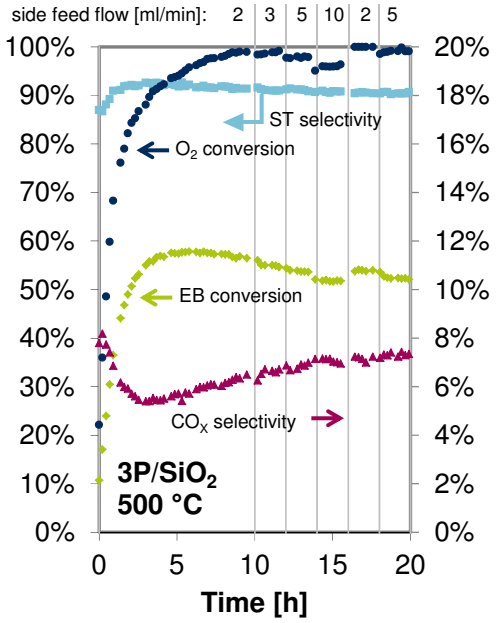

Figure 9.7: Performance versus time on stream of the 3P/SiO_2 sample in staged feeding with 6 reactors and varying side feed flows. Conditions: 500 mg sample/reactor, 500 °C, He diluent, 1 g EB/h (3.6 ml/min EB vapour), 0.6 O_2:EB total feed ratio.

9.4 Discussion

These staged feeding experiments are prime examples to demonstrate the advantage of staged wise (cross flow) feeding of one of the reactants (Figure 9.2-10.4). By reducing the concentration of oxygen, it is used much more efficiently by the desired dehydrogenation reaction. Because the reaction stoichiometry between O_2 and EB for the two competing reactions 9.1 and 9.2 is very different (0.5 to 10.5), a small increase in ST selectivity is observed together with a larger increase in EB conversion.

The penalty that has to be paid for the lower O_2 concentrations is the increase in the amount of catalyst that is needed. Each reactor in the staged feeding experiment is loaded with the same amount of catalyst as the reactor used for the single feed experiment. At lower oxygen concentrations, the reaction rates are lower and more catalyst is required for full oxygen conversion, which is a requirement in the optimal ST selectivity operation (Chapter 8, 9, Figure 9.5).

From an operational perspective, the staged feeding option could offer a win-win-situation. Besides the improved styrene yield, staged feeding also gives the possibility to control the exothermic reaction by cooling in between the adiabatic reactors. For instance 80% conversion with only air as diluent would give an adiabatic temperature rise of more than 300 °C. This is not realistic. Either a diluent or the in-between cooling is necessary to restrain the temperature rise and the consequent byproduct formation due to cracking reactions. To reach the competitive targets for this dehydrogenation reaction, at least 7 or 8 reactors would be required, limiting the adiabatic temperature rise to only 30-40 °C per reactor. A fluidised bed with internal cooling and fractal oxygen injection is also an option. An alternative could also be a series of two-zone fluidised bed reactors, where the catalyst is regenerated continuously.[3, 4] These fluidised bed type reactors have not yet found a practical application.

It is intriguing to see that in the staged feeding experiment over $5P/SiO_2$ the EB conversion can be increased from 18% to 70% without a significant loss of the ST selectivity (Figure 9.4). And similarly for the Al_2O_3 sample where the EB conversion increases from 10% to 49% (Figure 9.2). It is much more common in selective oxidations that a product can react further, or that product inhibition takes place. The adsorbed oxygen on the catalyst prefers to react with EB and not with ST, even though that has a reactive double bond in its side chain.

Achieving full oxygen conversion with $5P/SiO_2$ is much harder than with γ-Al_2O_3. At 450 °C and even at 425 °C, all the oxygen is already converted over the alumina. With the P/SiO_2 sample it is necessary to go up to at least 500 °C for full oxygen conversion. At a temperature of 475 °C, the selectivity to styrene is already high (95%), but the O_2 conversion is incomplete (80%) and therefore, the EB conversion (60%) does not reach its potential conversion level (Table 9.2). Lowering the amount of diluent in the

side feeds also improves the catalyst activation (Figure 9.7). It is probably much more difficult to form sufficient coke on the 5P/SiO_2 sample to reach full oxygen conversion. The SiO_2 support itself does not form coke and does not become active for the ODH reaction at all (Ch. 7). Probably only the acidic sites that are formed by phosphorous deposition form a little coke and that is almost in balance with the amount of coke that is being gasified.

Another issue with the 5P/SiO_2 sample is its deactivation with *TOS* and after regenerations (Figure 9.5). It shows very nice optimum values of 64% EB conversion and 91% ST selectivity, but ten hours later already 10% points of EB conversion are lost and selectivity decreases 2% points. The deactivation slowly continues after the initial large decrease. Regeneration will not bring the catalyst back completely to its initial optimum of 70% EB conversion and 93% ST selectivity (Figure 9.6 and Table 9.2). The catalyst stability has to improve a lot before it can be applied in industry (lifetime of at least 2 years). The continuous coke deposition is believed to be the cause of the deactivation with *TOS* and the activity can be recovered to a large extent by regeneration for the P/SiO_2 catalyst. The cause for the permanent deactivation is still unclear. Perhaps a solid state reaction between the phosphorous and SiO_2 support occurs that deteriorates the ODH performance. The alumina sample does not show this initial fast deactivation, it deactivates much slower with *TOS* and it can be regenerated completely to its original performance. Unfortunately, this catalytic performance, in terms of EB conversion and ST selectivity, is worse than of the 5P/SiO_2 sample.

The activity of the 3P/SiO_2 samples could be improved by lowering the amount of diluent in the feed and in the side feeds without affecting the ST selectivity (Figure 9.7). The molar diluent:EB ratio was lowered from 21.7 to 8.3. This was not tested for the γ-Al_2O_3. Apparently, the total *GHSV* or diluent amount and by that the concentrations of O_2 and EB do not play a role for the ST selectivity. This indicates that for P/SiO_2 samples the selectivity depends only on the local (per reactor) feed ratio between O_2 and EB (Figure 9.4). Staged feeding effectively lowers this local O_2:EB feed ratio.

Another difference from these staged feeding experiments compared to the single feed experiments is the varying concentration of EB. It enters the first reactor with a concentration of up to 15 vol% and decreases due the dilution with the O_2 feed at each reactor inlet to 11 or 4.5 vol%, depending on the side feed flows. Decreasing the feed EB concentration on purpose by increasing the feed diluent flow did not give a measurable effect (not shown). The 6× increase in catalyst amount due to the 6× decrease in O_2 concentration already compensates enough for the decreased EB concentration. Also take notice that the total WHSV is 6× lower than of the single feed experiments.

In this chapter the concept of O_2 (ST) selectivity is introduced. This parameter directly shows what part of the O_2 is used for the selective oxidative dehydrogenation

reaction. Most results are obtained at a O_2:EB feed ratio of 0.6, a small excess of oxygen compared with the stoichiometric amount of 0.5 for full EB conversion. At the required full oxygen conversion, the maximum obtained O_2 (ST) selectivity is 32% for γ-Al_2O_3 sample and 55% for the 5P/SiO_2 sample. Further improvements are required to reach the desired O_2 (ST) selectivity of > 65% to meet the commercial targets of 80% conversion and 97% selectivity (Ch.2). The CO_X and ST selectivities do not change much above an O_2 (ST) selectivity of 50%. This new parameter helps to visualize the significance the improvements that have been achieved and that still need to be achieved.

9.5 Conclusions

Staged feeding is very advantageous in the ODH reaction of EB to ST. Conversion of EB and ST selectivity are a function of the total O_2 to EB feed ratio, but are drastically improved by staged feeding, maintaining low O_2 partial pressures in all reactors. The losses in ST selectivity and EB conversion due to CO_X production are effectively reduced. The selectivity losses are minimal when increasing the number of side feeds and, thereby, the EB conversion. The activity of the samples is lower when used in staged feeding, due to lower reactant concentrations. More sample is needed for complete O_2 conversion. The ST selectivity of the 5P/SiO_2 sample is mainly determined by the local O_2:EB feed ratio and not their absolute concentrations. The tested samples are not commercially interesting yet, as they suffer from poor stability (P/SiO_2) or mediocre performance (γ-Al_2O_3). The O_2 (ST) selectivity can help in assessing the performance of the catalyst samples.

References

[1] D. Lafarga, A. Varma, Chem. Eng. Sci. 55 (2000) 749-758.
[2] M.A. Pena, D.M. Carr, K.L. Yeung, A. Varma, Chem. Eng. Sci. 53 (1998) 3821-3834.
[3] J. Gascon, C. Tellez, J. Herguido, A. Menendez, Chem. Eng. J. 106 (2005) 91-96.
[4] J. Herguido, M. Menendez, J. Santamaria, Catal. Today. 100 (2005) 181-189.

10

Catalyst coking in the oxidative dehydrogenation of EB to ST

Abstract

A packed bed microbalance reactor setup (TEOM-GC) is used to investigate the formation of coke as a function of time on stream on γ-Al_2O_3 and 3P/SiO_2 catalyst samples under different conditions for the ODH reaction of ethylbenzene to styrene. The product gas is analysed by an online GC, so both the weight and performance of the catalyst with time on stream are recorded. On alumina based catalyst samples a fast initial coke build-up takes place, the coverage of coke does not stabilize but grows with time on stream, although the rate of coke deposition decreases with time on stream. On the 3 wt% P/SiO_2 sample the initial coke build-up is slow and the coke deposition rate increases with time. All samples show a linear correlation of the styrene yield with the initial coverage of coke. When the styrene yields reach their maximum, the data diverges from this correlation. The CO_X production increases with the coverage of coke. A higher oxygen partial pressure gives more coke, a higher temperature gives less coke and the coverage of coke on the catalyst varies with the position in the bed. The optimal coverage of coke should be sufficient to convert all O_2, but as low as possible to prevent selectivity loss by CO_X production and depends on all the parameters: temperature, O_2:EB ratio, reactant concentrations and the type of starting material.

10.1 Introduction

Studies on the catalyst coking are usually performed to gain insight on the catalyst deactivation. In catalytic cracking, the carbon deposits block the acid sites that are active for the cracking reactions, causing the catalyst deactivation.[1, 2] The oxidative dehydrogenation reaction is an exception to this. The reaction is not catalysed by the catalyst that is loaded into the reactor, but by the coke that is formed during the reaction.[3-5] By studying the coke formation, information on the real catalyst in ODH is obtained. Coke can be formed in several ways: oligomerisation of olefins, poly-alkylation of aromatics and condensation of aromatics.[2]

For ODH it is generally accepted that the oxygen groups on the surface of the deposited coke, like the quinone and hydroquinone groups, are the catalytically selective active sites. These can undergo a redox reaction where ethylbenzene (EB) is the reducing agent and the oxygen is the oxidizing agent.[6] It is also possible that (oxygen) radicals take part in the dehydrogenation mechanism.[7] In the past, a few studies focused on the formation of the carbon deposits on aluminas[8] and metal pyrophosphates.[5] There are several factors that influence the formation of coke on Al_2O_3 in ODH:[8]

- A higher oxygen partial pressure will give more coke,
- A maximum is present when varying temperature,
- The acidity of the catalyst increases the coke formation.

According to Lisovskii *et al*. these factors result in a stable amount of coke on a Al_2O_3 catalyst, a monolayer, that covers the catalyst surface.[8] For a specific surface area of 100 m^2/g this coke monolayer is about 4 wt%, at 200 m^2/g it amounts to 8-9 wt%. The amount of monolayer coke normalised for the specific surface area is equal: 0.54 mg/m^2.[8] For the metal pyrophosphate catalysts, a monolayer corresponds to about 0.8 mg/m^2.[5]

One of the tools that are available to study coke formation dynamics are microbalance reactors. A special type of microbalance reactor is the TEOM, an inertial microbalance that uses the natural frequency of the oscillating tapered element to determine the mass.[9] The TEOM reactor has a well-defined gas phase (fixed bed reactor), a high mass resolution and stability and can operate under experimental conditions that are relevant to practical operation.[10] It does not suffer from external mass transfer limitations or gas bypassing, as is the case for hanging basket type microbalance reactors.[9] The TEOM has found applications in many topics such as coke deposition, adsorption and diffusion in zeolites, gas storage, synthesis of carbon fibres.[11]

In Chapters 6-8 many catalyst samples have been tested and discussed. The optimal performances of four of these samples are given in Table 10.1. The γ-Al_2O_3 is the reference sample in this work. It reaches 29% ST yield at 82% ST selectivity. The addition of a phosphorous promoter improves the ODH performance of the Al_2O_3 to some

Table 10.1: Data on the performance in the ODH reaction.

Sample	Temp. [°C]	O_2:EB	ST yield	ST selectivity	CO_X selectivity
γ-Al_2O_3	450	0.6	29%	82%	16%
1.3P/Al_2O_3	475	0.6	31%	83%	15%
Al-1000	450	0.6	36%	86%	13%
3P/SiO_2	475	0.6	51%	91%	8%

extent, 2% points increase in ST yield and 1% point in ST selectivity. The high temperature (1000 °C) calcined Al_2O_3 sample Al-1000, shows a larger improvement of the performance with 36% ST yield and 86% ST selectivity. The 3 wt% P/SiO_2 sample is one of the best performing samples that was tested and reaches 51% ST yield at 91% ST selectivity.

The goal of this chapter is to obtain more detailed information on the formation of the carbon deposits on γ-Al_2O_3, Al_2O_3 calcined at 1000 °C, 1.3 wt% P/Al_2O_3 and 3 wt% P/SiO_2 catalyst samples. This will be done using a TEOM-GC reactor setup. This setup will generate continuous data on the catalyst sample mass and the catalyst performance in the ODH reaction with the time on stream.

10.2 Experimental

10.2.1 Catalyst preparation

The preparation of the catalyst samples that are used are described in Chapter 6. An overview of the catalyst samples and their properties is given in Table 10.2.

10.2.2 The TEOM reactor setup

The tapered element oscillating microbalance (TEOM) reactor setup is an excellent tool for measuring the mass changes of a catalyst sample under reaction conditions. This mass change can be the result of coke formation, adsorption, desorption, oxidation, or reduction. A mass change of less than 1 microgram can be measured. Already a change in the gas composition can be detected by this method. The reactor is a true fixed bed reactor, not a hanging basket that may suffer from external mass transfer.

Table 10.2: Specifications of the used catalyst samples.

Sample	S_A [m^2/g]	V_P [ml/g]	Sample Amount [mg]	other
γ-Al_2O_3	272	0.83	60.9	Ketjen CK300
Al-1000	119	0.49	77.6	Calcined at 1000 °C
1.3P/Al_2O_3	245	0.59	60.9	1.3 wt% P on Ketjen 3P
3P/SiO_2	164	0.76	46.1[a] / 50[b]	3 wt% P on SiO_2

[a] 20 h *TOS* experiment, Figure 10.11.
[b] 130 h *TOS* experiment, Figure 10.12.

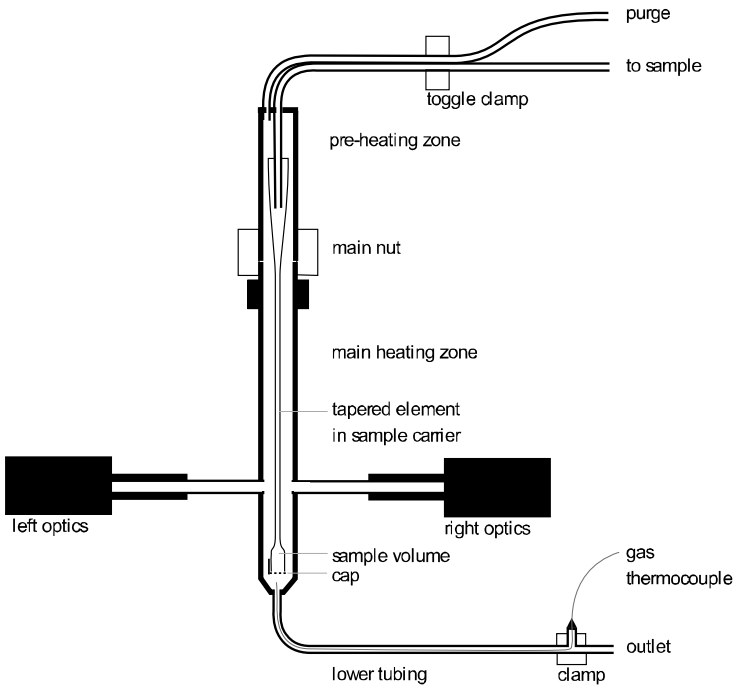

Figure 10.1: Schematic of the TEOM reactor part.

Internal mass transport limitations need to be checked, like for any other fixed bed reactor. A commercial (now discontinued) Rupprecht and Patashnick (R&P) 1500 Pulse Mass Analyser is used in this work. A schematic layout of the reactor part is shown in Figure 10.1.

The working principle of the balance is based on the natural oscillation frequency of the reactor that is at the end of a tapered element. The frequency of this oscillation depends on the weight of the sample. This frequency is accurately measured by an infrared beam, perpendicular to the oscillation. A change of the frequency from f_0 to f_1 from time t_0 to t_1 results in a total mass change (of gas and solids in the sample volume) that is calculated according to Eq. 10.1. The spring constant K_0 is determined by using a calibration weight with the reactor.

$$\Delta M = \Delta M_S + \Delta M_G = K_0 \left(\frac{1}{f_1^2} - \frac{1}{f_0^2} \right) \qquad 10.1$$

In the reactor setup, a catalyst sample of maximum 100 mg can be used. This is held in position by a quartz wool plug at the top and at the bottom. A metal cap with

small holes in it is used to close the reactor end. There are two temperature zones, a preheating zone that can be heated from 50 °C to 500 °C and a reaction zone that can be heated from 50 °C to 600 °C. The operating pressure is between 0 barg (ambient pressure) and 10 barg. A reaction mixture can be formed from three gases and one liquid feed that is evaporated. The flows are all accurately controlled by six mass flow controllers. The connected gases are helium (MFC1, max 500 Nml/min; MFC2, max 200 Nml/min; MFC5, max 100 Nml/min), air (MFC4, max 2 Nml/min) and carbon dioxide (MFC3, max 100 Nml/min). All flows are reported at the standard conditions of 20 °C / 1 atm. The ethylbenzene is fed as a liquid (LMFC, max 0.6 g/h).

At the start of an experiment, the reactor (450-500 °C) and preheating zone (200 °C) are heated up under a helium flow (25 Nml/min) through the reactor and a helium purge flow (100 Nml/min) along the reactor. When the sample mass is stabilised (normalised standard deviation < $3x10^{-6}$), the reaction was started by switching to the reactor feed that consists of air (0.12-1.07 Nml/min), helium (25 Nml/min) and the ethylbenzene vapour (0.13 g/h or 0.45 Nml/min vapour). This gives an EB concentration of 1.7 vol%. The helium purge flow is not changed. The O_2:EB molar feed ratio is varied between 0.05 and 0.5. The (diluent + O_2):EB molar feed ratio is 58. The W/F_{EB} is between 37 and 64 g-cat·h/mol. The $GHSV_{TOT}$ is 20.000 l/l/h.

The sample is regenerated in between experiments at the reaction conditions by switching off the EB feed. Only the ethylbenzene feed is removed from the reactant mixture during the regeneration, giving a diluted air mixture (0.1-0.9 vol% O_2). The data are highly reproducible after each regeneration.

An online GC, type Chrompack CP9001, with two channels was used for analysis of the product gas stream. One channel uses an FID for the analysis of hydrocarbons with a 2ft 12% UCW column. The other channel uses a TCD for the analysis of permanent gases (O_2, N_2, CO, CO_2) with a Poraplot Q and molsieve column. The molsieve column uses a bypass for CO_2 and H_2O analysis. The EB conversion, ST, coke and CO_X selectivities and ST yields are based on moles of ethylbenzene and calculated according to Eqs. 10.2-10.6. M_{coke} is 120 g/mol, assuming a molecular composition for coke of C_8H_8O. Although coke is measured, the overall carbon balance is not 100% due to difficult analysis of CO and CO_2 concentrations that are close to the detection limit of the GC.

$$EB\ conversion = \frac{EB_{in} - EB_{out}}{EB_{in}} \qquad 10.2$$

$$ST\ selectivity = \frac{ST_{out}}{EB_{in} - EB_{out}} \qquad 10.3$$

$$CO_X \ selectivity = \frac{(CO_{2,out} + CO_{out})/8}{EB_{in} - EB_{out}} \quad 10.4$$

$$coke \ selectivity = \frac{\Delta m_{coke} \cdot EB_{in}}{M_{coke} \cdot \Delta t \cdot F_{EB}} / EB_{in} - EB_{out} \quad 10.5$$

$$ST \ yield = EB \ conversion \times ST \ selectivity \quad 10.6$$

In addition to the calibration procedure of the TEOM setup itself, the setup is also calibrated by determination of the coke amount using a TGA. The coke as calculated from the TGA data is a little higher than measured by the TEOM. The ratio of coke wt% from TGA over TEOM for both samples is the same, 1.3. All TEOM mass data presented in this chapter is corrected accordingly. The TEOM calibration constant, K_0, is slightly temperature dependent, causing this deviation with the TGA data.

10.2.3 The 6-flow reactor setup

Details on this reactor setup and the reaction conditions can be found in Chapter 6.

10.2.4 Catalyst characterization

The amount of coke was determined by a TGA (MettlerToledo TGA/SDTA851^e, 20 mg sample of spent catalyst, 100 ml/min air, 50 ml/min He flow) using a ramp of 3 °C/min from RT to 723 °C.

Surface area, pore volume and pore size distribution were determined by N_2 adsorption at –196 °C (BET-method, Quantachrome Autosorb 6B). The samples were pretreated overnight in nitrogen at 250 °C.

10.3 Results

10.3.1 The ODH performance in the TEOM reactor

With the TEOM-GC setup, both the catalyst performance and catalyst weight are monitored with time on stream. A typical example of the catalyst performance of Al_2O_3 in the TEOM reactor is shown in Figure 10.3. At the 0.15 O_2:EB ratio, a styrene yield of 23 % at a 96% ST selectivity is reached after 20 h *TOS* and do not change up to a *TOS* of 70 h. These numbers are higher than would be expected from the 6-flow experiments (15% ST yield at 90% ST selectivity). The *TOS* required to reach this optimum performance is longer in the TEOM setup. Initially the coke selectivity is high, 15%, this quickly decreases to below 1% after 10 h *TOS*. Initial ST yield and ST selectivity are 8% and 77%, respectively. With *TOS* the ST selectivity and yield increase, coke selectivity and CO_X selectivity decrease. The catalyst performance stabilizes after about 10-20 h, depending on the reaction conditions. The O_2 conversion is around 95% during the whole experiment.

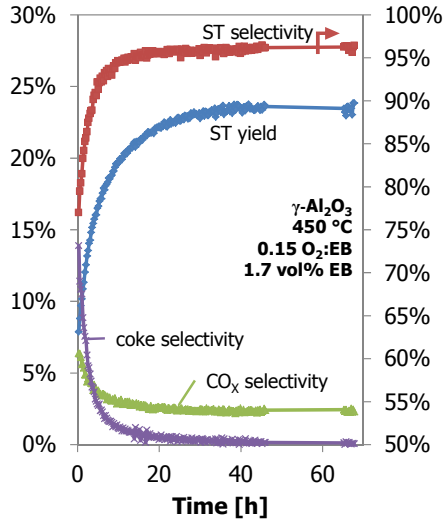

Figure 10.3: The performance of the Al_2O_3 sample in the TEOM reactor.

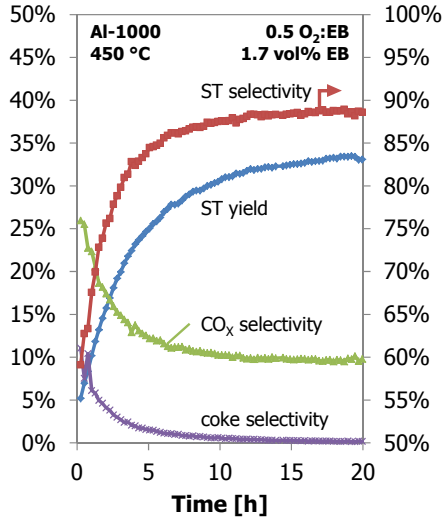

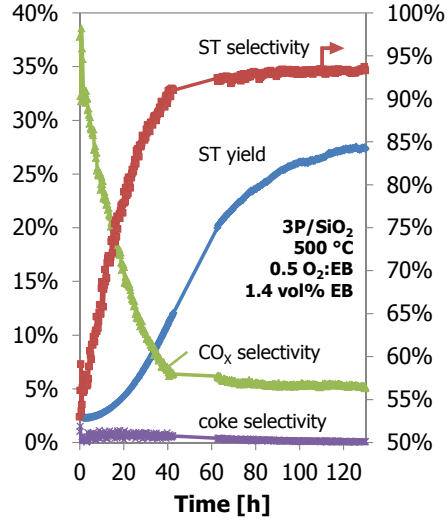

Figure 10.2: The performance as a function of time on stream for the Al-1000 and 3P/SiO_2 samples in the TEOM reactor.

The performances in the ODH reaction for the Al-1000 and 3P/SiO_2 samples are shown in Figure 10.2. With increasing *TOS*, the ST yield and ST selectivity increase. For the Al-1000 it increases from 5% to 34% and from 60% to 89%, respectively. For the 3P/SiO_2 it increases from 4% to 16% and from 57% to 87%, respectively. The oxygen conversion for Al-1000 increases from 50% to 90% after 20 h *TOS*. For the 3P/SiO_2 the oxygen conversion is constant at about 50%. Again, the ODH performance of the Al-1000 is better than expected from the 6-flow experiments. The ODH performance of the 3P/SiO_2 is worse than expected.

10.3.2 Catalyst coverage with coke

Many experiments are done with the bare γ-Al_2O_3, three temperatures and four O_2:EB feed ratios are tested. These results are shown in Figure 10.4. It is assumed that all the mass increase is only the result of carbon deposition. For the measured temperatures under the same O_2:EB ratio, the final coke coverage in about 20 h *TOS* decreases from 0.71 m^2/g to 0.38 m^2/g with an increasing temperature from 450 °C to 500 °C. Initially the coke coverage rates are the same, but at a higher temperature it levels off earlier in time. Looking at the effect of the O_2:EB ratio at a constant temperature, the final coverage of coke increases from 0.41 mg/m^2 to 0.72 mg/m^2 with an increasing O_2:EB ratio of 0.05 to 0.20. The initial coke coverage rates increase with an increasing O_2:EB ratio. With time on stream, the coke coverage rate decreases continuously, the coke deposition becomes slower.

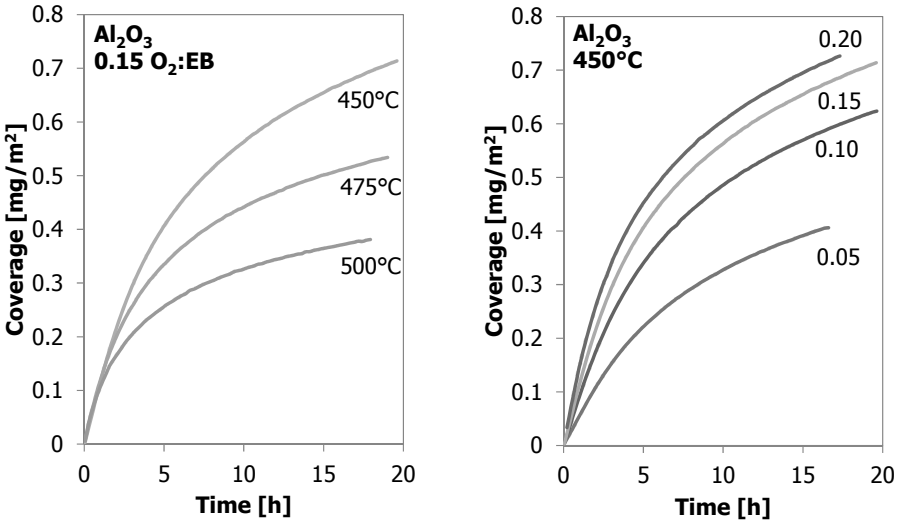

Figure 10.4: The effect of temperature (*left*) and O_2:EB feed ratio (*right*) on coke coverage for Al_2O_3 as a function of time on stream.

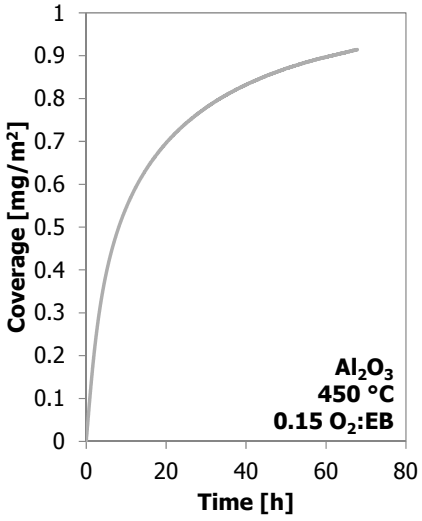

Figure 10.5: The coke coverage in time (*left*) for Al_2O_3 up to 70 h time on stream.

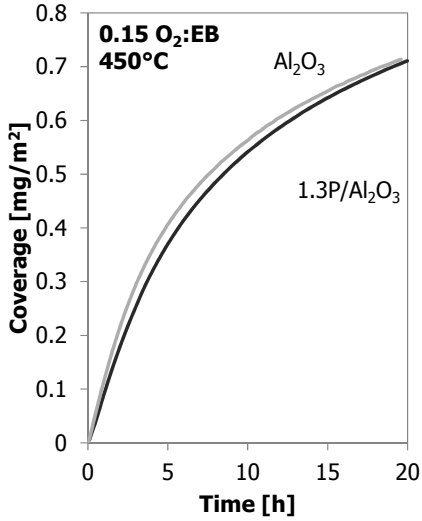

Figure 10.6: Coke deposition in time for Al_2O_3 and $1.3P/Al_2O_3$ samples.

When an experiment with Al_2O_3 is performed for 70 h *TOS*, a coverage by coke with time on stream as in Figure 10.5 is obtained. This shows that the coke coverage keeps increasing with the time on stream. The coke deposition rate decreases with the time on stream but does not become zero.

A phosphorous loaded alumina is also tested, the result of this sample compared with the bare alumina sample is shown in Figure 10.6. This sample shows a better performance in the ODH reaction. The coke coverage in time that is measured in the TEOM reactor is nearly identical to the Al_2O_3 sample, even though the Al_2O_3 supports and their surface areas are different (Table 10.2).

The Al-1000 sample has a better ODH performance than the γ-Al_2O_3 (Ch. 8). A phosphorous loaded silica support, such as $3P/SiO_2$, shows the best results in the ODH reaction (Ch. 6 & 7). Both samples are tested in the TEOM and their coverage by coke with time on stream is shown in Figure 10.7 The 1000 °C calcined alumina shows a similar behaviour as the bare alumina, but the coverage by coke is higher, 1.02 mg/m^2 for Al-1000 against 0.70 mg/m^2 for γ-Al_2O_3, after 20h *TOS*. The P/SiO_2 sample shows a completely different coke deposition behaviour. Initially the coke build-up is very slow, but it increases continuously in time. A higher temperature is required to observe sufficient coke formation and ODH on the P/SiO_2 sample. After 20 h *TOS* only 0.38 mg/m^2 of coke is deposited. The data of these two experiments are fitted with the "monolayer-multilayer" model[12, 13] that can describe the coking behaviour of these catalysts.

The experiment with the $3P/SiO_2$ sample was repeated under slightly different conditions (30 *vs.* 25 Nml/min helium carrier flow, 50 *vs.* 46.1 mg sample) to observe

the coke build-up during an enhanced time on stream (130 h *TOS*). The results are presented in Figure 10.8. Initially the coke build-up is very slow, but increases with *TOS*. After 60 h *TOS* or above 0.6 mg/m^2 coverage the development of the coke coverage on 3P/SiO_2 behaves more like the Al_2O_3 samples. The coke build-up becomes slower after about 60 h *TOS*. This dataset with the typical S-curve behaviour could not be fitted with a "monolayer-multilayer" model.

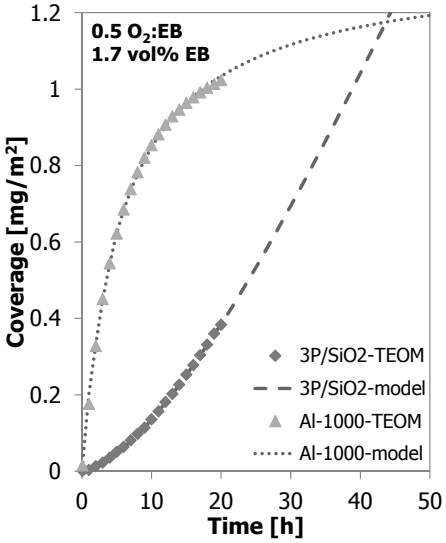

Figure 10.7: Coke coverage in time for Al-1000 at 450 °C and for 3P/SiO_2 at 500 °C.

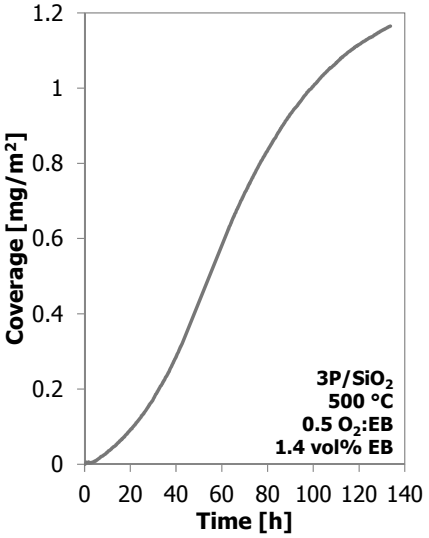

Figure 10.8: Coke coverage in time for 3P/SiO_2.

10.3.3 Styrene yield as a function of coke coverage

When the catalyst performance and mass data are coupled, a linear relationship is observed for the styrene yield as a function of the coverage of coke as is shown in Figure 10.9. The slope of the curve increases at a higher temperature. For higher O_2:EB ratios the slope does not change, but the off-set value of the ST yield at 0 mg coke increases. At the higher styrene yields and coke coverage, the data from the experiments start to deviate from a straight line. At the O_2:EB ratio of 0.15 and at 500 °C the deviation starts at a coverage of about 0.25 mg/m^2, at 475 °C it is 0.40 mg/m^2 and at 450 °C the deviation is not observed in Figure 10.9.

The styrene yield as a function of the coke coverage for a 70 h *TOS* experiment over the γ-Al_2O_3 is shown in Figure 10.10. Under these conditions the styrene yield increases linearly with the coverage of the coke up to 0.70 mg/m^2 (20 h *TOS*). The yield increases slightly, but above 0.80 mg/m^2 (35 h *TOS*) the styrene yield does not change

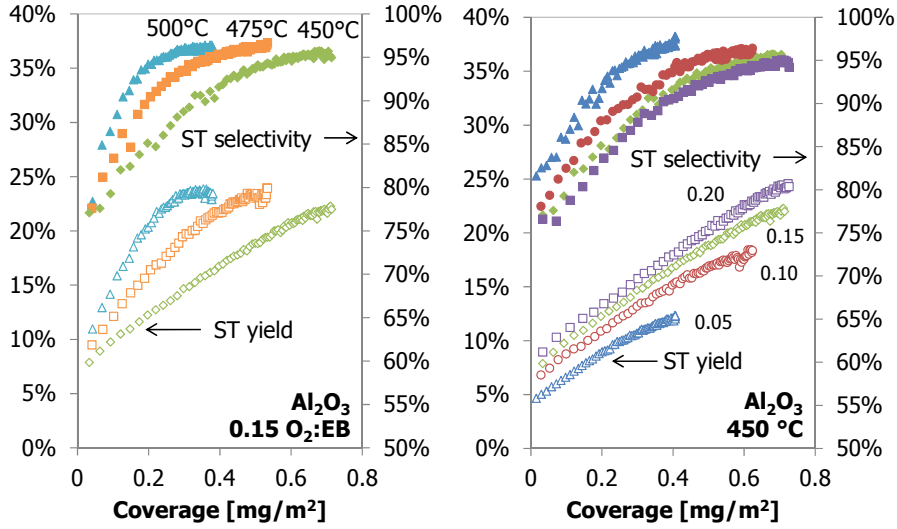

Figure 10.9: The styrene yield (open symbols) and selectivity (closed symbols) as a function of the coke coverage on the Al_2O_3, for different temperatures (*left*) and O_2:EB ratios (*right*) up to 20 h *TOS*.

anymore with an increase in the coke coverage. Above this point the data start to deviate from a linear correlation.

The styrene yield as a function of the coke coverage for Al-1000 and 3P/SiO_2 is shown in Figure 10.11. Although the temperature and sample amounts are different, both samples show an almost identical dependency of the styrene yield on the coverage of deposited coke. A linear fit gives a turnover number of 7 g styrene/g coke. Above a 30% styrene yield and a coverage of about 0.80 mg/m^2, the performance of the calcined alumina sample shows a deviation from the linear ST yield with coke coverage relationship.

The results of the experiment with the 3P/SiO_2 sample under slightly different conditions (30 *vs.* 25 ml/min helium carrier flow, 50 *vs.* 46.1 mg sample) are presented in Figure 10.12. The experiment shows a gap in the GC data due to a temporary GC failure. The styrene yield in-

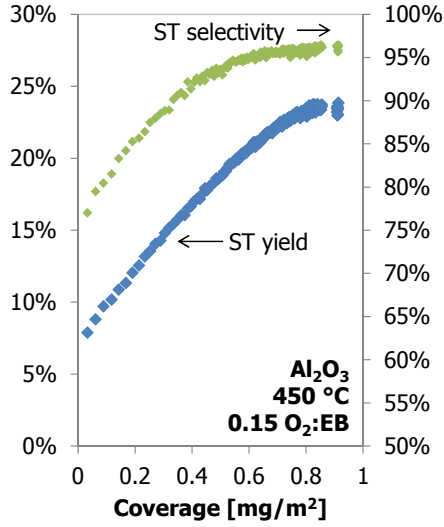

Figure 10.10: The styrene yield and selectivity versus coke coverage for Al_2O_3 up to 70 h time on stream.

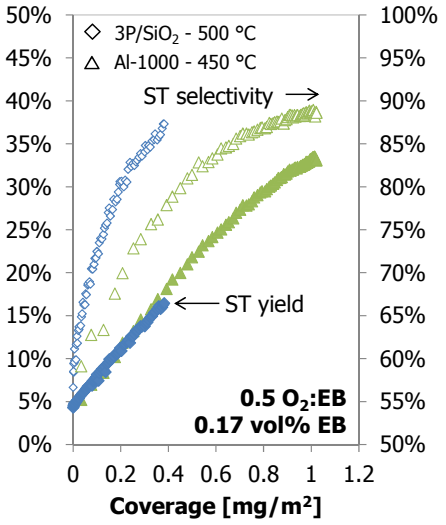

Figure 10.11: Styrene yield (closed symbols) and selectivity (open symbols) as a function of coke coverage for Al-1000 and for 3P/SiO$_2$.

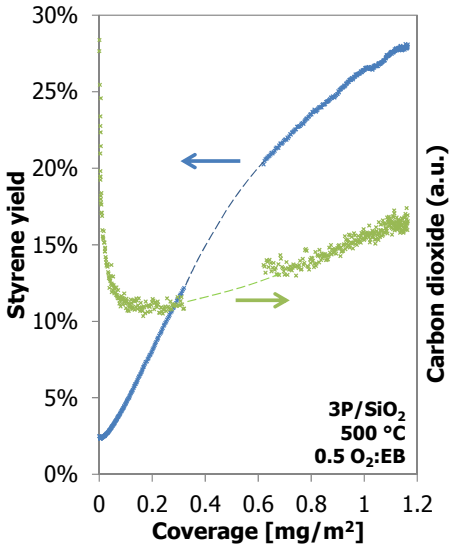

Figure 10.12: Styrene yield and carbon dioxide as a function of the coke coverage (*right*) for 3P/SiO$_2$.

creases linearly with the coke coverage up to about 20 % ST yield and a 0.6 mg/m^2 coverage and then it starts deviating from the initial linear relationship. The curve in Figure 10.12 is a little lower than in Figure 10.11 due to the different conditions, but they are exactly parallel to each other. Additionally, above a coke coverage of about 0.2 mg/m^2 the amount of carbon dioxide produced also shows a linear relationship with the coke coverage. The amount of CO_2 produced at this coverage of 0.2 mg/m^2 is the minimum amount.

10.3.4 TGA analysis

The spent Al_2O_3 (1000 °C) and 3P/SiO_2 samples are analysed by thermo gravimetric analysis (TGA) in air, their oxidation profiles are shown in Figure 10.13. The maximum oxidation temperature of the coke on 3P/SiO_2 is higher than for alumina based coke. Their temperature at the maximum weight loss rate is 565 °C and 480 °C, respectively. This indicates a higher reactivity of the coke on the Al_2O_3.

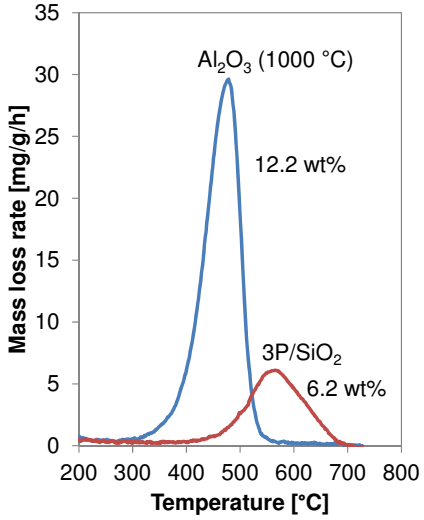

Figure 10.13: TGA in air profiles of the spent Al-1000 and 3P/SiO$_2$ samples.

10.3.5 Distribution of coke in a catalyst bed

An experiment was done in the 6-flow reactor setup with γ-Al_2O_3, where the catalyst bed was split up in 8 separate parts. This gives an idea of the build-up of coke over the catalyst bed with its height. This catalyst was tested using the standard testing protocol (Ch. 6). The coverage of coke with the bed height are shown in Figure 10.14. The maximum coverage of coke, 2 mg/m^2, is just below the top section of the catalyst bed. The top section of the catalyst bed has a lower coke coverage (1.2 mg/m^2). Towards the end of the bed the coverage of coke decreases to 0.75 mg/m^2. The reactor is operated in down-flow operation.

The characterisation by TGA also showed that the temperature of maximum soot oxidation had small variations: the top catalyst section at 466 °C, the next at 476 °C, the next two at 472 °C and the bottom four at 470 °C.

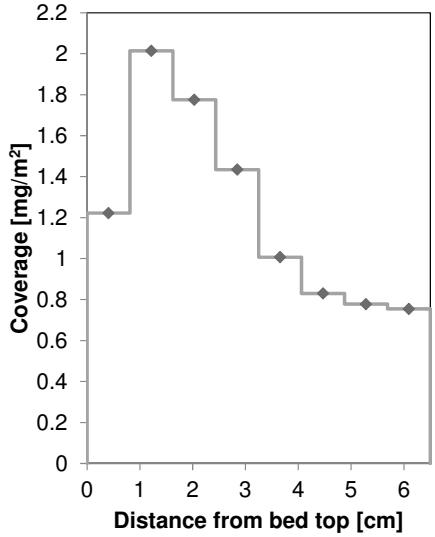

Figure 10.14: Distribution of the coke coverage on γ-Al_2O_3 as a function of the catalyst bed length, after the standard 62 h testing protocol from Chapter 6.

10.4 Discussion

The oxidative dehydrogenation reaction could be an attractive reaction to replace the industrially used endothermic direct dehydrogenation reaction that is equilibrium limited. The ODH reaction is catalysed by the coke that is formed and not by the initial 'catalyst'. Therefore it is very important to get more insight on this coke. So far some general correlations have been found, that are investigated in more detail in this chapter with the TEOM-GC setup.

10.4.1 The ODH performance in the TEOM reactor

The ODH performance over a bare alumina at different temperatures (450-500 °C) does not change much. In the 6-flow setup at an O_2:EB ratio of 0.2, the ST yield is around 14%, at a styrene selectivity around 88% and changing no more than 1% point with temperature. In the TEOM setup at an O_2:EB ratio of 0.15, the ST yield and ST selectivity reach 23% and 95%, respectively. The activation period of Al_2O_3 in the 6-flow setup is around 5 h, whilst in the TEOM reactor the activation is slower and takes 10-20 h. Such differences were not expected, as both setups operate under similar conditions and are both well-defined fixed-bed reactors. A possible explanation for these strange differences between the two setups is the reactant concentrations. These are lower in the TEOM reactor, the inlet EB concentration is 1.7 vol% against 9 vol% in the 6-flow reactor. At lower concentrations, the processes that occur (coke deposition, coke gasification and ODH) may become slower and more selective to ODH. Temperatures can also be slightly different between the two reactor types due to their design, but this does not have a large effect on the ODH reaction. Another possible explanation is the quality of the analysis. With the 6-flow this is more advanced because of the higher concentrations and a more accurate calibration. But even with these low concentrations, an error estimation results in only a ± 0.5% point ST selectivity difference and a ± 0.1% point difference in ST yield. An error in the O_2:EB ratio will result in a little larger deviation, but still smaller than the differences in ODH performance that are observed between both setups. Axial dispersion phenomena can also be responsible for the improved performance. This has been observed for the ODH reaction and is described in Appendix A.5. The Péclet number of the TEOM reactor is about 9× smaller than for the 6-flow reactors. This can lead to improved performance over an Al_2O_3 catalyst. However, in general it can be stated that the performance in the TEOM setup behaves similar to that in the 6-flow setup.

The worse than expected performance in the ODH reaction for the $3P/SiO_2$ sample is simpler to explain. In a blank experiment without any sample in the TEOM reactor, already quite some CO_2 production is measured. The tapered element reactor itself is made from quartz that is not active for the ODH or combustion reaction, but the con-

tainer in which the reactor is placed is made from Inconel that is active in ODH at those conditions (App. A.6). When there is still oxygen available after the reactor and that is the case with the 3P/SiO_2 sample, it will react further resulting in a lower performance than expected. Whenever possible in the experiments, full conversion of O_2 at the end of the reactor was aimed for, but with the 3P/SiO_2 sample this could not be achieved.

Despite the differences between the TEOM and 6-flow setup, it can be stated that the general observed trends are similar. Although the time scales and conditions are different, their performances with regard to temperature, molar O_2:EB ratio and catalyst samples are in agreement for both setups.

10.4.2 Coke coverage and ODH performance

Large differences are observed on the coke coverage as a function of time on stream with the different temperatures (Figure 10.4 (*left*)). Initially the coke formation rates with the time on stream are almost identical, but at a higher temperature the coverage of coke levels off earlier. With an increasing temperature, probably the coke gasification rate increases faster than the coke formation rate, without affecting the overall ODH performance. The balance between the ODH and gasification reaction remains unchanged. This seems strange, but actually this makes sense. The reaction rates over a normal catalyst also go up with temperature and less catalyst is needed for the same activity. Thus, less coke can form the same amounts of styrene and CO_X at a higher temperature. Within these results, a maximum in the coke coverage with temperature[8] was not found. No results were measured below 450 °C, because full oxygen conversion was not reached within a time span of 20 h. It can be imagined that the coke coverage decreases below this temperature because of incomplete oxygen conversion. The coke formation can be slower and the coke gasification can be higher due to the higher oxygen concentrations in the catalyst bed.

The deposition of coke is, just like the ODH performance, very dependent on the O_2:EB ratio (Figure 10.4 (*right*)). More oxygen yields more styrene and more coke. The relationship between oxygen, coke and yield is not linear, for every increase in the O_2:EB ratio the increase in the coverage of coke and in the styrene yield is smaller. Looking at the ST yield as a function of the coke coverage (Figure 10.9), an increase in the coke coverage gives a similar activity increase for all higher O_2:EB ratios. The final coverage will be higher due to the resulting balance between the ODH and gasification reaction, but the coke does not seem to be more active.

At high coke coverages, the linear correlation between the styrene yield and the coverage of coke does not hold anymore (*cf.* Figure 10.9). At the point that it starts to deviate from the initial linear correlation, sufficient coke is available to catalyse the ODH reaction. The coke formation continues, whilst the ODH performance does not

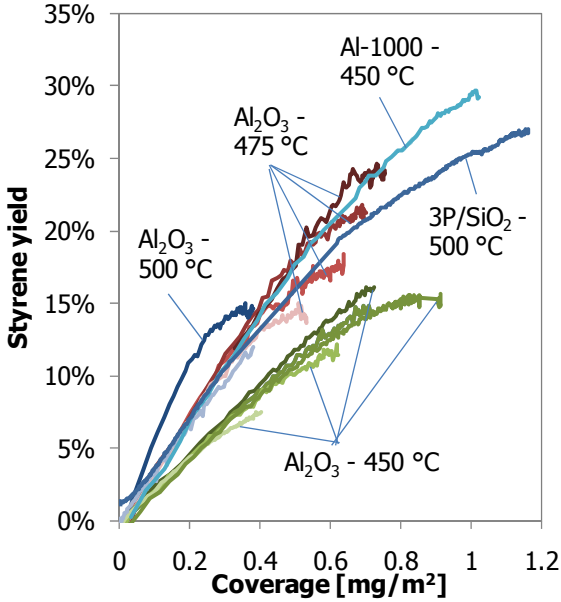

Figure 10.15: ST yields, corrected for the ST yield at zero coke coverage, as a function of coverage by coke for all experiments.

change. Overall, the coke catalyst becomes less efficient. Eventually the excess of coke will have an effect on the ODH performance, as more CO_X is produced and the styrene yield is decreasing (Figure 10.12 and Chapter 9).

In the literature it is claimed that adding a mineral acid, like phosphoric acid, changes the composition and reactivity of the coke.[8] Based on the data presented in this work, the largest factor that determines the performance is the coverage of coke. Its composition and reactivity can still explain some diverging results. The phosphorous loaded alumina shows nearly the same coke coverage as the γ-Al_2O_3 (Figure 10.6), but has a slightly better ODH performance in the 6-flow. Probably the TGA-profile of the 1.3P/Al_2O_3 sample has shifted to a slightly higher oxidation temperature, just like the difference between the calcined aluminas in Chapter 8.

The coke deposits on the 3P/SiO_2 and Al-1000 samples have the same turnover number, but at a different temperature (Figure 10.11) and the TGA data (Figure 10.13) also suggests different reactivities of the coke. Comparing the styrene yields to the ST yield of normal γ-Al_2O_3 at a similar coke coverage, the coke on Al-1000 is more active and the coke on 3P/SiO_2 is less active than of normal γ-Al_2O_3. The comparative data are shown in Figure 10.15. This is supported by the reactivity of the coke in TGA (see also Ch.8). The TGA profiles in Figure 10.13 cannot be compared directly to the profiles presented in other chapters because the heating rate was 3 °C/min compared to 10 °C/min in the other chapters. This causes a shift in the oxidation temperatures.

The activity of the catalyst is foremost an effect of the coke that is present and its

coverage. Sufficient coke needs to be present to convert all oxygen, but when much more coke is present than necessary this negatively influences the selectivity, giving more CO_X. For example the $3P/SiO_2$ catalyst does not have sufficient coke to convert all oxygen. Even at the end of a 130 h long run (Figure 10.12) not all oxygen is converted.

All experiments with the alumina based catalysts show the same behaviour of quick initial coke coverage and a decreasing coking rate with time on stream (Figure 10.4-11.7). For the catalyst stability this is preferred, as it means that the coverage of coke on the sample will not change much with longer time on stream. The ODH performance of alumina is quite stable with time, or in other words, the coke formation and gasification rates are nearly in balance. A very small net coke formation still takes place, but it takes a very long time (> 50 h *TOS* at 10 vol% EB) before the extra coke has a negative effect on the ODH performance (Chapter 8 and 9). The opposite in terms of the catalyst stability is presented by the $3P/SiO_2$ sample that displays a slow initial coke build-up, but increasing coking rates with time on stream (Figure 10.7). The ODH performance of $3P/SiO_2$ in the 6-flow setup shows an optimum after a 3 h *TOS*, with a minimum in CO_X and then deactivates (Ch. 9). This deactivation is caused by excessive coking that shifts the oxygen balance to CO_X production instead of styrene. The 130 h run with $3P/SiO_2$ also shows this increase in the CO_X production (Figure 10.12) after a minimum in the CO_2 production at low coke coverage of 0.2 mg/m^2. Any further increase in the coke coverage gives an increase in the CO_2 production. At the optimum ODH performance point, the coke formation, coke gasification and ODH reactions are not at equilibrium. The TEOM experiment with the $3P/SiO_2$ catalyst shows that the coking rate on the P/SiO_2 will eventually decrease with time (Figure 10.8). But at that point in time the performance of the P/SiO_2 will be far from its optimum.

The coke build-up experiments on $3P/SiO_2$ in Figure 10.7 and Figure 10.8 are done with the same amount of reactants, but with a different amount of diluent (25 *vs.* 30 ml/min helium) and thus different concentrations in the gas mixture. This has a large effect on the coke build-up. After 20 h time on stream the amount of coke in the first experiment is 0.38 mg/m^2, the second experiment needs 50 h *TOS* to reach this coke coverage. The reactant concentrations appear to have a large effect on the coke build-up at these very low concentrations.

In the ODH literature it appeared that a monolayer coverage of the coke is obtained when the pseudo steady-state is reached (optimal ST yield and selectivity), that was determined at 0.54 mg/m^2 over several Al_2O_3 samples (at O_2:EB = 1, 0.17 vol% EB and 425 °C).[8] In this TEOM study it is observed that the same coverage is obtained over the γ-Al_2O_3 and $1.3P/Al_2O_3$ under the same conditions, but not for the Al-1000 or $3P/SiO_2$ samples. Furthermore, the O_2:EB feed ratio and reaction temperature have a large influence on the coverage (also at the pseudo steady-state). The theoretical cover-

age of a monolayer of graphene of 0.76 mg/m^2 is even surpassed by the Al-1000 and 3P/SiO_2 samples, before reaching their optimal ST yield. Therefore, we hypothesize that coke formation occurs more like stacks of islands (3-dimensional) instead of monolayer (2-dimensional) in the case of graphene-like structures on the support surface, where every layer has a similar ODH activity. The surface density of such coke islands can be higher for supports with a high acid site density such as γ-Al_2O_3 and lower for supports with a low acid site density such as 3P/SiO_2. Coke is able to form at the acid sites and also at the edges and on top of existing coke ('multilayer') but at a slower rate.

The presented data does not support the claim by Lisovskii *et al*. that the amount of coke is stable. There is a continuous net build-up of coke on the catalyst (Figure 10.5), but this is very small and only clearly observed on a longer time scale of tens of hours. On an hour to hour basis the amount of coke is nearly constant, especially when less sensitive equipment than a TEOM is used to determine the amount of coke.

The build-up of coke along the catalyst bed in the 6-flow setup is intriguing (Figure 10.14). At the top section of the catalyst bed where the oxygen concentration is the highest, less coke is present than in the next section of the catalyst bed. The reactivity of the coke is also highest in this top section, as indicated by the temperature of maximum soot oxidation. Perhaps most of the CO_X is already formed in the top part of the catalyst bed, reducing the local coverage of coke. Most of the styrene will be formed in the top part of the bed that already contains sufficient coke to have full oxygen conversion. For coke to form, also O_2 needs to be available. The contributions of these 3 reactions (CO_X, ST and coke formation) result in an O_2 profile over the reactor like in Figure 10.16 and a coke profile over the reactor like in Figure 10.14. It is also possible that

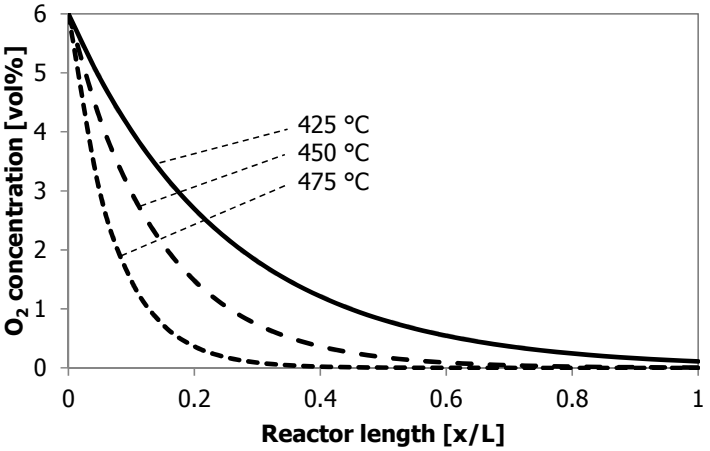

Figure 10.16: Scheme of the O_2 concentration as a function of the reactor bed length at the different reaction temperatures.

the top sections of the bed are already partly deactivated due to the high coke coverage. The slightly higher temperatures of maximum soot oxidation in the top sections of the bed could indicate this. The experiments are done in an integral mode and not in a differential mode. It is easily possible that this catalyst bed could reach higher yields with more feed.

10.5 Conclusions

This investigation into the formation of coke on several catalysts and under different conditions confirms the existing correlations:

- A higher oxygen partial pressure gives more coke, but it is not a linear correlation.
- At full oxygen conversion, a higher temperature gives less coke without changing the ODH performance.
- A catalyst sample with more coke produces more CO_X.
- The initial coke build-up shows a linear correlation with the styrene yield.

Different samples can give coke with different activities, but the above correlations hold. It was also found that the coverage of coke varies with the bed position, in addition to the temperature, O_2:EB ratio, reactant concentrations, time on stream and the type of starting material. For an optimal performance in ODH, a sufficient but low coverage of coke needs to be available. The exact optimal coverage depends on all the above mentioned parameters.

References

[1] D.L. Trimm, Appl. Catal. 5 (1983) 263-290.
[2] J.R. RostrupNielsen, Catal. Today. 37 (1997) 225-232.
[3] M.F.R. Pereira, J.J.M. Orfao, J.L. Figueiredo, Appl. Catal. A: Gen. 184 (1999) 153-160.
[4] F. Cavani, F. Trifiro, Appl. Catal. A: Gen. 133 (1995) 219-239.
[5] G.E. Vrieland, J. Catal. 111 (1988) 14-22.
[6] G. Emig, H. Hofmann, J. Catal. 84 (1983) 15-26.
[7] A. Schraut, G. Emig, H.G. Sockel, Appl. Catal. 29 (1987) 311-326.
[8] A.E. Lisovskii, C. Aharoni, Catalysis Reviews: Science and Engineering. 36 (1994) 25-74.
[9] D. Chen, A. Gronvold, H.P. Rebo, K. Moljord, A. Holmen, Appl. Catal. A: Gen. 137 (1996) L1-L8.
[10] W. Zhu, J.M. van de Graaf, L.J.P. van den Broeke, F. Kapteijn, J.A. Moulijn, Ind. Eng. Chem. Res. 37 (1998) 1934-1942.

[11] R.J. Berger, F. Kapteijn, J.A. Moulijn, G.B. Marin, J. De Wilde, M. Olea, D. Chen, A. Holmen, L. Lietti, E. Tronconi, Y. Schuurman, Appl. Catal. A: Gen. 342 (2008) 3-28.
[12] I.S. Nam, J.R. Kittrell, Ind. Eng. Chem. Proc. Dd. 23 (1984) 237-242.
[13] J. Gascon, C. Tellez, J. Herguido, M. Menendez, Appl. Catal. A: Gen. 248 (2003) 105-116.

Catalytic dehydrogenations of ethylbenzene to styrene

Summary, evaluation, conclusions and future prospects

Every ethylbenzene dehydrogenation is catalysed by coke

This research work on the catalytic dehydrogenation of ethylbenzene (EB) to styrene (ST) had a primary goal of developing improved catalysts for dehydrogenation processes both in CO_2 as well as with O_2 that can compete with the conventional dehydrogenation process in steam. In order to achieve this goal, all these processes need to be properly understood. After having worked on catalytic dehydrogenation reactions in steam, in nitrogen, in carbon dioxide and with oxygen, it appeared that these reactions show many parallels. Carbon deposit formation on the catalyst is closely connected to all dehydrogenation reactions of ethylbenzene to styrene. They always go hand-in-hand and cannot be separated. Yes, these coke deposits will also be a cause of deactivation. But foremost the coke is an active ingredient of the 'catalyst' in the ethylbenzene (EB) dehydrogenation reactions. In the oxidative dehydrogenation it is without any doubt that the selective dehydrogenation reaction proceeds over the deposited coke on the catalyst or support. The dehydrogenations experiments in CO_2 or N_2 in this thesis and characterizations of the samples also clearly show the involvement of coke in the dehydrogenation reaction to styrene (ST). Also in the direct dehydrogenation in steam, coke deposits play an important role in the dehydrogenation, based on literature and our experiments presented in this thesis (Ch. 2). By applying catalyst- and technology developments, a competitive process with O_2 appears to be within reach. This process applies a P/SiO_2 catalyst and staged feeding of O_2, whereby the stability of the catalyst as a function of the *time on stream* still remains a topic of concern.

The role of coke in all these reaction systems is briefly discussed separately and followed by my view on the role of coke in steam dehydrogenations.

Dehydrogenation in CO_2 or N_2

Still, a large number of authors hypothesize that their catalyst is doing the catalysis in the dehydrogenation of ethylbenzene in CO_2, for instance *via* a redox mechanism (references in Ch. 3-4). One of the first eye-openers in this PhD work was to recognise that coke is responsible for the selective dehydrogenation reaction of EB to ST in CO_2

or N_2 diluent.[1] The use of a 'clean' catalyst support, high purity γ-Al_2O_3, does not leave much room for other interpretations of our data on the EB conversion, ST selectivity and coke amounts with *time on stream* (*TOS)* (Ch. 3).

Also the data from the use of the alumina supported V, Cr and Fe catalysts with their similar EB conversions and ST selectivities after 10 h *TOS* in CO_2 points to a common catalytic origin. In the initial phase of operation these catalysts show some different EB conversions due to their different reverse water gas shift (RWGS) activities, but when the catalyst deactivates due to too much coke, the RWGS reaction has no effect on the EB conversion anymore. It also proves that an additional catalyst is required for the RWGS activity that would not deactivate under the applied conditions. A coked alumina has hardly any RWGS activity (Ch. 4).[2]

Another important aspect that emerged from the initial work on the dehydrogenation reaction in CO_2 is the necessity that dehydrogenation experiments should run at least 20 h *TOS*. Some good catalysts such as γ-Al_2O_3 or K/Al_2O_3 are hardly reactive in the first hours on stream, because not enough coke is formed yet to achieve the optimal styrene yield and selectivity. These would not be identified as potentially good catalysts if an experiment would only last 10 h *TOS* or less. The downside is that many catalysts that form a lot of coke, such as the alumina supported V, Cr and Fe catalysts, will already deactivate during the first hours on stream. From commercial or stability perspective, one can wonder if these quickly deactivating catalysts are interesting enough to investigate at all (Ch. 3, 5).

The coke is formed on the acid sites on the catalyst. These acid sites also participate in the cracking reactions leading to benzene and toluene byproducts, so when these sites become covered with coke this byproduct formation to benzene and toluene decreases and the catalyst becomes more selective and more active for the dehydrogenation reaction. The other contributor to the poor initial selectivity is the coke build-up itself that is also a byproduct. Initially coke build-up is very fast, especially with V, Cr and Fe catalyst, but as more of the catalyst surface becomes covered with coke, the rate of coke formation decreases. The optimal coverage is a monolayer on the catalyst surface. The coke formation does not stop when this monolayer is reached, coke is also formed on coke itself, leading to many layers (multilayers) of coke on top of each other that finally leads to a completely blocked catalyst support. At this point the system is still highly selective to ST, but due to the low available surface, the EB conversion will be low. This happens as well on carbon starting materials such as activated carbon or carbon nanotubes (Ch. 3).[1]

The dehydrogenation in CO_2 or N_2 is thought to proceed over the defects and edges of the coke, which can be hydrogenated by EB. Consequently the EB is converted into ST and the hydrogenated defects and edges are subsequently thermally dehydro-

genated. When CO_2 is used and a RWGS catalyst is also present on the catalyst system, the hydrogen can spill-over from the coke to the RWGS catalytic part and react by a redox mechanism with CO_2 to CO and H_2O. Molecular H_2 itself does not induce this effect (Ch. 4).[2]

The γ-Al_2O_3 catalyst can be improved by adding a potassium promotor. Potassium moderates the most active acid sites, giving a lower formation of cracking products and improved ST selectivity, but also a slower coke build-up and thus a slower activation and deactivation of the catalyst. Catalyst deactivation could not be prevented. Potassium also enhances the catalyst activity by promoting the CO_2 activation, yielding higher RWGS activities (Ch. 6).

The effect of CO_2 on the dehydrogenation reaction of EB to ST is limited. The EB conversion initially increased 5-10% points with the tested catalysts, but did not yet show the theoretical nearly 20% point increase that would really make it a competitive process. Catalysts with good stability and with higher RWGS activities need to be developed. The other ascribed effect of CO_2, coke gasification that should prevent catalyst deactivation by too much coking, has not been observed under any of the applied reaction conditions in this study. Temperatures above 650 °C are required to activate the gasification with CO_2 (reverse Boudouard reaction). This is not feasible due to a severe loss of ST selectivity under those conditions. Catalyst development for coke gasification and stabilisation of the catalyst is perhaps more important than its RWGS activity development (Ch. 4 and 5).[2]

The dehydrogenation of EB to ST in CO_2 shows similar very high ST selectivities as the steam dehydrogenation process. This is quite an achievement, but the enhancement of EB conversion is not as good as was expected on the basis of thermodynamic calculations. Furthermore, the catalyst stability is far from achieving a desired commercial catalyst lifetime of several years. Adding to this the challenges of the CO_2 supply, separation, compression, recycling and a CO conversion unit, it will be difficult for a dehydrogenation process with CO_2 to compete with the conventional technology of steam aided dehydrogenation. This subject was investigated only for a limited amount of time and therefore, this process is not yet completely evaluated. But the improvements will be time-consuming and perhaps neither rewarding nor worthwhile.

Oxidative dehydrogenation

Kinetic and mechanistic aspects

The formation of styrene *via* oxidative dehydrogenation (ODH, Eq. 1) has many advantages over direct dehydrogenation, such as no equilibrium limitations and a lower reaction temperature. The largest challenge for ODH is to achieve a comparable high ST selectivity (> 96%), especially because the EB can be easily oxidised completely (Eqs. 2 and 3). But more side reactions occur that become significant at the desired high ST selectivity. An overview of the main global reactions that take place during ODH:

$$C_8H_{10} + ½O_2 \rightarrow C_8H_8 + H_2O \quad (1)$$

$$C_8H_{10} + 10½O_2 \rightarrow 8CO_2 + 5H_2O \quad (2)$$

$$C_8H_{10} + 6½O_2 \rightarrow 8CO + 5H_2O \quad (3)$$

$$C_8H_{10} + O_2 \rightarrow precursors \rightarrow coke \quad (4)$$

$$coke + O_2 \rightarrow CO + CO_2 + H_2O \quad (5)$$

$$C_8H_{10} + O_2 \rightarrow oxygenated\ products \quad (6)$$

$$C_8H_{10} + H_2 \rightarrow C_7H_8 + CH_4 \quad (7)$$

$$C_8H_{10} \rightarrow C_6H_6 + C_2H_4 \quad (8)$$

The formation of benzene and toluene (Eqs. 7 and 8) increases with increasing temperature. The selectivity to other oxidised products (Eq. 6) and coke precursors (Eq. 4) increases with decreasing temperature. For γ-Al_2O_3 the temperature optimum for ST selectivity is 450 °C (Ch. 6). A reaction network scheme for ODH is shown in Figure 1. Most reactions run in parallel, the formation of coke and CO_X from coke, are series reactions. Once ST has desorbed and is in the gas phase, it does not react further under ODH reaction conditions at 525 °C in the presence of per cent of oxygen in the gas phase (Ch. 9).

The formation of CO_X consumes far more O_2 relative to EB (6.5-10.5) than the ODH reaction (0.5). It was observed that an increase in the O_2:EB ratio, or a higher O_2 concentration, leads to more coke build-up, higher CO_X selectivity, lower ST selectivity and lower EB conversion (Ch. 6-10). This indicates different reaction orders in O_2 for ST and CO_X formations. The reaction order for ODH is the lowest, formation of CO_X has the largest reaction order.

The difference in reaction orders of O_2 can also be used beneficially,[3] as was

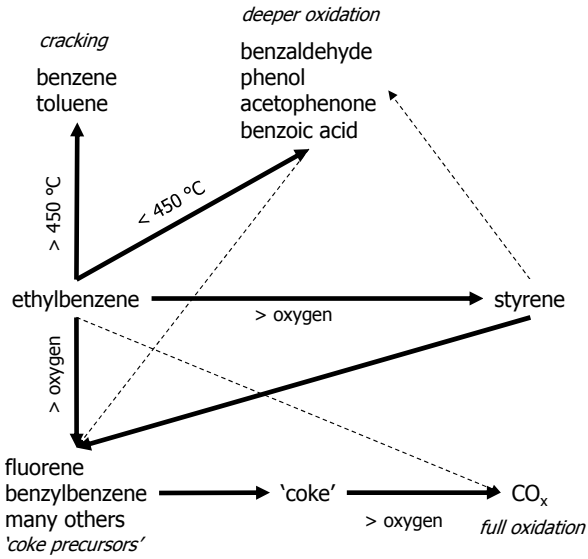

Figure 1: Scheme of the reaction pathways in ODH for carbon species.

demonstrated with the staged feeding experiments. By distributed feeding of the O_2 amount over 6 reactors instead of co-feeding all O_2 and EB in 1 reactor, the ST selectivity (+4% points) and EB conversion (+15% points) improved drastically. By increasing the number of reactors and total amount of O_2 (fixed amount per reactor), the EB conversion can be increased linearly as the ST selectivity remains almost constant. This also proved that the ST reactivity is very low under severe reaction conditions. The penalty that has to be paid is an increase in the amount of catalyst because the reaction rates are lower at low O_2 concentrations (Ch. 9).

The role of coke

For the oxidative dehydrogenation reaction of EB to ST it is well documented that coke is the actual catalyst.[4, 5] In fact, some of the reported best catalysts are carbon-based materials. The research group of Schlögl *et al*. is investigating the use of all kinds of structured carbon materials for the oxidative dehydrogenation reaction of EB to ST and butane to butenes.[6-15] The advantage of starting with a carbon material is that the catalysts are active and selective from the start. However, this is no guarantee for better (more selective) catalysts than the best ones tested in this thesis, as can be concluded from the comparative overview of catalyst performances in Table 1. There are a number of differences between the experiments in this table: the O_2:EB molar feed ratios, O_2 conversions and in this study an integral reactor was used and in Schlögl *et al.*'s studies a differential reactor was usually employed. These factors can explain part of the differences in the catalyst performances.

Table 1: Reaction conditions and performance data of several catalysts from this study and Schlögl *et al.*

Sample	Ref.	Temp. [°C]	O_2:EB ratio	ST yield	ST selectivity	O_2[b] conversion	O_2 (ST)[b] selectivity
γ-Al_2O_3	Ch. 6	450	~0.6	29%	82%	100%	23%
Al-1000	Ch. 8	450	~0.6	36%	86%	100%	28%
γ-Al_2O_3[a]	Ch. 9	450	~0.6	42%	86%	100%	32%
5P/SiO_2	Ch. 7	500	~0.6	48%	89%	100%	38%
3P/SiO_2	Ch. 7	475	~0.6	51%	91%	100%	41%
5P/SiO_2[a]	Ch. 9	500	~0.6	65%	93%	100%	55%
OLC	[10]	517	2.5	62%	68%	100%	12%
CMK-3	[11]	400	2.5	52%	76%	80%	13%
CNF	[9]	515	1	23%	81%	60%	20%
CNF	[9]	440	1	38%	81%	95%	20%
CNF	[16]	400	2.6	13%	85%	10%	25%
CNF	[9]	425	1	19%	89%	26%	32%
CNT	[15]	400	0.5	11%	95%	22%	47%

[a] 6 reactor staged feeding configuration
[b] Calculated from the available data; if no data was available, a 1:1 mixture of CO_2 and CO by-products was assumed to calculate O_2 conversion and O_2 (ST) selectivity.

Starting from a carbon based material has the disadvantage that the material is not stable under reaction conditions, as observed with the activated carbon (AC) samples (Ch. 8). If a hotspot is generated in the reactor, the entire catalyst inventory can be lost easily. During the ODH process the reaction surface is continuously rejuvenated so the composition of the carbon material in the reactor changes.[5] In our tests with carbon nanotube (CNT) samples we observed the formation of more reactive carbon deposits during the ODH reaction (a shift to lower temperature for oxidation in thermo gravimetric analysis (TGA) in air, App. A.9). Therefore, from an application point of view this seems not the way to proceed and the use of an inorganic material is the better starting point, although this will mean that a break-in period is required to develop activity. This way the catalyst can be regenerated and possibly the type and amount of coke can be influenced by catalysis.

The work with the fixed bed microbalance reactor coupled with a gas chromatograph (TEOM-GC setup) has very nicely shown the direct linear relationship between the amount of coke on a catalyst and its EB conversion and ST selectivity. This holds very well initially, but when the coke coverage approaches a monolayer, the relationship deviates from this linear behaviour until an ODH performance plateau is reached where a change in the amount of coke has no effect on the overall ODH performance. Very severe coking in combination with related high coke coverage will eventually result in a loss of ODH performance (Ch. 10).

As was mentioned earlier, the type of coke is an important parameter in the ODH performance. The type of coke is defined here by its reactivity with O_2 as analysed by

TGA. This type is a result from the coke composition (CH_XO_Y) and the influence of the support or catalyst on the coke gasification. Ideally the coke should be very unreactive (nearly inert) towards O_2, in combination with a non-oxidizing support. The high temperature calcination of γ-Al_2O_3 had a positive effect on the ODH performance and the TGA profile for the coke oxidation shifted to slightly higher temperatures. For the P/SiO_2 catalysts, the TGA profiles of the coked catalysts shift to even higher temperatures and their EB conversion and ST selectivity are much higher than of γ-Al_2O_3. The regeneration of the catalyst under reaction conditions (without EB) takes much longer for P/SiO_2 samples (>10 h) than for the Al_2O_3 catalysts (2-4 h). The low reactivity of the coke works in two ways: (1) less coke is gasified to CO_X, improving the ST selectivity; (2) the activity for the selective ODH reaction is also lower, so either more coke or higher temperatures are required to achieve comparable activity. The inorganic starting material and promotors clearly have a pronounced effect on the type of coke (Ch. 6, 8, 10).

Clear structural pictures of the coke deposit have not been obtained in this research, but with respect to the reactivity next to the accessibility the degree of dehydrogenation-aromatisation is an important parameter. The dehydrogenation is thought to take place at the (oxidized) edges of the graphene structures,[6, 17] where also the gasification takes place.[18] The local oxygen partial pressure and the coke reactivity then determine the ST selectivity on these edges.

Reactor performance

During this work on ODH, several factors were identified that have a significant impact on the reactor performance. One is the need to have full O_2 conversion at the end of the reactor, making the catalyst testing more complex. The two reactants EB and O_2 are required around their stoichiometric ratio (O_2:EB = 0.5). In the examples where not all O_2 is converted at the end of the reactor (Ch. 6-10), relatively more CO_X and heavy condensates are produced at the expense of ST selectivity, due to the higher overall concentration of O_2 in the reactor. This negative effect on ST selectivity becomes smaller for coke that is less reactive with O_2 (*i.e.* gasification and combustion), like on P/SiO_2 catalysts. Additionally it is also required for safety and economic reasons: high EB conversion and low EB recycle are desired, while risks of explosion or runaway should be avoided.

Another factor is the degree of plug-flow behaviour that can have an effect on the reactor performance under the applied testing conditions (A.5). The fact that full oxygen conversion and high EB conversion are desired drives the need to have near perfect plug-flow behaviour. Several reactor designs were used throughout this work and for the γ-Al_2O_3 catalyst it appeared that less ideal plug-flow reactor behaviour had a positive

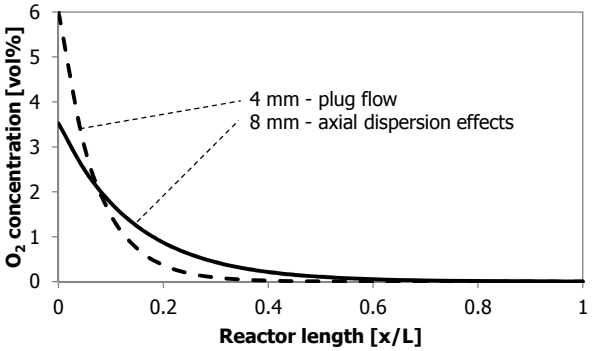

Figure 2: The O_2 concentration as a function of the catalyst bed length at different reactor diameters.

effect on its ODH performance. Shorter and wider catalyst beds yield a lower Péclet number, moving away from the ideal plug-flow towards a slightly more mixed reactor type. In the ODH process there are two main competing reactions that use both EB and O_2 reactants, dehydrogenation and CO_X formation. Because these two reactions have different reaction orders for O_2, the reaction with the lowest reaction order benefits from the lower O_2 concentrations due to the mixing or axial dispersion effects. The effect on O_2 is the largest because as limiting reactant it is consumed completely. The effect of axial dispersion on the O_2 concentration along the reactor is shown in Figure 2. The P/SiO_2 catalysts are less sensitive for this effect of axial dispersion and perform better with more ideal plug-flow behaviour, since these catalysts are not as very active as the γ-Al_2O_3 and show lower CO_X formation.

One more factor is the contact time, reciprocally expressed in the *WHSV* value. Under varying *WHSV* conditions the catalyst showed very peculiar behaviour (A.1). The *WHSV* could be increased (or decreased for that matter) almost 6× before a significant change in the ODH performance was observed. Apparently all these *WHSV* values are located within the ODH performance plateau that was observed with the TEOM-GC system and coke mass characterizations (Ch. 8 and 10). The key to this behaviour are the coke amount (and coverage) and the oxygen concentration profiles along the reactor. At the lowest *WHSV* much more coke was present than was required for full O_2 conversion, but not too much that it would affect the ODH performance. For the highest *WHSV* that was tested, just enough coke is available to have full O_2 conversion at the end of the reactor and optimal ST selectivity. Only when the temperature was lowered, the activity of the catalyst decreased and the O_2 conversion and ST selectivity decreased, leading to conclude that insufficient coke was present to catalyse the selective ODH reaction (A.1). Another nice example that illustrates the effect of having sufficient coke is shown in Figure 3. Initially, full O_2 conversion is not achieved by the catalyst at 475 °C and an

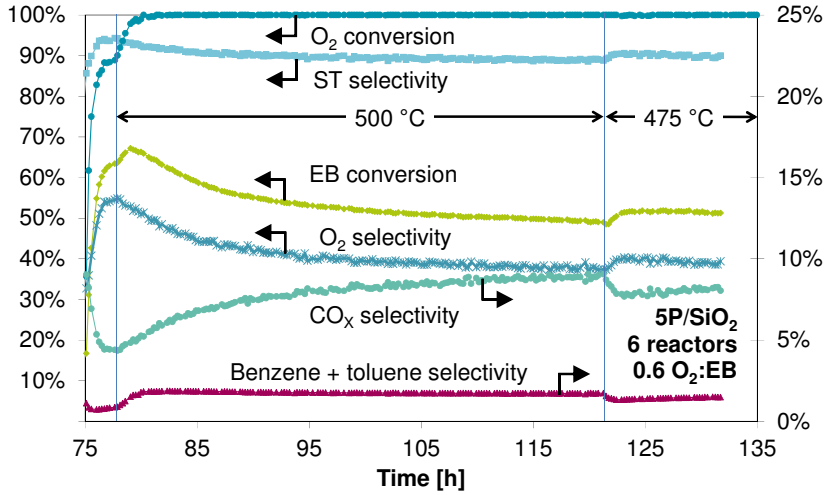

Figure 3: Performance with time on stream for the 5P/SiO_2 sample in staged feeding with 6 reactors. When the reaction temperature is decreased after 40 h *TOS*, sufficient coke is available for full O_2 conversion and the performance improves: EB conversion and ST selectivity increase, CO_X and BT selectivity decrease. Deactivation due to coke build-up still occurs.

increase of temperature up to 500 °C is required, but 30 h later enough coke is present to operate the process at 475 °C with full O_2 conversion. This even gives a temporary improvement of the performance due to decreased selectivities to CO_X, benzene and toluene. Clearly O_2 is the limiting reactant under these reaction conditions as it is completely converted.

These effects of plug-flow behaviour and contact time are very interesting observations that were made during this work. Only preliminary testing was done in order to get some understanding of these effects. Clearly more research is needed to fully understand the consequences of these effects on the oxidative dehydrogenation reaction

Catalyst testing

It was a challenge to have good and reliable analysis of the product gas stream by gas chromatography in the ODH experiments. This is partly caused by the design of the experiments, with CO_2 as one of the used diluents (Ch. 6, A. 4) and partly for the many byproducts that are formed in this reaction. The challenge of the CO_2 diluent was solved by regularly measuring the feed gas composition as a reference for the oxygen balance calculations for each of the product gas-stream measurements. In this way the measured CO_2 amount could be split into the amount of CO_2 that was produced as a byproduct and into the amount of CO_2 that was fed (Ch. 6). The range of hydrocarbon byproducts in the ODH process is large and contains molecules such as methane, ethene, benzene, toluene, acetophenone, benzoic acid and many more (A.4, A.8). The ethylbenzene, sty-

rene and smaller hydrocarbons are easy to identify and detect. The challenges arise with the hydrocarbons that are larger, heavier and less volatile than the styrene product. These heavy condensates can constitute over 1% of the total product stream (typically 0-0.5%). They can accumulate in the GC column, causing problems like peaks shifting with elution time, or baseline changes. The carbon balance will also be flawed if these heavy condensates are not properly measured. In these studies, a ramp to high temperature during the analysis prevented any issues and gave a very reliable carbon balance where only carbon on the catalyst (coke) is missing from the total mass balance.

With the optimised product gas stream analysis by a GC, the catalyst performance could be accurately followed with *TOS*. With an improving catalyst performance, the differences in ST selectivity became smaller and smaller due to the large difference in O_2 consumption between the two main and competing reactions of dehydrogenation and full oxidation, 0.5 and 10.5 O_2 for each EB molecule, respectively. With an improving catalyst performance at full O_2 conversion, the amount of O_2 used for the dehydrogenation increases more and more. Therefore, it makes good sense to calculate the selectivity of O_2 that is used to produce ST (Ch. 9, Table 1). With ST selectivities around 90% and higher, the O_2 (ST) selectivity clearly shows the improvements and should be used as an additional performance parameter. The EB conversion also increases with improving catalyst performance, but is also a function of the O_2:EB molar feed ratio. The O_2 (ST) selectivity is independent of the O_2:EB ratio.

Progress in ODH performance

When the condition of full O_2 conversion is fulfilled, the CO_X selectivity, EB conversion and ST selectivity are coupled. An increase in ST selectivity always concurred with an increase in EB conversion and a lower CO_X selectivity. This makes perfect sense, as O_2 can only react once, forming H_2O and either ST or CO_X. The selectivity to the other byproducts (benzene, toluene, heavy condensates) is usually quite low (< 1% point selectivity). Taking into account that both CO_2 (lower boundary) and CO (upper boundary) can be produced, the curve in Figure 4 can be calculated from the mole balances. When a similar graph is created with all the measured data, the observed trend is exactly same. The performance of some of the most important catalyst groups are indicated in Figure 4.

The figure also gives a nice impression of the performance development during this project in time. Large steps were made and it appears as if the target is within reach. For instance when more than 6 reactors are used in staged feeding with the $5P/SiO_2$ catalyst, it predicts that both EB conversion and ST selectivity improve further. Reality is that this catalyst and also other, deactivate with *TOS*. The TEOM-GC experiments showed that the coke build-up continues constantly on all catalysts, although the rate of

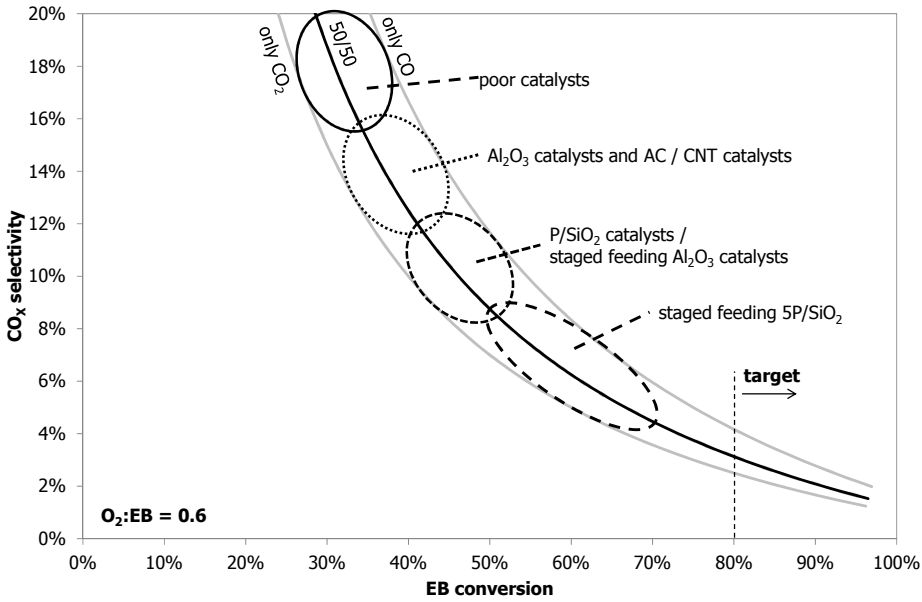

Figure 4: Relationship between CO_X selectivity and EB conversion at full O_2 conversion for an O_2:EB total molar feed ratio of 0.6. Black line is for 50/50 CO/CO_2 production, upper grey line is for only CO, lower grey line for only CO_2 production. Results from important catalyst groups are indicated.

coke formation is decreasing slowly. In order to maintain the optimal amount of coke on the catalyst, the catalyst should be (partly) regenerated continuously. Various options are known to achieve regeneration such as swing-operation, moving catalyst beds and fluidised bed reactors (2-zone or separate reactor/regenerator) (Ch. 9). Sofar, I did not observe a mechanism or method to control the amount of coke on the catalyst during operation. Feeding more oxygen increases the coke gasification and coke formation rate at the same time, maintaining a net coke build-up in time. Also there does not appear to be an inhibition mechanism on the coke formation that would stabilize the amount of coke.

Thoughts for further improvement

An idea that was explored for controlling the amount of coke is to add a second oxidant to the system. A good choice could be NO_2 that is known to enhance coke gasification in diesel exhaust gas treatment. Unfortunately, no stabilizing effect was observed comparing data with and without NO_2 for more than 100 h *TOS* using a NO_2 concentration between 100-800 ppm. Other secondary oxidants were not tested.

Another possibility is to add a volatile gasification catalyst such as KOH (in combination with steam). This could temporarily enhance the gasification rates[18] and the amount can be controlled in order to match the deactivation. Of course this will come at a penalty of O_2 and ST selectivity loss, because the rate of coke formation remains un-

changed and too high. Lastly, it could be attempted to limit the amount of coke by similar tricks as were applied in the H_2O dehydrogenation process: having low surface areas and high macroporosity. Less coke can be deposited and CO_X selectivity is not enhanced by mass-transport limitations (Ch. 8). But of course enough coke should be available for the catalyst activity and selectivity and the reactor volume may need to be increased for the desired conversion level.

Dehydrogenation in H_2O

Having discussed the two new options for EB dehydrogenation, many similarities are observed between the steam dehydrogenation process and the dehydrogenation in CO_2 or with O_2. The byproducts of the reaction largely correspond: benzene, toluene and heavy condensates are produced in all dehydrogenation reactions. Coke deposition occurs in all the ethylbenzene dehydrogenation reactions. For the dehydrogenation in CO_2 the deactivation by coke formation is very fast, EB conversion over γ-Al_2O_3 decreases from 62% to 25% in 100 h *TOS* (Ch. 3). In the oxidative dehydrogenation the deactivation is already much slower, EB conversion over γ-Al_2O_3 decreases from 35% to 30% in 100 h *TOS* (Ch. 6). In the steam dehydrogenation process the deactivation problem by coke formation is solved. Other processes dominate the catalyst deactivation, such as redistribution and loss of potassium during the catalyst lifetime. To compensate for these other deactivation effects, the reactor temperature is slowly increased (exit temperature 580-630 °C) during the >2 year lifetime in the presence of an excess of steam in the gas phase.[4, 19, 20]

Based on my experience with the three catalytic dehydrogenation reactions, I am convinced that also the dehydrogenation reaction in steam is catalysed by the coke. There are many indications that coke is an essential part of the catalyst system.

(1) The catalyst system needs about 20 h to reach steady state.[20, 21] One could say this is required to reach the optimal oxidation state of the catalyst, but it could also be due to the very slow build-up of a steady-state amount of coke (due to the gasification of coke with the excess of steam).

(2) The presumed active phase of the catalyst, $KFeO_2$,[21-23] is also a very good coal gasification catalyst.[24, 25] Perhaps that is also the dominant function of the $KFeO_2$ in the steam dehydrogenation process, to gasify the coke and control the steady-state amount of coke on the catalyst and that coke is the actual catalyst.

(3) Several authors report a steady-state amount of coke on the catalyst and that the more active catalysts contain more coke. One report mentions 0.024-0.050 wt% of coke,[21] while a commercial catalyst optimally contains 2-3 wt% of coke throughout the

catalyst bed.[26] With the very low specific surface area of the KFe catalyst (2-5 m^2/g) and the 0.54-0.76 mg/m^2 monolayer coke coverage (Ch. 10), the reported amounts are between sub-monolayer up to tens of layers of coke on the catalyst surface. Such large amounts of coke do not seem to hinder the dehydrogenation reaction from taking place.

(4) A low specific surface area and macroporous structure of the catalyst are favourable for the catalyst selectivity.[27] Of course, the macroporous structure will improve the internal mass transport and reduce possible byproduct formation due to consecutive reactions, but the resulting low surface area can also be a very good method to limit the amount of the coke (also a byproduct) that can form and improve the gasification of the coke, to have control over the coke amount and hence possible deactivation due to excessive coking.

(5) Potassium is known to be mobile[20] and is present on the surface of a coked KFe catalyst.[26] This can be favourable for the gasification of the coke, but also it can enhance the dehydrogenation reaction on the coke by a spill-over mechanism, as we have observed for the dehydrogenation in CO_2 (Ch. 5).

(6) Coke gasification has to occur *via* the temporary formation of oxygen groups on the coke surface. Possibly these short-living oxygen groups on the coke surface can perform a similar chemistry as in the ODH process. The operating temperature is about 150 °C higher, so reaction rates will also be much higher and much less coke is required for an active and selective catalyst (compared to 10-30 wt% in ODH, Ch. 8).

(7) The co-feeding of CO_2 over the KFe catalyst quickly deactivates the catalyst due to the formation of stable potassium carbonates (Ch. 2).[21, 22] This destroys the presumed active phase ($KFeO_2$) and it also disables the coke oxidation and gasification function of the potassium compounds in the catalyst. Without the presence of the oxygen groups on the coke surface, the reaction rates will plummet. The dehydrogenation in N_2 (no oxygen groups on the coke) at a comparable temperature and pressure requires larger amounts of coke to be active, about 20 wt% (Ch. 3). The experiments with the KFe catalyst and CO_2 showed that the selectivity of the catalyst remained very high, the EB conversion and the ST selectivity even slowly increased from 8 to 10% and 94 to 98%, respectively. Once CO_2 is removed, the oxygen groups on the coke slowly return as the potassium becomes available again. The observed deactivation is still due to excessive coke formation and loss of available surface for reaction.

(8) The short steaming treatment[22] could produce a higher concentration of oxygen groups on the coke and hence explain the temporary higher conversions.

(9) The claim that steam has no effect on the dehydrogenation reaction[23] can be understood. The coke gasification rate is not influenced by the steam-to-oil (S/O) ratio (oil being EB), only temperature has an effect (Ch. 2).[26] However, there is a critical minimum S/O ratio for each catalyst, if the amount of steam becomes lower severe

deactivation will occur. A steaming treatment is required to reactivate the catalyst.[26]

Following this idea that coke is the active phase in the steam aided dehydrogenation, a reaction mechanism like in Figure 5 is envisaged. Coke precursors (heavy condensates) are formed from styrene, which forms coke by further dehydrogenation and polymerisation reactions. This coke is oxidised with steam, forming quinone type species on the coke surface (possibly catalysed by potassium). Once this quinone is formed, there are two options: (1) gasification of coke, the quinone reacts with another water to H_2 and CO_2, or perhaps desorbs as CO[18] (and gaseous CO can react with H_2O to H_2 and CO_2); (2) dehydrogenation of EB, the quinone is reduced and H_2O and ST are formed.

From a classical catalysis perspective, the explanation of coke as the active phase might seem far-fetched, but one can also wonder how realistic it would be for the iron species to be accessible[21] if several tens of layers of coke are on the catalyst surface. The presumed active phase $KFeO_2$ has a coke gasification activity and $K_2Fe_{22}O_{34}$ and the iron phases act as a very good potassium reservoir with a very slow and controlled release of potassium to keep the catalyst in its active form (like a kind of a drug delivery system). Some of the earliest steam dehydrogenation catalyst research showed that it was potassium that increased the reaction rates by an order of magnitude, compared to an iron catalyst without potassium (or other alkali metal) and it also stabilised the catalyst performance with *TOS*.[20, 21] This can indeed mean that the steam activation for the oxidation of iron was improved, but it can very well be the formation of oxygen groups on the coke that improved the reaction rates. Especially in view of the current knowledge that ODH, dehydrogenation in N_2 and in CO_2 are all catalysed by coke.

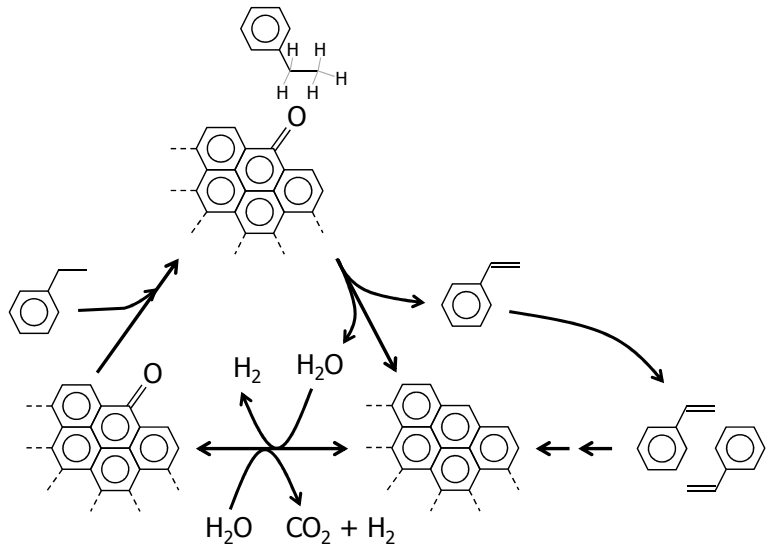

Figure 5: Reaction scheme for the dehydrogenation reaction in steam.

Conclusions and future prospects

The discovery and development of the KFe catalyst for EB dehydrogenation in steam was a success. Although it is not understood completely yet, this catalyst system manages to be very active, highly selective and shows very good stability. Comparing this with the alternative catalytic dehydrogenation operation with O_2, or CO_2, none is yet as good as the conventional catalyst. The catalysts for these new processes still need to find the right promotor to achieve a competitive activity, selectivity and stability where a balance is obtained between coke formation and removal, as is the case for the conventional catalyst. Part of the solution can also be found in the engineering tool box such as continuous catalyst regeneration and staged feeding. A thorough economic evaluation will have to prove if such solutions can provide enough incentive to commercialize the technology, such as with the SNOW/Advanced Styrene Monomer technology or SMART upgrade (Ch. 1). Despite the disadvantages of the steam dehydrogenation process, it appears that its advantages and track record still make it the most attractive process for styrene production.

References

[1] C. Nederlof, F. Kapteijn, M. Makkee, Appl. Catal. A: Gen. 417-418 (2011) 163-173.
[2] C. Nederlof, G. Talay, F. Kapteijn, M. Makkee, Appl. Catal. A: Gen. 423-424 (2012) 59-68.
[3] R. Krishna, S.T. Sie, Chem. Eng. Sci. 49 (1994) 4029-4065.
[4] F. Cavani, F. Trifiro, Appl. Catal. A: Gen. 133 (1995) 219-239.
[5] A.E. Lisovskii, C. Aharoni, Catal. Rev. - Sci. Eng. 36 (1994) 25-74.
[6] J.J. Delgado, X. Chen, J.P. Tessonnier, M.E. Schuster, E. Del Rio, R. Schlögl, D.S. Su, Catal. Today. 150 (2010) 49-54.
[7] J.J. Delgado, X.W. Chen, D.S. Su, S.B.A. Hamid, R. Schlögl, J. Nanosc. Nanotech. 7 (2007) 3495-3501.
[8] J.J. Delgado, D.S. Su, G. Rebmann, N. Keller, A. Gajovic, R. Schlögl, J. Catal. 244 (2006) 126-129.
[9] J.J. Delgado, R. Vieira, G. Rebmann, D.S. Su, N. Keller, M.J. Ledoux, R. Schlögl, Carbon. 44 (2006) 809-812.
[10] N. Keller, N.I. Maksimova, V.V. Roddatis, M. Schur, G. Mestl, Y.V. Butenko, V.L. Kuznetsov, R. Schlögl, Angew. Chem., Int. Ed. 41 (2002) 1885-1888.
[11] D.S. Su, J.J. Delgado, X. Liu, D. Wang, R. Schlögl, L.F. Wang, Z. Zhang, Z.C. Shan, F.S. Xiao, Chem. As. J. 4 (2009) 1108-1113.
[12] D.S. Su, N. Maksimova, J.J. Delgado, N. Keller, G. Mestl, M.J. Ledoux, R. Schlögl, Catal. Today. 102 (2005) 110-114.
[13] D.S. Su, N.I. Maksimova, G. Mestl, V.L. Kuznetsov, V. Keller, R. Schlögl, N. Keller, Carbon. 45 (2007) 2145-2151.

[14] J. Zhang, X. Liu, R. Blume, A.H. Zhang, R. Schlögl, D.S. Su, Science. 322 (2008) 73-77.
[15] J. Zhang, D.S. Su, A.H. Zhang, D. Wang, R. Schlögl, C. Hebert, Angew. Chem., Int. Ed. 46 (2007) 7319-7323.
[16] J.J. Delgado, X.-W. Chen, B. Frank, D.S. Su, R. Schlögl, Catal. Today. 186 (2011) 93-98.
[17] M.F.R. Pereira, J.J.M. Orfao, J.L. Figueiredo, Appl. Catal. A: Gen. 184 (1999) 153-160.
[18] S.G. Chen, R.T. Yang, F. Kapteijn, J.A. Moulijn, Ind. Eng. Chem. Res. 32 (1993) 2835-2840.
[19] D.H. James, W.M. Castor, "Styrene", in: Ullmann's Encyclopedia of Industrial Chemistry, Wiley-VCH Verlag GmbH & Co. KGaA, 2002.
[20] E.H. Lee, Cat. Rev. - Sci. Eng. 8 (1973) 285-305.
[21] T. Hirano, Appl. Catal. 26 (1986) 65-80.
[22] T. Hirano, Appl. Catal. 26 (1986) 81-90.
[23] M. Muhler, J. Schütze, M. Wesemann, T. Rayment, A. Dent, R. Schlögl, G. Ertl, J. Catal. 126 (1990) 339-360.
[24] M. Muhler, R. Schlögl, G. Ertl, J. Catal. 138 (1992) 413-444.
[25] J. Carrazza, W.T. Tysoe, H. Heinemann, G.A. Somorjai, J. Catal. 96 (1985) 234-241.
[26] Personal communication with G.R. Meima on Styrene monomer production at DOW, 2012.
[27] G.H. Riesser, Dehydrogenation Catalyst, 1979, U.S. patent 4144197.

Katalytische dehydrogeneringen van ethylbenzeen naar styreen

Samenvatting, evaluatie, conclusies en vooruitzichten

Elke ethylbenzeendehydrogenering wordt gekatalyseerd door coke

Dit onderzoek aan de katalytische dehydrogenering van ethylbenzeen (EB) naar styreen (ST) had als primair doel om een betere katalysatoren te ontwikkelen voor zowel het dehydrogeneringsproces in kooldioxide als in zuurstofhoudende atmosfeer die kunnen concurreren met het huidige proces van styreenvorming in stoom. Om dit te kunnen bereiken moeten al deze processen tot in detail begrepen worden. Na gewerkt te hebben aan katalytische dehydrogeneringsreacties in stoom, in stikstof, in kooldioxide en in zuurstofhoudende atmosfeer, blijkt het dat deze reacties vele overeenkomsten vertonen. De vorming van coke op deze katalysatoren is nauw verbonden met alle dehydrogeneringsreacties van EB naar ST. Deze twee elementen, coke en katalysator, zijn altijd samen aanwezig en kunnen niet los gezien worden van elkaar. De cokeafzettingen zullen naar verwachting voor deactivering zorgen. Maar bovenal is de coke een selectieve ingrediënt van de 'katalysator' in de dehydrogenering van EB naar ST in verschillende atmosferen. In de oxidatieve dehydrogenering staat niet meer ter discussie dat de reactie verloopt over de afgezette coke op de katalysator of het dragermateriaal. De dehydrogeneringsexperimenten in CO_2 of N_2 in dit proefschrift en de karakteriseringen van de katalysatoren laten duidelijk de betrokkenheid van coke bij de dehydrogeneringsreactie naar ST zien. Ook in de directe dehydrogenering in stoom spelen de cokeafzettingen een belangrijke rol. Dit wordt door zowel de literatuur als eigen resultaten in dit proefschrift ondersteund (Hoofdstuk 2). Door toepassing van zowel katalysator- als technologieontwikkeling lijkt een concurrerend proces met zuurstofhoudende atmosfeer binnen handbereik. Hierin worden een P/SiO_2-katalysator en de getrapte toevoer van O_2 toegepast.

De rol van de cokeafzetting in al deze reactiesystemen zal afzonderlijk besproken worden, gevolgd door mijn inzichten over de rol van de cokeafzettingen in de dehydrogeneringsreactie in stoom.

Dehydrogenering in CO_2 of N_2

Nog altijd zijn er vele auteurs die beweren dat de katalysator waar zij de experimenten mee beginnen verantwoordelijk is voor de katalyse van de dehydrogenering van EB in CO_2, zoals bijvoorbeeld *via* een redox-mechanisme (referenties in Hoofdstukken 3 en 4). Het besef dat cokeafzettingen de werkelijke selectieve katalysator zijn voor de omzetting van EB naar ST in CO_2 of N_2 was een zeer belangrijke stap in dit onderzoekswerk.[1] Door een 'schone' katalysatordrager te gebruiken, γ-Al_2O_3 van zeer hoge zuiverheid, rest er weinig anders te concluderen uit de gegevens van EB-omzetting, ST-selectiviteit en hoeveelheid cokeafzetting als functie van de '*time-on-stream*' (tijd dat de katalysator wordt getest, verder aangeduid als *TOS*) (Hoofstuk 3).[1]

Ook de gegevens van de toegepaste aluminagedragen V-, Cr- en Fe-katalysatoren wijzen op een gemeenschappelijke katalytische oorsprong door hun vergelijkbare EB-omzettingen en ST-selectiviteiten na 10 uur *TOS* in CO_2. In de initiële testfase laten deze katalysatoren nog verschillen zien in de EB-omzetting als gevolg van verschillende 'reverse-water-gas-shift'- (RWGS, of omgekeerde-water-gas-reactie) activiteiten. Wanneer de katalysator gedeactiveerd raakt door een overmaat aan cokevorming, heeft deze RWGS-reactie geen effect meer op de EB-omzetting. Dit bewijst tegelijkertijd dat een extra katalytische functie nodig is die niet gevoelig is voor deactivering door coke onder deze reactiecondities. Een ingekoolde alumina vertoont nauwelijks nog activiteit voor de RWGS-reactie (Hoofdstuk 4).[2]

Een ander belangrijk aspect dat naar voren kwam uit de eerste dehydrogeneringsexperimenten in CO_2 is dat de *TOS* ten minste 20 uur zou moeten bedragen. Enkele goede katalysatoren, zoals γ-Al_2O_3 of K/Al_2O_3 zijn nauwelijks actief in de eerste uren van de test, omdat nog niet voldoende coke is gevormd om de optimale EB-omzetting en ST-selectiviteit te halen. Als een experiment 10 uur of korter zou duren, dan zouden deze katalysatoren niet als potentieel goede katalysatoren geïdentifi-ceerd zijn. Het nadeel van zulke lange metingen is dat veel katalysatoren zoveel coke produceren, zoals de Fe-, Cr- en V-katalysatoren, dat ze al binnen enkele uren sterk deactiveren, ook voor de dehydrogenering. Vanuit een commercieel- of stabiliteits-oogpunt kan men zich afvragen of het wel interessant is om zulke katalysatoren te onderzoeken (Hoofdstukken 3 en 5).

De coke wordt op de zure plaatsen van de katalysator gevormd. Deze zure plaatsen leiden ook tot de vorming van bijproducten als benzeen en tolueen door middel van kraakreacties. Als deze plaatsen door coke bezet worden zal de vorming van deze bijproducten afnemen en wordt de katalysator selectiever en actiever voor de dehydrogeneringsreactie. De andere bijdrage aan een matige selectiviteit komt door de cokevorming zelf, wat natuurlijk ook een bijproduct is in het proces. Initieel is de cokeopbouw zeer snel, zeker met de Fe-, Cr- en V-katalysatoren, maar met de tijd

worden meer en meer zure plaatsen door coke bezet en neemt de snelheid van de cokeopbouw af. De optimale bedekkinggraad is een monolaag van coke op het katalysatoroppervlak. De vorming van coke stopt niet na het bereiken van de monolaag bedekking, coke wordt ook gevormd op de coke zelf, wat leidt tot stapeling van vele lagen (multi-laags-) coke. Dit leidt uiteindelijk tot een volledig ingekoolde en gesloten katalysatordrager. Zelfs dan is de katalysator nog zeer selectief, maar door het lage beschikbare (externe) oppervlak zal de omzetting laag zijn. Dit gebeurt overigens ook over andere, op koolstof gebaseerde startmaterialen zoals actieve kool of koolstof-nanobuisjes (Hoofdstuk 3).[1]

Het idee is dat de dehydrogenering in CO_2 en N_2 verloopt over de defecten en randen van de cokestructuur (grafeenranden), welke door EB gehydrogeneerd kunnen worden. Als gevolg daarvan wordt de EB omgezet naar ST en de gehydrogeneerde defecten of randen worden vervolgens weer gedehydrogeneerd door de hoge temperaturen. Als CO_2 wordt gebruikt en als er een RWGS-katalysator aanwezig is in het katalysatorsysteem dan kunnen de gevormde waterstofatomen gemakkelijk 'overlopen' (spill-over) van de coke naar de RWGS-katalysator om vervolgens verder te reageren *via* een redox-mechanisme met CO_2 naar CO en H_2O. Met moleculair waterstof (H_2) wordt dit effect niet waargenomen (Hoofdstuk 4).[2]

De γ-Al_2O_3-katalysator kan worden verbeterd door een kaliumzout toe te voegen. Kalium beïnvloedt de meest actieve zure plaatsen, waardoor er minder kraakproducten, een verbeterde ST-selectiviteit, maar ook een langzamere cokeopbouw en dus een tragere activering en deactivering van de katalysator. De deactivering van de katalysator kon niet worden voorkomen. Kalium verbetert ook de katalysatoractiviteit door de activering van CO_2 te promoten, wat resulteert in een hogere RWGS-activiteit (Hoofdstuk 6).

Het effect van CO_2 op de dehydrogeneringsreactie van EB naar ST is beperkt. De omzetting van EB is initieel zo'n 5-10% punten hoger bij de geteste katalysatoren, maar heeft niet de theoretisch mogelijke 20% punten verhoging laten zien die het daadwerkelijk tot een competitief proces zou maken. Hiervoor moeten katalysatoren met een goede stabiliteit en met hogere RWGS-activiteiten worden ontwikkeld. Een ander effect dat CO_2 zou moeten geven is de vergassing van coke, die de deactivering van de katalysator door een teveel aan coke tegen zou moeten gaan. Dit is onder geen van de toegepaste reactiecondities waargenomen. Om de vergassing van coke met CO_2 (de omgekeerde Boudouard-reactie) te activeren zijn temperaturen van 650 °C of hoger en de aanwezigheid van een katalysator nodig. Een aanzienlijk verlies van ST-selectiviteit onder die condities maakt dit niet werkbaar. De ontwikkeling van katalysatoren met een cokevergassingsfunctie en een goede stabiliteit zijn daarom nog belangrijker dan de verbetering van de RWGS activiteit van de katalysator (Hoofdstukken 4 en 5).[2]

De dehydrogenering van EB naar ST in CO_2 vertoont een vergelijkbare, zeer hoge ST-selectiviteit als bij de dehydrogenering in stoom. Dat op zich is al een hele prestatie, maar de verbetering van de EB-omzetting was lang niet zo goed als verwacht kon worden vanuit thermodynamische beschouwingen. Daarbij is de stabiliteit van de katalysator ver verwijderd van de gewenste commerciële levensduur van enkele jaren. Wanneer deze aspecten bij de resterende uitdagingen van CO_2 toevoer, scheiding, compressie, hergebruik en een benodigde CO omzettingsinstallatie worden opgeteld, wordt het erg lastig voor een dehydrogeneringsproces gebaseerd op CO_2 om te concurreren met de gebruikelijke technologie van dehydrogenering in stoom. Hierbij moet wel de kanttekening worden geplaatst dat dit onderwerp maar voor een beperkte tijd is onderzocht en op basis daarvan geen goede evaluatie gemaakt kan worden. Daarentegen is het vrijwel zeker dat verbeteringen enorm veel moeite zullen vergen. Het is de vraag of dat het wel waard is.

Oxidatieve dehydrogenering

Kinetische en mechanistische aspecten

De vorming van ST *via* oxidatieve dehydrogenering (ODH, Vgl. 1) heeft vele voordelen ten opzichte van de directe dehydrogenering in stoom, zoals het ontbreken van evenwichtsbeperkingen en een lagere reactietemperatuur. De grootste uitdaging voor ODH is daarentegen om een vergelijkbare hoge ST-selectiviteit (>96%) te behalen, aangezien de EB zeer gemakkelijk volledig geoxideerd kan worden (Vgl. 2 en 3). Maar er zijn nog meer zijreacties die belangrijk zijn voor de gewenste hoge ST-selectiviteit. Een overzicht van de belangrijkste reacties die plaatsvinden tijdens ODH:

$$C_8H_{10} + \tfrac{1}{2}O_2 \rightarrow C_8H_8 + H_2O \quad (1)$$

$$C_8H_{10} + 10\tfrac{1}{2}O_2 \rightarrow 8CO_2 + 5H_2O \quad (2)$$

$$C_8H_{10} + 6\tfrac{1}{2}O_2 \rightarrow 8CO + 5H_2O \quad (3)$$

$$C_8H_{10} + O_2 \rightarrow precursors \rightarrow coke \quad (4)$$

$$coke + O_2 \rightarrow CO + CO_2 + H_2O \quad (5)$$

$$C_8H_{10} + O_2 \rightarrow oxygenated\ products \quad (6)$$

$$C_8H_{10} + H_2 \rightarrow C_7H_8 + CH_4 \quad (7)$$

$$C_8H_{10} \rightarrow C_6H_6 + C_2H_4 \quad (8)$$

De vorming van benzeen en tolueen (Vgl. 7 en 8) neemt met toename van de temperatuur toe. De selectiviteit naar andere, geoxideerde producten (Vgl. 6) en voorproducten van coke (Vgl. 4) nemen met afnemende temperatuur toe. De ST-selectiviteit over γ-Al_2O_3 is optimaal bij een temperatuur van 450 °C (Hoofdstuk 6). Een schema van het ODH-reactienetwerk is in Fig. 1 afgebeeld. De meeste reactie verlopen parallel aan elkaar, de vorming van coke en CO_X (CO plus CO_2) uit coke zijn volg-reacties (Vgl. 5). Zodra ST gedesorbeerd is en in de gasfase is dan reageert het niet verder, zelfs onder reactiecondities van 525 °C in de aanwezigheid van één procent zuurstof in de gasfase (Hoofdstuk 9).

De vorming van CO_X verbruikt veel meer O_2 ten opzichte van EB (6.5-10.5) in vergelijking met de ODH-reactie (0.5). Er is waargenomen dat een toename van de ratio O_2:EB, of een hogere O_2 concentratie, leidt tot een hogere cokeopbouw, een lagere ST-selectiviteit en lagere EB-omzetting (Hoofdstukken 6-10). Dit is een indicatie van verschillende reactieordes van O_2 in de reacties naar ST en CO_X, waarbij de reactieorde van ODH de laagste is en de reactieorde van de volledige oxidatie de hoogste.

Het verschil in reactieordes van O_2 kan ook op een slimme manier gebruikt worden, zoals gedemonstreerd wordt door de getrapte O_2-voedingsexperimenten. Door de O_2-toevoer te verdelen over 6 reactoren in plaats van alle O_2 en EB tezamen aan 1 reactor toe te voeren, zijn de ST-selectiviteit (+4% punten) en EB-omzetting (+15% punten) sterk toegenomen. Door zowel het aantal reactoren als de totaal gevoede hoeveelheid O_2 (gelijke hoeveelheid per reactor) te verhogen, neemt de EB-omzetting

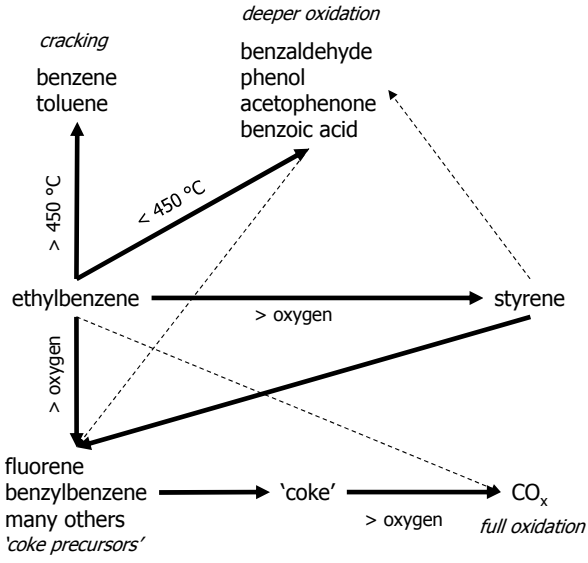

Fig. 1: Het reactienetwerk van de koolwaterstoffen in ODH.

lineair toe bij een vrijwel gelijkblijvende ST-selectiviteit. Dit bewijst ook dat de ST eigenlijk niet verder reageert onder deze hevige reactieomstandigheden. De prijs die hiervoor betaald moet worden is een grotere hoeveelheid katalysator, aangezien de reactiesnelheden lager liggen door de lagere O_2 concentraties (Hoofdstuk 9).

De rol van coke

Voor de ODH-reactie is het al sterk in de literatuur onderbouwd dat coke de werkelijke katalysator is.[4, 5] Het is zelfs zo dat de beste katalysatoren die bekend zijn uit koolstof zijn opgebouwd. De onderzoeksgroep van Schlögl bestudeert het gebruik van allerhande gestructureerde koolstof materialen voor de ODH-reacties van EB naar ST en butaan naar butenen.[6-15] Het voordeel van het uitgaan van uit koolstof bestaande materialen is dat deze katalysatoren direct actief en selectief zijn voor ODH. Overigens is dit geen garantie dat deze katalysatoren beter (selectiever) zijn dan de best geteste katalysatoren in dit proefschrift, wat ook geconcludeerd kan worden uit het overzicht in Tabel 1. Er zijn een aantal verschillen tussen de experimenten in deze tabel: de verhoudingen van O_2:EB, omzetting van O_2 en het gebruik van een integrale reactor, waar Schlögl *et al.* vooral een differentiële reactor gebruikten. Deze factoren kunnen voor een deel de verschillen in katalysatorprestaties verklaren.

Uitgaan van een koolstofmateriaal heeft als nadeel dat dit materiaal niet stabiel is onder reactieomstandigheden, wat aan den lijve met geactiveerde kool-(AC-)monsters is ondervonden (Hoofdstuk 8). Wanneer er een 'hot-spot' ontstaat in de reactor kan het gemakkelijk gebeuren dat het volledige monster verloren gaat. Gedurende het ODH-proces wordt het reactieoppervlak continu vernieuwd, wat er ook voor zorgt dat de samenstelling van het koolstofmateriaal verandert.[5] Eigen tests met koolstofnanobuisjes

Tabel 1: Reactiecondities en prestaties van verschillende katalysatoren uit dit proefschrift en werk van Schlögl *et al.*[6-15]

Monster	Ref.	Temp. [°C]	O_2:EB ratio	ST productie	ST selectiviteit	O_2[b] omzetting	O_2 (ST)[b] selectiviteit
γ-Al_2O_3	H6	450	~0.6	29%	82%	100%	23%
Al-1000	H8	450	~0.6	36%	86%	100%	28%
γ-Al_2O_3[a]	H9	450	~0.6	42%	86%	100%	32%
5P/SiO_2	H7	500	~0.6	48%	89%	100%	38%
3P/SiO_2	H7	475	~0.6	51%	91%	100%	41%
5P/SiO_2[a]	H9	500	~0.6	65%	93%	100%	55%
OLC	10	517	2.5	62%	68%	100%	12%
CMK-3	11	400	2.5	52%	76%	80%	13%
CNF	9	515	1	23%	81%	60%	20%
CNF	9	440	1	38%	81%	95%	20%
CNF	16	400	2.6	13%	85%	10%	25%
CNF	9	425	1	19%	89%	26%	32%
CNT	15	400	0.5	11%	95%	22%	47%

[a] getrapte O_2 voeding met 6 reactoren

[b] Berekend uit beschikbare gegevens; bij ontbrekende gegevens is uitgegaan van een 1:1 verhouding van CO_2 en CO bijproducten om O_2 omzetting en O_2 (ST) selectiviteit te berekenen.

(CNT) lieten zien dat er tijdens de ODH-reactie een reactievere koolstofhoudende afzetting wordt gevormd (een verschuiving naar lagere oxidatietemperaturen in de thermogravimetrische analyses (TGA) in lucht, Appendix 9). Daarom is het vanuit praktisch oogpunt niet de route die verder gevolgd moet worden en is het gebruik van een anorganisch materiaal een beter uitgangspunt, ook al betekent dit dat een inloopperiode noodzakelijk is om de ODH-reactie op gang te krijgen. Op deze manier kan het systeem geregenereerd worden en mogelijk zelfs *via* katalyse vat krijgen op het type en de hoeveelheid coke die gevormd wordt.

Het werk met de gepakt-bed-microbalans-reactor opstelling in combinatie met een gaschromatograaf (TEOM-GC) heeft laten zien dat er een lineaire relatie bestaat tussen de hoeveelheid coke op de katalysator en de EB-omzetting en ST-selectiviteit. Initieel gaat deze relatie heel goed op, maar op het moment dat een monolaag coke is afgezet, begint het werkelijke gedrag af te wijken totdat een ODH-prestatieplafond wordt bereikt waar een verandering van de hoeveelheid coke geen effect meer heeft op de algehele prestaties van de katalysator. Uiteindelijk leidt een combinatie van ernstig inkolen en bijbehorende hoge katalysatorbedekking tot een vermindering van de ODH-prestaties (Hoofdstuk 10).

Zoals eerder al was genoemd is het type coke een belangrijke parameter voor de ODH-prestaties. Het type coke wordt hier gedefinieerd door de reactiviteit met O_2 in de TGA-analyse. Dit is een direct resultaat van de cokesamenstelling (CH_XO_Y) en wordt beïnvloed door het effect van het dragermateriaal of katalysator op de vergassing van de coke. Idealiter is de coke zeer onreactief (bijna inert) met O_2, in combinatie met een niet oxiderende drager. Het calcineren van γ-Al_2O_3 bij hoge temperaturen had een positief effect op de ODH-prestaties en de reactiviteit van de coke. Het TGA-profiel van de ingekoolde monsters verschoof naar iets hogere oxidatietemperaturen. De TGA-profielen van de ingekoolde P/SiO_2-katalysatoren verschoven zelfs naar nog hogere oxidatietemperaturen, waarbij de betreffende EB-omzetting en ST-selectiviteit ook veel hoger lagen dan die van γ-Al_2O_3. Het regenereren van P/SiO_2-monsters onder reactiecondities (zonder EB) duurde veel langer (>10 uur) dan voor de γ-Al_2O_3-monsters (2-4 uur). De lage reactiviteit van de coke heeft twee gevolgen: (1) er wordt minder coke vergast naar CO_X, wat de ST-selectiviteit ten goede komt en (2) de activiteit voor de selectieve ODH-reactie is ook lager, waardoor hogere temperaturen of meer anorganisch startmateriaal nodig zijn om vergelijkbare activiteit te krijgen. Het anorganische startmateriaal en promotoren hebben duidelijk een sterk effect op het type coke dat gevormd wordt (Hoofdstukken 6, 8 en 10).

Duidelijke transmissie-electronenmicroscopie opnames van de structuur van de cokeafzettingen zijn niet verkregen in dit onderzoekswerk, maar voor de reactiviteit zijn de toegankelijkheid en de mate van dehydrogenering/aromatisering van de coke ook

zeker van belang. Het idee is dat de dehydrogeneringsreacties plaatsvinden op de (geoxideerde) randen van de grafeen structuren,[6, 17] waar ook de vergassing plaatsvindt.[18] De ST-selectiviteit op deze randen wordt dan bepaald door de lokale O_2 partiaaldruk en reactiviteit van de coke.

Reactorprestaties

Tijdens de ODH-reactie zijn er verschillende factoren geïdentificeerd die een significante invloed hebben op de reactorprestaties. Één daarvan is het vereiste om volledige O_2 omzetting aan het einde van de reactor te behalen, wat het testen van de katalysatoren bemoeilijkt. Voor een hoge en selectieve omzetting zijn de twee reactanten, EB en O_2, rond de stoichiometrische reactieverhouding nodig (O_2:EB = 0.5). In de gevallen waar niet alle O_2 aan het einde van de reactor is omgezet (Hoofdstukken 6-10), worden er ten koste van de ST-selectiviteit relatief meer CO_X en zware condensaten gevormd, als gevolg van de hogere gemiddelde O_2 concentratie in de reactor. Dit negatieve effect op de ST-selectiviteit wordt wel kleiner in het geval dat de coke minder reactief is met O_2 (verbranding), zoals bij de P/SiO_2-katalysatoren. Daarnaast is het ook noodzakelijk om veiligheids- en economische redenen: hoge EB-omzettingen en kleine recyclestromen zijn gewenst, gelijktijdig moeten 'runaway'- en explosierisico's voorkomen worden.

Een andere factor is de mate van 'plug-flow'-(propstroom-)gedrag dat een effect kan hebben op de reactorprestaties onder de toegepaste testcondities (Appendix 5). Het vereiste van volledige O_2 conversie en gewenste hoge EB-omzetting sturen de behoefte om vrijwel perfect propstroomgedrag te hebben. Verschillende reactorontwerpen zijn gebruikt in dit werk en voor γ-Al_2O_3 bleek het zo te zijn dat minder ideaal propstroomgedrag juist een positief effect had op de ODH-prestaties. Kortere en bredere katalysatorbedden hebben een hoger Péclet getal, wat betekent dat het gedrag meer richting een gemengde reactor gaat in plaats van een propstroomreactor. In het ODH-proces zijn er twee belangrijke concurrerende reacties die beide zowel O_2 als EB consumeren, de dehydrogenering en vorming van CO_X. Omdat deze twee reacties verschillende reactieordes hebben in O_2, profiteert de reactie met de laagste orde van de lage O_2-concentraties van de axiale dispersie of mengeffecten. Vanuit dit oogpunt is een ideaal gemengde reactor met lage zuurstof partiaalspanning juist gewenst (Hoofdstuk 9). De gevolgen met betrekking tot O_2 zijn het grootst omdat deze reactant volledig wordt geconsumeerd. Een situatieschets van het effect van axiale dispersie op de O_2-concentratie is in Fig. 2 getekend. De P/SiO_2-katalysatoren zijn opnieuw minder gevoelig voor dit effect van axiale dispersie en presteren inderdaad beter bij ideaal propstroomgedrag, aangezien deze katalysatoren minder actief zijn dan γ-Al_2O_3 en minder CO_X-vorming vertonen.

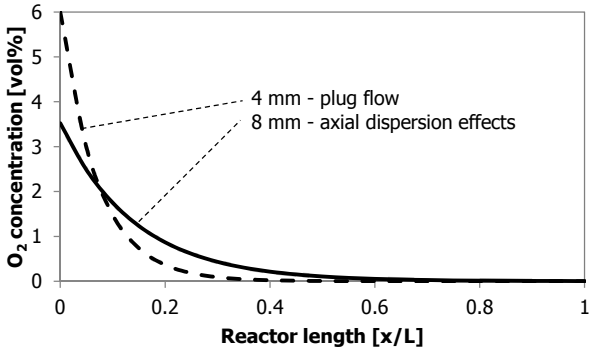

Fig. 2: De concentratie van O_2 als functie van de positie in de reactor bij verschillende reactor diameters.

Nog een belangrijke factor is de contacttijd van de reactanten met de katalysator, welke reciprook in de 'weight-hourly-space-velocity'-waarde (*WHSV*, massadebiet per katalysatorgewicht per uur) wordt uitgedrukt. Onder verschillende *WHSV*-condities vertoont de katalysator vrij bijzonder gedrag (Appendix 1). De *WHSV* kon bijna zesvoudig worden verhoogd (of verkleind) voordat er een significante verandering optrad in de ODH-prestaties van de katalysator. Klaarblijkelijk vallen al deze *WHSV*-waardes binnen het prestatieplafond dat werd waargenomen met de TEOM-GC-opstelling en bepalingen van de cokebelading (Hoofdstukken 8 en 10). De sleutel die dit gedrag verklaart is een combinatie van de hoeveelheid coke (en bedekking) en de O_2-profielen over de reactor. Bij de laagste *WHSV*-waarde is er veel meer coke aanwezig dan strikt noodzakelijk voor volledige O_2-omzetting, maar ook weer niet teveel dat het een negatief effect heeft op de ODH-prestaties. Bij de hoogste *WHSV*-waarde die is getest was er juist precies genoeg coke aanwezig om een volledige O_2-omzetting en de optimale ST-selectiviteit te bereiken. Pas wanneer de temperatuur omlaag werd gebracht, ging de activiteit van de katalysator naar beneden tegelijk met de ST-selectiviteit en de O_2-omzetting. Dat leidt tot de conclusie dat er onvoldoende coke aanwezig was om het selectieve ODH-proces te katalyseren (Appendix 1). Een mooi illustrerend voorbeeld van dit effect van onvoldoende coke is in Fig. 3 te zien. In dit voorbeeld lukt het niet om tussen 75-78 uur volledige O_2-omzetting te behalen. Na het verhogen van de temperatuur en 40 uur extra *TOS* is er wel voldoende coke gevormd om bij een temperatuur van 475 °C alle O_2 om te zetten. Op dat moment verbeteren ook de andere prestaties (de EB-omzetting en de ST-selectiviteit nemen toe, de selectiviteit naar CO_X, benzeen en tolueen nemen af). De deactivering door cokeopbouw gaat onveranderd verder. Het mag duidelijk zijn dat O_2 onder al deze omstandigheden de limiterende reactant is.

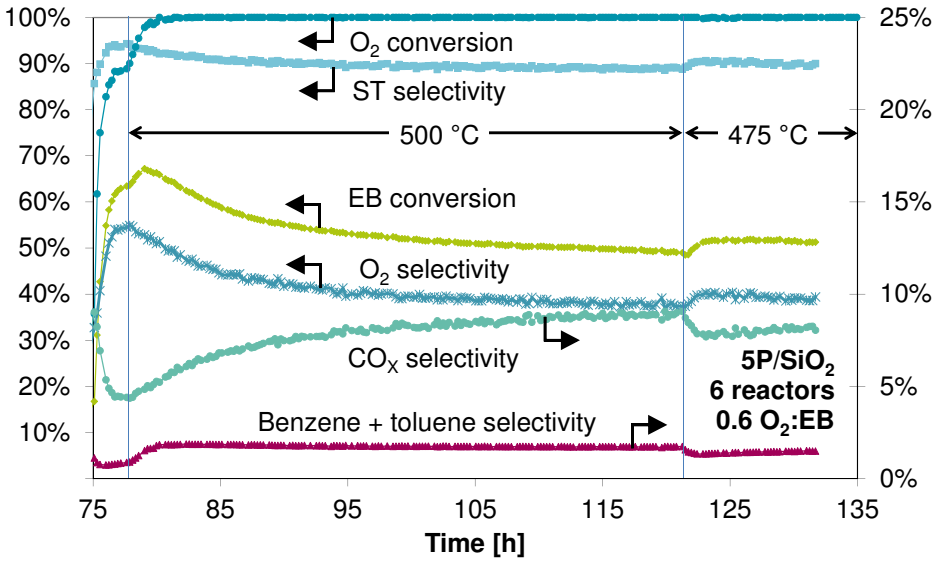

Fig. 3: Prestaties als functie van de *TOS* van het 5P/SiO_2-monster in een getrap voedingsexperiment met 6 reactoren. Tussen 78-122 uur is de temperatuur ingesteld op 500 °C, op andere tijden is het 475 °C.

Deze geobserveerde effecten van propstroomgedrag en contacttijd zijn zeer interessant. Om de consequenties van deze effecten op de ODH-reactie volledig te begrijpen is aanzienlijk meer onderzoek nodig.

Katalysatortests

Het ontwikkelen van een goede en betrouwbare procedure voor de analyse van de productgasstroom was een uitdaging. Dit kwam enerzijds door de opzet van de experimenten met CO_2 als één van de gebruikte verdunningsmiddelen (Hoofdstuk 6, Appendix 4) en anderzijds door het brede spectrum aan bijproducten die tijdens het ODH-proces worden gevormd. De eerste uitdaging, het gebruik van CO_2, werd opgelost door de voedingsgassamenstelling regelmatig te analyseren als referentiepunt voor de O_2-balansberekeningen voor elke productgasstroomanalyse. Op deze manier kon bepaald worden welk deel van de gemeten concentratie CO_2 uit de voeding komt en welk deel tijdens het proces werd gevormd (Hoofdstuk 6). Het spectrum aan bijproducten uit het ODH-proces is zeer breed en bevat ondermeer moleculen als methaan, etheen, benzeen, tolueen, acetophenon, benzoëzuur en nog heel veel meer (Appendices 4 en 8). Sommige moleculen, zoals EB, ST en kleine koolwaterstoffen zijn eenvoudig te identificeren en detecteren. De uitdaging zit hem met name in de koolwaterstoffen die groter, zwaarder en minder vluchtig zijn dan ST, het gewenste product. Zulke zware condensaten kunnen tot wel 1% van de totale productstroom uitmaken (meestal 0-0.5%). Ook kunnen ze zich ophopen in de GC-kolom, waardoor analyseproblemen

kunnen ontstaan zoals verschuivende piekposities, of een verhoging van de basislijn. Als deze zware condensaten meegenomen worden in de analyse door een matige meetprocedure, zal de koolstofbalans niet sluiten. Deze problemen zijn in dit werk opgelost door de GC-kolom iedere analyse tot hoge temperaturen (240 °C) te verwarmen, waardoor een zeer betrouwbare koolstofbalans is verkregen waarin alleen nog de koolstof die is achtergebleven op de katalysator (coke), ontbreekt.

Dankzij de geoptimaliseerde analyse van de productgasstroom konden de katalysator prestaties zeer nauwkeurig gevolgd worden gedurende de *TOS* van een test. Bij betere katalysatorprestaties worden de verschillen in ST-selectiviteit steeds kleiner terwijl er tegelijkertijd grote verschuivingen in het O_2-gebruik plaatsvinden door de grote verschillen in O_2-consumptie van de twee concurrerende reacties, dehydrogenering en volledige oxidatie. Deze bedragen respectievelijk 0.5 en 10.5 O_2 voor elk molecuul EB. Elke verbetering van de katalysatorprestaties onder volledige O_2-omzetting betekent dat de hoeveelheid zuurstof die wordt door de dehydrogeneringsreactie geconsumeerd sterk toeneemt. Om dit goed te beseffen is het zinvol om de selectiviteit van O_2 voor de vorming van ST te berekenen (Hoofdstuk 9, Tabel 1). Bij ST-selectiviteiten van boven de 90% laat de O_2 (ST)-selectiviteit de prestatieverschillen duidelijk zien en is dus inderdaad en zinvolle extra prestatieparameter. De EB-omzetting neemt ook toe bij betere katalysatorprestaties, maar deze is ook sterk afhankelijk van de ingestelde verhouding van O_2:EB. De O_2-selectiviteit voor de EB-omzetting naar ST is niet direct afhankelijk van deze verhouding.

Voor(ui)tgang van de ODH-prestaties

Als tegemoetgekomen is aan de vereiste volledige O_2-omzetting is het zo dat de CO_X-selectiviteit, ST-selectiviteit en EB-omzetting aan elkaar gekoppeld zijn. Een toename van de ST-selectiviteit gaat altijd samen met een toename van de EB-omzetting en een afname van de CO_X-selectiviteit (en omgekeerd). Dit is volstrekt logisch aangezien elk O_2-molecuul maar één keer kan reageren waarbij of CO_X, of H_2O en ST worden gevormd. De selectiviteit naar de andere bijproducten is meestal zo laag (< 1% punt van de selectiviteit) dat dit hierin amper meeweegt. Er rekening mee houdend dat zowel CO (bovengrens) als CO_2 (ondergrens) gevormd kunnen worden, dan volgt de niet-lineaire trend in Fig. 4 rechtstreeks uit de molbalansen. Als alle gemeten data op een soortgelijke wijze worden uitgezet dan ziet de trend er exact hetzelfde uit. De resultaten van enkele belangrijke groepen katalysatoren zijn ook in Fig. 4 aangegeven.

Deze figuur geeft ook een goede indruk van de ontwikkeling van de katalysatorprestaties binnen dit project. Er zijn grote stappen gezet en het lijkt zelfs alsof de gestelde doelen binnen bereik zijn. Bijvoorbeeld door het gebruik van meer dan 6 reactoren met getrapte O_2-voeding met de 5P/SiO_2-katalysator zou een hogere EB-

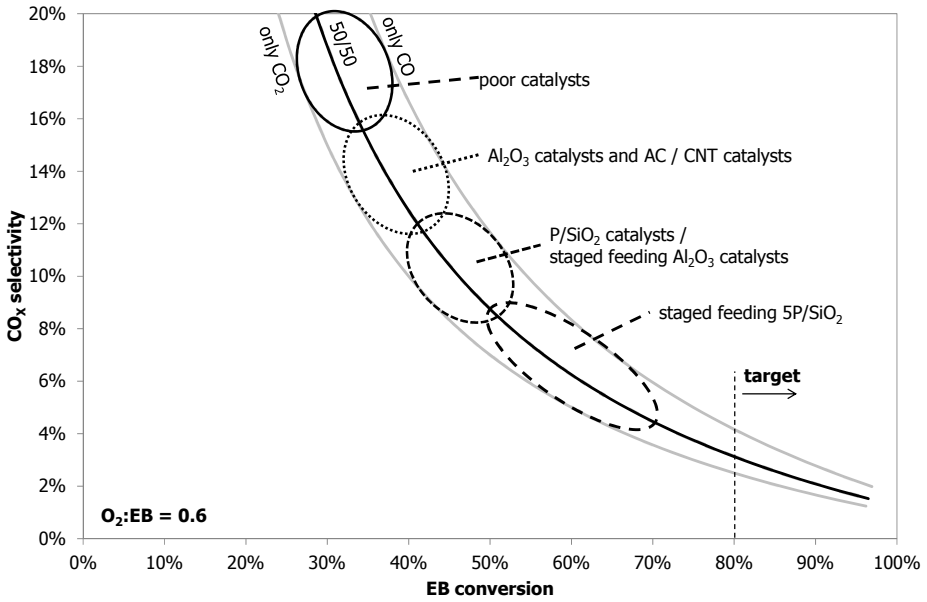

Fig. 4: De relatie tussen CO_X selectiviteit en EB-omzetting bij volledige O_2 omzetting voor een totale voedingsverhouding van O_2:EB = 0.6. De zwarte lijn is voor 50/50 CO/CO_2 productie, de bovenste grijze lijn is voor alleen CO-vorming, de onderste grijze lijn is voor alleen CO_2-vorming. De resultaten van belangrijke groepen katalysatoren zijn aangegeven.

omzetting en ST-selectiviteit behaald moeten kunnen worden. De realiteit is echter minder simpel, aangezien deze en ook andere katalysatoren deactiveren tijdens de *TOS*. De TEOM-GC-experimenten hebben laten zien dat de cokeopbouw continu doorgaat bij elke geteste katalysator, alhoewel de snelheid waarmee dit gebeurt wel langzaam afneemt met de *TOS*. Om de optimale cokehoeveelheid op de katalysator vast te houden, zou de katalysator ononderbroken (deels) geregenereerd moeten worden. Er zijn meerdere opties bekend om dit te bereiken, zoals 'swing-operation' (afwisselen van werkingsregimes met twee reactoren, één in operatie, de ander in regeneratie), stromende/bewegende katalysatorbedden of gefluïdiseerde katalysatorbedden (met aparte reactor/regenerator of twee werkingszones in één) (Hoofdstuk 9).

Tot op heden is het niet gelukt om een mechanisme of een methode te ontdekken die erin slaagt om de hoeveelheid coke op de katalysator onder controle te krijgen tijdens het ODH-proces. Er kan wel meer O_2 gevoed worden om meer oxidatie van coke te krijgen, maar tegelijkertijd wordt er dan ook meer coke gevormd waardoor er netto toch een toename van coke is en de selectiviteit naar ST daalt. Ook is er geen enkele aanwijzing gevonden die wijst op een inhiberend mechanisme die de cokeopbouw zou kunnen stabiliseren.

Ideeën voor verdere verbetering

Een van de ideeën die nog is uitgeprobeerd, is het toevoegen van een tweede oxidant aan het proces. Een goede kandidaat hiervoor is mogelijk NO_2, waarvan bekend is dat het de verbranding van roet verbetert tijdens de reiniging van dieseluitlaatgassen. Helaas had de toevoeging van NO_2 geen effect op de stabiliteit van het ODH-proces. Een vergelijking van experimenten met en zonder NO_2 (in een concentratie van 100-800 ppm) met meer dan 100 uur *TOS* liet geen verschil zien. Andere secundaire oxidanten zijn niet getest.

Een andere mogelijkheid is om een vluchtige vergassingskatalysator toe te voegen zoals KOH in combinatie met stoom. Dit zou tijdelijk de verbranding kunnen verbeteren[18] en de hoeveelheid kan worden aangepast om evenveel verbranding als vorming van coke te krijgen en zo een stabiel proces te krijgen. Dit zal wel tot een verlies van O_2 en ST leiden omdat de snelheid van cokevorming niet verandert en te hoog blijft.

Een laatste optie waar aan gedacht kan worden is afgekeken van het dehydrogeneringsproces in stoom: lage specifieke oppervlaktes en hoge gehaltes macroporositeit. Op deze manier is het oppervlak om coke af te zetten beperkt en is het bovendien goed toegankelijk, zonder last te hebben van stoftransportbeperkingen en samenhangende CO_X-selectiviteitsverhoging (Hoofdstuk 8). Echter zal er wel voldoende coke aanwezig moeten zijn om een actief en selectief katalysatorsysteem te zijn. Daarvoor moet mogelijk het reactorvolume worden vergroot om tot de gewenste conversie en selectiviteit te komen.

Dehydrogenering in stoom

Na het bespreken van de twee nieuwe opties voor EB-dehydrogenering is het opvallend hoeveel overeenkomsten er zijn met het dehydrogeneringsproces in stoom. De bijproducten van de reacties komen grotendeels overeen: benzeen, tolueen en zware condensaten worden in alle drie de processen gevormd. Ook cokeafzetting vindt plaats in alle drie de processen. In het dehydrogeneringsproces met CO_2 is de cokeopbouw heel snel, de EB-omzetting over γ-Al_2O_3 neemt af van 62% naar 25% in 100 uur *TOS* (Hoofdstuk 3). In het oxidatieve dehydrogeneringsproces is de deactivering een stuk langzamer, de EB-omzetting over γ-Al_2O_3 neemt af van 35% naar 30% in 100 uur *TOS* (Hoofdstuk 6). En in het dehydrogeneringsproces met stoom is de deactivering als gevolg van coke opgelost en zijn er andere deactiveringsmechanismen die plaatsvinden, zoals de herverdeling en het verlies van kalium gedurende de levensduur van de katalysator. Om voor deze andere deactiveringsmechanismen te compenseren wordt de reactortemperatuur langzaam omhoog gebracht (de uitgangstemperatuur stijgt van 580 naar 630 °C) gedurende de meer dan twee jaar die de katalysator wordt gebruikt in het

stoomdehydrogeneringsproces.[4, 19, 20]

Op basis van mijn ervaringen met de drie katalytische dehydrogeneringsreacties ben ik van mening dat ook het dehydrogeneringsproces in stoom door de coke wordt gekatalyseerd. Er zijn vele aanwijzingen te vinden die er op wijzen dat coke een essentieel onderdeel is van het katalysatorsysteem.

(1) Het katalysatorsysteem heeft ongeveer 20 uur nodig om 'steady-state' (stabiele toestand) te bereiken.[20, 21] Het is mogelijk dat deze tijd nodig is om de optimale oxidatie toestand van de katalysator te bereiken, maar het kan ook zo zijn dat de stabiele hoeveelheid coke maar heel langzaam wordt bereikt (door de continue vergassing van de coke met een overmaat stoom).

(2) De veronderstelde actieve stof van de katalysator, $KFeO_2$,[21-23] is ook bekend als een zeer actieve kolenvergassingskatalysator.[24, 25] Wellicht is dat ook de dominante functie van de $KFeO_2$ in het stoomdehydrogeneringsproces, om de coke te vergassen en zo een stabiele hoeveelheid coke in de hand te houden, maar dat de coke de werkelijke dehydrogeneringskatalysator is.

(3) Verschillende auteurs rapporteren een stabiele hoeveelheid coke op de katalysator én dat de actievere katalysatoren meer coke bevatten. Zo wordt er in één publicatie 0.024-0.050 wt% (gewichtsprocent) genoemd,[21] terwijl een commerciële katalysator optimaal wel zo'n 2-3 wt% coke door het gehele katalysatorbed kan bevatten.[26] De zeer lage specifieke oppervlaktes van de KFe-katalysator (2-5 m^2/g) en de 0.54-0.76 mg/m^2 voor een monolaag cokebedekking (Hoofdstuk 10) laten zien dat de gerapporteerde hoeveelheden net onder één monolaag liggen tot aan mogelijk wel tientallen lagen coke op het katalysatoroppervlak. Zulke grote hoeveelheden coke lijken niet te verhinderen dat de dehydrogeneringsreactie gewoon plaatsvindt.

(4) Een laag specifiek oppervlak en macroporeuze structuur van de katalysator bevorderen de selectiviteit van de katalysator.[27] Natuurlijk zal de macroporeuze structuur voor een goed interne stoftransport zorgen en de kans op mogelijke vervolgreacties verkleinen, maar het bijkomende lage specifiek oppervlak is ook een hele goede methode zijn om de hoeveelheid coke (ook een bijproduct) te beperken, de vergassing van deze coke te verbeteren en zo de hoeveelheid aan coke te kunnen beheersen en daarmee de mogelijke deactivering door overmatige cokevorming.

(5) Het is bekend dat kalium mobiel is[20] en aanwezig is op het oppervlak van een ingekoolde KFe-katalysator.[26] Dit kan gunstig zijn voor de vergassing van de coke, maar het kan ook de dehydrogeneringsreactie helpen door een 'spill-over'-mechanisme zoals is waargenomen bij de dehydrogenering in CO_2 (Hoofdstuk 5).

(6) De vergassing van coke zal moeten plaatsvinden *via* de vorming van tijdelijke zuurstofhoudende plaatsen op het cokeoppervlak. Het is niet onwaarschijnlijk

dat deze kortlevende zuurstofhoudende plaatsen op het cokeoppervlak soortgelijke chemie vertonen als in het ODH-proces. De werktemperatuur voor het stoomdehydrogeneringsproces ligt ongeveer 150 °C hoger, dus ook de reactiesnelheden zullen vele malen hoger zijn en is er veel minder coke nodig voor een actieve en selectieve katalysator (vergeleken met de 10-30 wt% in ODH, Hoofdstuk 8).

(7) Door het bijvoeden van CO_2 over de KFe-katalysator deactiveert deze razend snel door de vorming van het stabiele kaliumcarbonaat (Hoofdstuk 2).[21, 22] Dit zorgt voor de verdwijning van de veronderstelde actieve stof ($KFeO_2$) alsook de katalytische werking van de kaliumverbindingen op de cokevergassing en -oxidatie. Zonder de aanwezigheid van de zuurstofhoudende plaatsen op het cokeoppervlak zullen de reactiesnelheden sterk afnemen. De dehydrogeneringsreactie in N_2 (zonder zuurstofhoudende plaatsen op de coke) heeft onder vergelijkbare omstandigheden ongeveer 20 wt% coke nodig om actief te zijn (Hoofdstuk 3). De experimenten met de KFe-katalysator en CO_2 laten ook zien dat de ST-selectiviteit zeer hoog bleef. De omzetting van EB en de ST-selectiviteit gingen zelfs langzaam omhoog, respectievelijk van 8 naar 10% en van 94 naar 98%. Zodra CO_2 van de voedingsstroom wordt afgesloten, komt de kalium weer beschikbaar om zuurstofhoudende plaatsen te genereren en komt de activiteit van de katalysator terug. De waargenomen deactivering zal een gevolg zijn van overdadige cokevorming en verlies van het beschikbare reactieoppervlak.

(8) Een korte stoombehandeling[22] zou een hogere concentratie van zuurstofhoudende plaatsen kunnen genereren en daarmee de tijdelijke hogere ST-vorming verklaren.

(9) De bewering dat stoom geen effect heeft op de dehydrogeneringsreactie[23] kan worden begrepen. De cokevergassingssnelheid wordt niet door de verhouding S/O (stoom en olie(EB)) beïnvloed, alleen de reactietemperatuur heeft effect (Hoofdstuk 2).[26] Let wel op dat iedere katalysator een kritieke minimum S/O ratio heeft, bij een lagere S/O zal de katalysator ernstig deactiveren. Een stoombehandeling is dan nodig om de katalysator weer te reactiveren.[26]

Een verdere uitwerking van dit idee dat coke de actieve stof is in de stoomdehydrogenering leidt tot een beoogd reactiemechanisme als in Fig. 5 is weergegeven. Voorproducten van coke (zware condensaten) worden gevormd uit ST, welke verder reageren tot coke door dehydrogeneringen en polymerisatiereacties. Deze coke wordt door de stoom geoxideerd en chinon-achtige verbindingen worden op de coke gevormd (mogelijk gekatalyseerd door kalium). Als deze chinon is gevormd zijn er twee vervolgopties: (1) vergassing van de coke waarbij de chinon reageert met nog een watermolecuul tot H_2 en CO_2, of zelfs desorbeerd als CO[18] (gasvormig CO kan met H_2O reageren tot H_2 en CO_2); (2) dehydrogenering van EB, de chinon wordt gereduceerd en

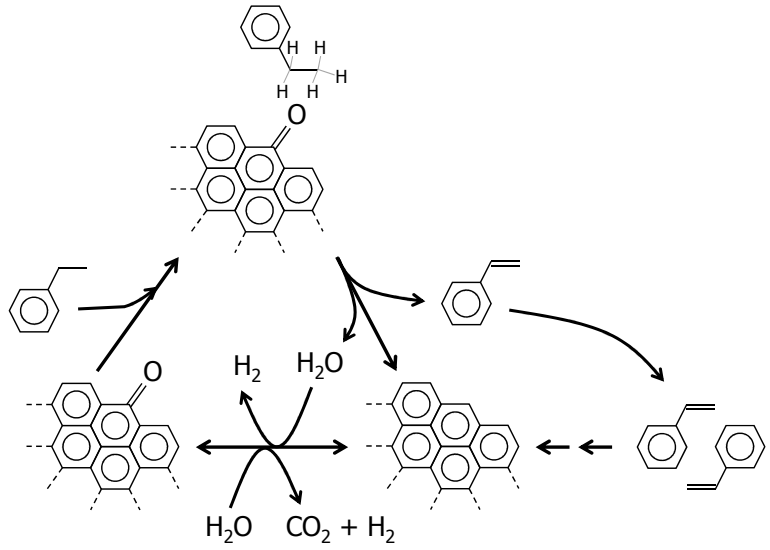

Fig. 5: Schema van het beoogd reactiemechanisme voor de dehydrogenering in stoom.

H_2O en ST worden gevormd.

Vanuit een klassiek katalyse-oogpunt lijkt deze verklaring van coke als de actieve stof misschien onwaarschijnlijk, maar men kan zich ook af vragen hoe realistisch het is dat de $KFeO_2$ nog toegankelijk is[21] als er tientallen lagen coke bovenop liggen. De veronderstelde actieve stof $KFeO_2$ vertoont ook activiteit voor de vergassing van coke, waarbij $K_2Fe_{22}O_{34}$ en andere ijzerverbindingen ook heel goed een rol kunnen hebben als buffervoorraad voor de gecontroleerde afgifte van kalium om de katalysator in zijn actieve toestand te houden (zoals een modern medicijnafgiftesysteem). Het vroege onderzoekswerk aan de ontwikkeling van een katalysator voor het stoomdehydrogeneringsproces heeft laten zien dat kalium verantwoordelijk is voor een toename van de reactiesnelheid met wel een factor tien in vergelijking met een ijzerkatalysator zonder kalium (of ander alkali metaal) en het stabiliseren van de katalysator prestaties tijdens de *TOS*.[20, 21] Dit kan inderdaad betekenen dat de activering van de stoom voor de oxidatie van het ijzer was verbeterd, maar het zou ook heel goed kunnen betekenen dat de vorming van zuurstofhoudende plaatsen op de coke de reactiessnelheid verhoogde. Vooral in het licht van de huidige kennis dat ODH, dehydrogenering in N_2 en in CO_2 allemaal door coke worden gekatalyseerd.

Conclusies en vooruitzichten

De ontdekking en verdere ontwikkeling van de KFe-katalysator voor de dehydrogenering van EB in stoom is nog steeds een succes te noemen. Alhoewel het nog steeds niet volledig wordt begrepen, lukt het dit katalysatorsysteem om zeer actief, selectief en stabiel te zijn. In de vergelijking met de alternatieve katalytische dehydrogeringsprocessen met O_2 of in CO_2, is het gebruikelijke katalytische proces nog veruit het beste. Voor katalysatoren van de nieuwe processen moeten nog steeds de juiste promotor afgedwongen worden om een concurrerende activiteit, selectiviteit en stabiliteit te bereiken, waarin een balans is gevonden tussen de vorming en verwijdering van coke zoals het geval is voor de katalysator in het stoomproces. Een deel van de oplossing kan gevonden worden in de gereedschapskist met technologische concepten zoals de continue regeneratie van de katalysator en het getrapt voeden van één van de reactanten. Een grondige economische evaluatie zal moeten uitwijzen of zulke oplossingen voldoende aansporing geven om de technologie te commercialiseren, zoals is gebeurd met de SNOW/Advanced Styrene Monomer technologie of de SMART modernisering (Hoofdstuk 1). Ondanks de nadelen van het stoomdehydrogeneringsproces lijkt het er sterk op dat de voordelen en de staat-van-dienst het nog altijd het meest aantrekkelijke proces maken voor de productie van styreen.

Referenties

[1] C. Nederlof, F. Kapteijn, M. Makkee, Appl. Catal. A: Gen. 417-418 (2011) 163-173.
[2] C. Nederlof, G. Talay, F. Kapteijn, M. Makkee, Appl. Catal. A: Gen. 423-424 (2012) 59-68.
[3] R. Krishna, S.T. Sie, Chem. Eng. Sci. 49 (1994) 4029-4065.
[4] F. Cavani, F. Trifiro, Appl. Catal. A: Gen. 133 (1995) 219-239.
[5] A.E. Lisovskii, C. Aharoni, Catal. Rev. - Sci. Eng. 36 (1994) 25-74.
[6] J.J. Delgado, X. Chen, J.P. Tessonnier, M.E. Schuster, E. Del Rio, R. Schlögl, D.S. Su, Catal. Today. 150 (2010) 49-54.
[7] J.J. Delgado, X.W. Chen, D.S. Su, S.B.A. Hamid, R. Schlögl, J. Nanosc. Nanotech. 7 (2007) 3495-3501.
[8] J.J. Delgado, D.S. Su, G. Rebmann, N. Keller, A. Gajovic, R. Schlögl, J. Catal. 244 (2006) 126-129.
[9] J.J. Delgado, R. Vieira, G. Rebmann, D.S. Su, N. Keller, M.J. Ledoux, R. Schlögl, Carbon. 44 (2006) 809-812.
[10] N. Keller, N.I. Maksimova, V.V. Roddatis, M. Schur, G. Mestl, Y.V. Butenko, V.L. Kuznetsov, R. Schlögl, Angew. Chem., Int. Ed. 41 (2002) 1885-1888.
[11] D.S. Su, J.J. Delgado, X. Liu, D. Wang, R. Schlögl, L.F. Wang, Z. Zhang, Z.C. Shan, F.S. Xiao, Chem. As. J. 4 (2009) 1108-1113.
[12] D.S. Su, N. Maksimova, J.J. Delgado, N. Keller, G. Mestl, M.J. Ledoux, R. Schlögl, Catal. Today. 102 (2005) 110-114.

[13] D.S. Su, N.I. Maksimova, G. Mestl, V.L. Kuznetsov, V. Keller, R. Schlögl, N. Keller, Carbon. 45 (2007) 2145-2151.
[14] J. Zhang, X. Liu, R. Blume, A.H. Zhang, R. Schlögl, D.S. Su, Science. 322 (2008) 73-77.
[15] J. Zhang, D.S. Su, A.H. Zhang, D. Wang, R. Schlögl, C. Hebert, Angew. Chem., Int. Ed. 46 (2007) 7319-7323.
[16] J.J. Delgado, X.-W. Chen, B. Frank, D.S. Su, R. Schlögl, Catal. Today. 186 (2011) 93-98.
[17] M.F.R. Pereira, J.J.M. Orfao, J.L. Figueiredo, Appl. Catal. A: Gen. 184 (1999) 153-160.
[18] S.G. Chen, R.T. Yang, F. Kapteijn, J.A. Moulijn, Ind. Eng. Chem. Res. 32 (1993) 2835-2840.
[19] D.H. James, W.M. Castor, "Styrene", in: Ullmann's Encyclopedia of Industrial Chemistry, Wiley-VCH Verlag GmbH & Co. KGaA, 2002.
[20] E.H. Lee, Cat. Rev. - Sci. Eng. 8 (1973) 285-305.
[21] T. Hirano, Appl. Catal. 26 (1986) 65-80.
[22] T. Hirano, Appl. Catal. 26 (1986) 81-90.
[23] M. Muhler, J. Schütze, M. Wesemann, T. Rayment, A. Dent, R. Schlögl, G. Ertl, J. Catal. 126 (1990) 339-360.
[24] M. Muhler, R. Schlögl, G. Ertl, J. Catal. 138 (1992) 413-444.
[25] J. Carrazza, W.T. Tysoe, H. Heinemann, G.A. Somorjai, J. Catal. 96 (1985) 234-241.
[26] Personal communication with G.R. Meima on Styrene monomer production at DOW, 2012.
[27] G.H. Riesser, Dehydrogenation Catalyst, 1979, U.S. patent 4144197.

Acknowledgements

Performing my PhD research work and ending up with the contents of this thesis would not have been possible, or as enjoyable, without the presence of many people and the financial contributions from STW and Lummus Technology. I would like to take the opportunity here to show my appreciation for all these contributions.

During the project, I have had the pleasure to work with five Master students whom did their MSc thesis work under my daily supervision. In chronological order, these were Thomas Isherwood (TGA as a screening method for dehydrogenation of isobutane in CO_2), Rogier Quak (Raman studies on coke formation and TAP-investigations), Güliz Talay (role of RWGS in the dehydrogenation of EB in CO_2), Pieter Vijfhuizen (coke studies on the oxidative dehydrogenation of EB to ST in the TEOM-GC setup) and Caroline Stemmer-Korsman (the effectivity of NO_X as a secondary oxidant in the oxidative dehydrogenation of EB to ST). All their results and discussions helped me a lot in creating a better understanding of the catalytic dehydrogenation reactions. A large part of their work can be found in this thesis, showing the great work that these students did, thanks once again.

Although I could manage to fix a lot of the emerging issues on the used setups, there were still many occasions that I needed the assistance of the very good technical support team that we have in our Catalysis Engineering group: Harrie Jansma, Kevin Mouthaan and Bart van der Linden proved to be more than capable time and time again. Also Willy Rook supported me quite a lot by doing many N_2-adsorption measurements and instructing me for the NH_3-TPD analyses. And I want to thank Patricia Kooyman for her work on taking the nice TEM-micrographs and EELS-analyses of several of my catalyst samples.

The secretary of the section Catalysis Engineering, staffed by Els Arkesteijn, Elly Hilkhuijsen and Caroline Monna, are also appreciated for their help with administrative matters concerning my PhD and finding available meeting times with my promotors. Els, I would like to thank you as well for your help with printing and distributing the draft thesis during my absence from Delft.

The key enabler for this project has been Michiel Makkee. The pleasant cooperation and supervision, starting from my Master thesis project, continued during this PhD work. I have always felt very welcome to share and discuss my latest results as well as many topics outside the scope of this project.

I have also very much appreciated the involvement of Freek Kapteijn as promotor in this project. Having a little distance from the project, there was always a good atmos-

phere to discuss the scientific developments in the project and their possible explanations or consequences. I found these meetings always very helpful.

Outside Delft there were also a couple of people involved in this project that was actually a combined project with University of Groningen, STW, Lummus Technology in the USA, and Delft University of Technology. I want to thank Barbara Kimmich from Lummus Technology for the many interesting WebEx meetings that we had, you proved to be a good commercial, but also stimulating reference point in the project. I also appreciated our scientific discussions on my publications.

In Groningen our project members were PhD candidate Valeriya Zarubina and her daily supervisor Ignacio Melián-Cabrera. I want to thank Valeriya for all her work in making a lot of catalysts for the ODH reaction and characterizations of these catalyst samples and wish her all the best in finalizing her PhD thesis. I also want to thank Ignacio for enabling this project and his participation in the WebEx discussions and presentations.

Finally, I would like to thank all the colleagues in the Catalysis Engineering section for their contribution to the great atmosphere in this group, during the Friday drinks, coffee breaks, Thursday lunches, Christmas dinners and all other social and professional activities that we enjoyed together.

List of publications

Articles

- Nederlof, C; Kapteijn, F; Makkee, M; Oxidative dehydrogenation of ethylbenzene to styrene: Staged O_2 feeding, Chemical Engineering Journal, *in preparation*.
- Nederlof, C; Vijfhuizen, P; Kapteijn, F; Makkee, M; Catalyst coking in the oxidative dehydrogenation of EB to ST, Chemical Engineering Journal, *in preparation*.
- Nederlof, C; Zarubina, V; Melián-Cabrera, I; Heeres, E; Kapteijn, F; Makkee, M; Oxidative dehydrogenation of ethylbenzene to styrene over alumina: effect of calcination, Catalysis, Science & Technology, 2012, *submitted*.
- Nederlof, C; Talay, G; Kapteijn, F; Makkee, M; The role of RWGS in the dehydrogenation of ethylbenzene to styrene in CO_2, Applied Catalysis A: General, Volumes 423–424, 7 May 2012, Pages 59-68
- Nederlof, C; Kapteijn, F; Makkee, M; Catalysed ethylbenzene dehydrogenation in CO_2 or N_2—Carbon deposits as the active phase, Applied Catalysis A: General, Volumes 417–418, 29 February 2012, Pages 163-173
- Almeida, RM de, Li, J, Nederlof, C, O'Connor, P, Makkee, M & Moulijn, JA (2010). Cellulose conversion to isosorbide in molten salt hydrate media. Chemsuschem, 3(3), 325-328.

Oral presentations

- Nederlof, C; Kapteijn, F; Makkee, M; Carbon deposits as the active phase in CO_2 ODH for ethylbenzene to styrene, NAM 22 (Detroit, USA), 6 June 2011.
- Nederlof, C; Kapteijn, F; Makkee, M; A fresh perspective on CO_2 oxidative dehydrogenation,
    - NPS 10 (Veldhoven, The Netherlands), 26 October 2010,
    - NCCC 11 (Noordwijkerhout, The Netherlands), 1 March 2011

Poster presentations

- Nederlof, C; Makkee, M; Catalyst surface in dehydrogenation. NPS 9 (Veldhoven, The Netherlands), 26-28 October 2009
- Nederlof, C; Kapteijn, F; Makkee, M; CO_2 oxidative dehydrogenation for hydrocarbons to styrene and olefins. XIth Netherlands Catalysis and Chemistry Conference (Noordwijkerhout, The Netherlands),1-3 March 2010

Curriculum Vitae

Christian Nederlof was born on the 30th of October, 1982 in Bernisse (Zuidland), the Netherlands. He obtained his Atheneum diploma in 2000, after which he started his Bachelor studies in Chemical and Biochemical Engineering at Delft University of Technology. He continued at the same university with his Master studies in Chemical Engineering. As a part of his Master studies he did a four month internship, on the topic of renewable energy and biomass conversions at the Statoil research center in Trondheim, Norway. The Master thesis work focused on the catalytic conversion of cellulose to polyols under the supervision of professor dr. Jacob A. Moulijn and dr.ir. Michiel Makkee, in the section Catalysis Engineering. He graduated in 2007, with honours. That same year he started his PhD research work under the supervision of professor dr. Freek Kapteijn and professor dr.ir. Michiel Makkee, entitled 'CO_2 oxidative dehydrogenation of hydrocarbons to styrene and olefins'. The results of that project are described in this thesis.

Since April 2012, Christian is working as a research engineer at Ford Research & Advanced Engineering in Aachen, Germany.

Appendices contents

b

A

A Experimental aspects of dehydrogenation experiments

Introduction

During the PhD study on the catalyst development for the dehydrogenation of EB to ST, many experimental issues were encountered. Some needed to be solved to be able to perform good experiments, where others are only described and a choice or assumption was made to continue with the work. These appendices are a summation of these issues that we encountered during the experimental work, plus supporting material for the thesis.

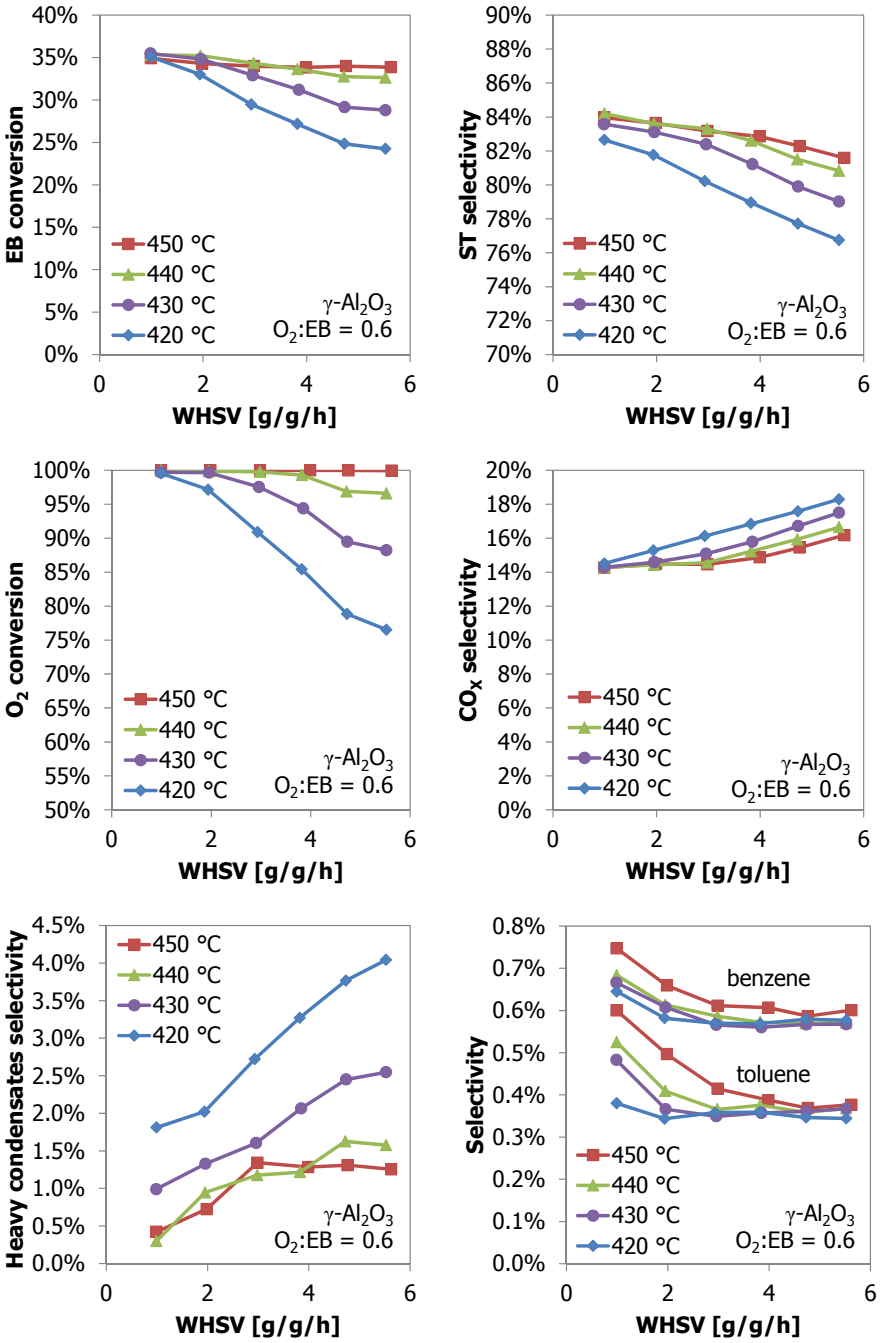

Figure 1: The ODH performance (conversion of EB and O_2, selectivity to ST, CO_X, heavy condensates, benzene and toluene) at different temperatures as a function of the *WHSV* for γ-Al_2O_3. 500 mg of catalyst, 10 vol% EB feed, CO_2:EB feed ratio of 5, balance gas N_2.

A.1 Variation of Weight Hourly Space Velocity (*WHSV*)

A.1.1 Results

In the optimisation of the testing conditions for our reference catalyst γ-Al_2O_3, one of the parameters was the *WHSV* [g EB / g cat / h]. The results are presented as a function of the *WHSV*. The ODH performance parameters are shown in Figure 1. At 450 °C, the ODH performance shows only very little variation under different *WHSV* conditions. At the highest *WHSV*s the ST selectivity decreases marginally due to an increase in the CO_X formation. At the lowest temperature that was tested, 420 °C, the ODH performance at a *WHSV* of 1 g/g/h is equal to that at 450 °C. For higher *WHSV* values, the ODH performance becomes worse both in EB conversion and ST selectivity. The O_2 conversion decreases from 100% to 77% for a *WHSV* of 1 to 5.5 g/g/h. Thereby, the EB conversion is decreased, but also ST selectivity decreases with less O_2 converted. This is due to a higher CO_X formation and increased formation of heavy condensates. The only parameter that is positively influenced by an increase in the *WHSV* is the selectivity to benzene and toluene. Both decrease at higher *WHSV* values, although it represents only a reduction of 0.1-0.2 % points in selectivity, with respect to just above 1% normally. For the other temperatures of 430 and 440 °C the same trends are observed. At a certain 'critical' *WHSV*, the O_2 conversion becomes incomplete and the ODH performance deteriorates in both EB conversion and ST selectivity. This 'critical' *WHSV* is 3.8 at 440 °C, 2.0 at 430 °C and 1.0 at 420 °C.

A.1.2 Discussion

The variation of the *WHSV* gave an unexpected result. At 450 °C, the *WHSV* could be increased from 1 to 5.6 g/g/h without affecting the ODH performance (both ST yield and selectivity). The small differences that are observed can be ascribed to small variations in the O_2:EB ratio that is around 0.6. At lower temperatures the *WHSV* can also be varied without changing the ODH performance, but only up to a certain critical limit. Above this limit, the O_2 conversion is not complete anymore, thereby decreasing the EB conversion, but also the ST selectivity decreases due to higher amounts of CO_X and heavy condensates. The selectivity to benzene and toluene improve a little at higher *WHSV*, but this is hardly significant compared with the other changes.

From literature and this work, it is clear that oxidative dehydrogenation is a complex process. The main function of the initial catalyst is to form coke and provide the surface area for the reactions. The coke is the active phase in ODH and this is not a constant amount (Chapter 10). The amount of coke, its surface coverage and its reactivity depends on the reactant concentrations, O_2:EB feed ratio, temperature, time on stream and possibly also on the *WHSV*. The maximum amount of coke will depend on the ab-

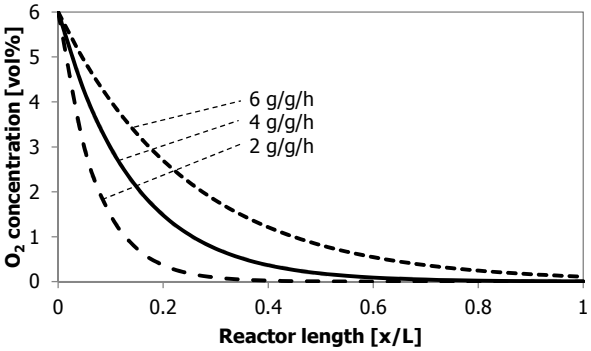

Figure 2: The O_2 concentration as a function of the catalyst bed length at different *WHSV* values.

solute amount of available surface and (pore) volume in the reactor. A plausible explanation for the fact that the *WHSV* can be varied without changing the ODH performance is that the (undetermined) amount of coke compensates for the new condition. When more EB and O_2 are fed, more coke will be formed. At some point the maximum amount of coke (or coverage) and maximum catalytic activity of the coke, is reached and full O_2 conversion is not possible anymore. When more O_2 and EB are fed, the ODH performance will deteriorate. The presented *WHSV* is the apparent *WHSV*, the intrinsic *WHSV* is an unknown fraction of the catalyst bed where oxygen is available (Figure 2). Probably the intrinsic *WHSV* is constant for the experiments where the EB conversion and ST selectivity remain constant at full O_2 conversion.

One thing that could be related to the *WHSV* is the selectivity to CO_X. At 450 °C, the amount of CO_X increases above 3 g/g/h while the EB and O_2 conversion are unchanged. The O_2:EB ratio is a little higher (up to +0.05) and usually a little higher EB conversion and CO_X selectivity are observed. When the *WHSV* is increased and comes closer to its critical *WHSV* for full O_2 conversion, it could happen that slightly more CO_X is produced because more O_2 flows over the coke.

For the small decrease in benzene and toluene selectivity the effect of *WHSV* could be much more straightforward. By increasing the *WHSV* the residence time (or space time) becomes shorter, the superficial gas velocity increases. Therefore, it can become more difficult for side reactions to take place, such as the acidic and thermal cracking to benzene and hydrocracking to toluene. The fact that these decrease with higher *WHSV* values implies that these reactions occur on the catalyst surface. Moreover, a higher amount of coke (or coverage) at higher *WHSV* values also reduces the number of accessible acid sites on the original catalyst surface.

An idea that keeps emerging is that at lower *WHSV* values, not all of the γ-Al_2O_3 catalyst is effectively used. At 450 °C and 2 g/g/h perhaps only the first 1/3 of the cata-

lyst bed is effectively used and all O_2 is consumed at this point. The rest of the catalyst is only a spectator that maybe adsorbs a few heavy condensate byproducts but nothing more. This idea is reinforced by the coke profile over the reactor length (Figure 10.14) that shows a higher coke coverage in the first part of the catalyst bed.

The deterioration of the ODH performance at incomplete O_2 conversion and possibly ineffective use of the catalyst at low *WHSV* values make it difficult to perform good differential catalyst testing or kinetics measurements. These experiments using γ-Al_2O_3 under different *WHSV* and temperature conditions already show the complexity of this process. In order to make a good evaluation of the catalysts that are screened, they should be tested over a wide range of conditions. Including several temperatures or *WHSV* values to find out what part of the catalyst is used effectively.

A.1.3 P/SiO_2

The most promising catalyst (P/SiO_2) was also tested at several *WHSV* values and temperatures. The ODH performance of both 3P/SiO_2 and 6P/SiO_2 are shown in Figure 3. The tests started at 475 °C at the lowest *WHSV* and the catalysts were regenerated with 6 vol% O_2 for 5 h before each higher temperature. For both samples the ST selectivity is the highest at 475 °C, 96% for 3P/SiO_2 and 97% for 6P/SiO_2. At 500 °C, 1% point ST selectivity is lost and again 1% point is lost at 525 °C. For the 3P/SiO_2 sample the ST selectivity is 2% points lower at 1 g/g/h compared with the other *WHSV* values. The O_2 conversion over the 3P/SiO_2 sample is 100% under all conditions. Its EB conversion is around 27%. At 475 °C it is 1% point higher, at 525 °C it is 1% point lower. The *WHSV* does not have an effect when the O_2:EB variations are taken into account. The O_2 conversion over the 6P/SiO_2 sample is complete at 525 °C, but at lower temperatures and high *WHSV* values not all oxygen is consumed anymore. At 475 °C the O_2 is not completely converted under all tested *WHSV* values. This has a large effect on the EB conversion, at 475 °C and 3.5 g/g/h the O_2 conversion is 52% resulting in a EB conversion of 15%, compared with full O_2 conversion and 27% EB conversion at 525 °C. For this P/SiO_2 catalyst the O_2 conversion does not have an effect on the ST selectivity.

The activation and deactivation of the P/SiO_2 catalysts make it a little more difficult to determine the effect of temperature and *WHSV*. The catalysts take a couple of hours to reach their optimal ST selectivity, hence the lower ST selectivities at 1 g/g/h for 3 P/SiO_2 (3-7 h *TOS*). The deactivation with *TOS* and loss in activity after regeneration explain the largest part of the decreasing selectivities at higher temperatures. The selectivity to cracking products (benzene and toluene, not shown) only increases 0.4% point with each 25 °C temperature increase.

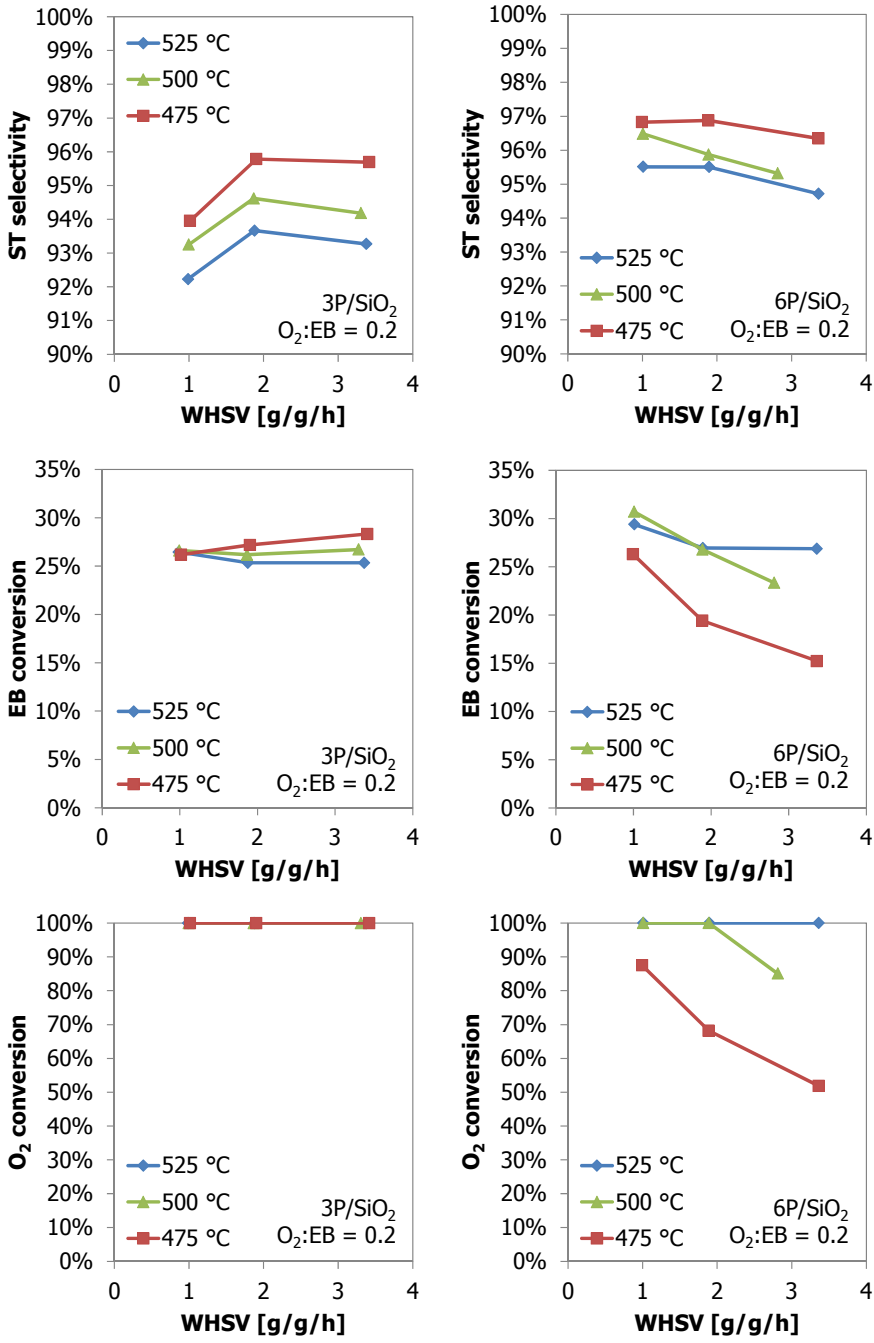

Figure 3: The ODH performance (EB conversion, ST selectivity and O_2 conversion) at different temperatures as a function of the *WHSV* for 3P/SiO_2 and 6P/SiO_2. 500 mg of catalyst, 10 vol% EB feed, CO_2:EB feed ratio of 5, balance gas N_2.

Otherwise, the *WHSV* and temperature variation for the P/SiO_2 catalysts show very comparable trends with γ-Al_2O_3. The EB conversion and ST selectivity are hardly changed at a different temperature of *WHSV* value. When not enough coke can be formed at lower temperatures and higher *WHSV* values, the O_2 conversion decreases and as a result the EB conversion decreases with it. The only difference with γ-Al_2O_3 is that the ST selectivity is not affected by a lower O_2 conversion over a P/SiO_2 catalyst.

A.2 Basis of comparison and testing

Our initial tests for ODH were all done with γ-Al_2O_3 or γ-Al_2O_3 supported catalysts. The density or specific surface area of these fresh catalysts was all roughly the same and could be compared without difficulty. For the screening phase of this project we would also be using and testing other supports and materials with completely different density and specific surface area. A catalyst activity can be defined in multiple ways, but usually it is mass or site specific. Most characterisation techniques will produce mass based data (*e.g.* NH_3-TPD, TPR, TPO, TGA, N_2-adsorption). With ODH, coke is the active phase, making the amount (or coverage) of coke an important parameter for comparison. This depends mostly on the available surface area of the catalyst and its acidity.

In this project a commercial party, Lummus Technology, participated. From an industrial perspective, the size and volume of a reactor are very important parameters as that affects the space that is required for a chemical plant. With some of the other materials that we tested (carbon nanotubes, mesoporous aluminosilicate, sintered alumina) their density and specific surface area resulted in a small variation in available surface areas in a constant catalyst testing volume. Testing the catalyst with a constant amount of volume was selected. (volume equal to 500 mg γ-Al_2O_3 of 212-425 μm particles = 0.8 ml; 65 mm bed height in the 4 mm ID quartz reactor tubes). A bed height of 65 mm was maintained in all experiments, unless otherwise specified.

A.3 Liquid feeding and evaporation

During our discussions with the equipment manufacturers, many options for the stable evaporation of the EB passed in review. The budget for the new high throughput setup was limited, so the best value for money was required. For liquid feeding there are many options. One can use individual liquid mass flow controllers (LMFC) that are fed by pressurised vessels, HPLC pumps, or even individual micro-rotary displacement pumps. Other options are direct feeding by Harvard micro-syringe pumps or ISCO syringe pumps. An overview of their pros and cons is given in Table 1.

Table 1: Liquid feeding options evaluation.

	LMFC + Pressurised vessel	LMFC + HPLC pump	LMFC + Micro-rotary displacement pumps	Harvard micro-syringe pumps	ISCO syringe pumps
Feeding range	+	+	+	+	+
Pressure range	+	+	+	0	+
Continuous use	0	+	+	0	0
Price	+	0	–	+	– –
Feeding stability	+	+	0	–	–

According to the data sheets of all the listed equipment, they all should be able to produce a constant flow in the range of 1 g/h of EB, by using different size syringes, internals, or sophisticated micro-step engines. As we also want to perform stability tests of weeks, or maybe months of continuous use, easy refilling without process interruption is very important. When using a pressurised vessel, the capacity of the vessel can be optimized, but the fact remains that it takes time and a feeding stop to refill. This is similar for the syringe pumps, their size can be optimized, or they can even be operated in parallel, but when switching from feeding to filling mode there is a short process disturbance. For the cost analysis, the basis of comparison is a feeding system for 6 reactors. This means that for some options there is a scale-out advantage (vessel, HPLC pump, or Harvard system). For the other options it scales linearly with the number of reactors. The ISCO syringe pumps are by far the most expensive (>20k€), although they are very robust and sophisticated. A Harvard syringe pump feeder costs much less (~5k€) and can handle multiple syringes. The force is limited, determining the size and number of syringes, depending on the required feed pressure. For the systems with a LMFC, the controller itself is the main investment. A pressurised vessel with connections and pressure regulators is the least expensive, followed by the single HPLC pump and most expensive the micro-rotary displacement pumps (but far less expensive than an ISCO pump).

Because the Harvard micro-syringe pump system looked quite promising, pressure is limited but sufficient, this was tested on a single flow setup with an online GC attached to it. The GC results, using different syringe sizes, are shown in Figure 4. Clearly, the EB vapour concentration is not very constant. Using a syringe of 50 ml, the ratio STD/AVG is 45% and for a 1 ml syringe pump it is still 5%. The smaller the syringe, the more process interruption disturbances (refilling), so these results are unacceptable for real use in the new setup. The micro-step engine in the Harvard system is not suitable for the stable feeding of the small flows that are required.

The TEOM setup is equipped with a LMFC/pressurised vessel that works very nicely, but during the experimental campaign the LMFC malfunctioned and an alterna-

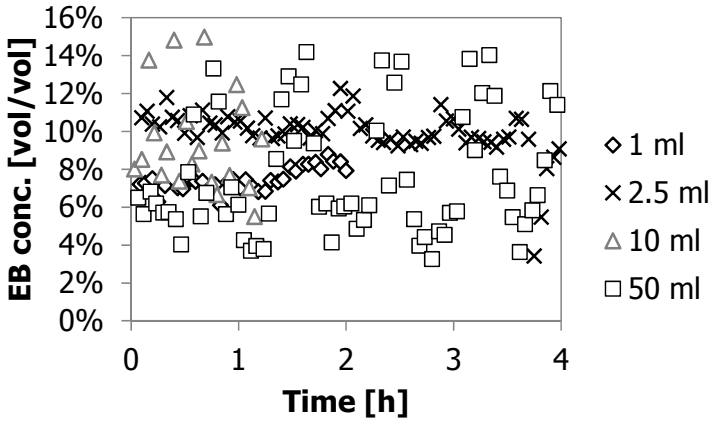

Figure 4: The EB concentration in the gas mixture with time, using different syringe sizes in a Harvard syringe pump system.

tive needed to be found. An unused ISCO pump was cleaned and implemented in the TEOM setup. Initially this appeared to work nicely too, but during our 20 h *TOS* tests the measured EB vapour concentration was changing. The reason was the ambient temperature in the room that fluctuated 5-10 °C, from day to night. Because of the density changes of the EB liquid and the large volume of the ISCO syringe this had a clear effect on the EB vapour concentration. The absolute volume displacement in the syringe was constant, but the mass displacement going out of the syringe was not. Heat tracing the syringe helped a little, but then the temperature control fluctuations affected the measured EB vapour concentration.

The only reliable choice left is a system with mass flow control. The pressurised vessel option cannot be used for very long experiments because of the limited volume and it can be difficult to control if one wants to test at different reactor pressures. The micro-rotary pumps are more expensive (and not proven for our context). The liquid feeding system with an HPLC pump was selected, with individual liquid mass flow controllers for each reactor and did not let us down thus far.

For the evaporation of the EB we could rely on previous experience. Preventing that the liquid is fed drop-wise is a very critical step. This can be achieved by using capillary sised tubing, of which the end is inserted into a bed of porous particles. The liquid will be absorbed and spread through the porous particles, ensuring a steady evaporation. This worked flawlessly, although the evaporation temperature needs to be sufficient but not too high that evaporation or boiling will already start in the capillary. Some optimisation was done to this end.

A.4 GC analysis & mole balances (O, C)

A good qualitative analysis is very important. Especially when the differences in the ODH performance of a variety of catalysts is within a couple of % points. A large improvement in the comparative analysis is the parallel (high throughput) reactor setup, where all reactors are analysed with the same equipment. The errors in the analysis or deviations from the calibration within one run are the same for each reactor and can therefore, be compared directly. Differences between runs are also small to negligible, but calibration of the GC was done regularly (when possible multiple times per month) to verify the GC response factors.

Calibration of the gas chromatograph (GC) was done using the pure gases and gas mixtures that were available: N_2, CO_2, air, H_2, the calibration mixtures (Table 2) and self-made gas mixtures using the mass flow controllers in the setup. For most components a one-point calibration is done and the GC data is assumed to be linear within a range of 0.1-100% for the TCD channel and 100 ppm – 10 vol% for the FID channel. Calculation of the several FID response factors is done by relative FID response factors [Dietz, 1967]. The elution peaks of ethane/ethane and propane/propene were overlapping for the column that was used (RTX-1 phase), so baseline separation and direct response factor calculation was not possible. The methane peak is used for the calculations. The response factor of EB was verified by a EB/N_2/CO_2 mixture at the end of each run. Typical GC curves for the FID and TCD channels are shown in Figure 5.

The online GC that was used did not sample a part of the reactor effluent gas flow, but instead all of the reactor effluent gas passed through the GC sample loop (20-100 ml/min, typically 40 ml/min). Depending on the flow, the pressure in the sample loops was a little higher than atmospheric pressure due to the pressure drop over the sample loops and additional tubing to the vent. This results in different amounts of gas that are injected into the GC columns. For long experiments in changing atmospheric conditions, the outside pressure fluctuations (940-1050 mbar) could also be observed in the

Table 2: Compositions of the calibration mixtures

Component	Mix 1 [vol%]	Mix 2 [vol%]	Synthetic air
Helium (He)	Balance		
Carbon dioxide (CO_2)	5	Balance	
Hydrogen (H_2)	2	5.014	
Oxygen (O_2)	2	1.213	21
Nitrogen (N_2)	5	30.05	79
Carbon monoxide (CO)	5	5.05	
Methane (CH_4)	4	3.076	
Ethene (C_2H_4)		2.022	
Ethane (C_2H_6)		1.493	
Propene (C_3H_6)		2.036	
Propane (C_3H_8)		1.507	

GC data. When necessary, all GC data was corrected for these pressure variations by a simple linear correction.

The calculation of conversions, selectivities and yields, are normally based on the inlet amounts of reactant (EB). Another method is to calculate the inlet amount from the measured amounts of reactant and products. This last method proved to give much nicer results, the variation between the measurements and the reactors is much smaller and better to compare. Of course, to be able to work properly with this method one needs to be sure that all products and byproducts are accounted for. In our case we are quite confident that all products and byproducts are measured. The GC method that is used

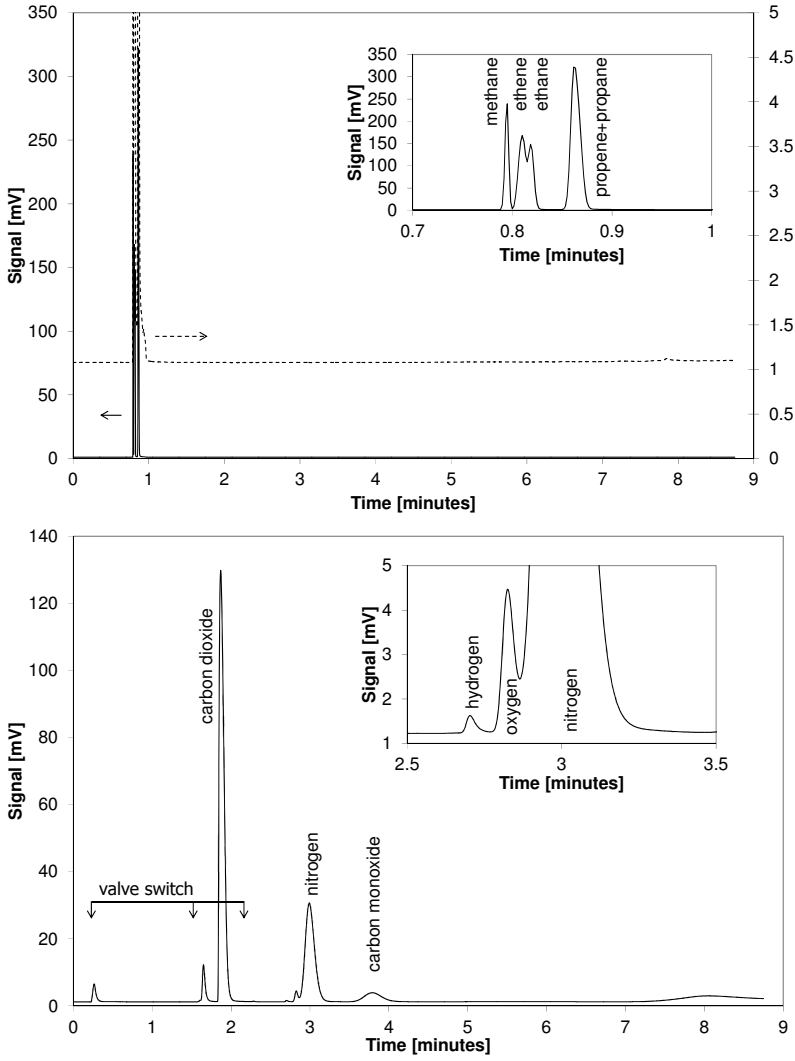

Figure 5: Typical GC curves from calibration gas mix 2. Top: FID channel (Hydrocarbons). Bottom: TCD channel (permanent gases).

measures all permanent gases and hydrocarbons with a temperature programmed method. Even the heavy condensates with a boiling point up to 240 °C are included. The final step is at 240 °C for one minute. In the last minutes of the analysis, hardly any products are measured. Typical GC curves for the FID and TCD channels are shown in Figure 6. Hydrogen is added to the gas flow downstream of the reactor and before the GC as an internal standard. Hydrogen is not produced in the ODH experiments.

Oxygen is the other reactant that is required for the oxidative dehydrogenation reaction. It reacts with ethylbenzene to the byproducts water, carbon monoxide and carbon dioxide. For simplicity it is assumed that other byproducts do not contain any oxy-

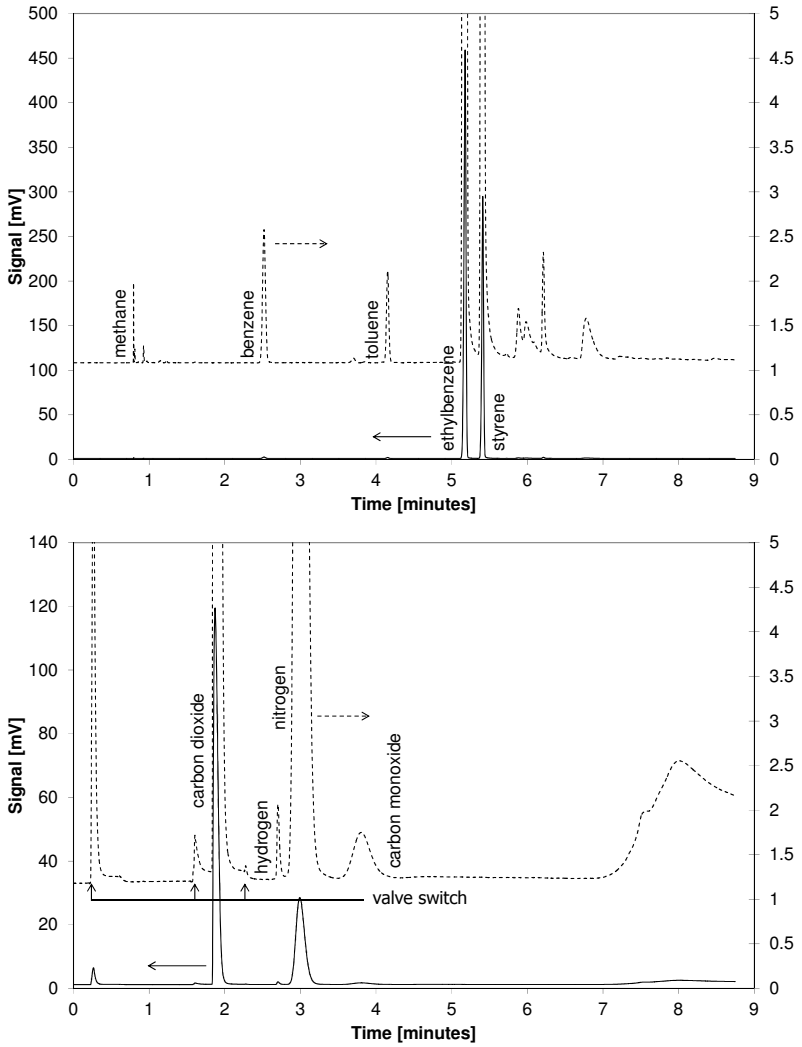

Figure 6: Typical GC curves from an ODH experiment. Top: FID channel (Hydrocarbons). Bottom: TCD channel (permanent gases).

gen. The oxygen balance is based on three main reactions, eqs. 1, 2 and 3. This includes the series reaction of the EB to coke and finally CO_X. Two product concentrations are unknown. The concentration of H_2O was not measured with the online GC because it does not give a linear response over a range of concentrations due to extreme tailing of the H_2O peak. The concentration of CO_2 is obscured because it is also used as a diluent. These two concentrations can be calculated by solving the oxygen balance, eqs. 4 and 5. In reality some byproducts may contain oxygen, but their concentrations are so low that they hardly make a difference to the oxygen balance and all-over mass balance.

$$C_8H_{10} + ½O_2 \rightarrow C_8H_8 + H_2O \quad (1)$$

$$C_8H_{10} + 10½O_2 \rightarrow 8CO_2 + 5H_2O \quad (2)$$

$$C_8H_{10} + 6½O_2 \rightarrow 8CO + 5H_2O \quad (3)$$

$$[CO_2] = \frac{16}{21}\left([N_2]\frac{21\%}{79\%} - \frac{1}{2}[C_8H_8] - \frac{13}{16}[CO] - [O_2]\right) \quad (4)$$

$$[H_2O] = \tfrac{8}{5}[CO_2] + \tfrac{8}{5}[CO] + \tfrac{1}{2}[C_8H_8] \quad (5)$$

A.5 Catalyst particle size effect

For good plug flow performance, the reactor length, reactor diameter and related Péclet number are important. For the case of wall effects to be negligible, the following rule of thumb (eq. 6) should be satisfied:

$$\frac{d_t}{d_p} > 10 \quad (6)$$

This leads to a maximum particle size of 400 µm for the selected reactor diameter size of 4 mm for the 6-flow setup. According to the Weisz-Prater criterion (Eq. 7) for negligible internal mass transfer, the EB conversion should be less than 10%. For the screening experiments, the EB conversion is usually much higher than 10%, also because we want to achieve full O_2 conversion for optimal ST selectivity.

$$\Phi = \eta_i \phi^2 \approx \frac{r_{v,obs} \cdot L^2}{D_{eff} \cdot c_s} \cdot \left(\frac{n+1}{2}\right) < 0.15 \quad (7)$$

Several tests were done to see the effect of particle size on the ODH performance over γ-Al_2O_3. Initially tests were done on the single flow setup with an 8 mm reactor diameter. These tests showed no effect of the particle size on the ODH performance. All measured particle sizes (90-150-300-425 µm) resulted in about 40% EB conversion. A

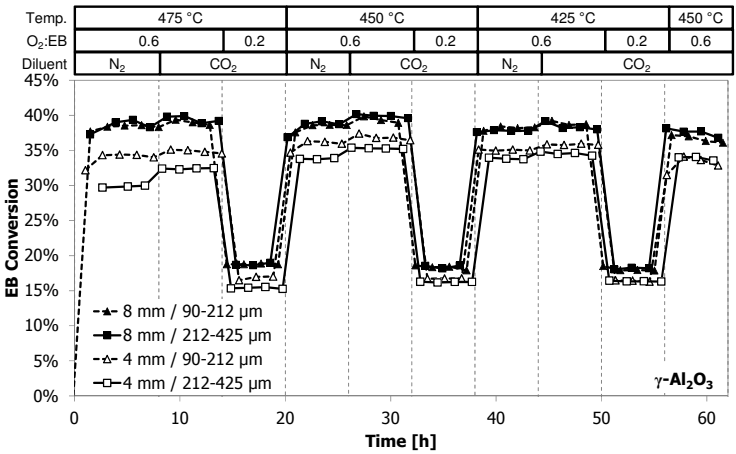

Figure 7: EB conversion as a function of time on stream over 500 mg γ-Al_2O_3 for different particle sizes (90-212 µm (*dashed lines,* ▲△) or 212-425 µm (*solid lines,* ■□)) and reactor diameters (4 mm (△□) or 8 mm inner diameter (▲■)).

particle size of 212-425 µm could be selected without any problems to do all other catalyst testing.

However, when the new 6-flow reactor setup with 4 mm reactors went operational and the same 212-425 µm γ-Al_2O_3 was used, the EB conversion went down to 36% at 450 °C and a 0.6 O_2:EB feed ratio. Because the testing criteria were still satisfied, our original thought was that this was due to improvements that were made in the GC analysis method and calculations. The O_2:EB ratio could have been slightly different and because the quality of the analysis improved due to the parallel testing with one GC, we wanted to trust these numbers over the old numbers.

To be completely sure about this (not being convinced completely), one 8 mm reactor was constructed for the 6-flow setup and once more the ODH performance was measured for several particle sizes and reactor diameters. The result is shown in Figure 7. At 450 °C and a 0.6 O_2:EB feed ratio (26-30 h *TOS*) the EB conversions are 40% in the 8 mm reactors with both particle sizes, 37% in the 4 mm reactor with the 90-212 µm particles and 35% in the 4 mm reactor with the 212-425 µm particles. Clearly there is an effect of particle size and reactor diameter and our initial assumptions were wrong, it was not a side-effect of the improved GC analysis. Unfortunately, this analysis was conducted by the end of the experimental work so it was undoable to repeat all experiments in a larger reactor or using smaller particle sizes. However, it is also shown in Chapter 6 that the data in the 4 mm reactors are very reproducible despite the possible mass transport influence. It is therefore, safe to say that all data are still comparable with each other, we see no reason to believe that another reactor diameter or particle size would give other trends and correlations.

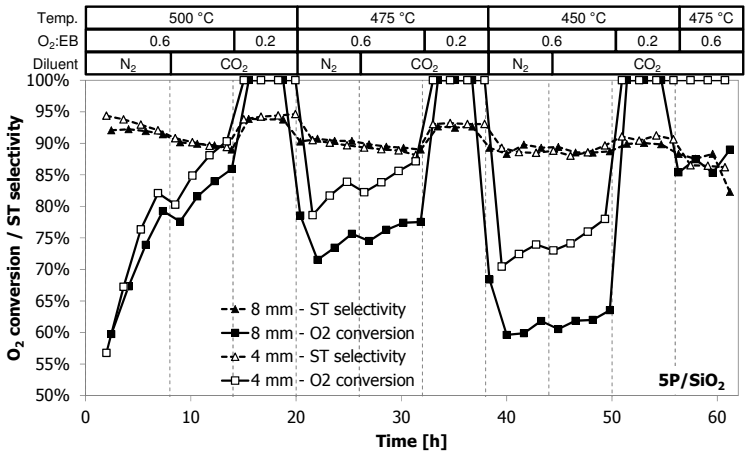

Figure 8: ST selectivity (*dashed lines,* ▲△) and O_2 conversion (*solid lines,* ■□) as a function of time on stream for 4 mm (△□) or 8 mm (▲■) reactor diameters using 212-425 µm particle sizes of 320 mg 5P/SiO_2 catalyst.

A similar experiment was done with the 5P/SiO_2 catalyst, the results are shown in Figure 8. The observed effects of the reactor diameter are much smaller compared with the γ-Al_2O_3. The ST selectivity is almost the same when using both reactor diameters. The main effect of reactor diameter is observed in the O_2 conversion and thus the direct activity of the catalyst. At an O_2:EB feed ratio of 0.2, full O_2 conversion is reached using both reactor diameters. At the O_2:EB feed ratio of 0.6, the O_2 conversion in the 4 mm reactor is higher than with the 8 mm reactor. For example at 30 h *TOS* the O_2 conversion in the 4 mm reactor is 86%, against 77% for the 8 mm reactor tube. In this case the EB conversion scales linearly with the O_2 conversion, because of the equal ST selectivities.

One can hypothesize about the reasons for the observed differences. The different particle sizes in the 4 mm reactor show that wall-effects may play a role here. Another large difference between these experiments is the superficial gas velocity that is at least 4 times smaller in the 8 mm tubes compared with the 4 mm tubes and oxygen may contact a larger fraction of the catalyst bed due to axial dispersion phenomena. The calculation of the Péclet numbers for the used reactors and the corresponding theoretical maximum conversion without axial dispersion and ideal plug flow behaviour (Eqs. 8-11) shows that the 8 mm reactor has an 8× lower Péclet number. The maximum O_2 conversion should be 80%, for 99.999% for the 4 mm tube. An overview of the data and calculation results is given in Table 3, including the data for the TEOM setup. The larger reactor behaves less ideal. As we have full O_2 conversion in both situations with γ-Al_2O_3, a relatively larger fraction of the reactor bed is used and the average O_2 concentration will be lower in that fraction of the bed, compared to the smaller bed fraction in

Table 3: Overview of reactor parameters and resulting Péclet numbers and maximum conversion.

Name	D_t [mm]	L [mm]	u [m/s]	D_{ax} [m^2s^{-1}]	Pe	Pe_p	X
4 mm	4	65	0.049	1.2E-5	236	1.5	99.999%
8 mm	8	16	0.012	4.5E-6	32	0.8	80%
TEOM	4	8	0.035	9.1E-6	26	1.3	72%

the thinner reactor (Figure 9). The staged feeding chapter (Ch. 9) nicely showed that a low O_2 concentration is favourable for EB conversion and ST selectivity. In the case of $5P/SiO_2$, there is no full oxygen conversion under all testing conditions. The relatively higher O_2 concentration in the 4 mm reactor gives higher conversions than for the 8 mm reactor. ST selectivity over P/SiO_2 catalysts is not affected so much by the O_2 conversion as γ-Al_2O_3 (Ch. 7). To investigate this further was outside the scope of this work. An important lesson is that assumptions should not be made easily and should be verified if possible.

$$Pe = \frac{L_b \cdot u}{D_{ax}} \qquad 8$$

$$Pe_p = \frac{d_p \cdot u}{D_{ax}} \qquad 9$$

$$D_{ax} = D_M + 0.5 \cdot u \cdot d_p \qquad 10$$

$$Pe > 20n \cdot \ln\left(\frac{1}{1-X}\right) \qquad 11$$

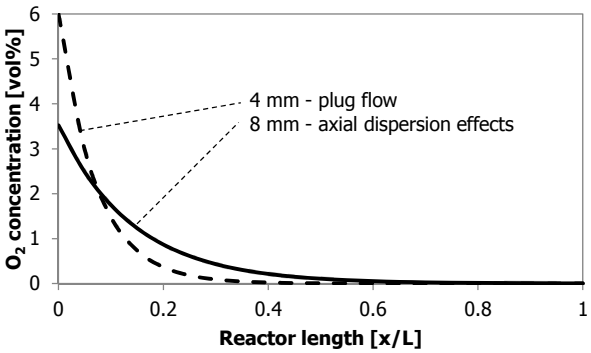

Figure 9: The O_2 concentration as a function of the catalyst bed length at different reactor diameters.

r

A.6 Reactor and diluent materials

The reactor design of the 6-flow reactors consisted of two Inconel half-shells in between which an Inconel reactor tube was placed. The advantage of this half-shell system is that one can easily replace it with another size of reactor. This was also a practical solution to the VCR connections of the reactors at the top and bottom. The size of the half-shells was a little larger than the size of the VCR-nuts, so the reactors could be removed from the reactor furnace for catalyst loading. One of the first tests that was done is to measure the 'background' conversion level of the reactors so that future experiments can be corrected for this, if necessary. The result is shown in Figure 10. This is a dramatic result. Not only does the EB conversion go up to almost 10%, it is also very different for each reactor. A small temperature variation (+/- 2 °C) between the 6 reactors was measured, but that cannot explain these differences. Possibly some scratches on the reactor surface cause these differences. It was concluded that the Inconel material was unsuited to do ODH experiments, because it seems like the reactor material itself has activity for the reaction.

Before the 6-flow setup arrived, many experiments were done using a single flow setup that had a quartz reactor tube. For this reactor material the measured background conversion was below 1%. A temporary construction with straight quartz tubes and rubber O-ring connections (VCO) at the top and bottom of the reactors were made and tested. These results are shown in Figure 11. As expected from the 1-flow setup, indeed the EB conversions are well below 1% and more important, almost equal for all reactors. Because this test was much more successful than with the Inconel reactors, new one-piece "half-shells" were made that had a permanent connection at the bottom and a

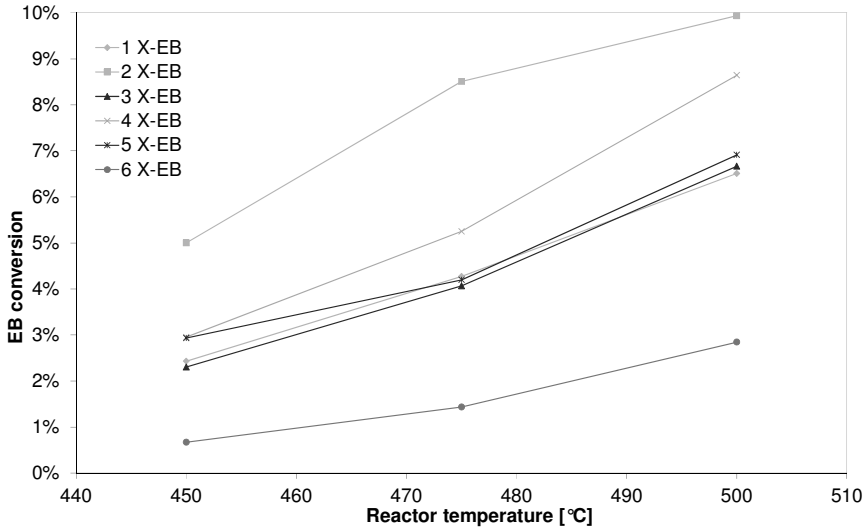

Figure 10: The EB conversion over the empty hastelloy reactors at different temperatures.

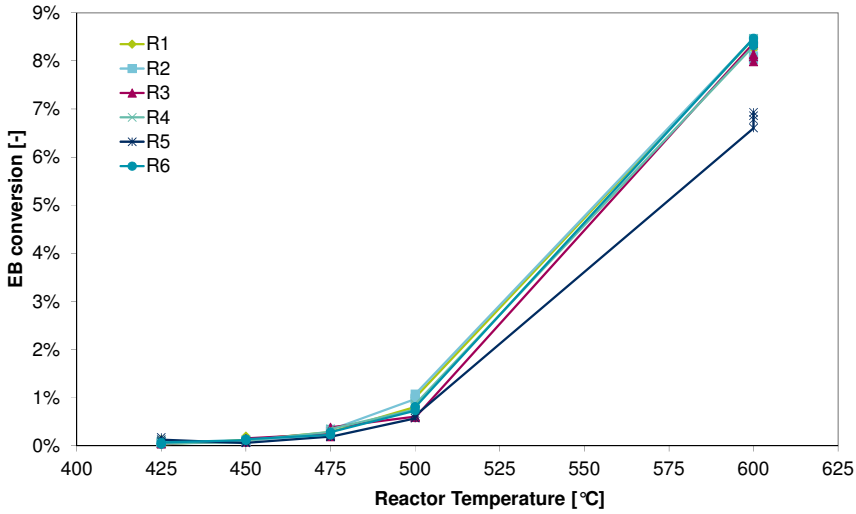

Figure 11: The EB conversion over the empty quartz reactors at different temperatures. quickly replaceable O-ring connection at the top for faster reactor replacements.

Besides the reactors themselves, also some diluent materials were tested for their 'background' conversion. These were silicon carbide, glass beads and quartz wool. Their conversion under different conditions is shown in Figure 12. This shows that the glass beads and quartz wool are also quite inert in the ODH reaction, but SiC, normally considered to be inert, is not inert and shows EB conversions well above 1%. In dehydrogenation with CO_2 diluent and at 600 °C, glass beads and SiC filled tubes have the lowest EB conversion. The glass beads had sintered together at 600 °C, so should not be used at these high temperatures. Quartz wool or an empty reactor shows higher EB conversion, these have the largest "open/free" volume. The shorter the time that the

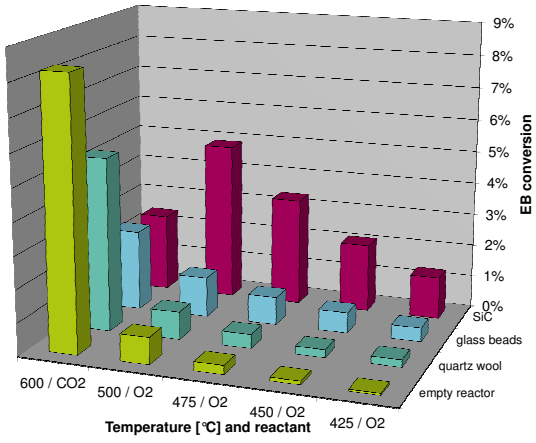

Figure 12: The EB conversion under different conditions over silicon carbide (SiC), glass beads, quartz wool and an empty reactor.

t

reactant is present in the reactor, the lower the conversion. Apparently quite some thermal decomposition takes place without any catalyst present. Under ODH conditions this should not be a problem and glass beads are the preferred diluent material. Quartz wool plugs are used to keep the catalyst + diluent bed in its position. In CO_2 and at 600 °C, SiC is the preferred diluent material.

A.7 Oxygen content of coke

During the TEOM experiment with the 3P/SiO_2 catalyst, it happened that the air feed switched off accidentally a first time and on purpose a second time. The sample mass change data are shown in Figure 13. During these periods the mass decreases and still a small amount of styrene was produced. This could be possible if the oxygen-surface-groups on the coke react with the EB. It seems like the coke acts as an oxygen storage medium. The oxygen content of the coke is quickly restored when the air feed was switched on again (65 h *TOS*). Also when the sample was regenerated (at 170h *TOS*) there is first a fast mass increase, attributed due to surface re-oxidation and then coke burn-off starts. During the first period (54.5-64.5 h *TOS*) 17.3 wt% is lost. During the second period (145.8-155.8 h *TOS*) this loss is 18.1 wt%. This could correspond to a molecular formula for coke of C_6H_6O, of which the O-content is 17% wt%.

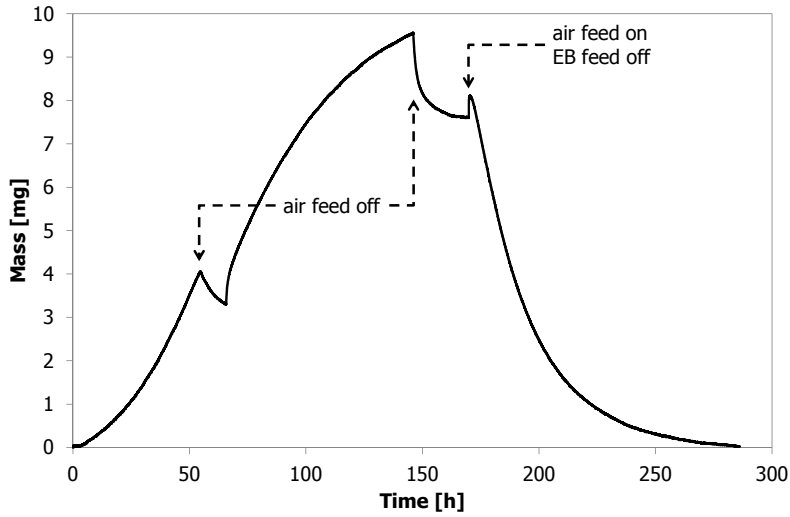

Figure 13: The mass data with time of the TEOM experiment with the 3P/SiO_2 catalyst.

A.8 Heavy condensate byproducts

In all dehydrogenation experiments (in CO_2, H_2O, or with O_2) a small amount of byproducts are formed that have higher boiling points than ST (longer elution time from the FID channel column). We refer to these as heavy condensates throughout this thesis, but in other work 'tars' or 'oxygenated aromatics' are also used. In a typical experiment, the selectivity to this group of byproducts is below 1%, but because of their high boiling points they still can cause problems in our laboratory setup as well as in commercially operated plants. In our laboratory setup these molecules condense on the tubing, even though it is heat-traced at 175-200 °C. Upon the replacement of the reactors with new ones, the setup and part of the heat-tracing has to be cooled down to work safely. On these occasions it happened multiple times that the tubing became blocked. The heavy condensates concentrate, usually at the bottom of a vertical part of the tubing and become very viscous or even solid. To recover from this situation, sometimes it was sufficient to heat up the heat-tracing and put a little gas pressure on the lines. On more severe occasions the tubing connections needed to be opened, clear the tubing with a thin metal wire and flow some acetone through the lines afterwards using a syringe. The acetone was one of the few solvents that worked well, it becomes very dark brown because of the dissolved heavy condensates.

The valve oven of the online-GC is also a bottleneck concerning the blockages due to these heavy condensates. The heating temperature is limited to 175 °C and the valves and lines are only heated indirectly by convection. Their actual temperature was measured by an additional thermocouple and was up to 25 °C lower. Taking apart the valves and cleaning with acetone worked well.

Similar considerations hold for the reactor selection valve in the reactor oven. It is at the lowest point of the setup and a lot of heavy condensates can collect at this point simply by gravity. For prevention measures, the valve rotor is cleaned between each experimental run. Dark brown deposits can usually be observed on this rotor after an experiment.

During our catalyst screening experiments, many different catalyst were tested and some catalysts yield more heavy condensates and problems than other catalysts. In the catalyst development the selectivity to heavy condensates should be minimised as it is a waste product and can cause big operational problems downstream of the reactor.

A.9 CNT reactivity before and after ODH

Several commercially available carbon nanotube (CNT) samples were tested for their performance in the ODH reaction. With increasing time on stream (*TOS*), the temparature of oxidation in thermogravimetric analysis increased for the catalyst material that was removed from the reactor tube after reaction. Three TGA curves are shown in Figure 14 that originate from the same CNT material. Clearly, the curves shift to lower temperatures for longer *TOS* in ODH conditions. This can be the result of two (combined) effects: (1) coke build-up on top of the CNT material, increasing the total mass of the material inside the reactor; (2) replacement or change of the CNT material by/to a more reactive type of carbon material. Because the ash content of the CNT material is very low and because of some small SiC diluent contaminations, it was not possible to analyse the amount of CNT or coke in these samples.

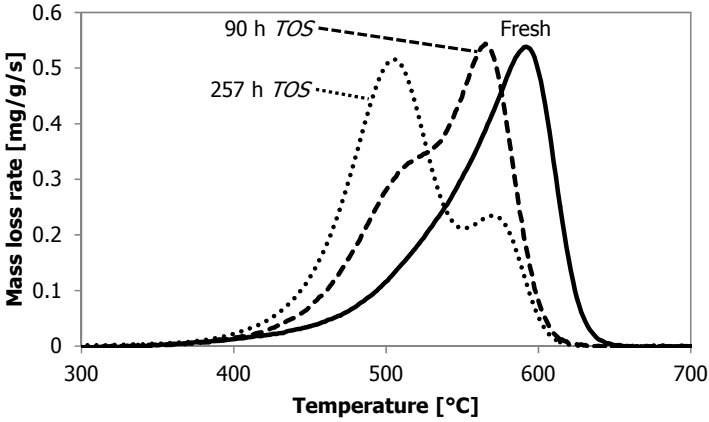

Figure 14: Mass loss rate curves from TGA for three CNT samples from the same starting material, after different *TOS* under ODH conditions.

A.10 Details of the Switch 6-flow setup

For the catalyst screening and kinetics testing, a parallel fixed bed reactor setup was designed and constructed. The order was carried out by Amtec GmbH from Chemnitz, Germany. It was designed for dehydrogenation experiments with operating conditions up to 10 barg and 700 °C. Typical operating conditions are atmospheric pressure and 450-600 °C. The setup can be divided into three sections: feeding, reactor and analysis. These are described in the next paragraphs. A picture with a simplified layout of the setup is shown in Figure 16.

A.10.1 Feeding section

There are 6 gas feeds (CO_2, N_2, H_2 or air, CO, CH_4, propane) that can be combined to make a common gas mixture that is fed to the reactors. Each gas feed has a separate mass flow controller (MFC). All gases are fed into a common pressure line that feeds the secondary MFC's to the individual reactors. The pressure in this common pressure line can be controlled by either a pressure control on the feed-MFC's, or by a pressure relief valve, dependent on the operators preference.

There are two separate liquid feeds, for ethylbenzene and for water. A liquid feed consists of a high pressure pump, pressure line to the feed MFC's and a pressure reducer. The flow in the pressure line is orders of magnitudes higher (>100×) than the required flow for the MFC's to ensure a stable pressure and flow. Excess flow is recycled into a buffer vessel that feeds the pump. Each reactor has an individual MFC for each liquid feed.

For each reactor the gas mixture, EB and H_2O, are first fed into an evaporator that is located in a large oven (Heraeus). The vapour/gas mixture is then fed to the reactor.

A.10.2 Reactor section

The reactor furnace consists of 6 heated zones with individual temperature control. All heating zones are surrounded by ceramic insulation material. The furnace height is 50 cm. Inside the furnace are 6 Inconel reactor shells that are designed to hold a quartz tube reactor of 6 mm outer diameter and 4 mm inner diameter. All reactors have an isothermal zone of over 20 cm. The temperature variation in this zone is +/- 0.5 °C, the temperature variation between reactors is +/- 1 °C, at a temperature setpoint of 600 °C (Figure 16).

Each reactor is supplied with a thermocouple (TC) that was only used to determine the temperature profile over the reactor length. The size of the reactors and catalyst material did not allow for a TC inside the catalyst bed during experiments. In front of each reactor, after the evaporators, an absolute pressure sensor is installed.

A.10.3 Analysis section

After the reactors, the product gas is fed to a selection valve with 2 outlets: a common outlet and an analysis outlet. Each outlet is connected to a pressure control system that sets the operating pressure of the reactors. This pressure control system can be bypassed for atmospheric operation. The common outlet leads to an ambient condensation vessel and the vent. The analysis outlet leads to an online GC system before going to another ambient condensation vessel and vent. All lines from the selection valve to the condensation vessels are heat-traced. The heat tracing is separated into 5 zones that are normally set to the same setpoint.

Just before the GC inlet, a small amount and constant amount of gas is added to the analysis line. This gas is used as an internal standard for the GC analysis. In most cases hydrogen is used.

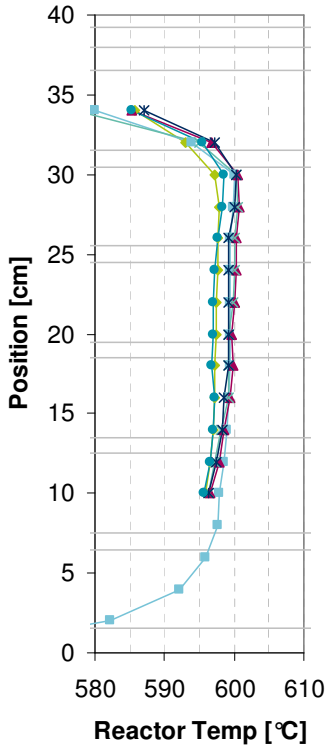

Figure 15: Temperature profiles of the 6 reactors over their reactor length (0 cm = bottom), temperature was set at 600 °C, all measured with one thermocouple.

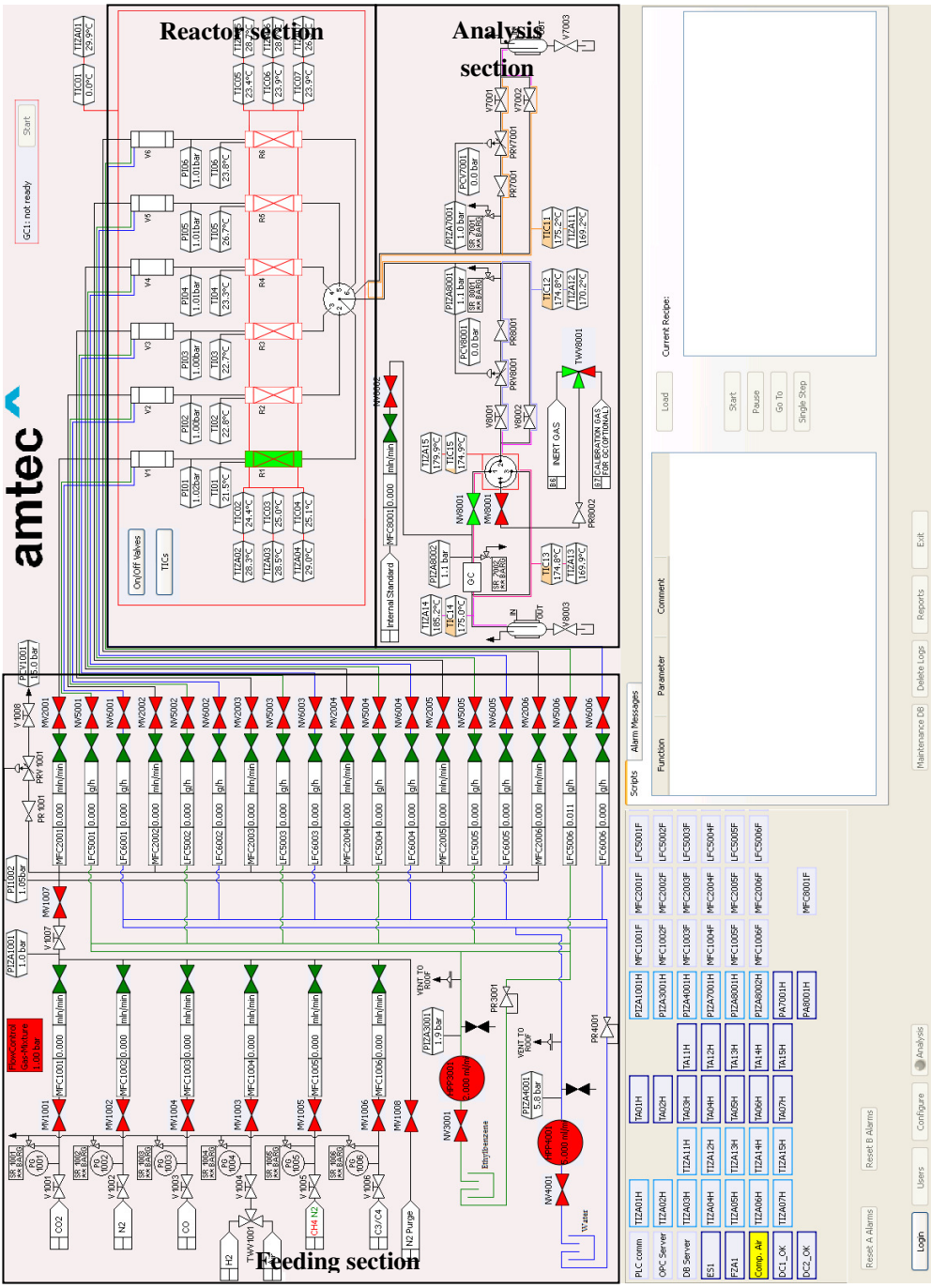

Figure 16: A simplified layout of the 6-flow setup.

A.11 Additional data P/SiO_2 samples

In Chapter 7 of this thesis, only a selection of the available data from the P/SiO_2 samples is presented. To better understand the origin and choice for those data, the full picture of these tests is shown here. Further characterization data are not available.

The performance data from the P/SiO_2 samples that were measured with the standard testing protocol from Ch. 6 (Table 4, test 1) is shown in Figure 17. A few samples (4P, 5P) were tested using a slightly different testing protocol and only the first 20 h *TOS* operated under equal conditions, are shown. The figure shows that all samples are still activating during 0-14 h *TOS*, although selectivity already starts decreasing after 3-5 h *TOS*. Break-in conditions (475 °C, O_2:EB = 0.6) were probably not optimal for the P/Si samples. All samples, except 2P, 3P and 15P, show a continuous increase in O_2 conversion. Based on these data it was recommended to increase the starting temperature to improve the break-in of the catalysts.

This higher starting temperature experiment (Table 4, test 2) was performed with six samples (2, 3, 4, 5, 6, 9 wt% P) and their results with *TOS* are shown in Figure 18. Like expected, it gave better activation of the samples in the 0-14 h *TOS* time window. The fastest activating catalyst sample was 3P/SiO_2, the slowest was 9P/SiO_2 (full order: 3>2>4>5>6>9). The faster activation resulted in higher initial ST yields, but unfortunately a similar decrease in selectivity after 3-5 h *TOS*.

A stability comparison based on a 30 h *TOS* difference was also made for both test series. The comparison of the first series (Figure 19) is not very useful as many samples were still activating (hence the Y10/Y5 > 1). The displayed deactivation of 2P and 3P samples (both nearly 20% yield loss) are a reason for concern, as this is much faster than shown by the reference γ-Al_2O_3 sample. The comparison of the second test series in Figure 20 is quite interesting; 25 °C higher activation temperature appears to be favorable for many samples. A higher wt% P loading appears to give a lower ST yield loss in 30 h *TOS*. However, the trend of increasing stability with P loading is clouded by the increasing O_2 conversion that partly balances the loss in ST selectivity due to increasing O_2 and EB conversions. Based on these data the 5P/SiO_2 sample appears to be the best, it has a comparable Y5 as the 3P/SiO_2 sample, but it has the best Y10.

These two series of tests show that a higher temperature improves the activation of the catalyst but will not improve the stability. Because of the better activation, higher ST yields can be obtained. More work is required for the break-in optimization. The loss of ST selectivity (coupled to increasing CO_X selectivity), rate of deactivation, and overall deactivation of these phosphorous silica based catalysts require intensive investigation. Understanding this is crucial for improvements to this catalyst system.

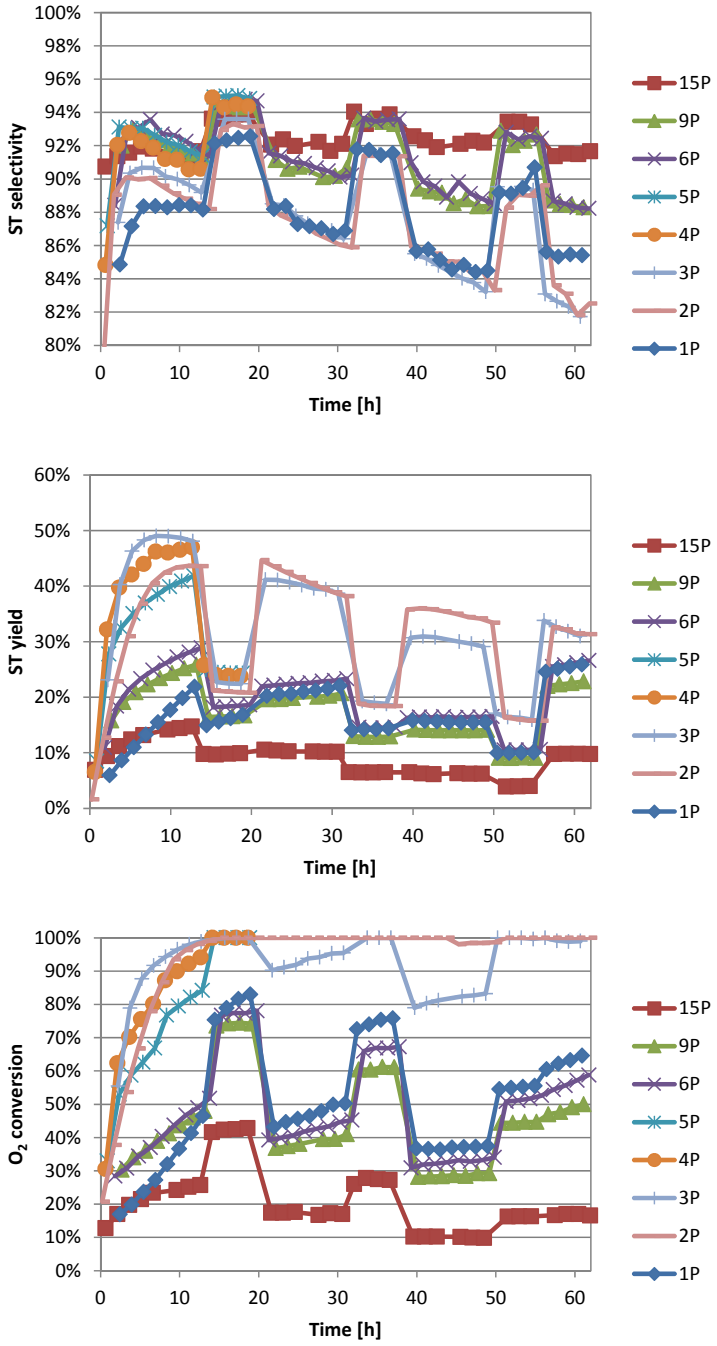

Figure 17: Catalyst performance (ST selectivity, ST yield, O_2 conversion) of the P/Si catalyst samples (wt% P in the legend) with *time on stream (TOS)*, using the standard testing protocol from Ch. 6. (475-450-425-450 °C).

bb

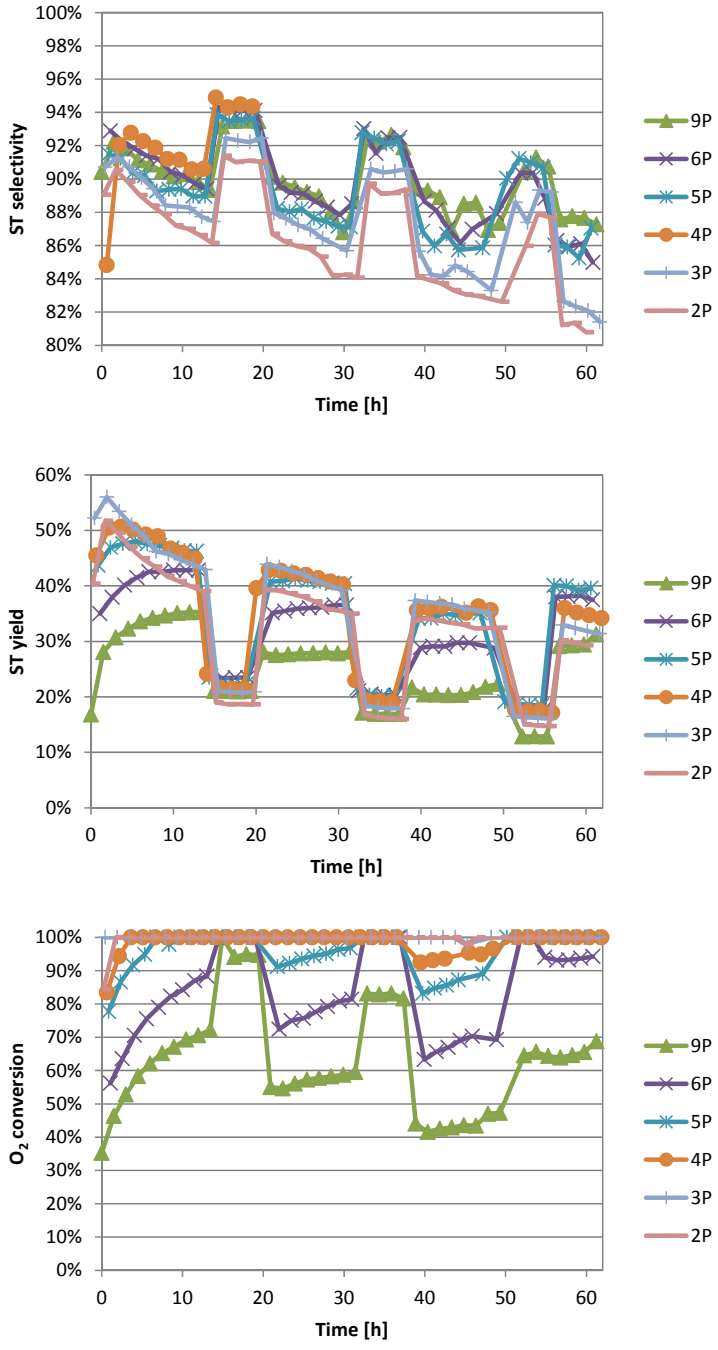

Figure 18: Catalyst performance (ST selectivity, ST yield, O_2 conversion) of the P/SiO_2 catalyst samples (wt% P in the legend) with time on stream, using an adjusted testing protocol. (25 °C higher reaction temperatures: 500-475-450-475 °C).

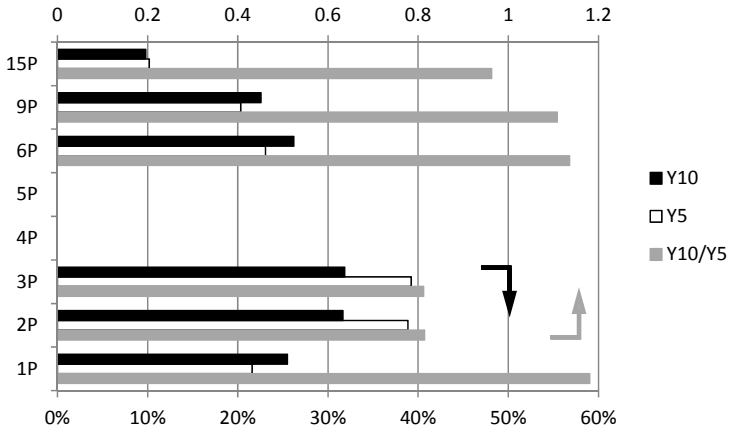

Figure 19: Comparison of the yields at the 5th (open) and 10th condition (closed) of the standard testing protocol (O_2:EB = 0.6, 450 °C) including the ratio of these two (grey). (5th = 26-32 h *TOS*, 10th = 56-62 h *TOS*, giving a 30 h *TOS* difference).

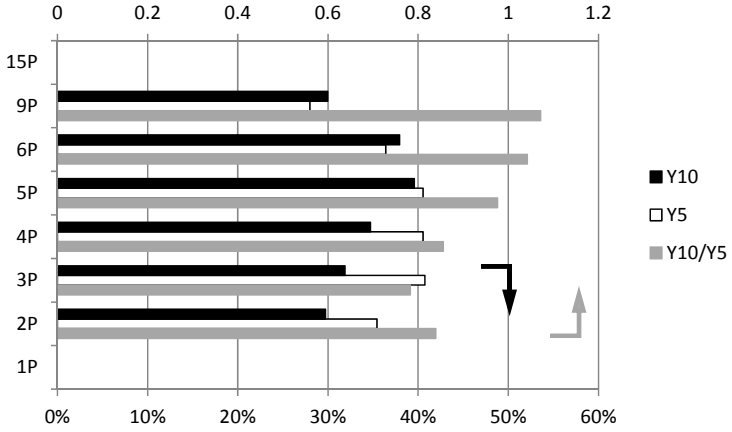

Figure 20: Comparison of the yields at the 5th (open) and 10th condition (closed) using an adjusted testing protocol (O_2:EB = 0.6, 475 °C) including the ratio of these two (grey). (5th = 26-32 h *TOS*, 10th = 56-62 h *TOS*, giving a 30 h *TOS* difference).

Table 4: Conditions of the two test series with P/SiO_2 samples.

Condition	1	2	3	4	5	6	7	8	9	10
TOS [h]	0-8	8-14	14-20	20-26	26-32	32-38	38-44	44-50	50-56	56-62
O_2:EB	0.6	0.6	0.2	0.6	0.6	0.2	0.6	0.6	0.2	0.6
Diluent	N_2	CO_2	CO_2	N_2	CO_2	CO_2	N_2	CO_2	CO_2	CO_2
Test 1 Temp. [°C]	475	475	475	450	450	450	425	425	425	450
Test 2 Temp. [°C]	500	500	500	475	475	475	450	450	450	475